Properties of enteric nervous system stem cells and their potential for clinical transplantation

Thesis submitted in accordance with the

requirements of the University of Liverpool for the

degree of Doctor in Philosophy

by

Sokratis Theocharatos

October 2011

CONTENTS

DECLARATION

This thesis is the result of my own work. The material contained in this thesis has not been presented, nor is currently being presented, either wholly or in part for any other degree or qualification.

The research was carried out at the University of Liverpool

ACKNOWLEDGEMENTS

I would like to thank my supervisors Prof David Edgar and Mr Simon Kenny for their helpful suggestions, criticisms and most importantly for the opportunity they gave me to become part of their team.

A big thank you to my family for their invaluable encouragement and support all these years.

I would also like to thank all my colleagues and friends who really made my time in Liverpool so enjoyable and pleasant.

ABSTRACT

The enteric nervous system (ENS), the intrinsic innervations of the gastrointestinal tract, consists of multiple neuronal and glial cells. However, during embryonic development, abnormalities in the colonization of the gut by ENS progenitors can result in lack of neurons in the colon and subsequent defective bowel function, a phenotype which characterizes the congenital disorder Hirschsprung's disease (HSCR). The current treatment of HSCR is surgery but chronic post-operative complications have stimulated research aimed at developing the use of ENS progenitor cell transplants as an adjunct therapy.

During the last two decades ENS progenitor cells and their neuronal and glial derivatives have been cultured in vitro as aggregates called neurospheres. Upon transplantation into explants of aganglionic embryonic colon, neurospheres have been shown to restore a normal pattern of contractility. However, the behaviour of neurosphere cells and the mechanisms controlling them either in the neurosphere or after

transplantation still need to be established. Consequently, the aim of this study was to investigate the proliferation, differentiation and migratory behaviour of ENS progenitors in vitro.

Results showed that although neurospheres are a mixture of cells expressing different markers, dividing cells follow a pattern. It was demonstrated that cells with high proliferation rate were localized at the periphery of the neurosphere. Upon division some of these cells moved towards the centre and slowed down or stopped proliferating, whereas the rest remained at the periphery and divided further. In both cases, their phenotype changed and they started expressing markers of differentiation. The phenotypic change and the proliferation rate were found to be regulated by the Notch signaling pathway. In addition, transplantation experiments in bowel explants showed that these cells were able to migrate into the gut in the presence or absence of an intrinsic ENS. Migration was also observed when neurospheres were transplanted to different tissues indicating the high migratory potential of these cells.

In conclusion the results of the present thesis give more light in understanding the properties and behaviour of neurosphere cells and represent one step closer to the treatment of bowel disorders such as HSCR.

LIST OF FIGURES AND TABLES

FIGURES

CHAPTER 4

TABLES

CHAPTER 1

CHAPTER 2

ABBREVIATIONS

- **B-FABP:** Brain-specific fatty acid binding protein
- **BrdU:** 5'-bromo-2'-deoxyuridine
- **BSA:** Bovine serum albumin
- **cDNA:** Complementary deoxyribonucleic acid
- **CGRP:** Calcitonin gene-related peptide
- **CNS:** Central nervous system
- **DAPI:** 4',6-diamidino-2-phenylindole
- **DAPT:** N-[N-(3, 5-difluorophenacetyl)-L-alanyl]-S-phenylglycine t-butyl ester
- **DMEM:** Dulbecco's modified eagle medium
- **DMSO:** Dimethyl sulfoxide
- **DNA:** Deoxyribonucleic acid
- **EDN3:** Endothelin-3
- **EDNRB:** Endothelin receptor B
- **EdU:** 5'-ethynyl-2'-deoxyuridine
- **EGFP:** Enhanced green fluorescent protein
- **EMT:** Epithelial mesenchymal transition

- **ENS :** Enteric nervous system
- **GDNF:** Glial cell line-derived neurotrophic factor
- **GFAP:** Glial fibrillary acidic protein
- **HSCR:** Hirschsprung's disease
- **NCCs:** Neural crest stem cells
- **NOS:** Nitric oxide synthase
- **NS:** Neurosphere
- **NSE:** Neuron specific enolase
- **O/N:** Overnight
- **PBS:** Phosphate buffered saline
- **PGP9.5:** Protein gene product 9.5
- **PNS:** Peripheral nervous system
- **qRT-PCR:** Quantitative Reverse Transcriptase Polymerase Chain Reaction
- **RNA:** Ribonucleic acid
- **RT: Room temperature**
- **TGF-β:** Transforming growth factor-β
- **TH:** Tyrosine hydroxylase
- **VIP:** Vasoactive intestinal peptide
- **YFP:** Yellow fluorescent protein

CHAPTER 1

Introduction

Hirschsprung's disease (HSCR) is a congenital disorder characterized by a lack of neurons in a variable length of the distal gut. The cause has been shown to be defective formation of the enteric nervous system (ENS) during early development (Swenson, 1996). In the last two decades although significant progress has been made in understanding the mechanisms regulating the formation of the ENS by neural crest cells, many questions remain unanswered. In the following paragraphs the origin and the mechanisms regulating the development of the ENS are discussed as well as current and potential treatments of HSCR.

1.1. Neural crest development and neural crest derivatives

The neural crest is derived from the embryonic ectoderm and was firstly described by His in 1868 in chick embryos as a group of cells located at the neural folds between the neural plate and the dorsal non neuronal ectoderm (Hall et al., 2008). Cells fated to become neural crest start expressing the paired-box transcription factor Pax7 and signaling induced by secreted molecules of the adjacent epidermal ectoderm such as bone morphogenetic-protein 4 (BMP-4) and fibroblast growth factor from the paraxial mesoderm are prerequisites for the generation of neural crest identity (Lemke et al., 2009). The dorsal lips of the neural folds during neurulation will fuse to form the neural tube. During and after the fusion, neural crest cells (NCCs) transit from an epithelial to

mesenchymal (EMT) state and migrate in different pathways giving rise to multiple cell types (Ruhrberg et al., 2010; Sieber-Blum et al., 2000; Gammill and Bronner-Fraser, 2003) (Fig. 1.1). The mesenchymal transition in neural crest cells is regulated by molecules such as the zinc finger transcription factors Snail-1 or Snail-2 which inhibit the role of cell-cell junction proteins cadherins and thus enable a migratory behaviour (Acloque, 2009).

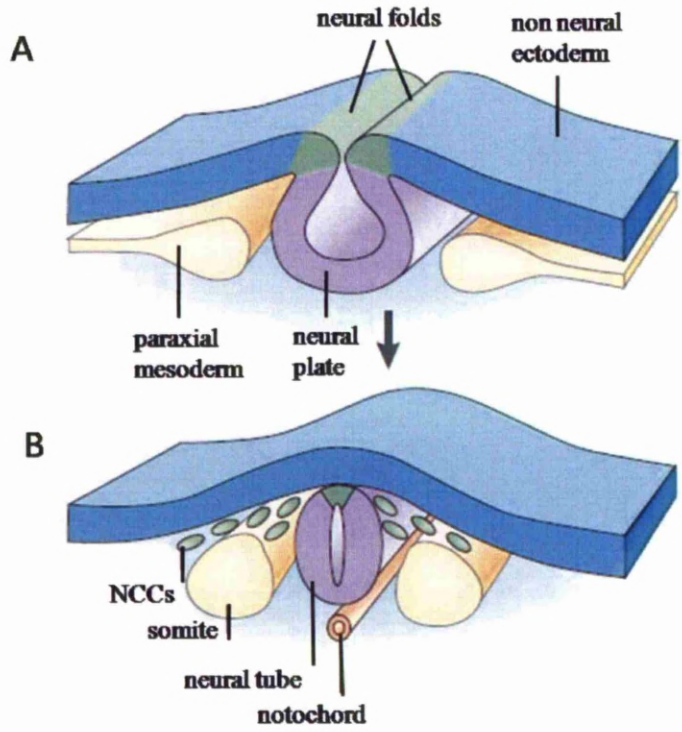

Figure 1.1. **Formation of neural crest during embryonic development.** Neural crest (green) is formed at the border between the non-neural ectoderm and the neuronal ectoderm (neural plate) (A). When the neural tube is formed, neural crest cells migrate to various locations where they form different cell types and tissues (B). NCCs= neural crest cells. (Picture was adapted and modified from Gammill and Bronner-Fraser, 2003).

Depending on their location and migratory pathways, NCCs can be divided in 4 groups:

1) cranial (cephalic), **2)** vagal and sacral, **3)** trunk and **4)** cardiac NCCs (Table 1.1). Cranial NCCs undergo dorsolateral migration and differentiate into bone, cartilage, cranial neurons, glia and connective tissues of the face (Gilbert, 2000). The vagal and sacral NCCs are responsible for the generation of enteric ganglia in the gastrointestinal tract (Le Douarin and Teillet, 1973; Pomeranz et al., 1991; Gilbert, 2000). The trunk NCCs migrate either dorsolaterally to give rise to melanocytes or ventromedially and differentiate into Schwann cells, chromaffin cells of the adrenal medulla and also give rise to dorsal root and sympathetic ganglia (Lemke, 2009). Finally, the cardiac NCCs, which are a vagal subpopulation (Kirby et al., 1990), give rise to melanocytes, neurons, cartilage and also to the connective tissue of the large heart arteries (Gilbert, 2000).

Neural crest type	Cellular derivative
Cranial neural crest	Mesenchyme Connective tissue (including muscle sheaths) Cartilage Bone Dentine (odontoblasts) Parafollicular cell (ultimobranchial bodies) of the thyroid gland. Cornea Sclera Ciliary muscle and muscles for eye attachment Inner ear (with otic placode) Sensory ganglia of cranial nerves V, VI, IX and X
Vagal and sacral neural crest	Neurons of parasympathetic nervous system of alimentary canal Neurons of parasympathetic nervous system of blood vessels Enteric ganglia
Trunk neural crest	Pigment Merkel cells Dorsal root ganglia Neurons and ganglia of the sympathetic nervous system Chromaffin cells of the adrenal medulla Epinephrine-producing cells of the adrenal gland
Cardiac neural crest	Connective tissue associated with the great vessels of the heart Aorticopulmonary septum of the heart Smooth muscles of the great arteries Ganglia (celiac, superior and inferior mesenteric, and aortical renal)

Table 1.1. **Neural crest derivatives.**

(Table was adapted and modified from Hall, 2008).

1.2. Enteric nervous system origin

Ablation experiments of vagal NCCs in chick embryos (Yntema and Hammond, 1954) and quail – chicken interspecies transplantations of segments from the neural axis (Le Douarin and Teillet, 1973) showed that most of the ENS progenitors derive from vagal neural crest cells, which emigrate at the level of the post-otic hindbrain and enter the foregut. Following that transition, cells migrate caudally through the gut wall and colonize the gastrointestinal tract (Burns 2005). There is also a small contribution from the sacral level of the neural tube where NCCs enter the gut mesenchyme and migrate in a caudal-rostral direction (Burns and Le Douarin, 1998; Burns et al., 2000; Kapur et al., 2000) (Fig. 1.2A).

The formation of ENS in the foregut is also contributed by trunk neural crest cells (Durbec et al., 1996). More precisely in chick, vagal neural crest cells that are located adjacent to somites 1-2 colonize mainly the oesophagus and the stomach whereas crest cells adjacent to somites 3-6 colonize the entire gut (Burns et al., 2000). In mice vagal NCCs adjacent to somites 1-5 give rise to enteric neurons along the entire gastrointestinal tract, whereas NCCs adjacent to somites 6-7 contribute only in the oesophagus. The sacral NCCs originate from the area caudally to somite 28 and 24 in chick and mouse embryos respectively (Anderson et al., 2006a).

In chick embryos the vagal NCCs enter the foregut on embryonic day 2.5-3 (E2.5-3), they reach the caecum on E6-E6.5 and colonization of the enteric gut is complete by E8.5 (Burns and Le Douarin, 1998). In mice vagal NCCs enter the foregut at embryonic day 9.5-10 (E9.5-E10), they arrive at the caecal region by E11.5 and reach the terminal hindgut at E14.5 (Young et al., 1998) (Fig. 1.2B). In humans, the entrance of vagal NCCs into the foregut takes place at week 4 and the colonization of the gut is completed by week 7 of development (Wallace et al., 2005).

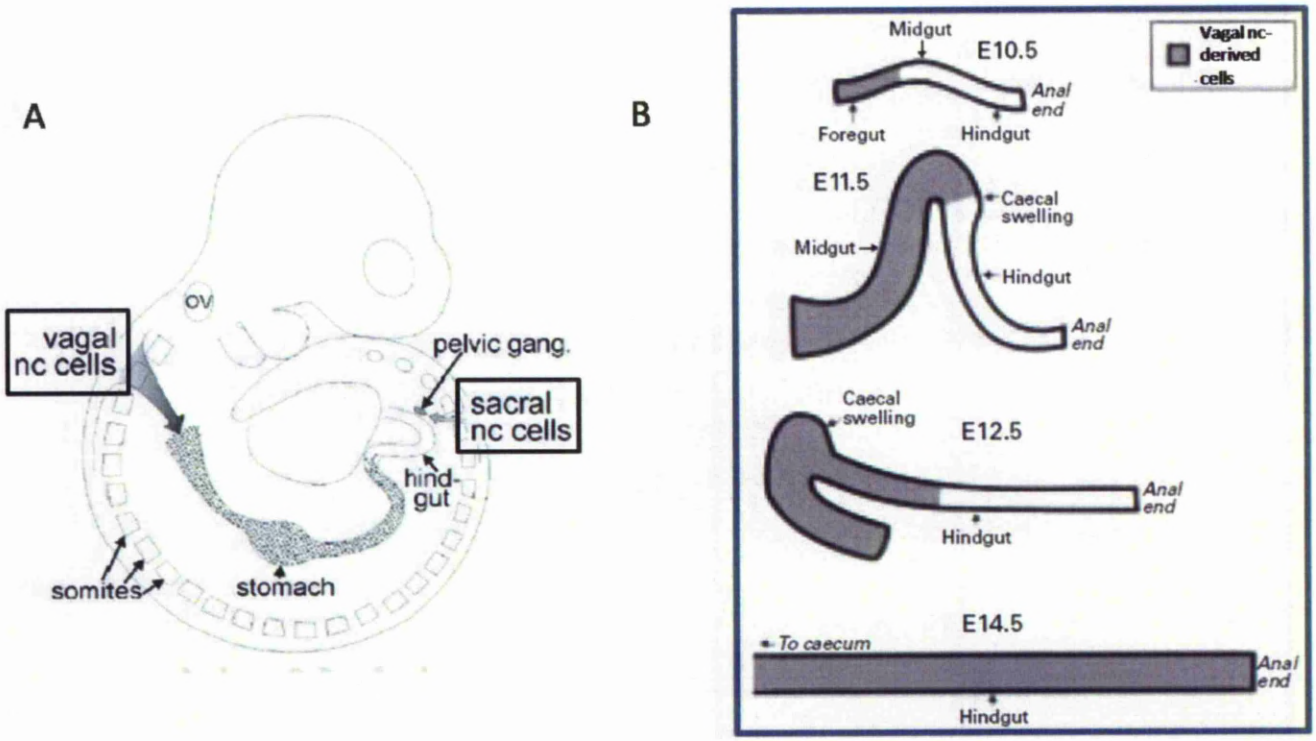

Figure 1.2. **Colonization of mouse embryonic gut from neural crest-derived cells.**

Neural crest cells from the vagal and sacral region enter and colonize the developing gut (A). Vagal neural crest-derived cells complete the colonization of the gut by E14.5 (B). NC= neural crest. (Pictures were adapted and modified by Anderson et al., 2006a (A) and Young et al., 2000 (B)).

In mice and humans, vagal NCCs migrate in the mesenchyme near to the periphery of the gut wall and form ganglia in the region where the myenteric plexus will form between the circular and longitudinal smooth muscle. Later on, a second migration takes place where NCCs migrate radially from the region of the myenteric plexus towards the circular muscle in order to give rise to the submucosal plexus (McKeown et al., 2001). A different migration pattern takes place in the colorectum of chick embryos. When vagal NCCs reach the proximal hindgut enter the inner layers of the circular muscle and migrate where the future submucosal plexus will form. Then they migrate outwards to form the myenteric plexus (Burns and Le Douarin, 1998).

The contribution of sacral NCCs is smaller in the generation of enteric ganglia and as it was demonstrated in the distal hindgut of E16 chicks, 17% of the enteric neurons derived from sacral NCCs (Burns and Le Douarin, 1998). In mice, sacral NCCs leave the neural tube at E9.5, form prospective pelvic ganglia at E11.5 and enter the distal hindgut at E13.5 which has not been colonized yet by vagal NCCs. Then caudal-rostral migration takes place guided by extended fibers of the pelvic ganglia into the hindgut (Wang et al., 2011). In chicks, sacral NCCs emigrate from the neural tube and form the nerve of Remak at E3.5. After E7 and in large numbers at E10, sacral NCCs colonize the distal hindgut guided by neuronal projections from the nerve of Remak in the

area of the myenteric plexus (Burns et al., 2005; Anderson et al., 2006a). In both mouse and chick, when sacral NCCs enter the hindgut give rise to neurons and glia (Burns et al., 1998; Wang et al., 2011).

1.3. Enteric nervous system structure and phenotypes of migratory and post-migratory vagal crest-derived cells

The ENS in the small intestine and colon consists of interconnected networks of neurons and glia which are grouped into two plexi; the myenteric (Auerbach's) plexus and the submucosal (Meissner's) plexus. The former is located between the inner circular muscle and the outer longitudinal muscle layers of the intestine, whereas the submucosal plexus is situated between the muscularis propria and the muscularis mucosa (Furness 2006).

Vagal crest-derived cells (called enteric NCCs from now on) express the neurotrophin receptor p75 (Chalazonitis et al., 1998). The expression of other markers has also been observed including the SRY-related High Mobility Group- box transcription factor Sox10 (Wegner et al., 1999), the Ret receptor protein tyrosine kinase (Pachnis et al., 1993), the transcription factors paired-like homeobox 2a (Phox2a) or homeobox2b (Phox2b) (Pattyn et al., 1999) and tyrosine hydroxylase (TH) (Gershon et al., 1984). Enteric NCCs colonize the gut in a rostral-

caudal direction and the formation of enteric neurons also follows a rostrocaudal wave (Rothman et al., 1982).

At the migratory wavefront all the neural crest $p75^+$ cells were $Phox2b^+$/ Ret^+/ $Sox10^+$/ $Phox2a^-$ (Young et al., 1999; Young et al., 2003) and represented undifferentiated enteric NCCs as examined in E10.5, E11.5, E12.5 and E13.5 mouse bowel (Young at al., 1999). All the Ret^+ cells were $p75^+$ but only a small number of $p75^+$ cells were expressing Ret. TH^+ cells were present not at the very caudal end of the wavefront but more rostrally. AT E10.5 around 15% of the $p75^+$ population was also TH^+. Cells expressing TH were present transiently in the foregut and midgut between E10-14 and they were never observed in the hindgut (Teitelman et al., 1981; Gershon et al., 1984). They gave rise to enteric serotonergic neurons but not neurons positive for the calcitonin gene-related peptide (CGRP) which seemed to be derived from TH^- progenitors (Baetge et al., 1990; Blaugrund et al., 1996).

In E12.5 mice, when the migratory wavefront is in the post-caecal hindgut, cells expressing nitric oxide synthase (NOS) were present in the oesophagus and midgut and they were $Ret^+/Phox2b^+/TH^-$ and weakly labeled for p75 (Young et al., 1999; Young et al., 2001a). Vasoactive intestinal peptide (VIP) was co-localized with NOS^+ neurons in adult mice but it appears later in embryonic life than NOS (Rothman

et al., 1984). The neurotransmitter acetylcholine can be detected as early as E10 (Hao and Young, 2009). $CGRP^+$ neurons were only found in the small intestine by E17 (Blaugrund et al., 1996) and they were not present in the oesophagus or the large intestine of E17 or P2 mice and their phenotypic profile was $p75^+$/ Ret^+/ $Phox2a^-$/$Phox2b^+$/NOS^- (Young et al., 1999).

Regarding glial cells, at E11.5, cells expressing the glial marker Brain-specific fatty acid binding protein (B-FABP) were present in the foregut and the proximal midgut, showing that they were rostral to the migratory wavefront which at that time point had colonized the caecum. The B-$FABP^+$ cells were all $p75^+$ and had low expression of Ret (Young et al., 2003). The calcium binding protein S100B was observed after E14.5 in small numbers in the duodenum and these cells were $p75^+$ with low expression of Ret. In addition the glial fibrillary acidic protein GFAP appeared for the first time at E16 (Rothman et al., 1986). When enteric NCCs commit towards the neuronal lineage the expression of Sox10 is downregulated whereas when they commit to the glial lineage Sox10 expression is maintained (Bondurand et al., 2003; Kim et al., 2003). The expression of all the above markers highlights the complexity in the formation of the ENS and the differentiation potential of enteric NCCs. This change in the phenotype of enteric NCCs during migration reflects changes in their proliferative and differentiating potential.

1.4. Functions of enteric nervous system

The ENS is capable of regulating gut motility reflexes without input from the central nervous system (CNS) (Gershon, 1999), due to the presence of interconnected neuronal networks consisting of sensory and intrinsic primary afferent neurons and excitatory and inhibitory neurons (Furness 2006). The ENS also regulates a series of functions such as secretion, absorption, electrolyte transport, immune and endocrine functions as well as blood flow within the gut tube (Furness 2008).

1.5. Migration pattern of enteric NCCs in the gut

Enteric NCCs migrate caudally in a complex and dynamic way in the gut mesenchyme. In chick embryonic gut, cells positive for the enteric NCC marker HNK-1 (Bronner-Fraser, 1986), migrate in chain formation which could be branched or not (Conner et al., 2003). A chain formation pattern of enteric NCCs has also been observed in mouse embryonic gut explants (Young et al., 2004) where the enteric NCCs were labeled with enhanced green fluorescent protein (EGFP) under the constitutive control of the promoter for the tyrosine kinase receptor gene, Ret, a marker for migrating NCCs in the gut (Pachnis et al., 1993). The trajectories of the chains showed great variations in terms of orientation and speed and also there were some individual cells which escaped

from the chain and migrated 50-100μm circumferentially and then joined the same or different chains of cells (Young et al., 2004).

A transgenic mouse model, using yellow fluorescent protein (YFP) under the control of the Wnt1 promoter, a marker for neural crest cells, demonstrated essential properties of the migration pattern in caecal and post-caecal regions. Migrating cells in the form of strands pause in the ileo-caecal border for 8-12h where more strands are forming. Individual 'advanced cells' from the wavefront migrate caudally and enter the caecum where they form new short strands which then join the network of strands located caudally to the leading wavefront. Repeat of this process results in the colonization of the distal gut (Druckenbrod and Epstein, 2005). It is worth mentioning that both groups (Young et al., 2004 and Druckenbrod and Epstein, 2005) observed a chain of enteric NCCs extending along the mesentery between the base of the caecum and the post-caecal hindgut, preceding the entry of the migratory wavefront in the mesenchyme of the intestinal wall, indicating the presence of a vagal crest cell-derived population with different migratory properties and maybe different response to the caecal mesenchyme as they can by pass it through the mesentery.

The migration pattern of NCCs in chains implicates the importance of cell to cell interactions in gut colonisation. Indeed cell contact

interactions have been shown to be present as the cell adhesion molecule L1 is expressed by enteric NCCs in embryonic mouse gut explants. Blockage of L1 function, with a L1-function blocking antibody decreased the migration rate and disrupted the chain formation at the leading wavefront of migration (Anderson et al., 2006b). Migration in chains is not a unique characteristic of crest-derived cells in the gut. Cardiac crest-derived cells migrate in cord formation as they colonize the heart (Poelmann et al., 1998). In addition, absence of gap junction protein connexin 43 (Cx43alpha1) has been shown to have a negative effect on the directionality and speed of cardiac neural crest cells (Xu et al., 2006). Furthermore, it has been demonstrated that the migration speed of enteric NCCs is approximately 35-40 μm/ h as has been shown in both fowl and mouse embryonic gut explants (Allan and Newgreen, 1980; Young et al., 2004).

1.6. Effect of cell number in the migration of vagal crest-derived cells

Various research groups, using neural crest ablation experiments, have demonstrated a relationship between the number of vagal crest cells and the length of the gut they colonize (Peters van de Sanden et al., 1993; Burns et al., 2000; Yntema and Hammond, 1954, Barlow et al., 2008). In embryonic mouse explants when part of the mesenchyme was removed, caudally to the migratory wavefront and without disturbing the

epithelium, the leading migratory cells showed reduced motility compared to controls (Young et al., 2004). A more detailed study which focused on the migration of ENS precursors in the hindgut, demonstrated that leading cells located caudal to the caecal colonic which was dissected out, were able to form an evenly distributed network only when they exceeded a minimum number (Druckenbrod and Epstein, 2005), suggesting that gut colonization depends on a 'population pressure' model from cells located rostral to the migratory wavefront. Using mathematical simulations and chimaeric experiments with embryonic chicken and quail gut, it was proposed that migratory cells at the leading wavefront proliferate more due to the fact the ENS density is low at the wavefront and therefore less population pressure is applied by the surrounding environment (Simpson et al., 2007).

1.7 Signaling pathways involved in the ENS formation

Two major signaling pathways have been shown to play important roles in the development of the ENS. These are the GDNF/Ret/GFRα1 and the endothelin-3/ endothelin receptor B pathways.

1.7.1. GDNF/Ret/GFRα1 signaling pathway

GDNF/Ret/GFRα1 signaling regulates the survival, proliferation and differentiation of enteric NCCs in vitro (Heuckeroth et al., 1998; Taraviras et al., 1999; Chalazonitis et al., 1998; Hearn et al., 1998).

Glial cell line-derived neurotrophic factor (GDNF) is a homodimer belonging to the transforming growth factor-β (TGF-β) superfamily which was initially found to promote the survival of embryonic midbrain dopaminergic neurons (Lin et al., 1993). GDNF is expressed by the gut mesenchyme (Young et al., 2001b) and attaches to GFRα1 which is bound to the cell membrane via a glycosyl phosphatidylinositol (GPI) anchor. Onto this complex the Ret receptor protein tyrosine kinase, which is expressed by the enteric NCCs, attaches and becomes activated (Airaksinen and Saarma, 2002; Pachnis et al., 1993). GFRα1 is expressed by both enteric crest and non crest-derived cells (Chalazonitis et al., 1998; Worley et al., 2000).

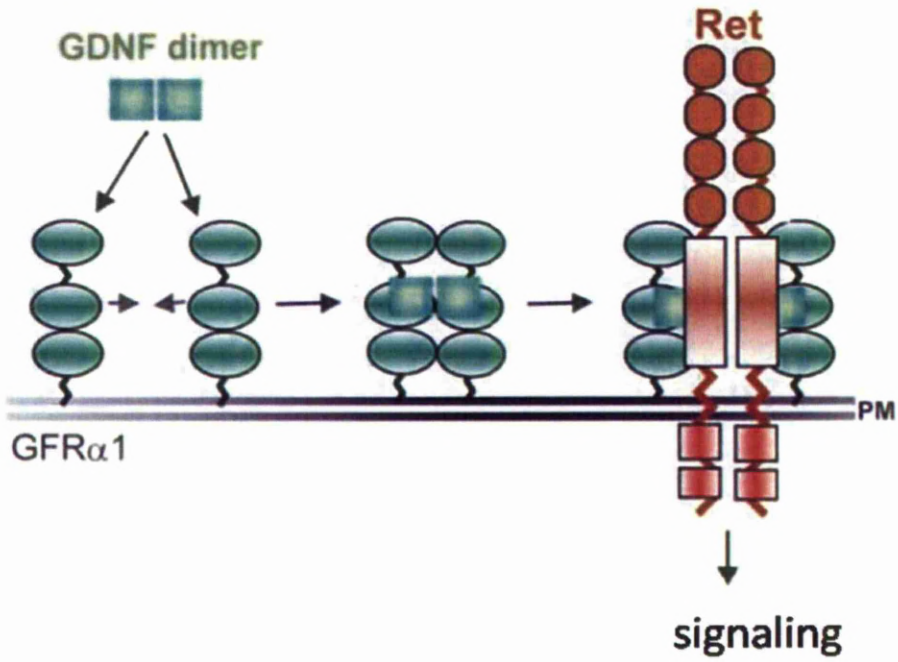

Figure 1.3. **GDNF/Ret/GFRα1 signaling pathway.**

A GDNF dimer binds and brings together two molecules of GFRα1. Onto this complex Ret molecules attach, followed by trans-phosphorylation and activation of their tyrosine kinase domains which initiates the signaling cascade. (Picture was adapted and modified from Sariola and Saarma, 2003).

Pre-enteric NCCs were chemo-attracted by GDNF when explants of mouse E9-9.5 post-branchial region were cultured in vitro with or without GDNF (Natarajan et al., 2002). Expression of GDNF mRNA in the gut mesenchyme of the foregut, midgut and caecum had been shown to precede migration of Ret^{+} enteric NCCs, consistent with a chemoattractive role of GDNF in vivo (Natarajan et al., 2002; Young et al., 2001b).

Experiments using transgenic mice showed that GDNF -/- (Moore et al., 1996), GFRα1 -/- (Enomoto et al., 1998, Cacalano et al., 1998) and Ret -/- (Schuchardt et al., 1994) mice die within 24 hours of birth. Aganglionosis in small and large intestine and renal agenesis or severe dysgenesis were observed in Ret -/- newborn mice (Schuchardt et al., 1994). In Ret -/- E17.5 mouse embryos, neurons and glia were present only in the esophagus and the proximal stomach, whereas in Ret +/- E17.5 embryos neurons and glia were present throughout the whole gastrointestinal tract (Durbec et al., 1996), indicating that Ret haploinsufficiency in mice is adequate for the entire colonization of the gut.

GDNF -/- E13.5 and P0 mice have no neurons in the small and large intestine as shown after immunostaining bowel sections for neuron specific enolase (NSE) and peripherin, although very few neurons could

be observed in the stomach area when compared to wild type (Moore et al., 1996). GDNF adult heterozygote mice have a reduced number of enteric neurons throughout the whole GI tract (Shen et al., 2002; Gianino et al., 2003) and that was shown to be due to fewer neuronal precursors identified by PGP9.5 and BrdU staining (Gianino et al., 2003) indicating the role of GDNF in influencing the number of enteric neurons by regulating the proliferation of their precursors. The degree of aganglionosis or hypoganglionosis may vary as shown in GDNF +/- newborn mice (Shen et al., 2002). On the other hand, adult Ret +/- mice do not have a decrease in the number of neurons but a reduction in neuron size was observed (Gianino et al., 2003). Both GDNF and Ret heterozygotes demonstrated abnormal contractility in the small and large intestine and a lower release of vasoactive intestinal peptide (VIP) and substance P (Gianino et al., 2003), suggesting that haploinsufficiency for the above genes is enough to provoke functional defects and loss of neuronal subpopulations.

Heterozygote GFRa1 mice appear healthy and reproduce normally (Enomoto et al., 1998). However GFRa1 -/- newborn mice have no ganglion cells in the small and large intestine but only in the oesophagus and stomach and do not survive more than a day after birth as mentioned previously (Enomoto et al., 1998). Also, in GFRa1 null mice agenesis or dysgenesis of kidneys was observed similar to

what has been shown for GDNF and Ret null mice (Shen et al., 2002; Gianino et al., 2003; Pichel et al., 1996; Sanchez et al., 1996). The similarity in the defects of the ENS and the kidney development in these mutants indicates the strong interaction between GDNF, GFRa1 and Ret and that they cannot compensate for the functional loss of the other one.

1.7.2. Endothelin 3/ Endothelin receptor B signaling pathway

The second important signaling pathway in ENS development is the endothelin 3 (EDN3) / endothelin receptor B (EDNRB) pathway. EDN3 interacts with the G protein-coupled seven trans-membrane receptor, EDNRB (Barlow et al., 2003). EDN3 is produced by the gut mesenchyme where its expression is higher in the caecum region as shown by in situ hybridization in mice embryos (Leibl et al., 1999). On the other hand EDNRB is expressed by the migrating enteric neural crest cells (Gariepy et al., 1998) and occasional mesenchymal cells in the embryonic jejunum (Barlow et al., 2003; Lee et al., 2003).

In mice there are natural mutants for EDN3 (lethal spotted-ls) and EDNRB (piebald lethal-sl). The lethal spotted mice have a mutation which blocks the proteolytic activation of EDN3 by the endothelin converting ezyme-1, ECE-1 (Baynash et al., 1994) whereas the piebald lethal mice have a deletion in the EDNRB gene resulting in absence of

a functional receptor (Hosoda et al., 1994). In both cases the phenotype of the mutants is distal bowel aganglionosis and coat colour spotting. Mice with targeted disruption of either the EDN3 or EDNRB gene have the same phenotype as the natural mutants (Baynash et al., 1994; Hosoda et al., 1994).

Studies in ls/ls mouse embryos showed that lack of EDN3/EDNRB signaling does not affect the survival or the proliferation of migratory enteric NCCs in the gut (Kruger et al., 2003; Woodward et al., 2003), although differences were observed in the spatial differentiation towards a mature neuronal phenotype (Woodward et al, 2003). In contrast, some groups reported a promotion of proliferation when EDN3 was present (Barlow et al., 2003; Nagy and Goldstein, 2006). These differences are more likely to be a result of different experimental approaches as in a study done by Barlow et al. (2003) they observed no difference in the total number of dividing cells in gut cultures of EDN3 ls/ls mice. However, they found a reduction in the number of dividing cells expressing the transcription factor and ENS progenitor marker Sox10, indicating the role of EDN3 in the proliferation of undifferentiated ENS progenitors (Barlow et al., 2003). Other evidence from experiments done in avian gut showed that EDN3 acts as an inhibitor of neuronal differentiation and in addition blocks the chemoattractive effect of GDNF on enteric crest-derived cells (Hearn et al., 1998; Nagy and

Goldstein, 2006). Thus, the EDN3/EDNRB pathway is responsible for maintaining an undifferentiated migratory population responsible for colonizing the hindgut (Wu et al., 1999; Bondurand et al., 2006).

1.7.3. Other signaling pathways involved in ENS development

1.7.3.1. Hedgehog signaling pathway

Sonic hedgehog (Shh) and Indian hedgehog (Ihh) have been both implicated in the normal development of the gut (Sukewaga et al., 2000; Ramalho et al., 2000). Both Shh and Ihh homozygous mutant mouse embryos displayed various abnormalities in the ENS. Shh -/- embryos have additional neurons into the villi and under the epithelium instead of them being localized only in the plexi. Ihh -/- mice displayed aganglionosis in regions of small intestine and colon (Ramalho et al., 2000).

Experiments in embryonic mouse bowel revealed expression of the Sonic hedgehog (Shh) receptor *Patched* (Ptc1) in Ret^{+} enteric NCCs. Further investigation in neurospheres formed by enteric crest-derived cells and in embryonic gut explants showed that Shh promotes proliferation and inhibits the chemoattractive effect of GDNF on enteric NCCs (Fu et al., 2004). In addition, the Shh pathway was shown to be necessary for the migration of vagal neural crest cells before entering

the bowel and for the migration of ENS precursors inside the gut (Reichenbach et al., 2008). Therefore, Hedgehog signaling seems to be necessary for the normal ENS development and further investigations to identify interactions with other pathways are essential.

1.7.3.2. Notch signaling pathway

Although the role of Notch signaling has been studied thoroughly in progenitors of the central nervous system and in other tissues or organs where it was shown to have an effect on cell proliferation and cell fate determination (Artavanis-Tsakonas et al., 1999; Andersson et al., 2011), very few studies have been published regarding its role for ENS precursors. Using adult rats with in situ hybridization and immunohistochemistry experiments it was shown that the receptor Notch-1 as well as the ligand Jagged-2 were expressed in ganglia along the gastrointestinal tract (Sander et al., 2003). Similarly, expression of Notch-1 and Jagged-2 was demonstrated in a recent study where human bowel was examined. It was shown that staining for Notch-1 or Jagged-2 was negative in patients with aganglionic bowel (Hirschsprung's disease) as their expression was low in segments lacking ganglia as demonstrated by Western blot analysis and RT-PCR (Jia et al., 2011).

Transgenic mice lacking a fucosyl-transferase (POFUT1) important for Notch signaling had a reduction in the number of $Sox10^{+}$ enteric NCCs due to premature differentiation towards a neuronal fate (Okamura et al., 2008). On the other hand, transient expression of the Notch pathway in neural crest cells induced gliogenesis (Morrison et al., 2000).

Finally a synergistic mechanism has also been implied between Shh and Notch signaling pathways during ENS development. Activation of Shh in enteric NCCs promoted their proliferation and glial differentiation, a reaction which was blocked by a Notch inhibitor, indicating that the induced proliferation and gliogenesis by Shh is caused through Notch signaling activation. In addition Shh activation promoted expression of the Delta-like 1 ligand (Dll1) and upregulation of the Notch signaling target gene Hes1 (Ngan et al., 2011). These data indicate the regulatory role of both Shh and Notch signaling pathways in ENS development.

1.8. Other molecules important for the ENS development

1.8.1. Transcription factor Sox10

A spontaneous mutation resulting in dominant megacolon appeared in the Jackson Laboratory in 1979 and was subsequently shown to involve the Sox10 transcription factor (Lane et al., 1984, Southard-Smith et al., 1998). Mice naturally or experimentally homozygous for the dominant megacolon (Dom mutation), $Sox10^{Dom/Dom}$, completely lack neurons from the gastrointestinal tract and the etiology was shown to be increased apoptosis of neural crest cells before entering the foregut (Kapur et al., 1999). On the other hand heterozygotes, $Sox10^{Dom/+}$, in both mice and humans demonstrate distal colonic aganglionosis in addition to pigmentation defects (Pingault et al., 1998, Southard-Smith et al., 1999, Walters et al., 2010), suggesting a critical role for Sox10 in ENS formation and survival of migratory NCCs. Additionally, the transcription factor Sox10 has been shown to maintain undifferentiated neural crest cells (Kim et al., 2003) and enteric NCCs (Bondurand et al., 2006)

A relationship between the transcription factor Sox10 and the gene EDNRB has been proposed as researchers have identified binding sites for Sox10 on the EDNRB gene (Zhu et al., 2004). Cross-breeding experiments between EDNRB and Sox10 mice mutants revealed that

aganglionosis in the double mutants was more severe than the one in the single mutants, as shown by staining of acetylcholine positive enteric neurons (Cantrell et al., 2004), indicating the presence of other mechanisms in ENS formation except their possible genetic interaction. Also, EDN3 and Sox10 double mutant mice had more severe aganglionosis than single mutants as demonstrated with Tuj1 immuno-histochemistry, implying that different mechanisms are regulating the role of Sox10 and EDN3 in ENS formation (Stanchina et al., 2006).

In addition Sox10 has been shown to bind to a 45bp sequence at the 3' end of the enhancer of the Ret promoter. Also, the transcription factor Pax3 binds in the same 45bp sequence (Lang et al., 2000). Mouse embryos (E12.5) lacking Pax3 have no enteric ganglia distal to the stomach (Lang et al 2000). In addition, a physical interaction between Sox10 and Pax3 in a protein-protein manner has been shown by immunoprecipitation experiments, suggesting a synergistic role for both Sox10 and Pax3 in the regulation of Ret expression (Lang et al., 2003).

1.8.2. Transcription factors Phox2b and Mash1

The transcription factor Phox2b has also been implicated in the normal development of the ENS. In mutant mouse embryos which lack Phox2b, enteric NCCs migrated only to the proximal stomach, a phenotype similar to Ret -/- mice (Pattyn et al., 1999). Also, Phox2b is needed for

the expression of the Ret gene as in transgenic mouse embryos lack of Phox2b results in loss of Ret expression (Pattyn et al., 1999). However an exact direct binding site of Phox2b on Ret has not been confirmed implying that Phox2b could control Ret expression indirectly (Leon et al., 2009).

The transcription factor Sox10 has been shown to be important for the initial induction of Phox2b and the proneural gene mammalian achaete-scute Homolog 1, Mash1, in neural crest cells. However, Sox10 expression decreases as $Phox2b^{+}$ and $Mash1^{+}$ cells commit towards the neuronal lineage (Kim et al., 2003). Transgenic mice lacking Mash1 (Mash1 -/-) die during the first day of birth (Guillemot et al., 1993).

Cultures of dissociated E12.5 rat bowel showed that most of TH^{+} cells were expressing Mash1. Often TH^{+}/ $Mash1^{+}$ cells were found as doublets suggesting a recent division but no doublets were observed in TH^{+}/ $Mash1^{-}$ cells. TH^{+}/$Mash1^{-}$ cells were larger and with long processes compared to TH^{+}/$Mash1^{+}$ cells, indicating that the latter are neural progenitor cells. Immunoreactivity of TH could not be observed in E12.5 Mash1 -/- rat bowel, whereas lack of Mash1 did not have an effect in Ret^{+} ENS progenitors (Blaugrund et al., 1996). These data suggest that Mash1 plays a critical role in the survival of TH^{+} neural progenitors in the gut.

1.8.3. Bone Morphogenetic Proteins

The bone morphogenetic proteins BMP-2 and BMP-4 are signaling molecules, that are part of the TGF-β family. They bind to BMP receptors and activate the Smad pathway through phosphorylation (Zwijsen et al., 2003). The BMPs participate in the induction and migration of neural crest cells (LaBonne et al., 1999) and play a role in the neuronal differentiation of enteric NCCs where BMP4 acts together with GDNF to promote enteric neuronal differentiation (Chalazonitis et al., 2004) and enteric NCCs' migration (Goldstein et al., 2005).

Overexpression of the BMP inhibitor noggin resulted in higher numbers of neurons in the small intestine (Chalazonitis et al., 2004), whereas in the hindgut fewer ganglionic neurons and a delay in the intestinal colonization were observed (Goldstein et al., 2005). These data are consistent with defects in the migration of enteric NCCs due to reduced BMP function. In the developing gut both BMP-2 and BMP-4 proteins are produced by enteric NCCs and by non-crest derived cells indicating an autocrine and paracrine role for BMPs on ENS cells (Chalazonitis et al., 2004).

BMP-2 has been shown to inhibit gliogenesis in rat neural crest cell colonies, a process which could be rescued by the presence of Sox10 (Kim et al., 2003). Also, BMP-4 promotes neuronal differentiation of

enteric NCCs in a manner independent from the EDN3/EDNRB signaling pathway (Kruger et al., 2003). Moreover, BMPs show a selective regulation in the survival of neurons expressing the neurotrophin-3 receptor TrkC (tyrosine kinase receptor C) (Chalazonitis et al., 2004). The above evidence shows that BMPs regulate the development of the ENS through complex mechanisms.

1.8.4. Vitamin A and retinoic acid

Retinoic acid, which is derived from the metabolism of vitamin A (Ott et al., 1979), has also been implicated in the development of the ENS. Regulation of Ret expression and the morphology of the gut are some of the roles of retinoic acid (Pitera et al., 2001). Mutant mice embryos which lack the synthesizing enzyme of retinoic acid retinaldehyde dehydrogenase 2 (RALDH2) die on embryonic day E10.5 due to heart abnormalities (Niederreither et al., 2001). However, exogenous addition of retinoic acid extended the lifetime of these embryos until the end of gestation demonstrating that there were defects in the development of the oesophagus and the stomach (Wang et al., 2006). Retinoic acid in vitro promotes the proliferation of a subset of enteric NCCs already committed to the neuronal lineage, as shown by expression of the immature neuronal marker Tuj1. In addition retinoic acid is responsible for the reduction of neurite length of enteric NCCs in culture expressing Ret and induces their neuronal differentiation (Sato et al., 2008). Finally,

distal enteric aganglionosis occurrs in transgenic mice lacking the vitamin A binding protein Rbp4, suggesting that reduction in retinoic acid levels due to low levels of vitamin A, results in defective gut colonization by the ENS progenitors (Fu et al., 2010).

1.8.5. Extracellular Matrix Proteins

The mesenchyme of the gut contains various extracellular matrix (ECM) proteins such as laminin, fibronectin, chondroitin sulfate proteoglycan and tenascin (Newgreen et al., 1995). Integrins are the main receptors of ECM proteins and they include 24 αβ heterodimers. Enteric NCCs express receptors for ECM proteins including α4, α6 and β1 integrins (Iwashita et al., 2003, Breau et al., 2006) and the LBP110 receptor of laminin-1 (Chalazonitis et al., 1997). In mice which have a tissue-specific homozygous mutation for β1-integrin, the enteric NCCs fail to colonize the whole length of the gut resulting in distal colonic aganglionosis. Moreover, ganglia formed aggregations in a disorganized pattern when compared to control ENS of P14 mice (Breau et al., 2006) indicating that normal interaction of enteric NCCs with the ECM proteins of the gut is crucial for their migration and colonization of the gut. This interaction was analyzed further, as it was demonstrated that enteric NCCs lacking β1-integrin failed to interact with the fibronectin in the hindgut which promotes their migration. As a result they receive the negative effect from tenascin which has been

shown to act as a negative regulator of cell adhesion and migration (Breau et al., 2009).

1.9. Hirschsprung's disease

In previous paragraphs the molecules and signaling pathways involved in the ENS development were analyzed, indicating the complexicity of the ENS formation and the different factors that could alter the normal colonization of the gut by enteric NCCs. The defective colonization of the gut by enteric NCCs and the consequent absence of ganglia in the distal colon is the typical phenotype of a disorder in humans called Hirschsprung's disease (HSCR).

HSCR is a congenital disorder which is characterized by the lack of enteric ganglia (aganglionosis) in both submucosal and myenteric plexi typically in the distal colon (Amiel et al., 2008). Children with HSCR have an extremely dilated proximal colon (megacolon). The length of the bowel which is affected may vary, but in 80% of the cases the aganglionic segment includes the internal anal sphincter, the rectum and a small part of the sigmoid colon and is classified as short segment HSCR (S-HSCR). When the aganglionosis is more extensive then it is termed long segment HSCR (L-HSCR). In addition different variants have been observed including total colonic aganglionosis (TCA), total

intestinal aganglionosis (where parts of the small intestine are involved), short segment aganglionosis (involving only the distal rectum) and finally the case where the aganglionic colon is rostral to ganglionic segment (Amiel et al., 2008).

Although HSCR was first reported in 1888 by the Danish paediatrician Harald Hirschsprung in two patients who died from chronic constipation and dilated bowel it was not until 1948 that the first effective surgical technique was developed to treat HSCR. Previous investigators were unaware that the etiology was the absence of ganglia caudal to the dilated bowel as demonstrated with histochemical examination and that was the segment that had to be removed (Swenson 1996). Surgery involved resection of the distal aganglionic bowel and a low anastomosis of ganglionic bowel to the rectum.

HSCR occurs in a ratio of 1:5000 live births (Bodian et al., 1963) but that number varies among different ethnicities (Kenny et al., 2010). In addition, there is a bias of males towards the occurrence of HSCR in a ratio of 4/1 (Kenny et al., 2010). Occurrence of HSCR could be identified as an isolated trait (70% of the cases) or it could be accompanied with a chromosomal defect such as trisomy 21 (12%). In the rest of the cases HSCR symptoms are part of another syndrome such as Waardenburg syndrome (Gershon, 2010).

Various genes have been implicated in the pathogenesis of HSCR with the most common being those involved in the Ret/GDNF and EDN3/ EDNRB signaling (Table 1). Mutations at the locus 10q11.2 of the proto-oncogene Ret are the most common ones as they have been identified in up to 50% familial and 35% sporadic cases. Mutations can be located in different positions of the gene and involve different types of mutations such as missense and nonsense mutations or even large deletions (Amiel et al., 2008).

ene	Abbreviation	Mutation frequency	Function
eceptor tyrosine nase	Ret	50% familial cases 15-35% sporadic cases	Expressed by ENCC. Promotes migration, survival and differentiation of ENCC
lial cell-line erived neurotrophic ıctor	GDNF	Rare, <5%, 6 cases reported	Produced by gut mesenchyme. Ret-ligand promoting migration, survival and differentiation of ENCC
eurturin	NTN	1 familial case reported	Co-ligand for GDNF. Produced by gut mesenchyme
ndothelin receptor	EDNRB	~5%	Expressed by ENCC. Maintenance of ENCC in undifferentiated state
ndothelin-3	EDN3	<5%	EDNRB ligand. Produced by gut mesenchyme particularly caecum
ndothelin onverting enzyme	ECE1	1 case report	Proteolytic conversion of endothelin-3 precursor to active form
RY-related MG-box 10	Sox10	Waardenburg-Shah syndrome	Expressed by ENCC, maintenance of ENCC in undifferentiated state, cell fate and glial cell differentiation
aired-like omeobox 2d	Phox2b	Congenital Central Hypoventilation Syndrome with HSCR	Expressed by ENCC. Essential for development of autonomic neural crest derivatives. Necessary for Ret expression.
nc finger omeobox 1b or nad interacting rotein 1	Zfhx1b/sip1	Mowat Wilson syndrome	Expressed by ENCC and derivatives. Essential for formation of vagal neural crest cells
anscription factor 4	TCF4	Pitt-Hopkins syndrome, occasionaly HSCR	Interacts with β-catenin that enters the nucleus as a result of Wnt signaling

Table 1.2. **Genes involved in human Hirschsprung's disease and their role. ENCC: enteric neural crest-derived cells, HSCR: Hirschsprung's disease.** (Table modified from Theocharatos et al., 2008 and Gershon, 2010).

Alternative splicing of the proto-oncogene Ret results in two isoforms, the RET9 and RET51 which differ only in their C-terminal ends (Tahira et al., 1990). Mice mutants expressing only one of the isoforms revealed an important role for RET9, because mice lacking only the RET9 isoform had colonic aganglionosis whereas $Ret51^{-}/Ret51^{-}$ mice had no apparent defect in the innervation of the gut (de Graaff et al., 2001). As discussed previously, mice heterozygotes for the Ret gene do not have any alterations in the number of enteric neurons (Gianino et al., 2003) whereas in humans Ret +/- genotype results in distal aganglionosis (Amiel and Lyonnet, 2001), implying a possible species difference regarding the role of HSCR related genes.

Nevertheless, many studies using transgenic animals including mouse and zebrafish knock-out models, as well as microarray assays, have identified the role of many genes, transcription factors and molecules involved in the normal development of the ENS and thus potential targets for HSCR therapy (Burzynski et al., 2009). In all cases where gut aganglionosis occurs the parameters discussed are the survival, proliferation, differentiation and migration of the enteric NCCs which for one or the other reason fail to colonize the whole gut and/or cannot keep up with the simultaneous growth of the bowel (Landman et al., 2007; Laranjeira et al., 2009).

The treatment of HCSR today is surgery and involves the approach described previously by Swenson where the aganglionic segment is removed (reviewed in Swenson et al., 1996). Although the same operational principle exists today with some modifications, the outcome of the surgery sometimes can lead to long-term complications as the aganglionic internal anal sphincter is required to remain in situ in order to maintain the function of the external anal sphincter (Theocharatos et al., 2008). These complications can involve chronic constipation or enterocolitis and social problems resulting in poor quality of life (Jarvi et al., 2010, Ieiri et al., 2010, Chumpitazi et al., 2011).

1.10. Stem cells of the enteric nervous system and their clinical potential

The possible post-operative complications of HSCR lead to the search for other adjunct therapies such as the use of neural stem cells. Previously, Reynolds and Weiss reported a protocol for maintaining neural stem cells in vitro isolated from the central nervous system (CNS) introducing a new era for the expansion of neural stem cells (Reynolds et al., 1992). The original protocol suggested that the presence of the epidermal growth factor (EGF) in combination with non adherent tissue culture conditions were the prerequisites for maintaining the proliferation of CNS stem cells. Due to proliferation and lack of adhesion to a culture substrate these cells

derived from mouse forebrain formed aggregates, named 'neurospheres' and they were able, upon attachment on adherent substrate, to give rise to neurons positive for the neuron-specific enolase (NSE), substance P and γ-aminobutyric acid as well as $GFAP^+$ glial cells (Reynolds et al., 1992) suggesting an in vitro way to propagate and maintain undifferentiated neural stem cells.

Regarding neural stem cells of the ENS, isolation and expansion of mouse enteric NCCs as neurospheres was demonstrated by Schafer et al. (2003). Thereafter progress has been made in isolating enteric NCCs from both mouse and human bowel samples (Bondurand et al., 2003; Almond et al., 2007; Metzger et al., 2009a, b). These groups demonstrated by immunostaining in gut-derived neurosphere sections the presence of neuronal markers including Tuj1, PGP9.5, NOS, VIP, substance P, CGRP and cholino- acetyltransferase (ChAT), indicating that the neuronal markers than can be found in the ENS in vivo, are also present in neurospheres. In addition, markers for enteric glia such as S100B and GFAP were also expressed. The fact that neurospheres upon multiple dissociations could regenerate and still express neuronal and glial markers suggests that neurospheres are a complex environment containing self-renewing progenitors and their progeny (Bondurand et al., 2003; Almond et al., 2007; Metzger et al., 2009a, b; Lindley et al., 2009). However, the

number and the location of stem cells in the neurospheres, how many of the cells express neuronal or glial markers or the mechanisms regulating cell differentiation within the neurosphere are still unknown.

Transplantation of neurospheres derived from bowel of HSCR patients into mouse aganglionic gut showed restoration of contractility indicating a functional role for neurosphere cells, and that neurosphere-cell transplantation in internal anal sphincter could be a therapy to treat HSCR (Lindley et al., 2008). In addition, neural stem cells derived from mouse embryonic brains were able to differentiate into NOS^{+} neurons and improve the gastric emptying after transplantation into the pyloric wall of NOS-/- adult mice (Micci et al., 2005). Also, when CNS neural stem cells isolated from the cortex of embryonic rats were transplanted into benzalkonium chloride-treated aganglionic rectum of adult rats, were able to differentiate into neurons and glia and recover the rectoanal inhibitory reflex as that was shown 8 weeks post-transplantation (Dong et al., 2008). However, it is unknown how and why these cells migrate in the gut explants. Also, it is not known if neurosphere cells behave in vitro in the same manner as enteric NCCs during bowel development.

Regarding proliferation, a small number of studies have demonstrated the presence of proliferating cells at the periphery of the neurosphere (Campos

et al., 2004). Again, we do not understand why these cells proliferate at such a great rate in culture compared to the in vivo conditions and most importantly how can we regulate their proliferation, a prerequisite for any potential transplantation in vivo as their continuous proliferation could lead to tumour formation.

Therefore, in this study we designed and performed experiments to answer the questions that rose above, because understanding the behaviour and the mechanisms controlling enteric stem cells in vitro could one day be the solution to treat enteric nervous system disorders such as HSCR.

Aims of the thesis:

- To investigate cell proliferation in neurospheres.
- To identify the relationship between cell proliferation versus cell differentiation in the neurospheres.
- To investigate the presence and the role of signaling pathways regulating cell proliferation and cell differentiation.
- To study the behaviour of neurosphere-derived cells following transplantation.

CHAPTER 2

Materials and Methods

2.1 Tissue dissection

Time mated CD-1 mice (Charles River Laboratories, Kent, UK) were sacrificed by inhalation of increasing concentration of carbon dioxide on embryonic day (E) 11.5 in accordance with UK Home Office regulations. Uterus containing embryos was dissected out and placed on a 60mm petri dish with 5ml of Dulbecco's Modified Eagle Medium, DMEM (Invitrogen, Paisley, UK) low glucose. Using forceps embryos were removed from the uterus and placed in a 60mm silicon based dissection dish. Embryonic caeca were isolated under a dissection microscope (Leica M165 FC) using fine forceps (No. 5 Dumont, Fine Science Tools, FST, Heidelberg, Germany). At the embryonic age E11.5 the wavefront of the migratory undifferentiated NCCs are located at the caecum (Druckenbrod and Epstein, 2005). At this stage in the caecum both GDNF (Young et al., 2001) and EDN3 (Leibl et al., 1999) are higly expressed by the gut mesenchyme, implying that enteric NCCs have been exposed to both GDNF and EDN3 signaling pathways at this stage. In addition, when mouse E11.5 colon containing few migratory enteric NCCs was dissected and cultured in vitro, enteric NCCs colonized the colon at similar density with what observed in intact gut and the number of NOS^+ neurons in both conditions remained unaltered (Sidebotham et al., 2002). These data indicate that the caecum at E11.5 contains ENS progenitors able for the colonization of the gut and therefore caecum was used as source of cells for our experiments.

2.2. Generation of embryonic mouse neurospheres

Dissected caeca (n= 12-16/ pregnant mouse) were centrifuged at 150g for 5 min. Caeca were incubated with 0.05% trypsin (Sigma Aldrich, Poole, UK) diluted in Dulbecco's phosphate buffered saline, DPBS (Invitrogen) for 15min at 37°C. The reaction was stopped by removing trypsin after centrifugation at 150g for 5min and by the addition of 1ml of neurosphere culture medium. Mechanical dissociation followed using 1ml Gilson pipette. The resulting single cells (2-3X10^5 cells/ ml) were transferred to 60mm non adherent dish (see 2.2.1.) and further 4ml of neurosphere culture medium were added. Cells were kept in a humidified incubator with 5% CO_2 (Heraeus, Thermo Fisher Scientific, Essex, UK).

After one week the first neurospheres had developed and by 2 weeks in culture they had reached the size of 100µm. Neurospheres were passaged by dissociation. They were incubated with 0.05% trypsin for 10min at 37°C. Upon centrifugation at 150g for 5min, the supernatant was removed and 1ml neurosphere culture medium was added. Mechanical dissociation with a 1ml Gilson pipette followed. Single cell suspension was split to 2 or 3 new 60mm non adherent dishes and complemented with medium to reach a final volume of 5ml.

2.3. Tissue culture

2.3.1. Tissue culture substrates

1. 60mm non adherent dishes (Sterilin, Scientific Laboratory Supplies, SLS, Nottingham) for the generation and propagation of the neurospheres as described in the previous paragraph.
2. Filter paper (Millipore, Watford, UK) with V-shape cut situated on top of a well in Terasaki 72-well plate (VWR, Lutterworth, UK) was used for the explant culture.
3. 8-well Permanox plastic Chambers (Sigma-Aldrich) for immunostaining of single cells derived from dissociated neurospheres.
4. 8-well Glass chambers (VWR), coated with 150 μg/ cm^2 poly-D-lysine (8h) (Sigma-Aldrich) and 1.5 μg/ cm^2 laminin (8h) (Sigma-Aldrich) with 3 rinses of PBS after each coating, for neurosphere attachment and neurosphere cell migration.

2.3.2. Neurosphere culture medium

Low glucose (1mg/ml) DMEM with 100U/ml penicillin and 100µg/ml streptomycin (Invitrogen), 2mM L-glutamine (Invitrogen), 2% v/v chick embryo extract (Sera Laboratories Int., Horsted Keynes, UK), 1% v/v N1-supplement (Sigma-Aldrich), 0.05mM 2-mercaptoethanol (Sigma-Aldrich), 20 ng/ml, epidermal growth factor (EGF, Sigma-Aldrich), 20 ng/ml fibroblast- growth factor-2 (FGF2, Autogen Bioclear, Calne, UK) and 1% fetal bovine serum (FBS, Invitrogen). The protocol was adapted from Almond et al. (2007). The culture medium was replaced twice a week; neurospheres were moved close to the centre of the dish by swirling and $^{2}/_{3}$ of the old medium were removed.

2.3.3. Explant culture medium and HEK293T medium

High glucose (4.5mg/ml glucose) DMEM with 100U/ml penicillin (Invitrogen), 10% FBS (Invitrogen) and 2mM L-glutamine (Invitrogen).

2.4. Sections and Immunostaining

2.4.1. Neurosphere sections

Neurospheres were firstly sectioned and then immunostained in order to identify protein localization in the middle of the neurosphere and avoid any antibody penetration issues resulting from wholemount immunostaining. Neurospheres with diameter 100-150μm were transferred to an embedding mold (peel-a-way truncated- T12, Park Scientific, Northampton, UK) with a glass Pasteur pipette (230mm, VWR). Excess medium was discarded and the mold was covered with 300μl of Shandon Cryomatrix (Thermo Fischer Scientific). Using a 200μl tip neurospheres were positioned in the centre of the mold. They were then centrifuged at 150g for 3min and as a result all the neurospheres were grouped at the bottom of the mold. They were stored at -80°C until sectioning. For the sections a Cryostat (HM505N, Thermo Fisher Scientific) was used, with disposable microtome blades (MX35, Thermo Fisher Scientific) and the sections were cut at 8μm thicken.

2.4.2. Explant sections

Explants including mouse embryonic E11.5 and neonatal P1 colon as well as neonatal P1 heart, liver and bladder were transferred to a 12-well plate (VWR) and fixed with 4% (w/v) paraformaldehyde (Sigma-Aldrich)

dissolved in Phosphate Buffered Saline (PBS), for 30min at RT followed by washing with PBS 3 X times. Explants were kept overnight (O/N) at 4°C embedded in 20% (w/v) sucrose dissolved in PBS. The following morning explants were transferred to freezing molds (peel-a-way truncated T12, Park Scientific, Northampton, UK) using forceps and covered with 300µl Shandon Cryomatrix. Tissue was stored at -80°C. Sections were taken as described in the previous paragraph.

2.4.3 Immunostaining on sections

Frozen sections were washed once with PBS. Cells were fixed with 4% paraformaldehyde for 10min at room temperature (RT). Fixative was removed with 3 X 5min washes of PBS. Incubation with 0.25% Triton X-100 (v/v) (Sigma-Aldrich) in PBS for 10 min at RT followed. Cells were washed 3 X 5min with PBS and a ring with a hydrophobic marker (Super HT Pap Pen, 4mm, Research products Int Corp, Illinois, USA) was drawn around each section in order to minimize the volume required for reagents in the next steps. Bovine serum albumin, BSA (2%, w/v in PBS) (Invitrogen), was added in each ring for 1h at RT prior to incubation with primary antisera diluted in BSA (2%, w/v in PBS) at 4°C, O/N. The next day, primary antibody was washed away with PBS 3 X 5 min times. Secondary antibody conjugated with fluorophore (see 2.14.2.) was added for 1h in the absence of light. Further washing 2 X 5 min with PBS followed. Sections

were incubated with 0.5μg/ml 4',6-diamidino-2-phenylindole (DAPI) for 5 min in the dark, 2 x 5 min washes with PBS followed. Sections were mounted with Mounting Medium (Dako) and covered with a coverslip. Sections were kept at 4°C until observation under the microscope.

2.4.4. Immunostaining on neurosphere-derived adherent cells

Following neurosphere dissociation, $5x10^3$ cells/ chamber/ $0.8cm^2$ were seeded onto Permanox chambers slides (Sigma-Aldrich). Counting was performed using a haemocytometer. In detail, 10μl from the single cell suspension were mixed 1/1 with Trypan Blue (Sigma-Aldrich) and half the volume was loaded to the haemocytometer for counting. Cells were fixed with 4% paraformaldehyde (150μl/ chamber) for 10min at RT. Cells were then processed as described in section 2.4.3.

2.4.5. BrdU immunostaining on frozen sections

BrdU solution was purchased from Becton Dickinson (Worthing, UK). It was diluted in neurosphere cell culture medium at a final concentration of 10μM. Sections were processed as normally but before adding 0.25% Triton X-100 (v/v), cells were treated with 4M HCl for 15min in order to denature the DNA. Washing with distilled water followed and 2X washes with PBS before continuing with the Triton X-100 step.

2.4.6. 5-ethynyl-2'-deoxyuridine (EdU) staining

For both sections and cells that were seeded on Permanox slides the process of EdU immunostaining was the same. Cells were fixed for 10min with 4% paraformaldehyde. Upon washing 3 X 5min times with PBS, 0.25% Triton X-100 was added for 20 min and then the process was continued according to the manufacturer's instructions (Click-it EdU imaging kit, Invitrogen). In contrast to antibody immunostaining, retrieval of incorporated EdU was based in the bond created by the azide group of the Click-it fluorophore Alexa594 and the alkyne group of EdU, a covalent reaction catalyzed by copper. The azide-containing fluorophore can enter the nucleus without prior HCl treatment.

2.4.7. Treatment of neurospheres with DAPT

For the inhibition of Notch signaling pathway the γ-secretase inhibitor N-[N-(3, 5-difluorophenacetyl)-L-alanyl]-S-phenylglycine t-butyl ester (DAPT) was used (Sigma-Aldrich). DAPT (5mg) was dissolved in pure (99.7% v/v) dimethyl sulfoxide (DMSO) at a final concentration of 10mM. It was added to neurosphere culture medium so that the final concentration was 10μM. In the control an equal amount of pure DMSO was added to the medium.

2.5. Transplantation assay

Colon was dissected from E11.5 mouse embryos and P1 mouse neonates. In embryos the explant originated from the caecal-colonic junction until the most caudal end that could be dissected (Fig. 2.1A). In the case of neonates ~3mm of bowel was dissected in between the appendix and anus. Colon from either E11.5 or P1 mice was transferred onto a square filter paper into which a V-shape cut had been made so that ends of the colon explants rested on the paper while most of the explants extended across the V-shaped gap. The paper (Millipore) was then transferred to a Terasaki well containing 11.5 µl transplantation culture medium. The middle of the bowel was suspended free in the medium whereas the edges remained attached to the paper. This technique allowed the bowel to maintain its tubular shape over time (Hearn et al., 1999). An $EGFP^+$ neurosphere was placed either at the rostral or the caudal end of the colon as indicated (Fig. 2.1B).

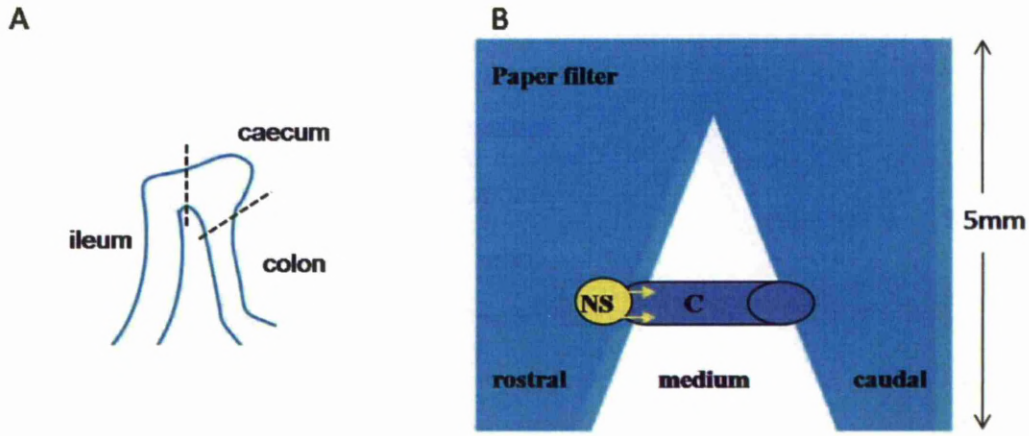

Figure 2.1. **Schemes demonstrating the origin of the embryonic mouse E11.5 colon and the transplantation design.**

Colon for transplantation experiments was dissected at the caecal-colonic junction and in cases where the caecum was included that was dissected at the boundary between ileum and caecum (A, dotted lines; Druckenbrod and Epstein, 2005). The transplantation design was adapted from Hearn et al., 1999 (B, NS=neurosphere; C=colon).

2.6. Production of lentivirus

2.6.1. Molecular cloning in bacteria and plasmid purification

For the production of the EGFP-expressing lentivirus, 3 plasmids were used. These were the pMDG.2, pCMVΔ8.74 and the pHR-SFFV-EGFP (Fig. 2.2). Plasmids were kindly provided by Dr Tristan McKay (University of Manchester). The plasmids were transformed (1μg) by heat-shock in One Shot Top10 competent E.coli bacteria (Invitrogen) according to the manufacturer's instructions. Selection of the successfully transformed bacteria was done by spreading them on LB/agar plates containing 100μg/ml ampicillin. For the plasmid purification Maxi-prep bacteriological cultures (500ml) were lysed and the lysate containing plasmid DNA was processed according to manufactures's instructions (Qiagen, Crawley, UK).

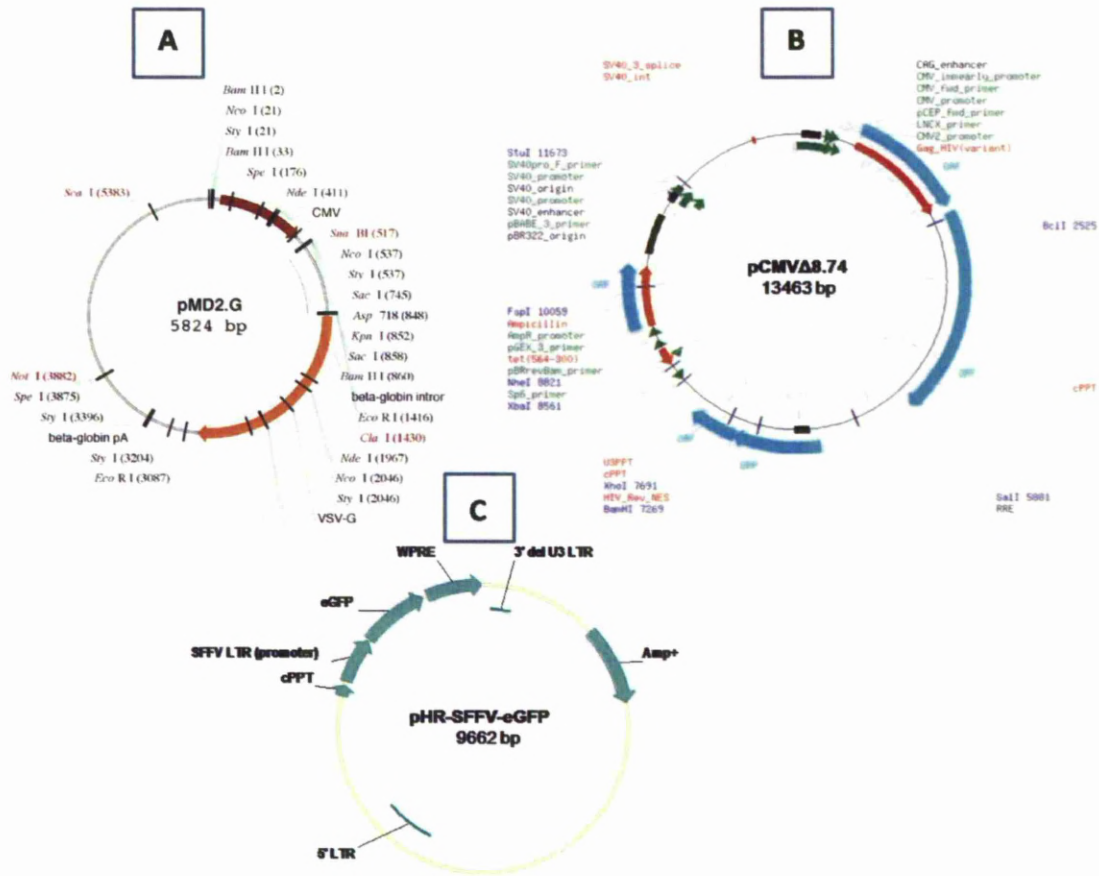

Figure 2.2. **Plasmids used for the transfection of the HEK 293T packaging cells.**

The plasmids used were pMD2.G (A), pCMVΔ8.64 (B) and pHR-SFFV-EGFP (C). The pMDG.2 plasmid contains the gene which encodes the envelope protein (vesicular-stomatitis-virus glycoprotein, VSV-G,), the pCMVΔ8.74 contains the genes gag (capsid protein) and pol (reverse transcriptase/ integrase activity) and the pHR-SFFV-EGFP plasmids contain an EGFP coding sequence which is

constitutively expressed under the control of the spleen focus-forming (SFFV) promoter (Restriction maps from Addgene, www.addgene.org).

2.6.2. HEK293T transfection

The packaging cell line HEK293T (provided by Dr Tristan McKay, University of Manchester) was triple transfected with the above plasmids using calcium phosphate precipitation. 12 X 10^6 HEK293T cells were seeded in a T175 ($175cm^2$) flask and kept O/N at 37°C, 5% CO_2. The following morning the three plasmids were added to a 50ml Falcon Tube containing 5ml DMEM (High Glucose, 4mg/ml), 25mM HEPES, 250µl $CaCl_2$ and the pH was adjusted to 7.1 with 1M HCl. The mixture was filtered with a 0.2µm filter (VWR) after pH adjustment and prior to plasmid addition. The amount of plasmids added were:

Plasmid	µg
pMG.2	17.5
pCMVΔ8.74	32.5
pHR-SFFV-EGFP	50

Table 2.1. **List of the plasmids used for the lentiviral production and their quantity for each HEK293T transfection.**

After plasmid addition, 3-4 gentle inversions of the tube followed and plasmids were left to incubate with $CaCl_2$ containing medium for 20min at RT. Medium from the HEK293T culture was removed and replaced with the medium containing the plasmids plus 20ml of 0.2µm filtered DMEM (High glucose) consisting of 10% FBS, 25mM HEPES whose pH was adjusted to 7.9 using 1M NaOH. Cells were left O/N at 37°C, 5% CO_2. The following day (Day 2), medium was discarded using Class 2 procedures and replaced with 20ml of HEK293T culture medium. Cells were kept O/N at 37°C, 5% CO_2. The next morning (Day 3) the 20ml of culture medium which contained the lentiviral particles was filtered through a 0.2µm pore size membrane (Sigma-Aldrich) in order to remove cell debris. Lentiviral supernatant was transferred to a Vivaspin 20 100kD MWCO filter tube (Sartorius Stedim, Epsom, UK) and centrifuged for 60min at 1500g at 4°C. The lentiviral supernatant was concentrated to a final volume of 300-500µl. The concentrated virus was aliquoted in 2 cryovials and kept at -80°C until further use.

2.6.3. Lentiviral transduction of embryonic mouse neurosphere cells

Embryonic mouse primary neurospheres after 2-3 weeks in culture in 60mm non adherent dishes were dissociated using 0.05% trypsin for 15 min at 37°C and mechanical agitation with a 1ml Gilson pipette. Single cells upon centrifugation at 150g were resuspended in 5ml of neurosphere culture medium and seeded into 60mm non adherent dishes. A viral aliquot was thawed from -80°C and transferred to the dish containing the single neurosphere cells. Virus was mixed with the medium by repetitive pipetting. Two days post-transduction, cell medium was discarded under Class 2 safety guidances and replaced with fresh neurosphere culture medium. After two weeks in culture $EGFP^+$ neurospheres of 100μm size were generated.

2.7. Formation of chimaeric neurospheres

$EGFP^+$ neurospheres 2-3 weeks old were dissociated. Single $EGFP^+$ neurosphere cells were counted and 5000 $EGFP^+$ cells were transferred to a small eppendorf tube together with an unlabeled neurosphere 2-3 weeks old. They were centrifuged in 150g for 5min and transferred at 37°C O/N. The next day, chimaeras had been formed inside the tubes. Using a 200μl Gilson pipette chimaeras were transferred to non adherent 96-well plate (Sigma-Aldrich) (1 chimaera/ well). Medium was changed every other day.

2.8. Flow cytometry

For the counting of $EGFP^+$ cells, labeled neurospheres were incubated with 0.05% trypsin for 15 min at 37°C and then centrifuged at 150g for 5 min. The suspension was discarded and neurospheres were resuspended in 1% (w/v) BSA/ PBS and dissociated as previously described. Single cells were counted and diluted with 1% BSA in a concentration of 10×10^5 cells/ ml. Large cell clumps were removed by passing the cell suspension through a cell strainer (VWR) before loading the cells in the flow cytometer. Settings: FSC=E00, SSC=371, FL1=333.

2.9. Statistical analysis

Graph plotting and unpaired two-tailed t-tests with confidence intervals of 95% were performed using the software GraphPad Prism 5.03 (GraphPad Software Inc., California, USA). Differences were considered statistically significant when p value< 0.05.

2.10. Image Software

- Adobe Photoshop was used for image cropping, resizing and colour channel overlay.
- Adobe Illustrator and Microsoft Office PowerPoint 2007 were used for figure-panel formation and orientation.
- ImageJ was used for cell counting on pictures of neurosphere sections and for measuring the distance of the most distal cell in explants and on adherent substrate as well as the measurement of neurite length.

2.11. Microscopy

For Image acquisition a range of different light and confocal microscopes were used.

Microscope	**Camera**
Leica DM IRB (inverted)	Leica DFC 420C
Leica Leitz DMRB (upright)	Leica DFC 420C
Leica M165 FC (dissection microscope)	Leica DFC 425C
Leica TCS SPE (confocal)	Integrated

Table 2.2. **List of microscopes and cameras used in the experiments.**

2.12. Molecular Biology

2.12.1. RNA extraction from neurosphere cells

Neurospheres were transferred to a 15ml falcon tube and centrifuged at 100g for 5 min. The supernatant was discarded, neurosphere cells were lysed in 1ml Trizol Reagent (Invitrogen) and transferred to a 1.5ml eppendorf tube. The tube was inverted gently 2-3 times. Then 200µl of chloroform was added and the mixture following vigorous shaking, was incubated at RT for 5 min. The cell lysate was centrifuged at 12000g for 15 min at 4°C. The top aqueous phase contained the RNA, the interphase DNA and the bottom one proteins and lipids. The RNA phase was transferred to a new 1.5ml eppendorf tube containing 20µg/ µl glycogen (Invitrogen) followed by 500µl isopropanol (Sigma-Aldrich). Samples were kept at -20°C O/N for higher RNA yield.

The next day the sample was centrifuged at 12000g for 10min at 4°C. RNA was visualized as a white pellet. The supernatant was discarded and the pellet washed with 75% ethanol in nuclease free water (Sigma-Aldrich) without disturbing the pellet. The sample was centrifuged at 4400g for 10min at 4 °C, ethanol was removed and the pellet was left to air-dry. The pellet was resuspended in 20µl of nuclease-free water. RNA concentration and RNA overall quality were assessed using a spectrophotometer

(Biophotometer, Eppendorf) and 1.5% agarose (Sigma) gel electrophoresis respectively (80V, 15min). RNA was kept at -20°C till further use.

2.12.2 DNAse treatment

Extracted RNA was diluted to a final concentration (200 ng/µl) using nuclease-free water. RQ1 DNase buffer (Promega, Southampton, UK) and (1 U/µl) DNase (Promega) were added in a volume of 1µl each. The mixture was incubated (2720 Thermal Cycler, Applied Biosystems, Warrington, UK) at 37°C for 30mins and the reaction was inactivated with 1µl of Stop Buffer (Promega) and a further 15min incubation at 60°C.

2.12.3. cDNA synthesis

The sample from the previous step was incubated at 65°C for 5 min in the presence of 1µl of 100ng/µl random examers (Abgene, Epsom, UK) and 1µl of 10mM dNTPs mix (Bioline Ltd, London, UK). The mixture was chilled on ice for at least 1 min. Then, 4µl of 5X First Strand buffer (Bioline), 1µl of 100 mM dithiothreitol (DTT) (Bioline) and 1µl of 200U/µl Superscript III reverse transcriptase (Promega) were added. The incubation protocol was as follows: 25°C for 5min, 50°C for 60 min and 70°C for 15 min. The synthesized cDNA was stored at -20°C in order to be used for a PCR template later on.

2.12.4. qPCR reaction

The mix of the PCR reaction consisted of 10μl KAPA-SYBR hot start master mix (KAPA BIOSYSTEMS, Luton, UK), 1μl of forward primer (10μM diluted in 1X Tris-EDTA, TE), 1μl of reverse primer (10μM diluted in 1X TE), 1μl of cDNA template and 7μl H_2O in order to reach a total volume of 20μl/reaction.

The PCR mixture was incubated as follows: denaturation at 95°C for 7min, 94°C for 5 sec, primer annealing at 62°C for 30 sec, primer extension at 72°C for 30sec and final extension at 72°C for 7min. The number of cycles was 40. The thermal cycler used was the Rotor-Gene RG-3000 (Corbett Research).

2.12.5. Agarose gel electrophoresis

PCR products (10μl) were mixed with 2μl loading buffer (Loading buffer III, Maniatis) and loaded to a 2% agarose gel in 1X Tris-acetate-EDTA (TAE) buffer with 0.5 μg/ml ethidium bromide. Gel products were visualized using a transilluminator (Geneflash, SLS).

2.13. Buffers

Phosphate buffered saline (1X)

- 8g of NaCl
- 0.2g of KCl
- 1.44g of Na_2HPO_4
- 0.24g of KH_2PO_4
- Total volume 1L dH_2O
- pH adjusted to 7.4 with 1M HCl

Tris-EDTA (TE) buffer, 10X

- 10mM Tris-Cl, pH 7.5
- 1mM EDTA
- pH adjusted to 8.0 with 1M NaOH

Tris-acetate-EDTA (TAE) buffer, 10X

- 48.4 g Tris Base (Sigma-Aldrich)
- 20 ml 0.5 M EDTA (Sigma-Aldrich)
- 11.42 ml glacial acetic acid (Sigma-Aldrich)
- pH adjusted to 8.0 with 1M NaOH

Loading buffer, 6X

- 0.25% Bromophenol blue
- 0.25% Xylene cyanol FF
- 30% glycerol
- Dilute 1:6 in 40% glycerol

2.14. Antibodies

2.14.1. Primary antibodies

Primary Antibody	Host	Dilution	Supplier
p75	rabbit	1:500	Abcam
GFAP	Rabbit	1:1000	Dako
GFAP	Mouse	1:500	Sigma
Sox10	Goat	1:100	Santa Cruz
Tuj1	Mouse	1:500	Abcam
S100	Rabbit	1:800	Abcam
NOS	Rabbit	1:800	Abcam
BrdU	Mouse	1:25	Dako
PGP9.5	rabbit	1:1000	AbD serotec

Table 2.3. **List of primary antibodies used in immunostaining.**

2.14.2. Secondary antibodies

All the secondary antibodies were supplied by Invitrogen and they were used in 1:1000 dilution in 2% BSA in PBS

Secondary Antibody	Host	Fluorophore (nm)
Anti-rabbit	Donkey	488
Anti-rabbit	Goat	488
Anti-rabbit	Donkey	594
Anti-mouse	Donkey	488
Anti-mouse	Donkey	594
Anti-goat	Donkey	568
Anti-goat	Donkey	488

Table 2.4. **List of secondary antibodies used in immunostaining.**

2.15. Primer sequences

Gene	Sequence	Amplicon size (base pairs)
hes1	F: 5'-GCACAGAAAGTCATCAAAGCC-3' R: 5'- TTGATCTGGGTCATGCAGTTG-3'	354
hes5	F: 5'- AGTCCCAAGGAGAAAAACCGA -3' R: 5'- GCTGTGTTTCAGGTAGCTGAC-3'	183
β-actin	F: 5'-CGTTGACATCCGTAAAGACC-3' R: 5'-CAGGAGGAGCAATGATCTTGA-3'	143

Table 2.5. **Sequences of the primers used in the qRT-PCR.**

CHAPTER 3

Neurosphere cell proliferation

3.1. Introduction

3.1.1. Aim

The aim of this chapter is to investigate the number and the location of proliferating cells in embryonic mouse gut neurospheres. Understanding the behaviour of enteric stem cells is a prerequisite to developing a cell-based therapy for Hirschsprung's disease (HSCR). In the following paragraphs the location of proliferating cells in the embryonic gut *in vivo*, as well as in gut-derived neurospheres *in vitro* is described.

3.1.2. Proliferating cells in the enteric nervous system

Proliferation of vagal neural crest-derived cells during embryonic life is one of the main forces that lead to the colonization of the gut by enteric NCCs resulting in formation of ENS (Simpson et al., 2007). The migratory wavefront consists of undifferentiated ENS progenitors whereas cells located rostrally differentiate towards the neuronal or glial lineage (Young et al., 1999; Young et al., 2003). When proliferation was investigated in embryonic bowel *in vivo*, over 40% of neural crest-derived cells were dividing along the migratory wavefront in both E11.5 and E12.5 mice as well as rostrally to the leading cells (Young et al., 2005), indicating a high proliferation capacity of ENS progenitors.

3.1.3. Isolation and propagation of ENS progenitors *in vitro*

At E11.5 mice the migratory wavefront which consists of the proliferating ENS progenitors is located at the caecum (Sidebotham et al., 2002; Druckenbrod and Epstein, 2005). In addition, in a study where E11.5 colon was dissected just distal to the caecum to include a few cells from the migratory wavefront, it was shown that just these few enteric NCCs were able to colonize the entire colon *in vitro* (Sidebotham et al., 2002) indicating the potential of caecal crest-derived cells at this developmental stage.

Cell sorting of enteric NCCs from embryonic rat bowel at E14.5, followed by clonal cell cultures showed that these cells contain stem cells as they can self-renew and give rise to glia, neurons and myofibroblasts (Bixby et al., 2002). Enzymatic dissociation of the caecum from E11.5 mice and under specific conditions in culture (described in Materials and Methods) allow enteric NCCs give rise to neurospheres (Almond et al., 2007). These aggregates contain both stem cells and their progeny as after multiple passaging they generate new neurospheres that contain glial and neuronal cells (Lindley et al., 2009). Neurospheres can also be generated from embryonic or neonatal human colon (Lindley et al., 2008; Metzger et al., 2009a, b) as well as neonatal mouse small intestine (Bondurand et al.,

2003). In addition, neurospheres can be generated from human gut mucosal biopsies derived from HSCR patients (Metzger et al., 2009a).

3.1.4. Cell proliferation in neurospheres

Experiments from different research groups have revealed a localization of dividing cells at the periphery of embryonic neurospheres derived from either E15.5 rat brain (Campos et al., 2004) or E11.5 mouse caeca (Almond et al., 2007). Due to the fact that these studies examined neurospheres straight after a single BrdU pulse (30min for CNS and 4h for enteric-derived neurospheres), it is still unknown whether these peripheral cells are the only dividing population or whether there are other slow dividing cells in different locations within the neurosphere. The slow dividing cells could be the stem cells which give rise to the proliferating cells at the periphery and to cells with mature phenotype.

On the other hand, when dividing cells in adult human gut neurospheres were stained using the marker BrdU continuously for 2 weeks, labeled cells were at the periphery and the centre of the neurosphere. However, the BrdU staining was not examined in neurosphere sections but in wholemount and as a result conclusions whether $BrdU^+$ cells are at the periphery or the centre could not be made (Metzger et al., 2009b). Thus, in order to resolve the ambiguities raised from previous work, a series of

experiments were designed which aimed to investigate the proliferation rate of cells in the neurosphere, their location and their behaviour over time.

3.2. Results

3.2.1. Generation of embryonic mouse neurospheres

Neurospheres were developed from dissociation of mouse embryonic caeca (E11.5) under non adherent conditions. In Fig.1 the location of the caecum (Fig. 3.1A and 3.1B) and the morphology of a typical neurosphere (Fig. 3.1C) after two weeks in culture are shown. All the neurosphere cells were positive for the marker p75 indicating their neural crest origin (Fig. 3.1D).

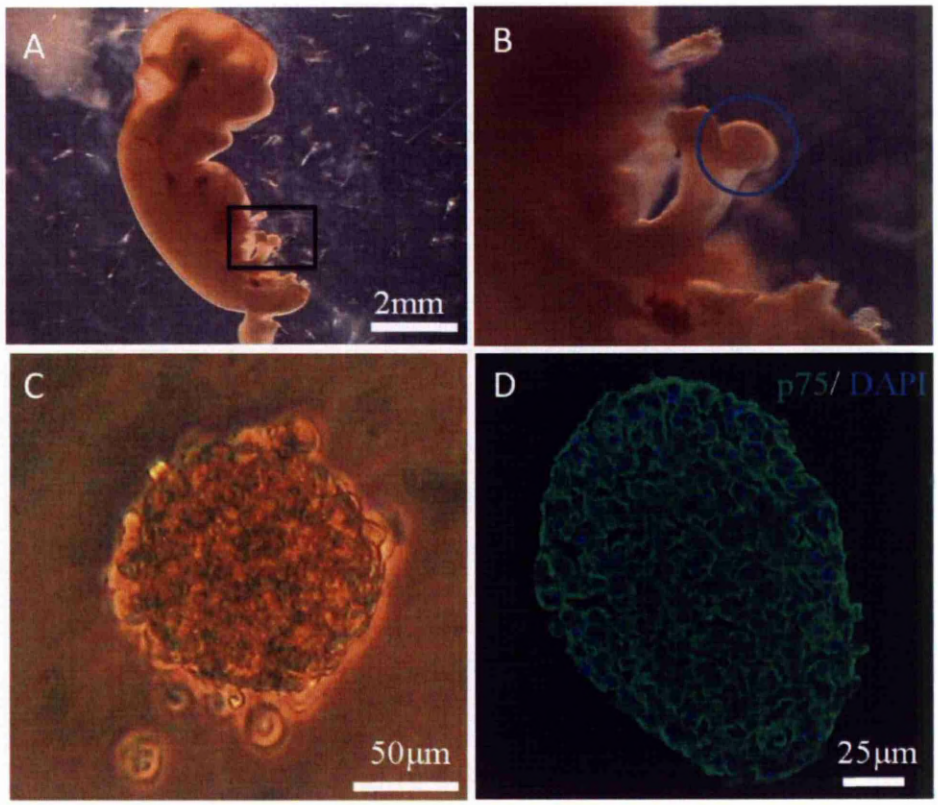

Figure 3.1. **Generation of embryonic mouse neurospheres from dissected caeca.**

Caeca were dissected from E11.5 mice and dissociated enzymatically as described in Materials and Methods (2.2). **A:** E11.5 mouse, **B:** higher magnification of the area defined by the square in A; blue ring indicates the location of caecum. **C:** Two week old primary neurosphere derived from dissociated caeca, **D:** immunostaining for the neural crest marker p75 in 8μm thick equatorial section of a 15 days old primary neurosphere. Nuclei stained with DAPI.

3.2.2. Cell proliferation in embryonic mouse neurospheres

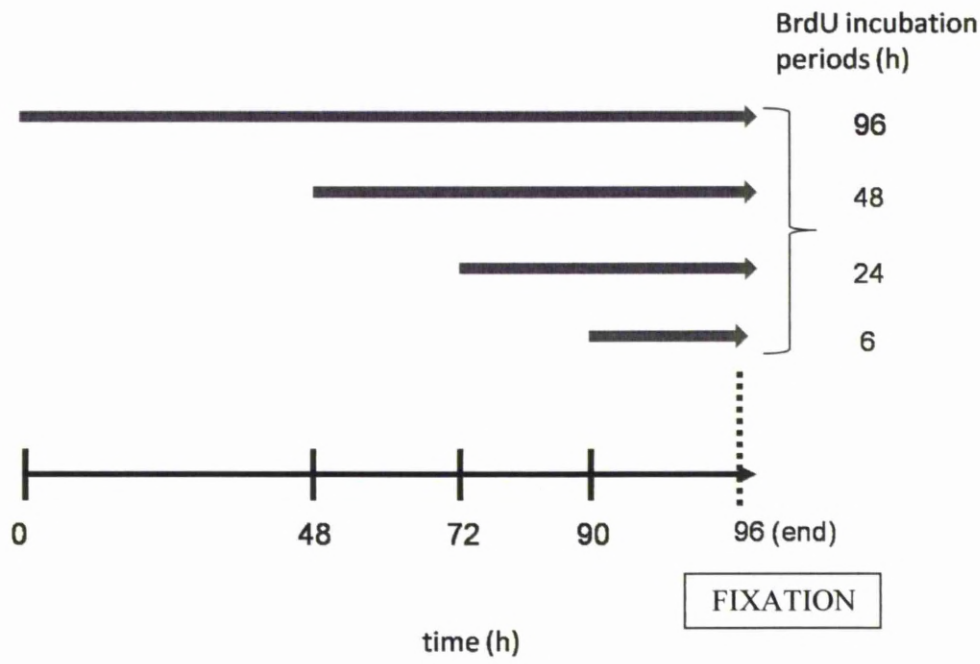

Figure 3.2. **Scheme for continuous labeling with BrdU of embryonic mouse neurospheres.**

Primary embryonic mouse neurospheres after 15 days of culture were aliquoted into 4 x 60mm suspension dishes (6-9 neurospheres per dish) and incubated in culture medium containing 10μM BrdU for 96h (0+96h with BrdU then fix), 48h (48h without+48h with BrdU then fix), 24h (72h+24h BrdU) and 6h (90h+6h BrdU) as shown in the diagram. After 96h the BrdU containing medium was removed from all the dishes, neurospheres were washed and processed for sectioning and immunostaining. The experiment was repeated twice.

When neurospheres were labeled continuously for 6h, BrdU positive nuclei were detected mainly at the periphery, although some were also present nearer to the centre of the neurosphere (Fig. 3.3E). After 24h labeling, the number of BrdU positive nuclei had increased and they were now randomly distributed throughout the neurosphere (Fig. 3.3F). This general distribution remained at 48 and 96 hours but the number of positive nuclei had obviously increased even more (Fig. 3.3G and 3.3H). The nuclei had similar but varying fluorescence levels irrespective of their location (Fig. 3.3m1 and 3.3m2, yellow and blue arrowheads).

Higher magnification after 6h continuous labeling shows that some of the BrdU positive nuclei were located exactly at the periphery of the neurospheres, whereas some of them were 1-2 cell layers deeper in the neurosphere (Fig. 3.3m1 and 3.3m2). The intensity of labeling of both peripheral and centrally located nuclei was variable and even after 96h continuous labeling there were nuclei located both centrally and peripherally that had not incorporated BrdU (Fig. 3.3H and 3.3I). Counts of BrdU labeled nuclei confirmed an increase from 16% at 6h to 82% after 96h continuous labeling (Fig. 3.4).

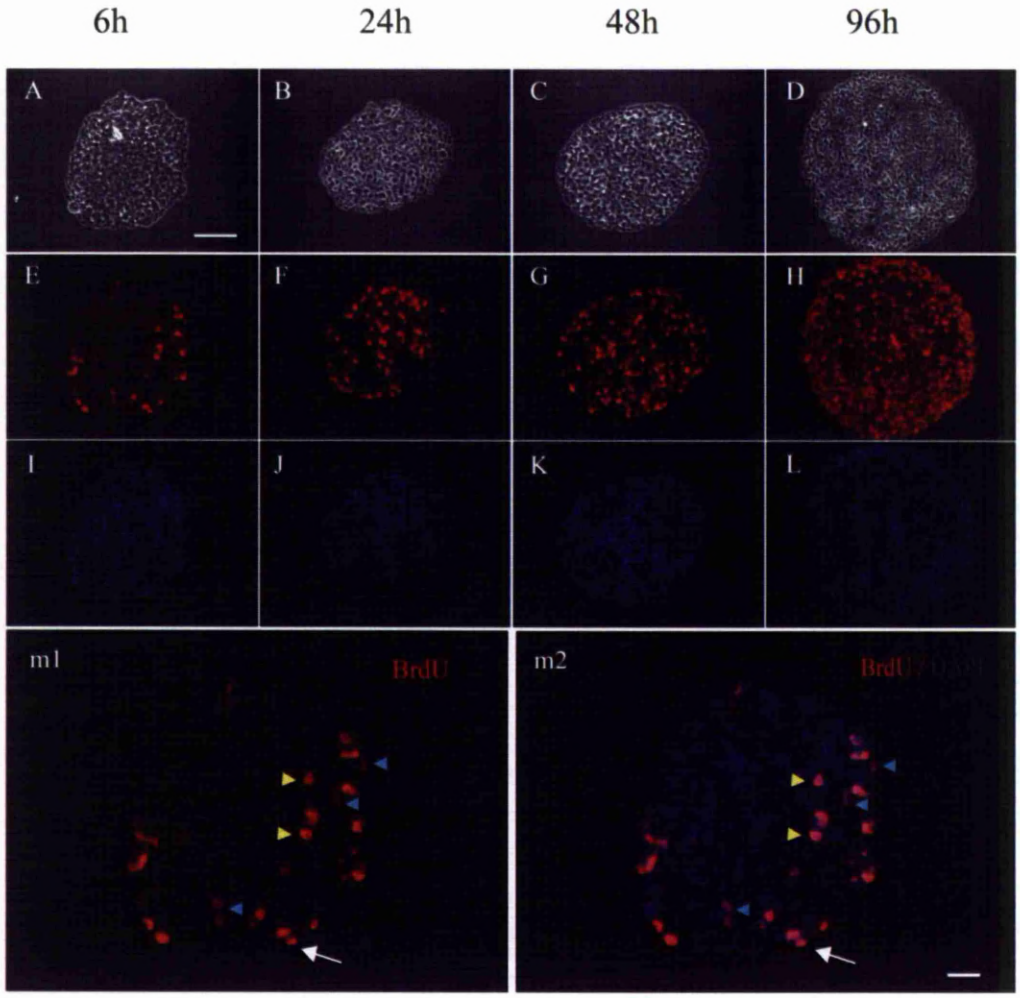

Figure 3.3. **Continuous labeling with BrdU in embryonic mouse neurospheres.** Immunostaining for BrdU in 8μm thick sections taken from the central region of neurospheres after different periods of continuous labeling with 10μM BrdU. **A-D**: phase contrast micrographs; **E-H**: BrdU immunostaining; **I-L**: nuclei staining with DAPI; **m1-m2**: higher magnification of Fig. E and Fig. I; $BrdU^+$ nuclei localized at the periphery (arrows) of the neurosphere or located more centrally (yellow

arrowheads). In both locations nuclei with similar BrdU levels were detected, however a few nuclei with lower BrdU levels could also be identified (blue arrowheads). Scale bar for A-L is 50μm and for m1, m2 is 25μm.

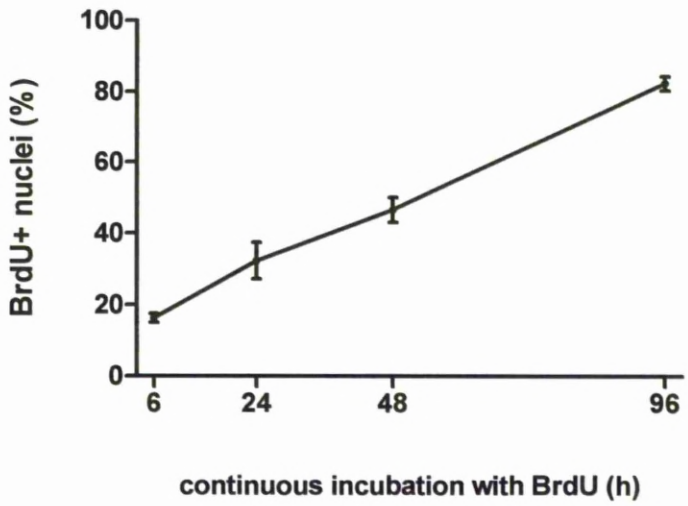

Figure 3.4. **Graph depicting the percentage of BrdU positive nuclei in neurosphere sections after different BrdU incubation periods.**

The number of BrdU positive and total DAPI stained nuclei was determined in sections cut across the centre of neurospheres (n= 6-9 neurospheres/ time point). The number of BrdU+ nuclei increased throughout the 96h continuous labeling with 10μM BrdU. Error bars represent range of the average of $BrdU^+$ nuclei counted in central neurosphere sections as calculated from 2 experiments.

In summary continuous labeling with BrdU indicates that there are differences in the behaviour of central and peripheral neurosphere cells which could be explained by differing rates of proliferation and/or migration of cells from the periphery to the centre of the neurosphere, or even rate of penetration of BrdU into the neurosphere (see Discussion, 3.3). In order to determine the reason for the differential labeling of central and peripheral cells it was therefore necessary to check which cells initially incorporated BrdU using a shorter labeling period, and to design a pulse-chase experiment to track the fate of proliferating cells.

3.2.3. Tracking of proliferating cells in embryonic mouse neurospheres

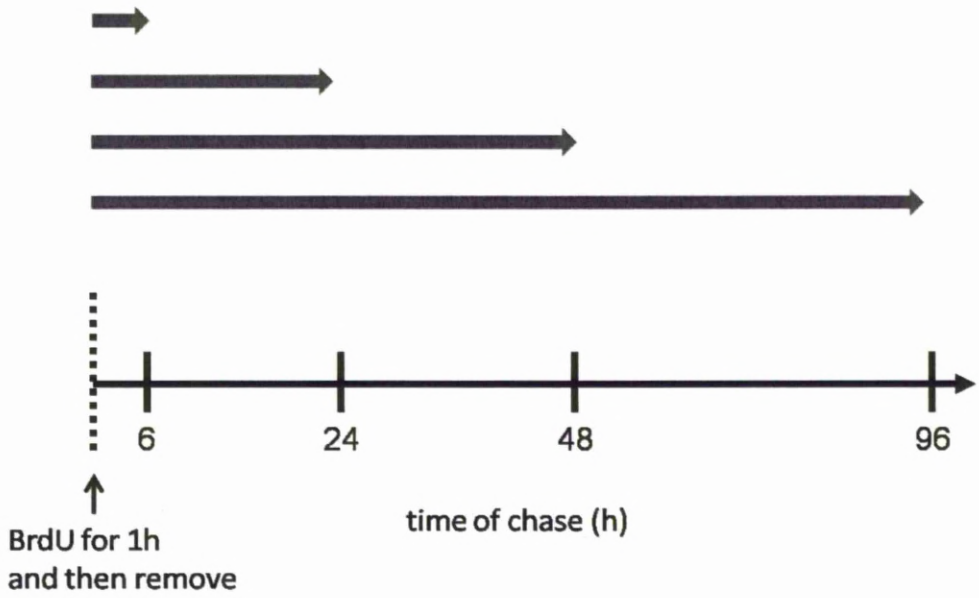

Figure 3.5. **Scheme for pulse/chase experiment with BrdU in embryonic mouse neurospheres.**

Primary embryonic mouse neurospheres after 15 days of culture were incubated with 10μM BrdU for 1h (pulse). At the end of incubation medium containing BrdU was removed, neurospheres (n= 5-13) were washed and fresh culture medium was added. Neurospheres were removed from culture at different time points (chase) as shown in the scheme and processed for sectioning and immunostaining in order to detect nuclei with incorporated BrdU. Each xperiment was repeated twice.

After 1h pulse with BrdU, labeled nuclei were restricted close to the periphery of the neurosphere (Fig. 3.6F). When BrdU was removed from the culture medium and neurosphere cells were chased for 6h, the majority of $BrdU^+$ nuclei were still located close to the periphery (Fig. 3.6G) but there was now a small increase in the number of labeled nuclei located more centrally.

After 24 (Fig. 3.6H), 48 (Fig. 3.6I) and 96h (Fig. 3.6J) of chase, $BrdU^+$ nuclei were randomly distributed in the neurosphere. However, after 48h and more evidently after 96h the strongly labeled cells were mainly located close to the centre of the neurosphere (Fig. 3.6p1, 3.6p2, white arrow), whereas weakly labeled $BrdU^+$ nuclei were observed mainly close to the periphery (Fig. 3.6p1, 3.6p2 yellow arrow). The percentage of cells with incorporated BrdU was increased after 6h (Fig. 3.7).

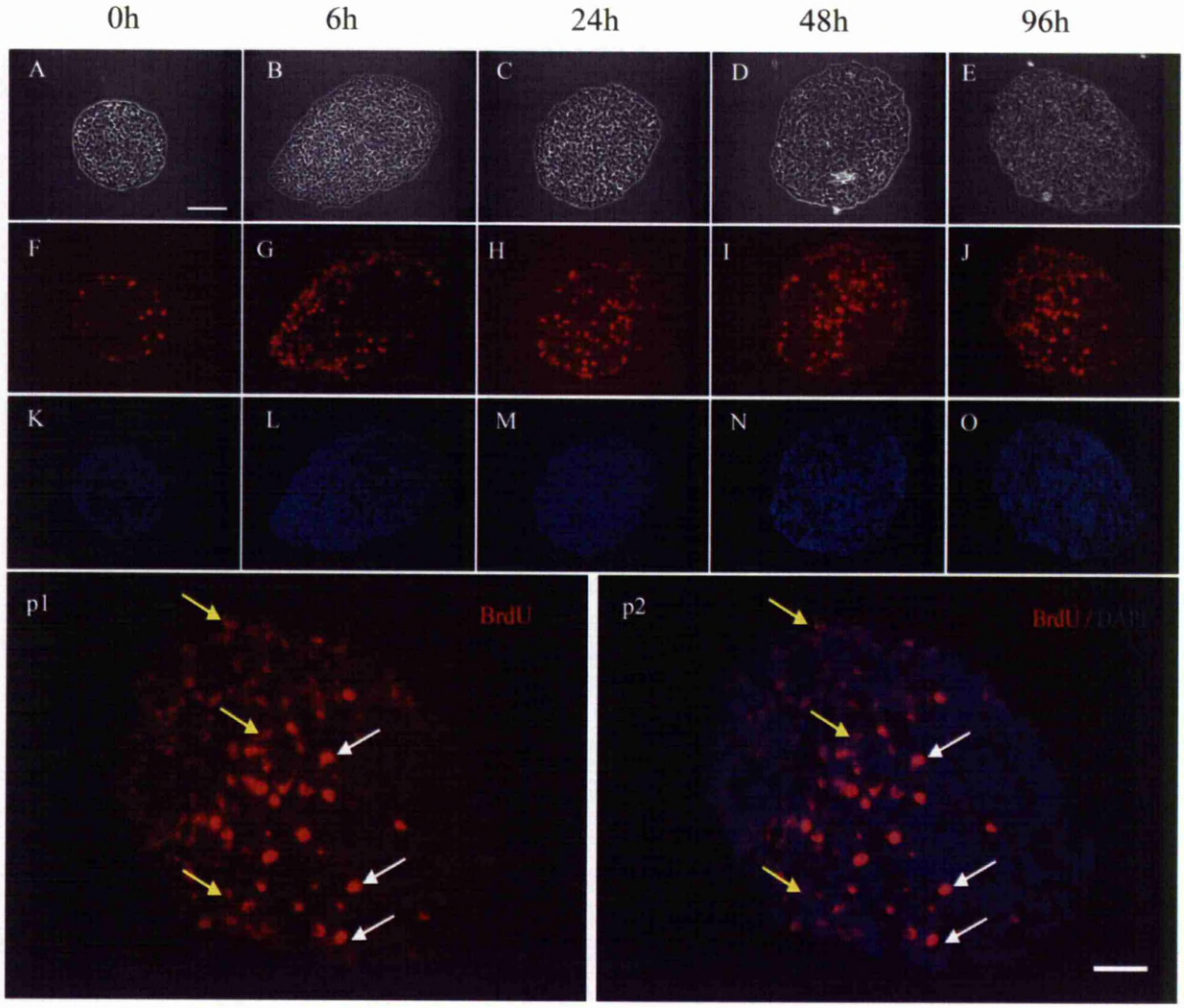

Figure 3.6. **Pulse/chase of BrdU labeled cells in embryonic mouse neurospheres.**

Primary embryonic mouse 15d neurospheres were pulsed with 10μM BrdU for 1h (A, F, K). Upon BrdU removal and washing, neurospheres were cultured for increasing times of chase (B-E, G-J, and I-O). Immunostaining for BrdU in 8μm thick sections taken from the central region of neurospheres. A-E: phase contrast

pictures; F-J: BrdU immunostaining; K-O: DAPI staining for nuclei; p1 and p2: higher magnification of Fig. J and Fig. O. After 4 days of chase nuclei with high (white arrows) and low BrdU levels (yellow arrows) could be easily distinguished. Scale bar for A-O is 50μm and for p is 25μm.

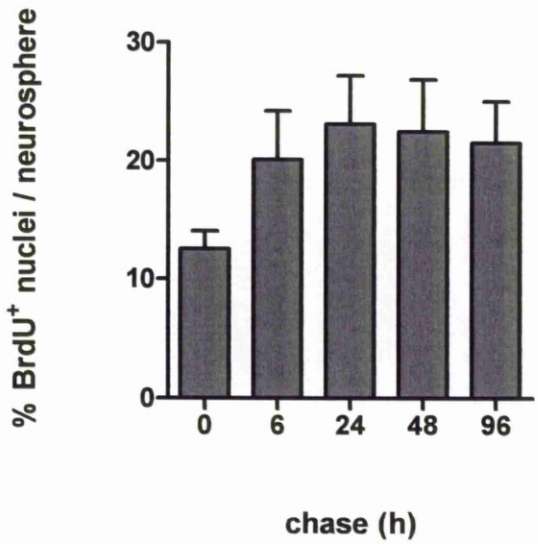

Figure 3.7. **Graph showing the percentage of BrdU$^+$ nuclei per neurosphere for each chase period.**

The number of BrdU positive nuclei was counted in 8μm sections cut across the central area of the neurospheres. The total number of nuclei in each section was counted after staining nuclei with DAPI. After pulse the number of BrdU positive nuclei initially increased. Each experiment was repeated twice. Error bars

represent range between 2 independent experiments. Number of neurospheres per time point: n= 7-13 for experiment 1 and n= 5-6 for experiment 2.

Cells which are proliferating rapidly will completely lose the incorporated BrdU over time. On the other hand cells which proliferated once during the pulse and stopped or proliferated at a slower rate will maintain BrdU labeling throughout the 96h chase. Therefore, the strongly labeled nuclei at the end of the chase (Fig. 3.6p1 and 3.6p2, white arrow), represent slow proliferating cells or cells which divide only during the 1h pulse and the weakly labeled ones (Fig. 3.6p1 and 3.6p2, yellow arrow), are cells which were dividing multiple times during the chase.

In order to quantify the presence of $BrdU^+$ cells closer to the centre of the neurosphere we divided the neurosphere section in concentric circles resulting in an inner and outer area of the neurosphere (Fig. 3.8). The counting showed that the ratio inner/outer of $BrdU^+$ nuclei was increasing over the time of chase indicating a movement of cells from the periphery towards the centre of the neurosphere (Fig. 3.9).

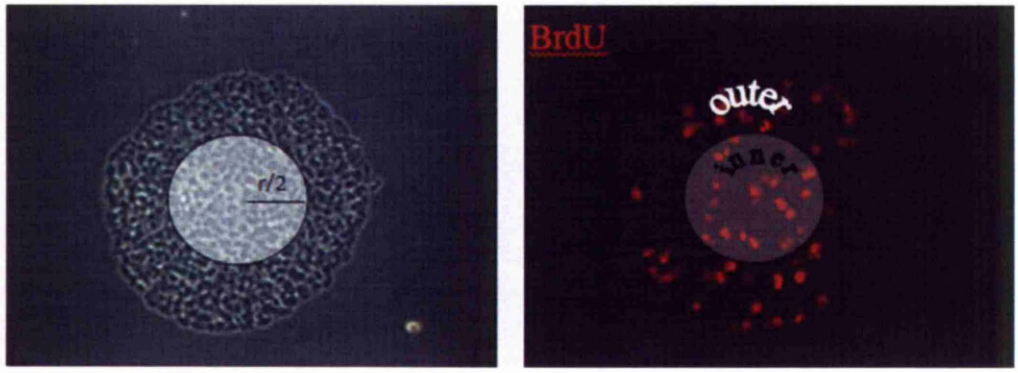

Figure 3.8. **Scheme showing subdivision of neurospheres for determination of the location of BrdU positive nuclei.**

Labeled nuclei were counted in two domains of the neurospheres: an inner area which represented a circle with half the radius of the whole neurosphere ($\pi r^2/4$) and an outer area which represented the space between the peripheral boundaries of the neurosphere and the inner area ($3\pi r^2/4$), as shown in the figure. The pictures shown are from an 8μm thick section of the central region of a neurosphere immunostained for BrdU 24h after the pulse.

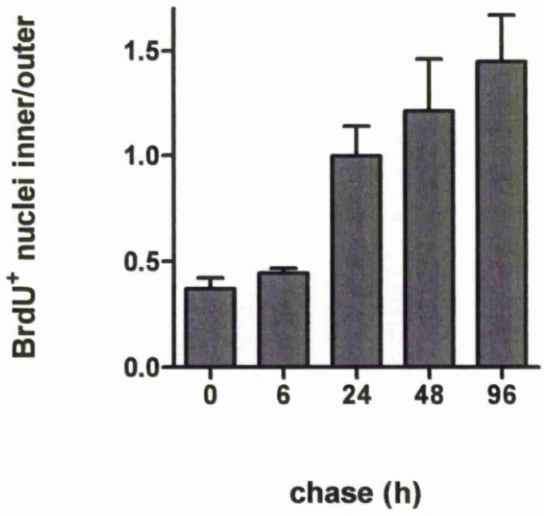

Figure 3.9. **Graph depicting the ratio of inner/outer BrdU$^+$ nuclei per neurosphere after increasing chase periods.**

The number of cells inside the inner area has been multiplied by 3 in order to normalize the areas measured. The number of BrdU$^+$ nuclei was counted in equatorial sections of neurospheres. The ratio inner to outer of BrdU labeled nuclei increased over time of chase. Error bars represent the range between 2 independent experiments (number of neurospheres = 7-13 for experiment 1 and n= 5-6 for experiment 2).

The pulse-chase experiment is consistent with the hypothesis that there is a movement of cells from the periphery towards the inside of the neurosphere. This movement could be passive due to the pushing from the peripheral cells due their higher proliferation rate, or it could be an active migration where cells develop processes and migrate in the inside of the neurosphere. In order to confirm that there is a movement either passive or active we designed an experiment with chimaeric neurospheres consisting of an already formed neurosphere in combination with EGFP expressing neurosphere-derived cells. The aim was to see whether the $EGFP^+$ cells would be able to mix with the unlabeled neurosphere cells.

Generation of $EGFP^+$ neurospheres is described in Materials and Methods (2.6.3.). When unlabeled peripheral neurospheres cells were covered with a cell suspension of neurosphere-derived $EGFP^+$ cells, their location in the chimaera switched from peripheral to central. After the first day of the chimaera formation its shape was irregular where the labeled cells had been added (Fig. 3.10A). After 4 days in culture the whole chimaera had a more spherical shape with $EGFP^+$ cells occupying one hemisphere and the unlabeled neurosphere the other one (Fig. 3.10B). Sections cut across the centre of the chimaera showed that a low number of single $EGFP^+$ cells had migrated into the unlabeled area of the chimaera and some of them had distinct processes (Fig. 3.10C, arrow). When chimaeras were labeled

for 1h with BrdU after 4 days in culture, immunostained sections showed that $BrdU^+$ nuclei were in both EGFP labeled and unlabeled cells located at the periphery of the chimaera. $BrdU^+$ nuclei were not present at the remaining interface of labeled and unlabeled cells of the chimaera (Fig. 3.10D).

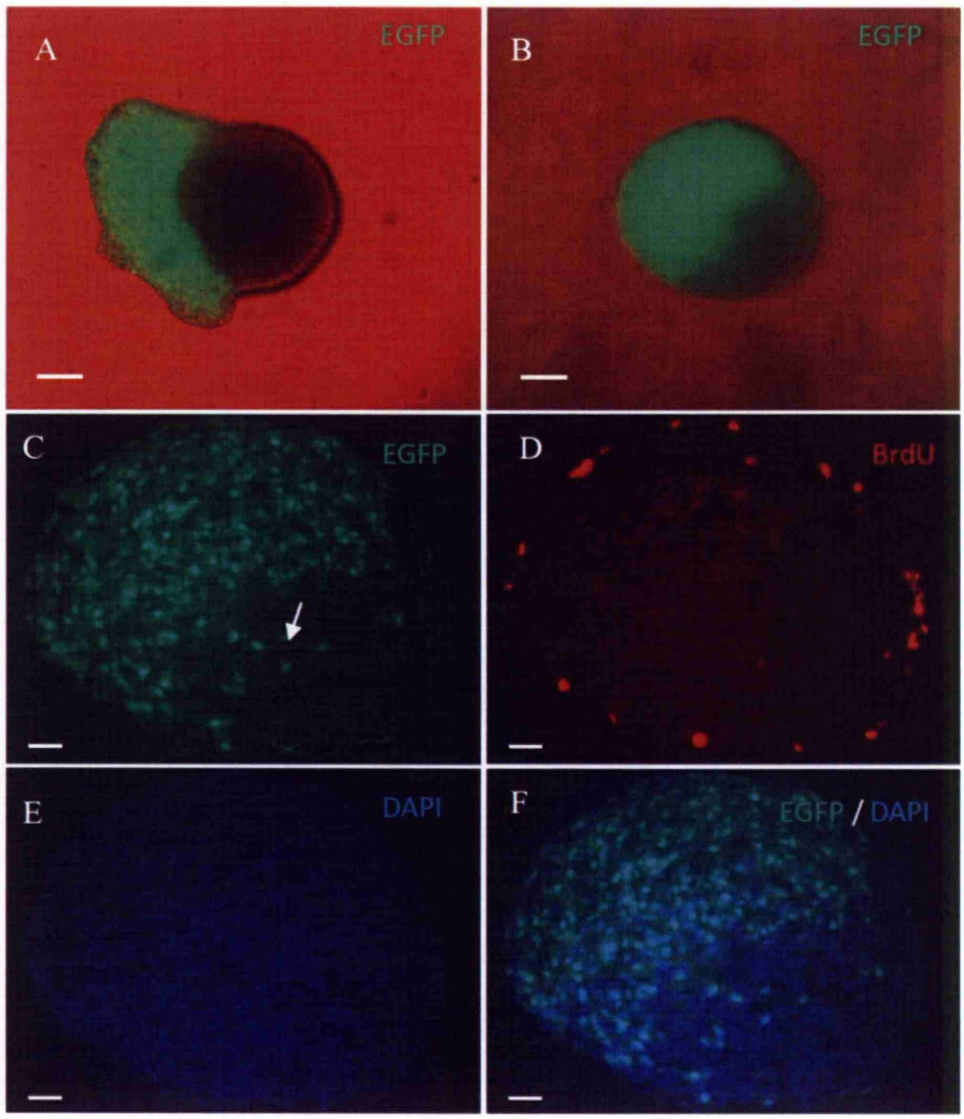

Figure 3.10. **Formation of chimaeras containing EGFP labeled neurosphere-derived cells and unlabeled neurospheres.**

Single $EGFP^+$ positive cells derived from 2-3 week old $EGFP^+$ neurospheres were combined by centrifugation with 2-3 week old unlabeled neurospheres in order to

form chimaeras and cover with two distinct segments. Whole mount pictures after 1 day in culture (A) show that $EGFP^+$ cells were situated at the side of the unlabeled neurosphere. After 4 days in culture, the shape of the chimaera was spherical (B). Sections 8μm thick at 4 days (C- F) showed that some $EGFP^+$ cells had migrated into the region occupied by the unlabeled cells and some had developed long processes (C, arrow). After short incubation for 1h with BrdU (D), $BrdU^+$ nuclei were identified at the periphery of the chimaera but no $BrdU^+$ cells were present at the interface between labeled and unlabeled cells. Each experiment was repeated twice. Scale bar 100μm for A-B and 25μm for C-F.

The fact that there were no $EGFP^+$ cells labeled with BrdU after 1h incubation in the centre of the chimaera implies a reduction and/or inhibition of the proliferation in these cells, as they were derived from dissociated $EGFP^+$ neurospheres containing both peripheral and central cells. Moreover, the side of the unlabeled neurosphere which wasn't covered by $EGFP^+$ cells had $BrdU^+$ nuclei at the periphery whereas the side which was covered didn't have any $BrdU^+$ nuclei.

These data support the hypothesis that peripheral cells can stop or slow down their proliferation rate when they are located closer to the centre of the neurosphere. Furthermore, the integration of $EGFP^+$ cells in the unlabeled neurosphere indicates that neurospheres are complex and dynamic systems where cells have the ability to migrate inside them.

The above experiments raise the question whether there is a phenotypic difference between the $BrdU^+$ cells at the beginning of the chase with the ones at the end of it, as there were differences in their location and BrdU incorporation.

3.3. Discussion

In this chapter we tried to answer questions regarding the location of the proliferating cells in an embryonic mouse gut neurosphere and what is their fate over time. We concluded that fast dividing cells are located at or close to the periphery of the neurosphere and over time some of them move/migrate towards the centre which could result in inhibition or reduction of their proliferation rate.

3.3.1. Cells closer to the periphery of the neurosphere divide faster.

Our data suggest that the neurosphere cells which are located at the periphery, or a few cell layers beneath the surface, are proliferating faster than the ones closer to the centre. The possibility that this result could be an artifact due to inadequate penetration of BrdU seems unlikely. This is because a gradient in the signaling of BrU^{+} cells after a short pulse was not observed. Also, some cells which were a few layers deeper from the periphery sometimes had more incorporated BrdU compared to others at the periphery. In addition, neurospheres at the end of the chase had strongly BrdU labeled cells close to the centre whereas cells at the periphery were weakly labeled, consistent with a faster proliferation rate at the periphery (Fig. 3.6). It could be argued that cells with low BrdU levels after the chase could be cells which were entering the S-phase at the end of the pulse and then stopped proliferation, therefore the BrdU

incorporation is low after 4 days. However, most of the cells with low BrdU at the end of the chase, had actually lower levels that what observed after the pulse implying that they proliferated over the period of chase.

Previous groups have also identified proliferating cells at the periphery of neurospheres derived from E11.5 embryonic mouse bowel (Almond et al., 2007) and E14 embryonic mouse forebrain cells (Santos et al., 2011). In addition, in neurospheres derived from neonatal rat brain, cells positive for the proliferation marker Ki-67 (Gerdes et al., 1983), which is expressed in the nucleus of cells which are in G1, S, G2 and M phase but not G0, had peripheral localization (Andersen et al., 2011) supporting the data obtained from our BrdU experiments. The fact that fast dividing cells are located closer to the periphery could be explained by inadequate penetration of nutrients in the inner layers of the neurosphere.

Also a closer look to a neurosphere section after pulse shows a variation of BrdU labeling (Fig. 3.3m1). That could be explained due to the fact the BrdU is incorporated only in the nuclei of cells which are through the S-phase of their cycle (Kee et al., 2002) thus, if during the pulse a cell is just entering the S-phase its nucleus will incorporate more BrdU than a cell which is exiting the S-phase. Also, it has been suggested that BrdU could be incorporated in nuclei which undergo DNA repair which requires DNA

synthesis (Rakic, 2002). However, labeling for BrdU together with other proliferating markers such as Ki-67 showed that $BrdU^+$ cells also express Ki-67 soon after labeling, whereas $BrdU^+ki\text{-}67^-$ nuclei were not present, failing to make a correlation between BrdU incorporation and DNA repair (Cooper-Kuhn et al., 2002).

3.3.2. A subpopulation of BrdU labeled cells stops proliferating over time

The number of $BrdU^+$ nuclei increased over time and their distribution became even throughout the neurosphere (Figs. 3.3 and 3.4). After 96h of labeling, almost all the cells in the neurosphere were $BrdU^+$. Also, the increase in the percentage of $BrdU^+$ cells with time is linear (Fig. 3.4, not analyzed statistically) indicating that the $BrdU^+$ cells were derivatives of one cell population which was proliferating just at the beginning of the experiment. However, to support this hypothesis it has to be assumed that all the cells are proliferating with the same rate and continuously until the end of the experiment. If that continuously dividing population was mixed with other cells which started proliferating the pulse, the line of the graph would have a sigmoid shape. However, it has been shown previously that ENS neurospheres contain terminally differentiated cells (Almond et al., 2007) implying that the population of proliferating progenitors contains a

subpopulation which differentiates towards a mature neuronal phenotype and stops proliferating (Ishizaki, 2006).

Thus, the most likely explanation which can account for the linear increase in the percentage of $BrdU^+$ cells (Fig. 3.4) is that over the duration of the experiment some of the cells with incorporated BrdU either slow down or stopped their proliferation and differentiate (see results and discussion in chapter 4) whereas other cells keep proliferating. This is consistent with what was shown at the end of chase where there were weakly and strongly BrdU labeled cells (Fig.3. 6).

3.3.3. Movement of peripheral cells towards the centre of the neurosphere

Results from the pulse/chase experiment suggested that peripheral cells, upon proliferation, end up towards the centre of the neurosphere. As shown in Fig. 3.9 the inner/outer ratio of $BrdU^+$ cells is increasing over time further supporting the above conclusion. If cells were not moving towards the centre the result at the end of the chase would be a $BrdU^-$ neurosphere core surrounded by $BrdU^+$ cells organized in multiple layers resembling a stratified epithelium like the oesophagus (Alyassin and Toner, 1977), something that we did not observe.

This cell behaviour is comparable to what is happening in vivo in the subependymal zone (SEZ) of the lateral ventricles in adult mouse brain where progenitors proliferate in the SEZ and then migrate away from the ventricle (Kazanis et al., 2010). Results from the chimaeric neurosphere experiment (Fig. 3.10) also suggested a migration of peripheral $EGFP^+$ cells towards the inside of the neurosphere implying that the neurosphere periphery could resemble the subependymal zone.

3.3.4. Cell location in neurosphere affects proliferation rate

Cells which are closer to the periphery of the neurosphere divide faster as demonstrated by the long $BrdU^+$ incubation and pulse/chase experiments. Also at the end of the chase we observed cells with high levels of incorporated BrdU located closer to the centre implying that these cells which migrated away from the periphery either stopped proliferation or slowed it down. However, a closer look at neurosphere sections at the end of chase (Figs. 3.6p1 and 3.6p2) shows the presence of some BrdU strongly labeled cells very close to the periphery and some weakly labeled ones in the centre of the neurosphere making it difficult to make a definite correlation between location in the neurosphere and proliferation rate. That could be because, there is always the possibility that cells with incorporated BrdU straight after the pulse either stop proliferating or divide multiple times before they move towards the centre of the neurosphere or

stay at the periphery. It has also been shown in embryonic mouse gut explants at E10.5 and E11.5 (Hao et al. 2008), that immature neurons can still migrate but at lower speeds than undifferentiated migratory enteric-crest derived cells (Druckenbrod and Epstein, 2005).

The experiment where we used chimaeric neurospheres with $EGFP^{+}$ cells (Fig. 310) cleared any ambiguities regarding the effect of neurosphere location and cell proliferation rate. Data suggest that when cells are losing their peripheral location and they get close to the centre of the neurosphere their proliferation rate is decreasing or it stops and exactly the opposite effect happens to cells which are exposed to the periphery (Fig. 3.11)

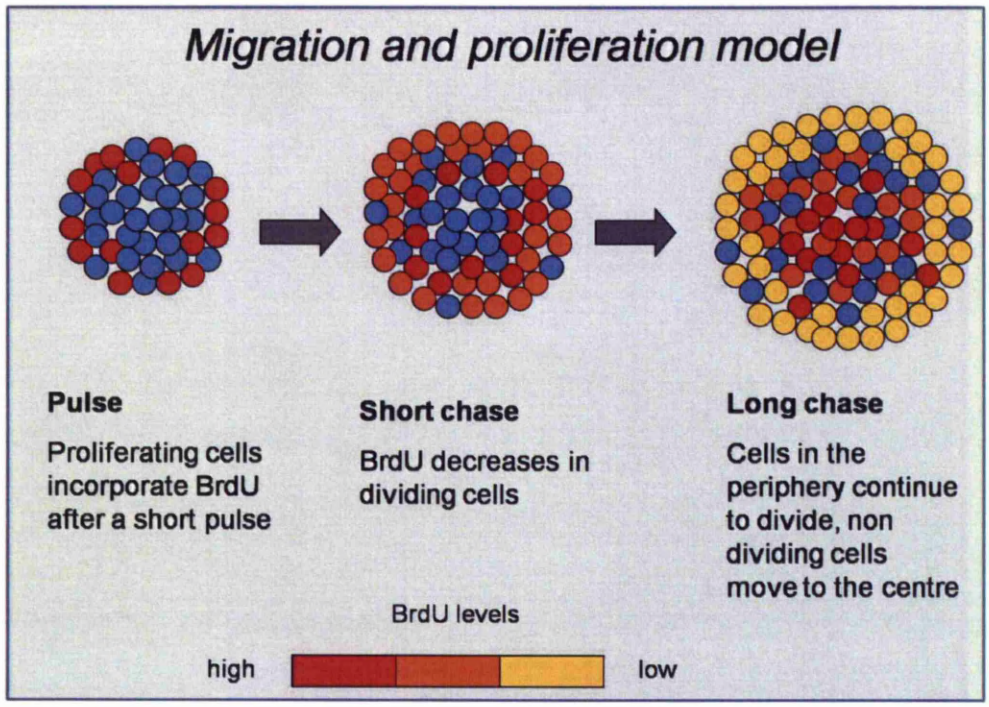

Figure 3.11. **Scheme describing the fate of peripheral dividing cells in the neurosphere.**

3.3.5. Conclusions

Neurospheres constitute a dynamic environment consisting of cells with different proliferation rates and migratory capacities. Peripheral cells divide faster than the ones closer to the centre and they can migrate in central neurosphere locations which have an effect on their proliferation rate. The neurosphere location might represent differences in the concentration of nutrients as large molecules might not reach the centre of the neurosphere. Moreover, activation or inactivation of signaling pathways such as Notch which are controlled by cell-cell contact can play a very important role in the proliferation and differentiation of neurosphere cells and especially those cells located at the periphery as they may have few cell-cell contacts.

CHAPTER 4

Neurosphere cell differentiation

4.1. Introduction

4.1.1. Aim

The experiments described in the previous chapter showed that neurosphere cells differed in their proliferation rate according to their location and also their position could change within the neurosphere over time. Briefly, neurosphere cells located at the periphery or close to it were proliferating faster compared to the cells which were residing at the centre. Moreover, cells which were dividing at the periphery could migrate towards the neurosphere centre while their proliferation rate decreased or stopped, whereas cells remaining at the periphery kept proliferating in faster rates.

Having analyzed cell proliferation in neurospheres the next step was to investigate the locations of cells expressing markers for progenitors and more mature neural cell phenotypes in the neurospheres, in order to identify any correlations between proliferation and differentiation. In the following text background information is given about the markers used and also their localization in the neurospheres.

4.1.2. Phenotypic markers of neural crest-derived cells in the gut

p75

The low affinity neurotrophin receptor p75 is a transmembrane protein which has been used to identify cells of neural crest origin in the bowel (Chalazonitis et al., 1998) as well as in gut-derived neurospheres (Almond et al., 2007; Metzger et al., 2009a and b). During development p75 is expressed in pre-enteric vagal neural crest cells and it is present in all the migratory ENS progenitors during bowel colonization (Young et al., 1999). It is also present in cells expressing the glial marker B-FABP and the marker S100B (Young et al., 2003).

Sox10

The transcription factor Sox10, which has been described in a previous chapter in detail (1.8.1.), is expressed in uncommitted ENS progenitors and enteric glial cells (Kim et al., 2003). During ENS formation, Sox10 is expressed in all the enteric NCCs at the migratory wavefront. It is not present is enteric neurons (Young et al., 2003). In addition, Sox10 is expressed in Schwann cells, melanoblasts as well as in oligodendrocyte progenitors where it is essential for their maturation (Wegner et al., 2005).

Tuj1 and NOS

The class III β-tubulin, Tuj1, is one of the earliest neuron- associated proteins expressed during mammalian development (Katsetos et al., 2003). In both chick and mouse, Tuj1 is expressed immediately before or after the final mitosis in almost all developing neurons (Dennis et al., 2002). It has been shown to be present early in the ENS as it is detected in transiently expressing tyrosine hydroxylase migratory cells at E11.5 (Hao et al., 2008) whereas nitric oxide synthase (NOS) is detected at E12.5. NOS catalyzes the production of nitric oxide from L-arginine. Nitric oxide is secreted by inhibitory motor neurons of the gut upon stimulation resulting in the relaxation of the smooth muscle, a Ca^{2+}-dependent process, and thus regulating the peristalsis of the bowel (Brookes, 1993). Due to the fact that Tuj1 and NOS are early neuronal markers and not transiently expressed they were selected for investigation of the neurospheres in this study.

GFAP and S100

The intermediate filament protein GFAP and the calcium binding protein S100B have been used by previous research groups to stain enteric glia (Bondurand et al., 2003; Young et al., 2003). However, in the CNS the role and expression of these proteins has been studied in more detail than in ENS. In adult CNS, dividing $GFAP^{+}$ cells are the precursors of neurons in the subependymal zone (SEZ) of the lateral ventricle and the subgranular

zone (SGZ) of the hippocampal dentate gyrus (Garcia et al., 2004). The protein S100 consists of dimers of alpha and beta subunits (Kligman et al., 1986). Heterodimers αβ form the protein S100A1 which is present in cardiomyocytes, skeletal muscle cells, renal cells and salivary epithelial cells (Rosario et al., 1999). On the other hand, homodimers ββ form the protein S100B which is abundant in glial cells of both central and peripheral nervous system, Schwann cells (Turker et al., 2011), adipocytes, melanocytes and chondrocytes (Rosario et al., 1999). Moreover, it was present in motor neurons of newborn rat brains (Iwasaki et al., 1997) and it was also expressed by a sub-population of cholinergic neurons in adult rat brain (Yang et al., 1996; Rickmann et al., 1995). In the CNS, S100B is also expressed in mature astrocytes (Platel et al., 2009), and in oligodendrocyte precursor cells (Deloulme et al., 2004). During embryonic brain development radial glial cells, progenitors of both neurons and glia, also co-express S100B and GFAP (Namba et al., 2005).

4.1.3. Localization of phenotypic markers in neurospheres

Depending on the methodology used to propagate neurospheres in vitro as well as the origin of the tissue which it is dissected from, the abundance and location of different phenotypic markers vary (Prajerova et al., 2009; Andersen et al., 2011). Immunoreactivity for p75 in sections of embryonic mouse and human neonatal colon derived neurospheres as shown by Almond et al. (2007) was found in all the neurosphere cells indicating the purity of the neurosphere in terms of its neural crest origin. In another study where cells were isolated from small and large intestine of adult humans, expression of p75 was only observed in a small number of neurosphere cells without a particular localization pattern (Metzger et al., 2009b). Also the culture conditions that the second group used involved coated substrates with fibronectin, laminin and poly-L-ornithine whereas Almond et al. used non-adherent conditions. This indicates the importance of the culture conditions and origin of tissue and how that can affect the interpretation of the results. When not all cells are $p75^+$, potentially there are cells of mesodermal origin in the neurosphere, because in the bowel, p75 is only expressed in cells of neural crest origin (Young et al., 1999).

In neurospheres derived from neonatal P0 rat forebrain $GFAP^+$ and $Tuj1^+$ cells were localized mostly in the centre (Campos et al., 2004). Central location of GFAP was also observed in rat subventricular-zone derived

neurospheres although Tuj1 immunoreactivity occured close to the periphery in that case (Andersen et al., 2011). In neurospheres derived from E12.0-E12.5 mouse telencephalon, Tuj1 immunoreactivity was detected only at the periphery (Prajerova et al., 2009). The topological differences of Tuj1 among the results demonstrated by different groups, imply once more the great influence of the origin of tissue and/or the propagation technique on the results.

For the markers S100, Sox10 and NOS there is not much literature demonstrating their presence in neurospheres. However where investigated S100 was present in few cells randomly distributed in the E11.5 mouse colon-derived neurosphere or cells were mainly located in the centre of neonatal human colon-derived neurospheres (Almond et al., 2007). Immunoreactivity for Sox10 in human postnatal gut neurospheres was present in a small number of cells located at the periphery and the centre of the neurosphere (Metzger et al., 2009b) whereas NOS immunoreactivity seemed to be stronger closer to the periphery (Almond et al., 2007), suggesting that cells expressing neuronal markers are closer to the periphery of the neurosphere.

The difference in the age and origin of the tissue that is used to generate neurospheres as well as the different culture conditions can influence the

expression and location of phenotypic markers, thus making it difficult to compare results between different research groups. Therefore, we decided to adapt the protocol that had been used before in our lab by Almond et al. (2007) where it has been shown that all the neurosphere cells are of neural crest origin. Also we tried to quantify neurosphere cells expressing different markers by dissociating neurospheres and seeding single cells on tissue culture substrate for a short period, just long enough to attach and then fix and stain them for various markers. The identification and quantification of the phenotypic markers will give us insight of a light of the cell types in a neurosphere and how are they compared with cells *in vivo* in order to get a better understanding of their behaviour.

4.2. Results

In this chapter we were interested in identifying the phenotypic profile of embryonic mouse-derived neurospheres, as well as to quantify and examine marker co-expression in single cells. In addition, as shown in Chapter 3, the fast dividing cells were located at the periphery of the neurosphere and over time their behaviour in terms of proliferation rate and location in the neurosphere changed. Therefore, we wanted to see what is the phenotype of these fast dividing cells and what is their fate over time.

4.2.1. Differentiation of cells in embryonic mouse neurosphere

Immunostaining was done in sections cut through the equator of neurospheres in order to be able to see cells both at the periphery and in the centre of the neurosphere on the same sections. In order to locate the equator, neurospheres were cut in serial sections and the ones where the neurospheres had the greatest diameter were considered as equatorial sections.

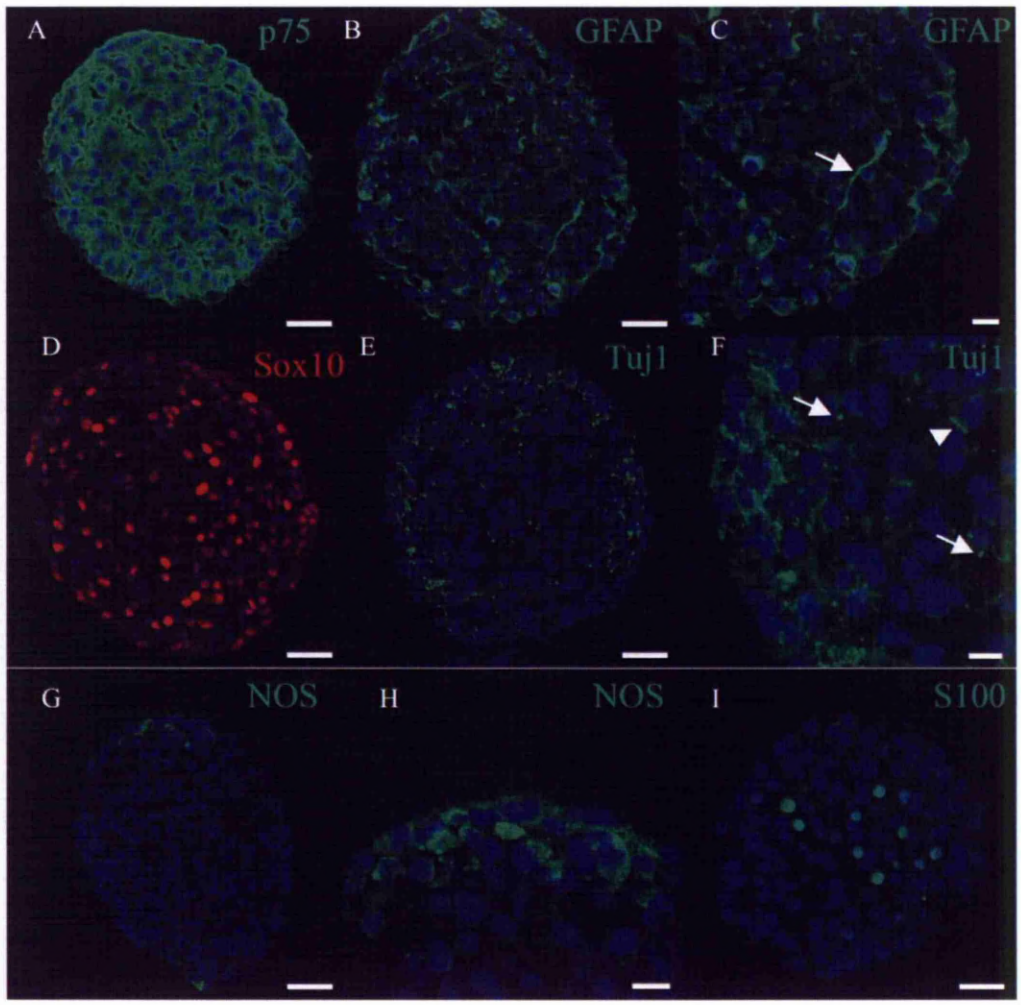

Figure 4.1. **Confocal images of phenotypic markers in embryonic mouse neurospheres.**

Primary embryonic mouse neurospheres after 15-19 day culture in 60mm non adherent dishes, were frozen and sliced in 8μm sections. Equatorial sections of neurospheres were selected, fixed and immunostained for the markers p75 (A),

GFAP (B, C), Sox10 (D), Tuj1 (E, F), NOS (G, H) and S100 (I). Figures C, F and H are higher magnifications of B, E and G respectively. Arrow in C indicates a strongly labeled cell process for GFAP. In F arrow and arrowhead indicate $Tuj1^{+}$ fibers either in vertical or horizontal plane respectively. Nuclei were stained with DAPI (blue). Scale bar is 10μm for C, F, H; 100μm for I and 25μm for the rest.

All the neurosphere cells are of neural crest origin as the marker p75 was expressed by all the cells (Fig. 4.1A). The glial marker GFAP was expressed in a high number of cells (Fig. 4.1B). Positive cells with fiber-like shape were observed throughout the neurosphere. It was difficult to quantify the number of GFAP positive cells, as the $GFAP^{+}$ cell processes were surrounding other cells and the intensity of labeling varied between cells (Fig. 4.1C arrow). However a similar distribution pattern in terms of cell location was observed for the progenitor and glial marker Sox10 (Fig. 4.1D) and because the Sox10 labeling was more clear-cut and restricted to nuclei, it was apparent that not all cells were immunopositive for Sox10. Nevertheless it could also be observed that some nuclei had a weaker Sox10 signal than others, implying that some of them could be differentiating towards the neuronal lineage (Young et al., 2003). The marker for immature neurons Tuj1 was mainly observed closer to the

periphery where strongly labeled fibers were present among the cells (Fig. 4.1E, F). Fibers with lower fluorescent signal were observed towards the centre of the neurosphere. Again, it was difficult to quantify $Tuj1^+$ cells as cell processes with Tuj1 immunoreactivity were surrounding neighbouring cells. Higher magnification of a confocal microscope images showed more clearly the presence and orientation of the $Tuj1^+$ fibers in a neurosphere section (Fig. 4.1F, arrow for vertical and arrowhead for horizontal orientation). The mature neuronal marker NOS was present in very few cells which were located at the periphery (Fig. 4.1G, H). Cells positive for the glial marker S100 were randomly distributed throughout the neurosphere and different levels of immunoreactivity were observed between those cells that were positive for this marker but their number was lower than the $GFAP^+$ cells (Fig. 4.1I). The antibody used in this study could detect both S100A1 and S100B isoforms, but because S100B is abundant in the peripheral nervous system (PNS) and S100A1 is not (Rosario et al., 1999), therefore S100 staining reflects S100B expression.

By examining the neurosphere sections it was difficult to count and decide if cells were positive or negative for markers such as Tuj1. A four day culture of neurosphere-derived cells in adherent conditions (see Fig. 4.2) showed that Tuj1 is present in fiber-like structures which run through the cell processes and the cell body and also in a few cells it was diffuse in the

cytoplasm. Negative cells had larger nuclei and more spread out morphology (Fig. 2A, arrowhead).

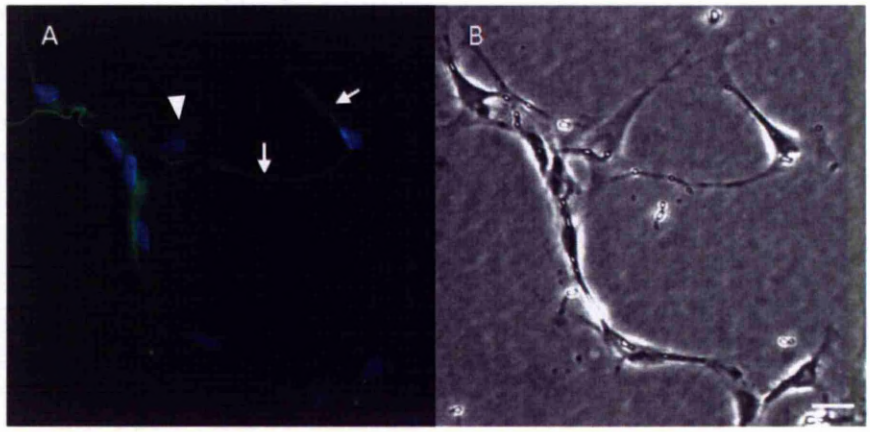

Figure 4.2. **Immunostaining for Tuj1 in dissociated neurosphere-derived cells after 4 days of culture in adherent conditions.**

Primary embryonic mouse neurospheres were dissociated after 21 days in suspension culture and $8x10^3$ single cells were cultured on 35mm tissue culture dishes for a further 4 days. Tuj1 (green) is located mainly in the cell processes (A, arrows). Nuclei were stained with DAPI (blue). Phase contrast picture (B). Arrowhead indicates a Tuj1 negative cell. Scale bar is 50 μm.

In order to quantify the number of cells expressing specific phenotypic markers and examine their co-expression, neurospheres were dissociated into single cells and seeded at low density in tissue culture dishes for 3h allowing a minimum time for the single cells to attach and begin to spread. This technique allowed a clear distinction to be made between cells that were positive and negative for all markers and therefore facilitated estimation of cell numbers. The 3h waiting period as well as the interaction of the cell with the tissue culture plastic raises the possibility that the neurosphere-derived cells might change phenotype and start expressing or losing markers that they did not have in the neurosphere environment. However as shown in the counting data in Fig. 4.3 the ratios of the phenotypic markers expressed in single cells in culture resembles the ratios observed in neurosphere sections, with GFAP being the most abundant marker and NOS being expressed only by very few cells (Fig. 4.1).

Quantitation of marker expression (Fig. 4.3) indicated that most of the neurosphere cells expressed the marker GFAP (60%), followed by Sox10 (44%), S100 (24%), Tuj1 (22%) and NOS (4%). Clearly these numbers add up to more than 100%, indicating that there must be overlap of marker expression. Dual immunostaining of neurosphere-derived cells for more

than one marker showed that there is indeed considerable and variable overlap (Figs. 4.4 and 4.5).

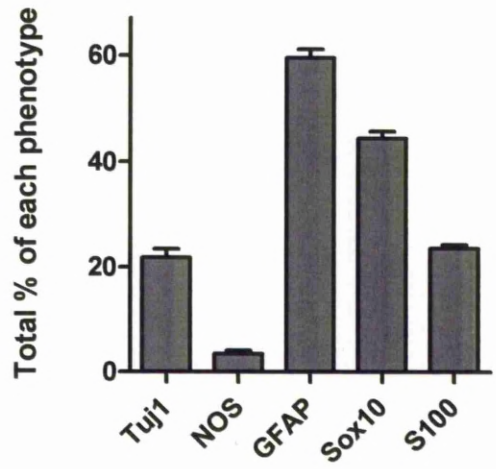

Figure 4.3. T**he percentage of neurosphere cells expressing different markers.**

Primary embryonic mouse neurospheres after 15 day culture in 60mm non adherent dishes were dissociated into a single cell suspension before seeding in adherent chamber slides ($5x10^3$ cells/chamber/ $0.8cm^2$). Neurosphere-derived cells were allowed to attach and spread for 3h then they were fixed and stained for the markers Tuj1, NOS, GFAP, Sox10, and S100. Immunopositive cells were counted in random optical fields (n= 10) of each chamber with a 40X oil objective. The total number of cells per optical field was quantified by counting the number of nuclei stained with DAPI. Columns and bars show means and range from 2 independent experiments.

4.2.2. Co-expression of phenotypic markers

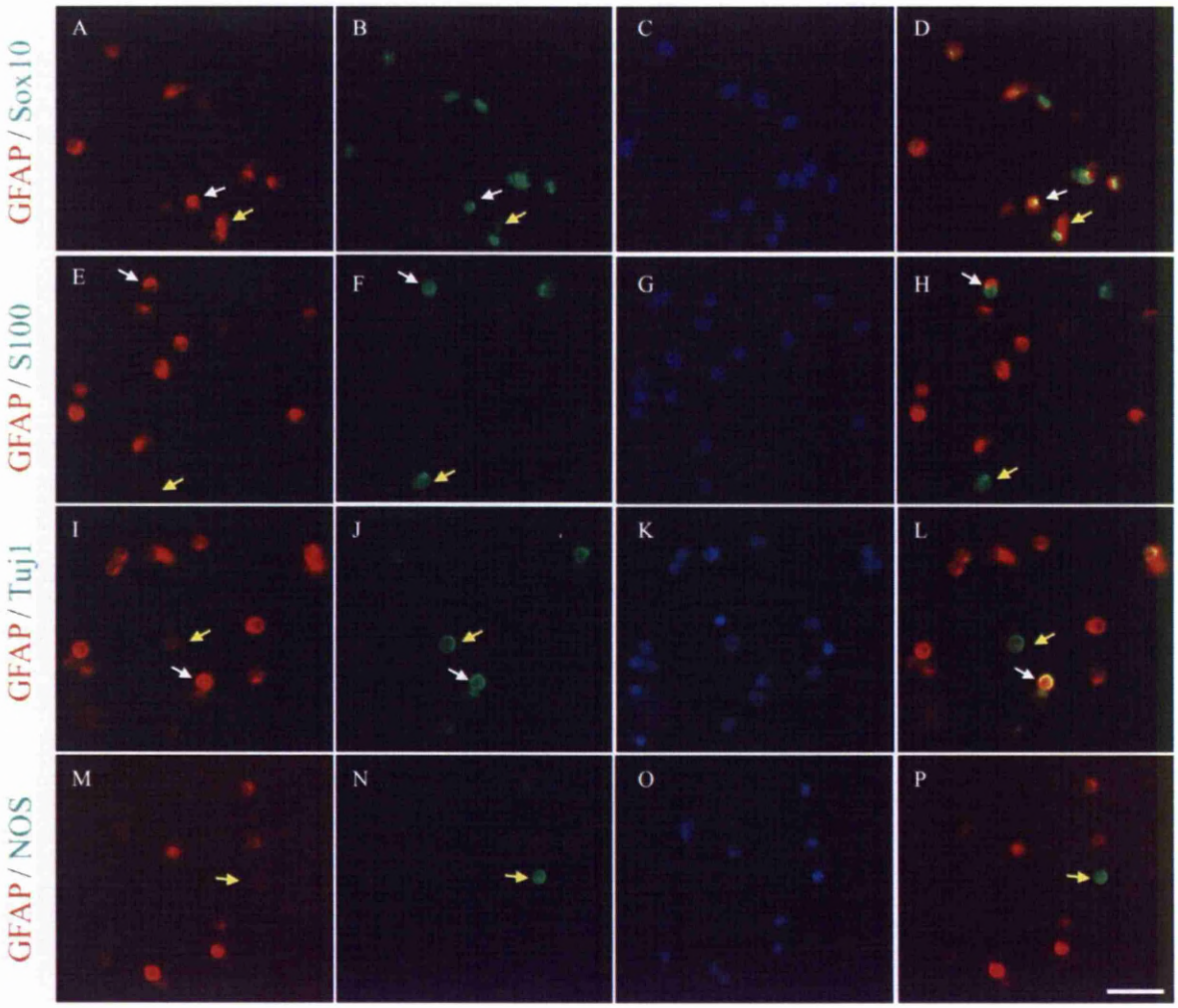

Figure 4.4. **Co-localisation of phenotypic markers in adherent cells dissociated from neurospheres [1].**

Primary embryonic mouse neurospheres after 15 day culture in 60mm non adherent dishes were dissociated into a single cell suspension before seeding in adherent chamber slides ($5x10^3$ cells/chamber/$0.8cm^2$). Neurosphere-derived cells were allowed to attach and spread for 3h when they were fixed and stained for the marker GFAP (A, E, I, M). They were also co-stained for the markers, Sox10 (B), S100 (F), Tuj1 (J) and NOS (N). Nuclei were stained with DAPI (blue); D, H, L, P : overlay of green and red channel. White arrows indicate co-localisation of GFAP with other markers. Yellow arrows represent cells that express only one marker after the co-staining in each row. Scale bar is 25μm.

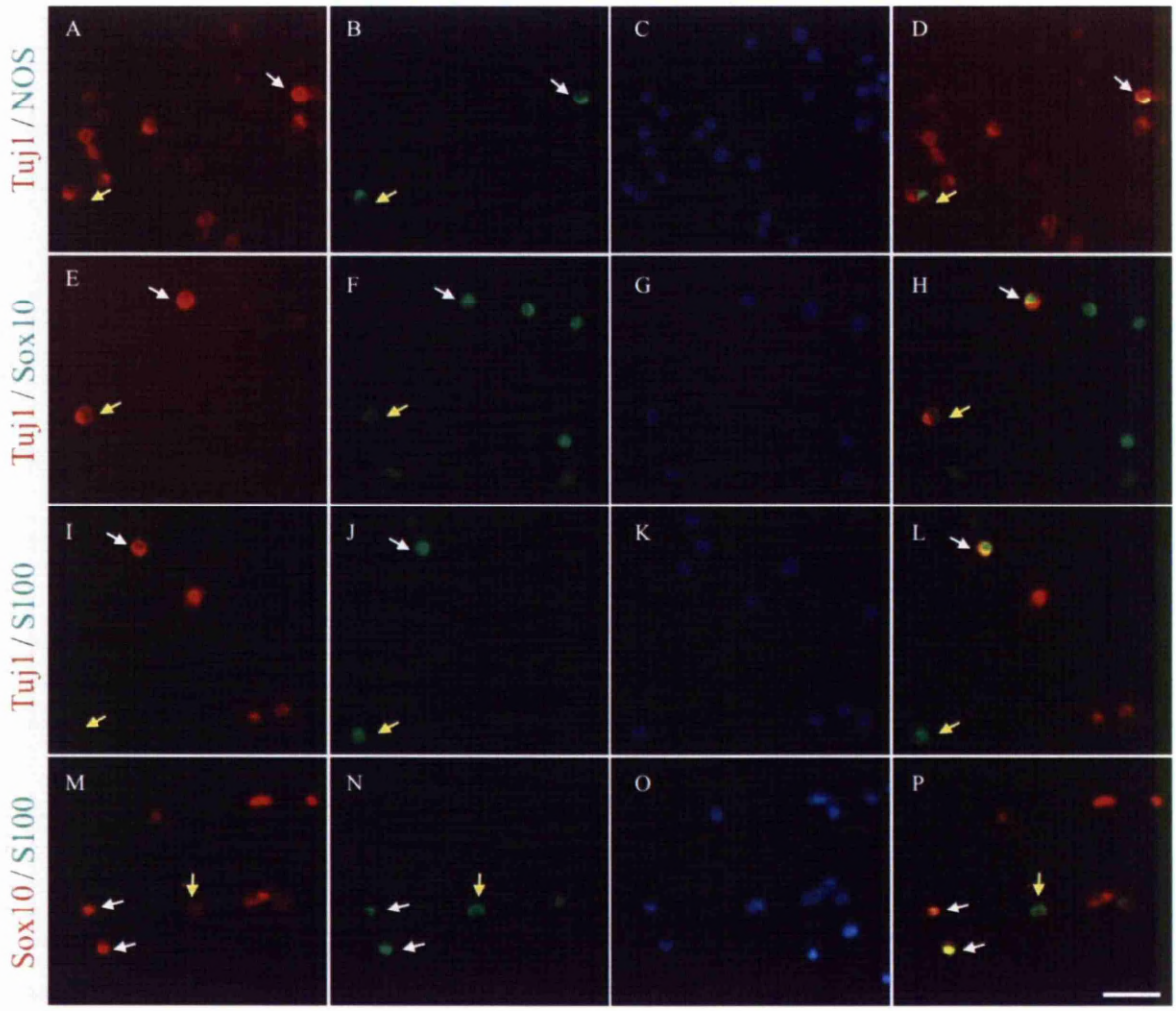

Figure 4.5. **Co-localisation of phenotypic markers in adherent cells dissociated from neurospheres [2].**

Primary embryonic mouse neurospheres after 15 day culture in 60mm non adherent dish were dissociated into a single cell suspension before seeding in adherent chamber slides ($5x10^3$ cells/chamber/$0.8cm^2$). Neurosphere-derived cells were allowed to attach and spread for 3h when they were fixed and stained for the

markers Tuj1 (A, E, I), NOS (B), Sox10 (F, M) and S100 (J, N). Nuclei were stained with DAPI (blue); D, H, L, P: overlay of green and red channel. White arrows indicate co-localisation of both markers in each row. Yellow arrows represent cells that express only one marker in each row. Scale bar is 25μm.

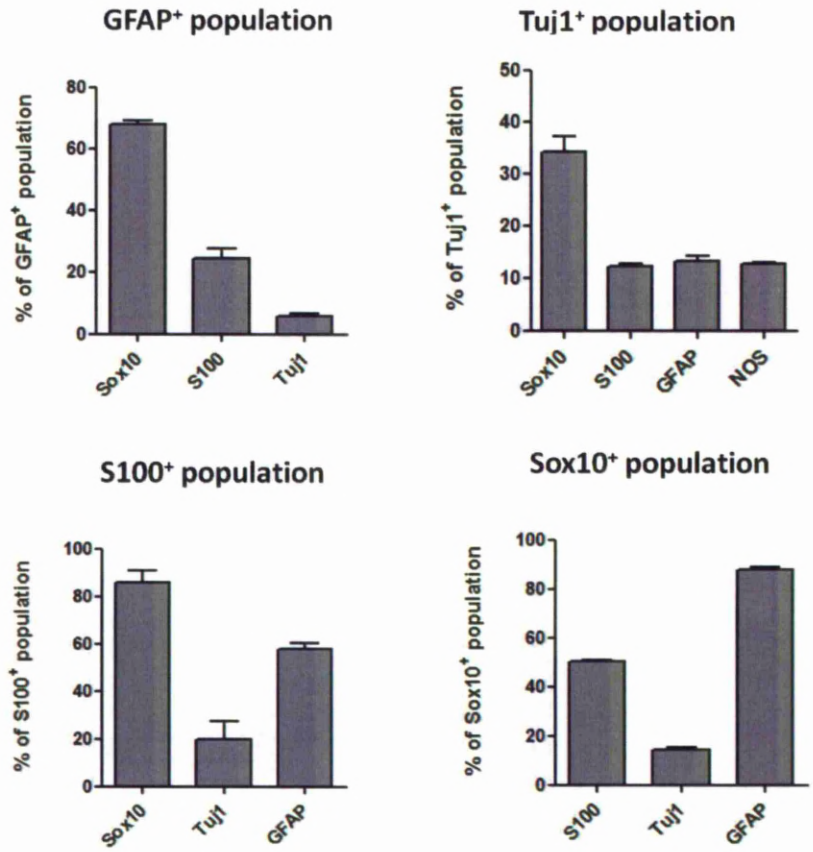

Figure 4.6. **Graphs showing the co-expression percentage of different markers.**

Conditions as described in legend of Fig. 4.5. Immunopositive cells were counted in random optical fields (n= 10) of each chamber using a 40X oil objective. The total number of cells per optical field was quantified by counting the total number of nuclei stained with DAPI. Columns and bars show means and range from 2 independent experiments.

A number of GFAP$^+$ cells also co-expressed all the other markers including Sox10, S100 and Tuj1 (Fig. 4.4 white arrows) but GFAP was not co-localized with NOS (Fig. 4.4P, yellow arrow), indicating that GFAP expression was absent in these mature neurons. Furthermore, a number of Tuj1$^+$ cells co-expressed either GFAP or NOS (Fig. 4.4L and 4.5D, white arrows), consistent with the idea that Tuj1$^+$ cells represent a transient population of cells from a progenitor state (GFAP$^+$) which differentiates towards a mature NOS$^+$ neuronal phenotype.

Also, there were Tuj1$^+$ cells which co-expressed Sox10 and S100 (Fig. 4.5H and L, white arrows). When cells were co-stained for Sox10 and S100, co-expression in most of the S100$^+$ cells was observed (Fig. 4.5P, white arrows). The vast majority of GFAP$^+$ cells co-expressed Sox10 (68%) followed by S100 (24%) and only a small number of them co-expressed Tuj1 (6%) (Fig. 4.6). In the Tuj1$^+$ cell population most of them also co-expressed Sox10 (34%) whereas for the markers GFAP, NOS and S100 the co-expression levels were very similar and in the range of 13%-15%. When the S100$^+$ cell population was examined a large number of them co-expressed Sox10 (86%), GFAP (58%) and Tuj1 (20%).

Finally, in the case of the $Sox10^+$ cell population, the great majority were $GFAP^+$ (88%), half of them co-expressed S100 (51%) and fewer Tuj (14%). Interestingly, Sox10 was co-expressed in many $GFAP^+$, $S100^+$ and $Tuj1^+$ cells (Fig. 4.6), implying that this transcription factor could be a general progenitor marker *in vitro* that remains detectable in the transition towards both the neuronal and the glial lineages.

4.2.3. Relationship between cell proliferation and differentiation

It was necessary to modify the previous BrdU proliferation assay as this staining technique required hydrochloric acid treatment in order to make the nucleus permeable to the anti-BrdU antibody, and this treatment caused loss in the antigenicities of many of the phenotypic markers displayed by the neurosphere cells (data not shown). This technical issue was solved by replacing BrdU with 5-ethynyl-2'-deoxyuridine (EdU), a thymidine analogue like BrdU but which does not require hydrochloric acid treatment; the EdU staining is based on the reaction between an alkyne (contained in EdU) and an azide (conjugated with a fluorophore) in the presence of copper which results in a stable triazole ring (Buck et al., 2008). The immunostaining and counting followed as described in the Materials and Methods Section (2.4.6.). Although BrdU and EdU act competitively when they are both together in the medium, in this experiment they were both present in the dividing cells. However, a

difference in the intensity of the labeling was observed between the EdU and the BrdU labeled cells implying their competition to incorporate in the cell DNA when they are together in the cell culture medium (Fig. 4.7). Therefore, EdU was used as equivalent of BrdU in the following experiments as they stain the same cells.

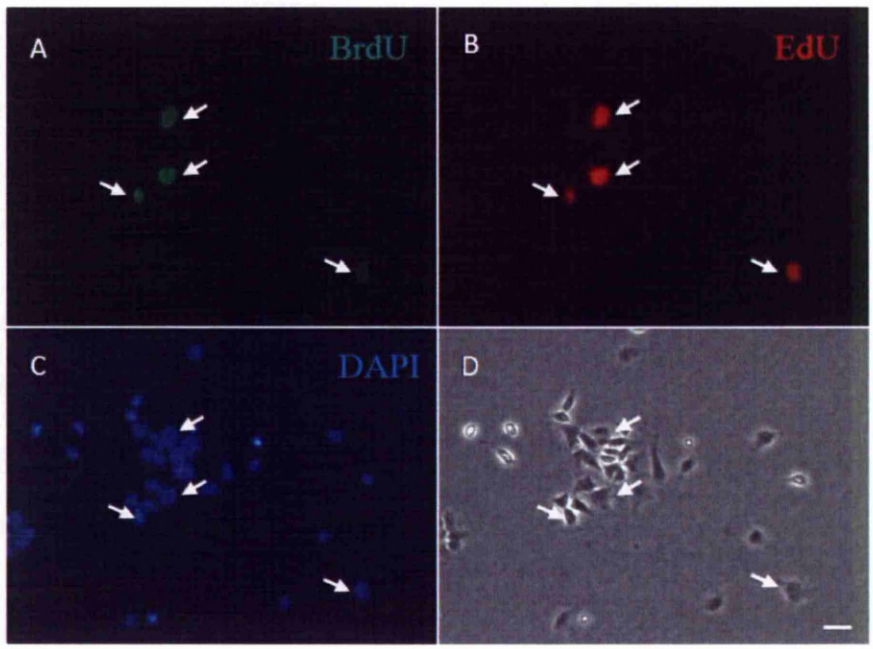

Figure 4.7. **Double staining for BrdU and EdU in neurosphere-derived cells.**

Primary embryonic mouse neurospheres after 15 day culture in 60mm non adherent dishes were incubated for a further 1h in medium containing both 10μM BrdU and 10μM EdU. Following dissociation $10x10^3$ single cells were seeded in 35mm tissue culture dishes and cultured for 3h, in the absence of BrdU and EdU. Fixation and staining for BrdU (A) and EdU (B) followed. Nuclei were stained with DAPI (Fig. C). Phase contrast picture (Fig. D). All nuclei which were positive for BrdU were positive for EdU and vice versa (arrows). Scale bar is 25μm.

Primary embryonic mouse neurospheres cultured for 15 days under non-adherent conditions were incubated with 10μM EdU for 1h with and without chase for 4 further days upon EdU removal, in order to examine the relationship between the different phenotypes and cell proliferation. Again, in order to quantitate numbers of cells of specific phenotype it was necessary to dissociate the neurospheres after these times and allow the cells to adhere briefly to chamber slides as described above.

Immunostaining and quantification of cells positive for each marker revealed that the phenotypic expression between neurosphere cells at the beginning of the chase (15d old) and neurosphere cells at the end of the chase (19d old) was very similar (Fig. 4.8) indicating there is a 'steady state' balance of the cell phenotypes in the neurosphere over these 4 days, although proliferation was occurring during the chase (see bars showing percentages of cells having incorporated EdU, Fig. 4.8). Specifically, a majority of the neurosphere cells expressed GFAP (56% before chase / 57% after chase), followed by the transcription factor Sox10 (43% / 33%), S100 (19% / 23%), Tuj1 (18% / 21%) and finally NOS (4% / 5%). None of these before/ after values were statistically different ($p > 0.05$). In contrast the number of EdU^+ nuclei increased significantly after the chase (16% before chase / 32% after chase, Fig. 4.8). This was expected as the cells

which incorporated EdU during the pulse continued to proliferate over the 4 days of chase.

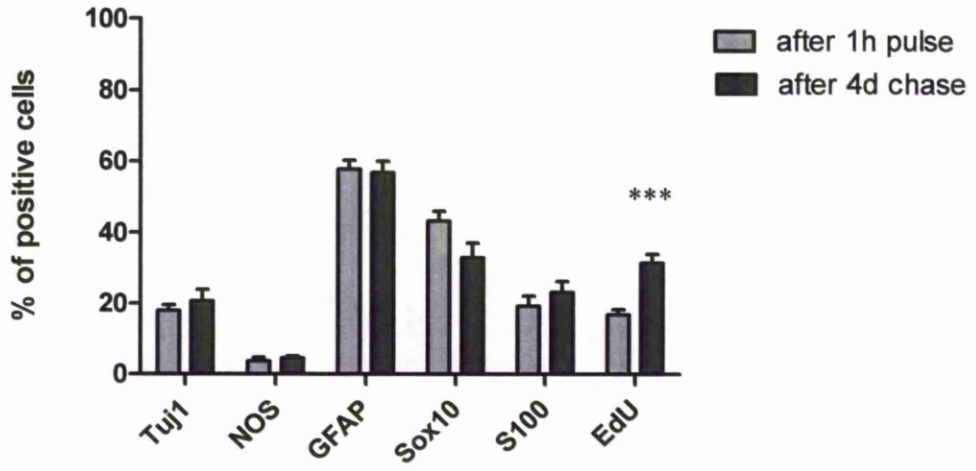

Figure 4.8. **The percentage of neurosphere cells expressing different markers or labeled with EdU with and without 4 day chase after EdU labeling.**

Neurospheres immediately after the EdU pulse and the 4 day chase following removal of EdU were dissociated into single cells which were allowed to attach and spread in adherent chamber slides for 3h ($5x10^3$ cells/chamber/$0.8cm^2$). Cells were then fixed and stained for different markers. Immunopositive cells were counted in random optical fields (n= 5-10) of each chamber using the 40X oil objective. The total number of cells per optical field was quantified by counting the total number of nuclei stained with DAPI. Error bars represent the SEM from independent experiments ($n \geq 3$). There was no significant difference between percentages of any of the phenotypic markers before and after the chase. A

significant increase was observed in the number of EdU^+ cells after the 4 day chase. ***= p value< 0.001

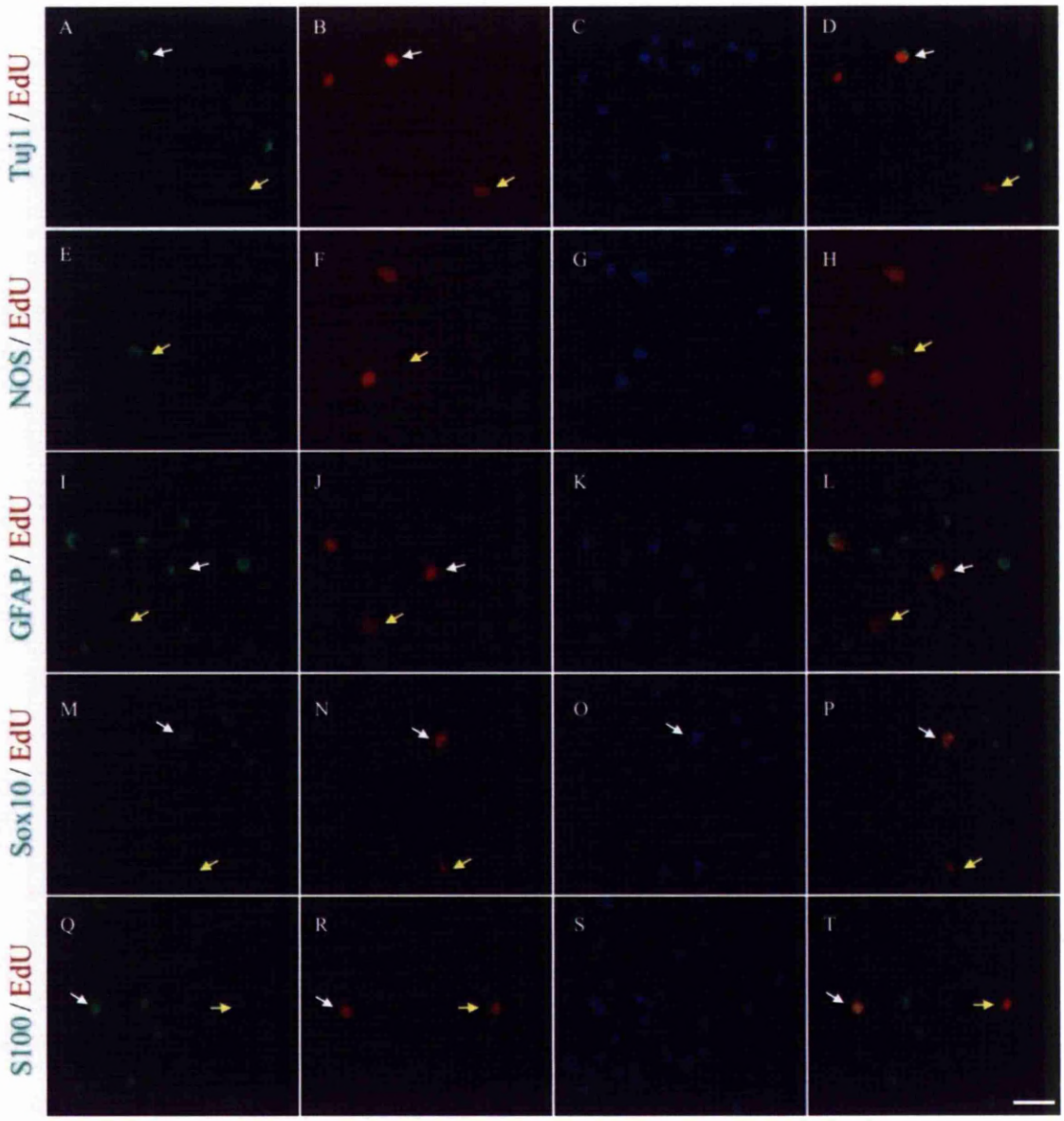

Figure 4.9. **Co-localisation of neurosphere-derived cell markers immediately after EdU incorporation.**

Primary embryonic mouse neurospheres after 15 day culture in 60mm non adherent dishes were incubated with 10μM EdU for a further 1h. EdU was removed, neurospheres were washed and dissociated into a single cell suspension before seeding in adherent chamber slides ($5x10^3$ cells/chamber/$0.8cm^2$). Neurosphere-derived cells were allowed to attach and spread for 3h when they were fixed and stained for Tuj1 (A), NOS (E), GFAP (I), Sox10 (M), S100 (Q) and EdU (B, F, J, N, R). Nuclei were stained with DAPI (blue); D, H, L, P, T: overlay of red and green channel. White arrows indicate co-localisation of EdU for each marker. Yellow arrows represent cells that are EdU^+ but negative for the relevant marker. Scale bar is 25μm.

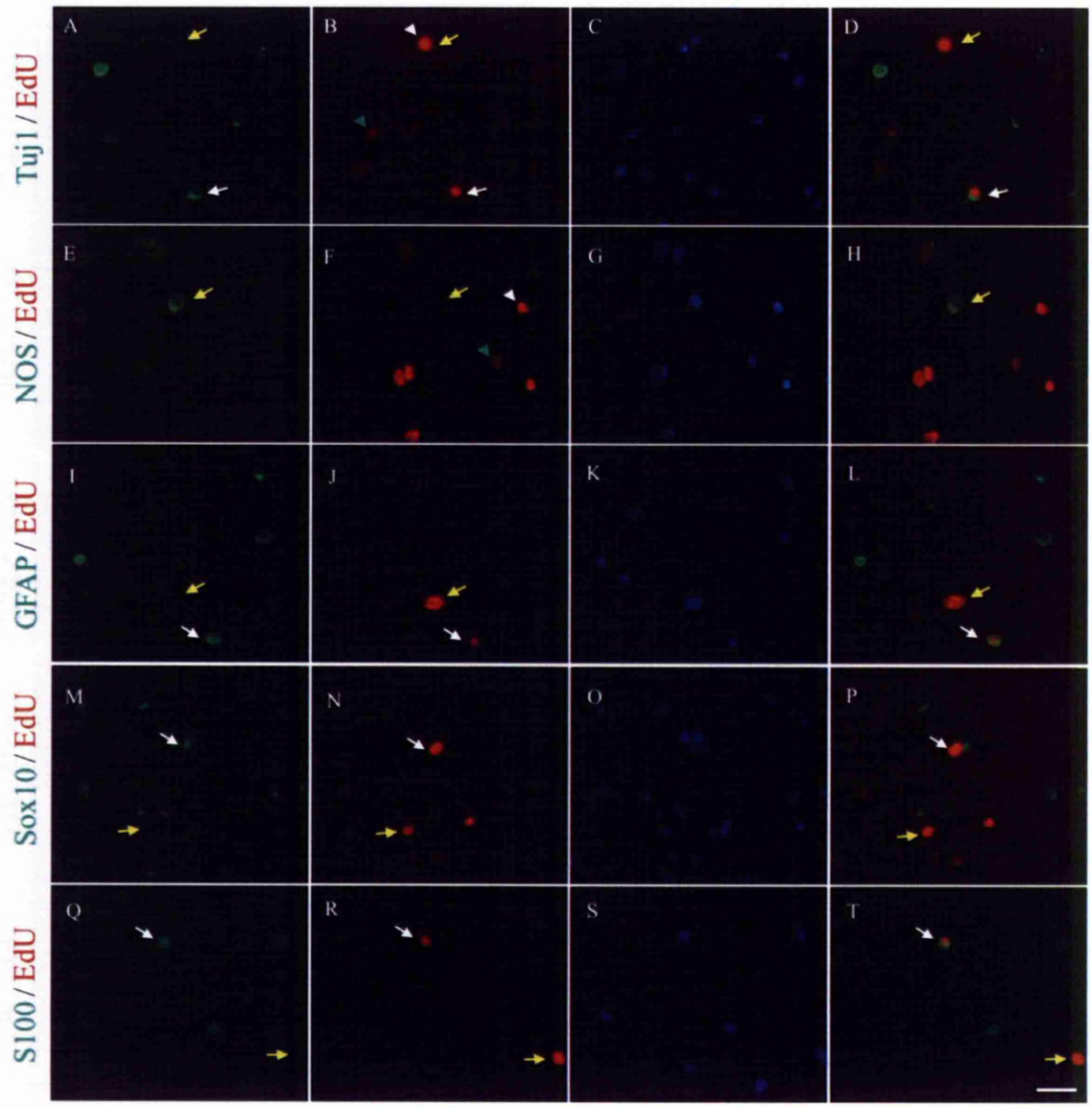

Figure 4.10. **Co-localisation of neurosphere-derived cell markers with EdU incorporation 4 days after EdU chase.**

Primary embryonic mouse neurospheres after 15 day culture in 60mm non adherent dishes were incubated with 10μM EdU for a further 1h and then cultured in absence of EdU for 4 days (chase). At the end of the chase neurospheres were dissociated and single cells were left to attach and spread for 3h in adherent chamber slides ($5x10^3$ cells/chamber/$0.8cm^2$). They were then fixed and stained for TuJ1 (A), NOS (E), GFAP (I), Sox10 (M), S100 (Q) and EdU (B, F, J, N, R). Nuclei were stained with DAPI (blue); D, H, L, P, T : overlay of green and red channel. White arrows indicate co-localisation of EdU for each different marker.Yellow arrows represent cells that are EdU^+ but negative for the relevant marker. White arrow head indicates a highly-labeled EdU nucleus and the green arrow head a low-labeled EdU nucleus (B, F). Scale bar is 25μm.

Moreover, the level of the EdU fluorescence signal was more variable after the 4 day chase compared to what was observed straight after the pulse (compare Fig. 4.10B, F, J, N and R). As shown in Fig. 4.10 F, at the end of the 4 day chase there were nuclei highly and weakly labeled with EdU (white and green arrowhead respectively), a picture similar to the one where proliferation at the same time point was examined in neurospheres using BrdU (Chapter 3, Fig. 3.6p1), indicating a variation in the rate of proliferation among neurosphere-cells. On the other hand, as with BrdU staining (Chapter 3, Fig. 3.3m1), the level of EdU fluorescence signal immediately after the pulse is very similar among the different positive nuclei (compare Fig. 4.9B, F, J, N and R), implying that for the short term of 1h there were not enough divisions to further dilute the incorporated EdU (See Discussion). At the end of the chase the EdU^{+} nuclei could be categorised under the microscope into low and high EdU labeled (Fig. 4.9F and Fig. 4.11). The number of cells with low EdU levels in their nucleus was higher.

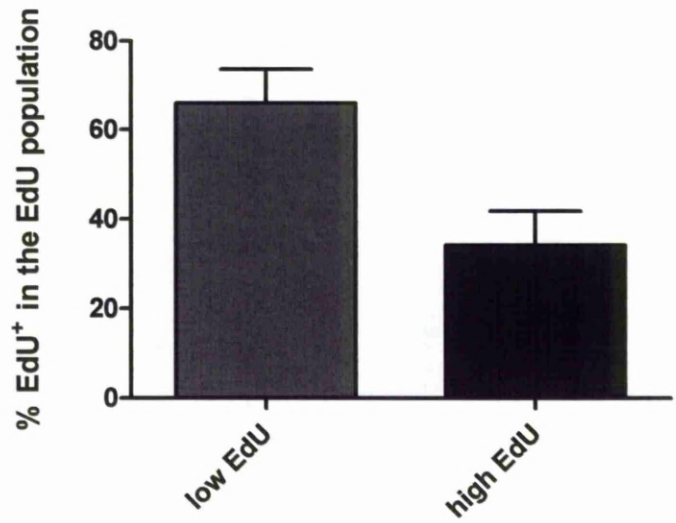

Figure 4.11. **The percentage of low and high signal EdU$^+$ cells in the EdU population after 4 days of chase.**

Neurospheres at the end of the chase were dissociated into single cells which were left to attach in adherent chamber slides for 3h (5x103 cells/ chamber). Cells were then fixed and stained for EdU. Positive nuclei were counted in random optical fields (n= 5) of each chamber and the objective 40x was used for it. (See Fig. 10F arrowheads for low and high EdU labeled nuclei). Error bars represent the SEM between 3 experiments (n= 3). *= p value < 0.05.

The phenotypic expression of cells which incorporated EdU after a 1h pulse, showed that variable proportions of cells with EdU^+ nuclei also express the markers Tuj1, GFAP, Sox10 and S100 (Fig. 4.12). A very low number of EdU^+ cells (0.3 %) were also positive for NOS. The vast majority of EdU^+ cells were $GFAP^+$ (82%). Then the markers Sox10 and S100 followed representing the 64% and 23% of EdU^+ cells respectively. The marker for immature neurons Tuj1 represented only the 5% of the EdU^+ population.

When cells were stained and counted at the end of the 4 day chase the majority of the EdU^+ population was still positive for GFAP (Fig. 4.10) but the percentage was reduced from 82% to 63% (Fig. 4.12). At the same time there was a decline of the $Sox10^+EdU^+$ population from 65% to 44%. On the other hand an increase of the $S100^+EdU^+$ cells was observed, from 23% to 40%, and even more strikingly a significant increase occurred in the $Tuj1^+EdU^+$ population, going from 5% to 20%.

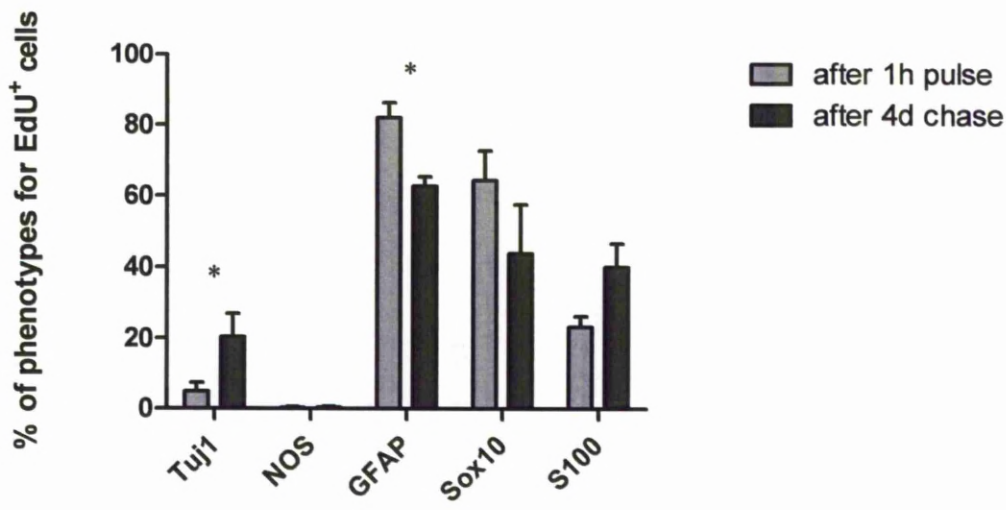

Figure 4.12. **Co-expression of different markers in EdU^+ cells with and without chase after EdU labeling.**

Neurospheres immediately after the EdU pulse and the 4 day chase following removal of EdU were dissociated into single cells which were allowed to attach in adherent chamber slides for 3h ($5x10^3$ cells/chamber/$0.8cm^2$). Cells were then fixed and stained for different markers and EdU. Immunopositive cells were counted in random optical fields (n= 5-10) of each chamber using the 40X oil objective. The total number of cells per optical field was quantified by counting the total number of nuclei stained with DAPI. Error bars represent the SEM from different experiments ($n \geq 3$). A two tailed unpaired t-test was performed for all the phenotypic markers: Tuj1 (p= 0.047), GFAP (p= 0.018), Sox10 (p= 0.27) and S100 (p= 0.08). * = p value< 0.05.

In summary, after 1h pulse with EdU most EdU^+ cells were positive for the marker GFAP whereas there was a low or almost no co-expression of the markers Tuj1 or NOS respectively. After 4 days of chase a significant increase in Tuj1 and an increasing trend of S100 expression were observed while the GFAP and Sox10 levels were reduced.

In order to identify any differences in terms of the differentiation status between low and high labeled EdU^+ nuclei at the end of the chase, counting was performed in EdU^+ cells which were also expressing the marker of immature neurons Tuj1, the marker with a significant increase at the end of the chase (Fig. 4.12). Interestingly, we were not able to identify differences between the expression of Tuj1 in low and high labeled EdU^+ nuclei (Fig. 4.13). These findings suggest that for the time period studied the cells which had not divided again during the chase had therefore higher levels of incorporated EdU had the same neurogenic potential as the cells which proliferated faster during the 4 days of chase.

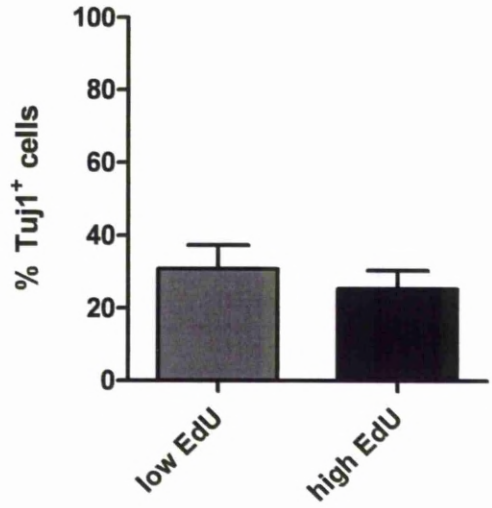

Figure 4.13. **Graph showing the percentage of $EdU^{+}Tuj1^{+}$ cells in the low or high labeled EdU population.**

Neurospheres at the end of the chase were dissociated into single cells which were let to attach in adherent chamber slides for 3h ($5x10^{3}$ cells/ chamber). Cells were then fixed and stained for Tuj1 and EdU. Positive nuclei were counted in random optical fields (n= 5) and the 40X oil objective was used for it. Error bars represent SEM between 3 independent experiments.

4.3. Discussion

In Chapter 3, we investigated the locations and proliferation rates of cells in embryonic mouse neurospheres. We demonstrated that cells closer to the periphery tended to divide faster than those closer to the centre of the neurosphere. Then in order to understand neurosphere cell behaviour we investigated the expression of phenotypic markers in neurosphere cells and we tried to see if there is any correlation between differentiation and proliferation rate.

4.3.1 Neurosphere cells express markers for ENS progenitors, neurons and glia

All the neurosphere cells were expressing in their cytoplasm the neural crest cell marker p75 (Fig. 4.1A) indicating their neural crest origin (Young et al., 1999). The marker glial fibrillary acidic protein GFAP was also present in the vast majority of the neurosphere cells whereas $S100^{+}$ cells were fewer and randomly distributed (Fig. 4.1B and 4.1I respectively). In the ENS, GFAP and the protein S100B have been used to identify glial cells (Bondurand et al., 2003; Young et al., 2003).

In the adult CNS, both markers have been used to label glial cells, particularly astrocytes, although S100B expression begins when astrocytes

mature, indicating that S100B is expressed later on in glial differentiation compared to GFAP (Platel et al 2009). In neonatal P2 and P8 mouse forebrain when astrocytes were still proliferating the vast majority of $GFAP^+$ cells were $S100B^-$. Increase in the number of $GFAP^+/S100B^+$ cells occurred at P15 in the parenchyma of the brain when astrocytes were mature (Deloulme et al., 2004). In the same study expression of S100B was present in slow dividing glial cells suggesting that S100B is expressed in more mature glial cells.

We showed that 24% of the $GFAP^+$ cells in embryonic mouse neurosphere cells are $S100^+$. We also observed that around 40% of the $S100^+$ population did not express GFAP. After a short pulse the vast majority of the fast proliferating cells expressed GFAP (82%) but only 23% expressed S100. We can conclude that some of $S100^+$ cells are a subpopulation of $GFAP^+$ and $S100^+$ cells do not represent the majority of the fast dividing cells, implying that S100 could represent a more mature glial phenotype. However, after the 4 day chase a smaller proportion of the EdU labeled cells expressed GFAP (63%) and a higher proportion S100 (40%), implying a maturation and commitment of the $GFAP^+$ cells towards the glial lineage over these 4 days which leads to the reduction of their proliferation rate.

In a study recently published by Laranjeira et al. (2011), glial cells isolated from small intestine of adult transgenic mice, where cells were expressing YFP under the control of the Sox10 promoter, which as described before is active in ENS progenitors and glia were able to give rise to adult enteric neurons in vivo, but neurogenesis with YFP co-localization could not be observed after the age of P84, indicating that these cells differentiated towards the glial lineage. However, upon dissociation of P84 mouse guts, $YFP^+/GFAP^+$ cells were able to give rise to different neuronal types in culture including NOS, VIP and neuropeptide Y, indicating that under specific conditions, cells expressing glial markers can give rise to neurons.

Consistent with these results, our data showed that neurospheres contained cells which were $Sox10^+/Tuj1^+$ as well as $GFAP^+/Tuj1^+$ possibly representing transient populations which differentiate towards the neuronal lineage, suggesting that the neurosphere environment provides the appropriate differentiation conditions similar to what was observed in monolayer culture by Laranjeira et al. by adding differentiation culture medium. Neurosphere generation may also resemble an injury model as embryonic tissue is dissociated and cells go from being attached to each other to become single cells until they start multiplying and forming new neurospheres.

In addition, ENS injury using topical application of benzalkonium chloride to myenteric ganglia generated cells positive for the pan-neuronal marker HuC/D, something that they could not observe in a steady-state bowel (Laranjeira et al., 2011). On the other hand, Joseph et al. (2011) failed to identify neurogenesis in almost all mice and rats tested (84 out of 85 animals) when BrdU was administered by injection and in the drinking water after local treatment of their distal ileum with benzalkonium chloride. Even after 11 months of chase without BrdU, they could not identify $BrdU^+/HuD^+$ cells at the site of benzalkonium chloride injury or in regions nearby. Moreover, even when they used adult transgenic mice, where cells were expressing EYFP under the control of the GFAP promoter, a very small number of HuD^+ derived from $GFAP^+/EYFP^+$ cells was observed (no more than 0.11%).

Joseph et al. (2011) suggested that there could be a mechanism which can promote neuronal differentiation from adult glial cells without prior proliferation as that would explain the absence of proliferating neuronal progenitors. In addition, there might be a $Sox10^+/ GFAP^-$ population in vivo which is responsible for the generation of neurons after injury of the adult ENS and thus the possible explanation of the neurogenesis observed by $Sox10^+$ cells in the mouse model by Laranjeira et al. (2011).

However, Joseph et al. (2011) managed to show that cells sorted using flow cytometry (a2-integrin$^+$/ CD45$^-$/ TER119$^-$/ CD31$^-$) from adult mouse gut were co-expressing GFAP and S100B as well as p75 and the neural stem cell marker nestin (GFAP$^+$/ S100B$^+$/ p75$^+$/ nestin$^+$/ Hu$^-$) similar to what is co-expressed in the adult gut. When these cells were cultured in vitro, could generate peripherin positive neurons and smooth muscle actin positive cells, indicating that GFAP and S100B can be expressed in cells which give rise to different cell types in vitro. Thus, GFAP$^+$ or S100B$^+$ cells in the neurosphere could represent mature glial cells as well as ENS progenitors which can give rise to both neurons and glia with or without division as suggested above.

4.3.2. Neurosphere cells require time to differentiate upon proliferation

The observation of more immature neurons (Tuj1$^+$ cells) at the end of chase (5% after the pulse and 20% at the end of the chase) indicates a commitment of progenitor cells towards the neuronal lineage over the chase period. Regarding the marker Sox10 which, as described in the introduction, is expressed in both ENS uncommitted progenitors and enteric glial cells (Kim et al., 2003). Therefore the reduction in the levels of Sox10 can be explained due to differentiation of Sox10$^+$ uncommitted cells to Sox10$^-$ neuronal precursors or glial cells to neurons. Together with the

results from GFAP and S100 at the end of the chase, we can conclude that dividing neurosphere cells over time differentiate towards a more mature phenotype which could be either glia or neurons.

In order to investigate whether the fast diving cells (low EdU levels) at the end of the chase will be more differentiated than the low- or non-proliferating cells (high EdU levels), we counted the presence of the marker Tuj1 in each group, as it was the marker with the highest increase. As shown in Fig. 4.13 there was not any difference in the expression of Tuj1 between slow and fast dividing cells, therefore a correlation between proliferation rate and differentiation could not be made. Also we did not observe any NOS^{+} cells with incorporated EdU at the end of the chase, indicating that maybe a period longer than 4 days is required for the dividing cells to acquire a terminally differentiated phenotype. However, other markers of mature neurons could be present but they were not investigated in this study.

4.3.3 Cells expressing neuronal markers are close to the periphery

Staining for the marker of immature neurons Tuj1, showed immunoreactivity close to the periphery of the neurosphere (Fig. 4.1E). Also, cells expressing the mature neuronal marker NOS were only present at the periphery of the neurosphere, organized in a group. There were no NOS^+ cells in the centre of the neurosphere. On the other hand the distribution of $GFAP^+$, $Sox10^+$ and S100+ cells in the neurosphere was random. These data suggest that cells expressing markers of the neuronal lineage are located at the periphery where the fast dividing cells have been shown to be (Chapter 3). As discussed in the introduction, peripheral Tuj1 immunoreactivity was also observed in rat subventricular-zone derived neurospheres (Andersen et al., 2011). However, the cell body of these cells could be located somewhere closer to the centre resembling interkinetic nuclear migration of neuroepithelial cells over their cycling period (Del Bene, 2011) but that is unlikely to be the case for all the $Tuj1^+$ cells because we observed less nuclei with adjacent Tuj1 immunoreactivity closer to the centre of the neurosphere.

4.3.4. Conclusions

Neurospheres are a mixture of cells expressing markers for ENS uncommitted progenitors, enteric glia and neurons. Also, they contain transient cell populations which co-express undifferentiated and more mature markers implying that differentiation is an on-going process in the neurosphere environment. In addition, we demonstrated that the majority of fast dividing cells were not expressing markers indicating differentiation, but that takes time to start expressing such markers. The next question would be what signaling pathways, if any, are involved in the regulation of the neurosphere cell behaviour that was described in this chapter.

CHAPTER 5

Notch signaling inhibition

5.1. Introduction

5.1.1. Aim

Previously, we showed that neurospheres contain cells which express markers for immature and mature neurons (Tuj1 and NOS) as well as for glia and ENS progenitors (GFAP, S100, Sox10). Proliferation and differentiation are two processes that occur continuously in the neurosphere environment but the ratios of different phenotypic markers remain stable, indicating the presence of a balance between progenitors and differentiated cells. In this chapter the aim was to test the hypothesis that the Notch signaling pathway regulates the proliferation and differentiation of neurosphere cells. Notch signaling has been shown to play a critical role in the cell fate of progenitor cells and in the following paragraphs, we discuss the presence and role of the Notch signaling pathway in the gut and especially in the ENS as well as previous evidence of Notch signaling in neurospheres.

5.1.2. The notch signaling pathway regulates proliferation and differentiation of neural stem cells

The Notch signaling pathway plays a key role in the maintenance of neural stem cells and their differentiation (Artavanis-Tsakonas et al., 1999; Hitoshi et al., 2002). Notch signaling is controlled by cell-cell contact. Typically a cell which has undergone differentiation will be the ligand-presenting cell which will activate the Notch receptor in neighbouring cells and thereby inhibit their differentiation, a process called lateral inhibition (Cornell et al., 2005). In mammals there are 4 Notch receptors (Notch 1-4) and the ligands are the Delta-like (Dll1, 3, 4) and Jagged (Jag1, 2) proteins (Artavanis-Tsakonas et al., 1999). The extracellular domain of Notch receptors consists of 36 tandem epidermal growth factor (EGF) repeats whereas the intracellular domain consists of a sequence rich in the amino acids proline, glutamic acid, serine and threonine (PEST) (Artavanis-Tsakonas et al., 1999). Upon activation of Notch receptor with the binding of the ligand a series of cleavages begin. The extracellular domain of Notch receptor is cleaved by the ADAM protease and the γ-secretase protein complex cleaves and releases in the cytoplasm the Notch intracellular domain (NICD) (Brou 2009) (Fig. 5.1). This will then translocate to the nucleus where it binds with the proteins Rbp-Jκ (also known as CBF1) and Mastermind-like protein to de-inhibit expression of target genes such as Hes1, Hes5 and Hey genes (Pierfelice et al., 2011).

These genes encode factors which block neuronal differentiation and thus maintain the undifferentiated and proliferating status of the cell (Iso et al., 2003).

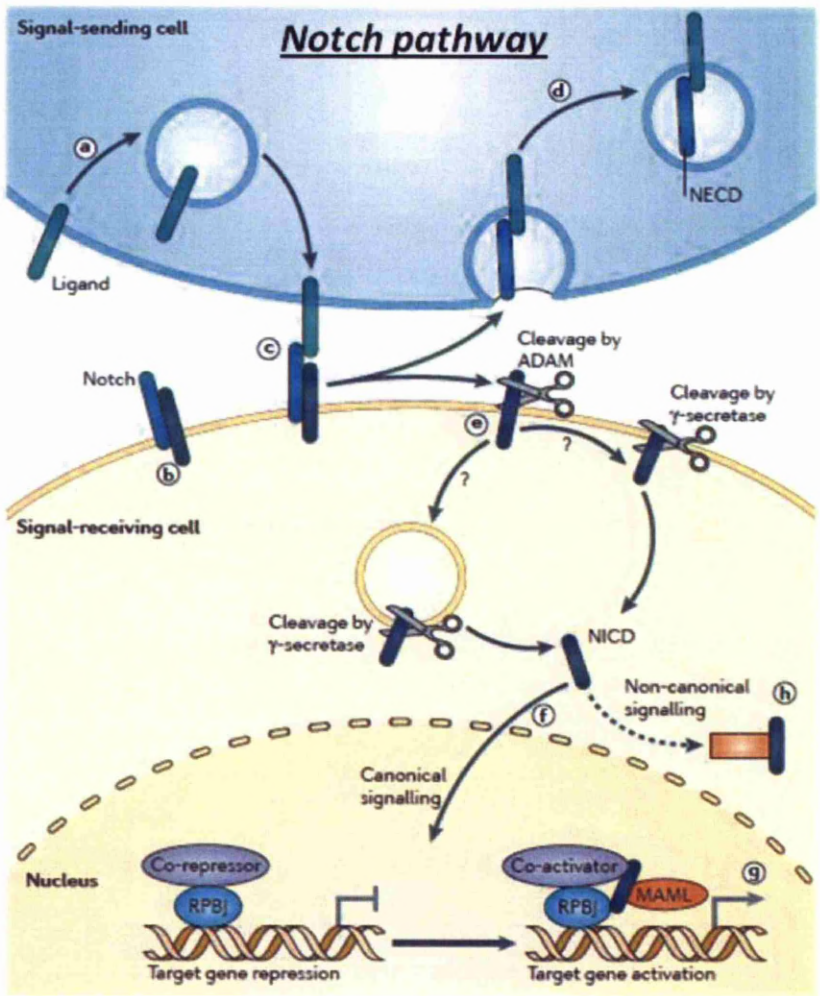

Figure 5.1. **Canonical Notch signaling pathway.** (Figure was adapted and modified from Ables et al., 2011).

In addition to the canonical Notch signaling pathway which was just described, studies have indicated the Rbp-Jκ independent Notch signaling activation. This Rbp-Jκ independent pathway can involve Notch receptor cleavage but it activates other signaling pathways like Wnt, Hedgehog and TGF-β in order to activate the transcription of downstream genes. But it can also be independent of γ-secretase cleavage of the Notch-receptor for its activation (Sanalkumar at al., 2010) demonstrating the great complexity and interactions of Notch signaling pathway.

5.1.3. Role of Notch signaling pathway in the gut

The presence of Notch signaling has been implicated in many regulatory roles of the gut. One of them is the maintenance of the intestinal epithelial stem cells of the crypts. Conditional inactivation of the Rbp-Jk transcription factor, a key part of the Notch cascade, resulted in the loss of proliferating crypt stem cells and their subsequent differentiation to post-mitotic goblet cells in adult mouse small intestine (van Es et al., 2005). In addition, constitutive expression of Notch1 in cells of the intestinal epithelium and the crypt stem cells, showed that goblet and endocrine cell differentiation was impaired. On the other hand the number of proliferating cells in the crypts was increased (Fre et al. 2005), confirming the regulatory role of Notch signaling pathway in the cell fate decision.

Although the Notch signaling pathway has been studied in more detail in the intestinal epithelium and regarding its involvement in bowel cancers (Radtke et al., 2005), there is little evidence in the literature regarding its role in the ENS. Sander et al. (2003) demonstrated that in the submucosal and myenteric plexi in adult rat gut the receptor Notch1 and the ligand Jagged2 are present, whereas the receptor Notch2 and the ligand Jagged1 could not be detected. Receptor Notch-1 was present in a subset of cholinergic neurons but was not co-localized with NOS^+ or $calretin^+$ neurons. On the other hand, the ligand Jagged2 was expressed in all the above subclasses of neurons (Sander et al., 2003). The presence of Notch-1 in post-mitotic neurons has also been described in non-proliferative neurons in the CNS regarding its role in inhibiting neurite outgrowth (Berezovska et al., 1999) and enhancing dendrite branching and blocking dendritic growth (Redmond et al., 2000), implying a possible common role for Notch signaling in both ENS and CNS.

Although Sander et al. (2003) suggested rather than showed a role for Notch signaling pathway in the ENS, Okamura et al. (2008) demonstrated that Notch signaling is essential for ENS development and maintenance of the proliferating migratory enteric NCCs by deleting the gene encoding the O-fucosyl-transferase 1 (Pofut1), in cells expressing the neural crest

promoter Wnt1. Pofut1 is responsible for the transfer of O-fucose to the extracellular EGF repeats of the Notch receptor therefore critical for the activation of the receptor by the ligand (Okamura et al., 2008). In this study, it was demonstrated after Notch signaling inhibition that ENS progenitors differentiated prematurely towards the neuronal lineage as that was shown by Tuj1 immunostaining. In addition, Notch signaling inhibition promoted a reduction in the proliferation of ENS progenitors, indicating a role of Notch signaling in the differentiation and proliferation of ENS progenitors during development.

5.1.4. Notch signaling pathway in neurospheres

As Notch signaling maintains the undifferentiated state of neural progenitor cells it is quite likely that the Notch pathway will have a pivotal role in the behaviour of neurosphere cells. In fact, expression of the receptor Notch-1 has been shown previously in sections of neurospheres derived from embryonic or postnatal forebrain (Campos et al., 2006). Also, inhibition of Notch signaling with the γ-secretase inhibitor L-685, 458 resulted in a decrease in the cell number of neurospheres derived from human fetal brains (Mori et al., 2006). Moreover, there was lower rate of increase in the cell number of human glioblastoma-derived neurospheres upon administration with the γ-secretase inhibitor GSI-18 and they also failed to generate secondary neurospheres upon dissociation (Fan et al., 2010) implying a role for Notch signaling in neurosphere cell proliferation.

Although Notch signaling has been shown to have an effect on neurosphere cell behaviour as described above, direct evidence for Notch signaling involvement in proliferation correlated to differentiation has not been demonstrated in either CNS or ENS neurospheres. In the previous chapter we showed that neurosphere cells which have just proliferated changed phenotype during the following 4 days. Briefly, when 15 day old primary neurospheres were labeled for 1h with EdU and then chased for 4 days, significantly higher expression of the markers Tuj1 was observed at

the end of the chase in EdU^+ cells, indicating a relationship between proliferation and differentiation. We were then interested to examine if this relationship can be regulated by blocking a signaling pathway. Because the Notch pathway has been shown to play a key role in the cell fate of neural progenitors and also because there is evidence as described above concerning its involvement in ENS development, we decided to study the effect of Notch inhibition on neurosphere cell behaviour.

5.2. Results

We were interested in investigating the role of the Notch signaling pathway in the proliferation and differentiation of neurosphere cells. Due to the fact that in the previous chapter we found a correlation between proliferation rate and differentiation, we wanted to examine further if this pattern is regulated by Notch signaling and thus being one step closer to learning how to control the behaviour of the neurosphere cells, a prerequisite for future clinical applications.

5.2.1. Inhibition of Notch signaling promotes neuronal differentiation and decreases proliferation in neurosphere cells

Notch signaling was inhibited using 10μM (Hansen et al., 2010) of the γ-secretase inhibitor DAPT, an inhibitor which is widely used to block Notch signaling (Dovey et al., 2001; Crawford et al., 2007). Initial experiments were designed to see if the Notch inhibitor had any effect on the proliferation and differentiation of neurosphere cells.

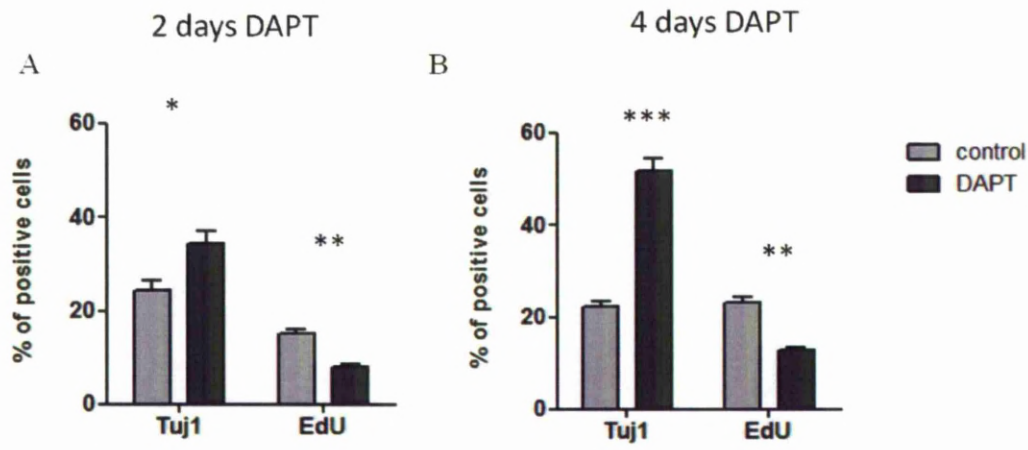

Figure 5.2. **The percentage of neurosphere cells positive for Tuj1 and EdU after treatment with DAPT.**

Embryonic mouse primary neurospheres (n=60-80) after 15 day culture in 60mm non adherent dishes were split in same type of dishes and incubated for 2 (A) or 4 (B) days with medium containing either DAPT (10μM final concentration) dissolved in DMSO or with the DMSO vehicle alone (0.1% (v/v) final dilution, control). At the end of treatment neurospheres were incubated with 10μM EdU for 1h, washed and dissociated into a single cell suspension before seeding in adherent Permanox chamber slides ($5x10^3$ cells/ chamber/ 0.8 cm^2). Neurosphere-derived cells were allowed to attach and spread for 3h with or without DAPT after which they were fixed and stained for the markers Tuj1 and EdU. Immunopositive cells were counted in random optical fields (n= 5) of each chamber with a 40X oil

objective. The total number of cells per optical field was quantified by counting the number of nuclei stained with DAPI. Error bars represent the SEM between different optical fields. A two tailed unpaired t-test was performed for the markers Tuj1 [$p= 0.02$ (A) and $p< 0.001$ (B)] and EdU [$p= 0.003$ (A) and $p= 0.002$ (B)]. * = p value < 0.05, ** = p value < 0.01, *** = p value < 0.001.

After 2 days in the presence of DAPT there was an increase of the proportion of $Tuj1^+$ population from 25% to 35% and a decrease of EdU^+ nuclei from 15% to 8% relative to controls (Fig. 5.1). These differences became greater after 4 days of inhibition: the percentage of $Tuj1^+$ cells was double that of controls (from 22% to 52%) whereas that of EdU labeled cells decreased to about half that of controls (from 23% to 13%) (Fig. 5.1; see also Fig. 5.2). These data indicate that there is a greater effect in the expression of Tuj1 in neurosphere cells when the inhibitor is used for 4 days instead of 2. Consequently, the DAPT exposure period of 4 days was selected for subsequent experiments.

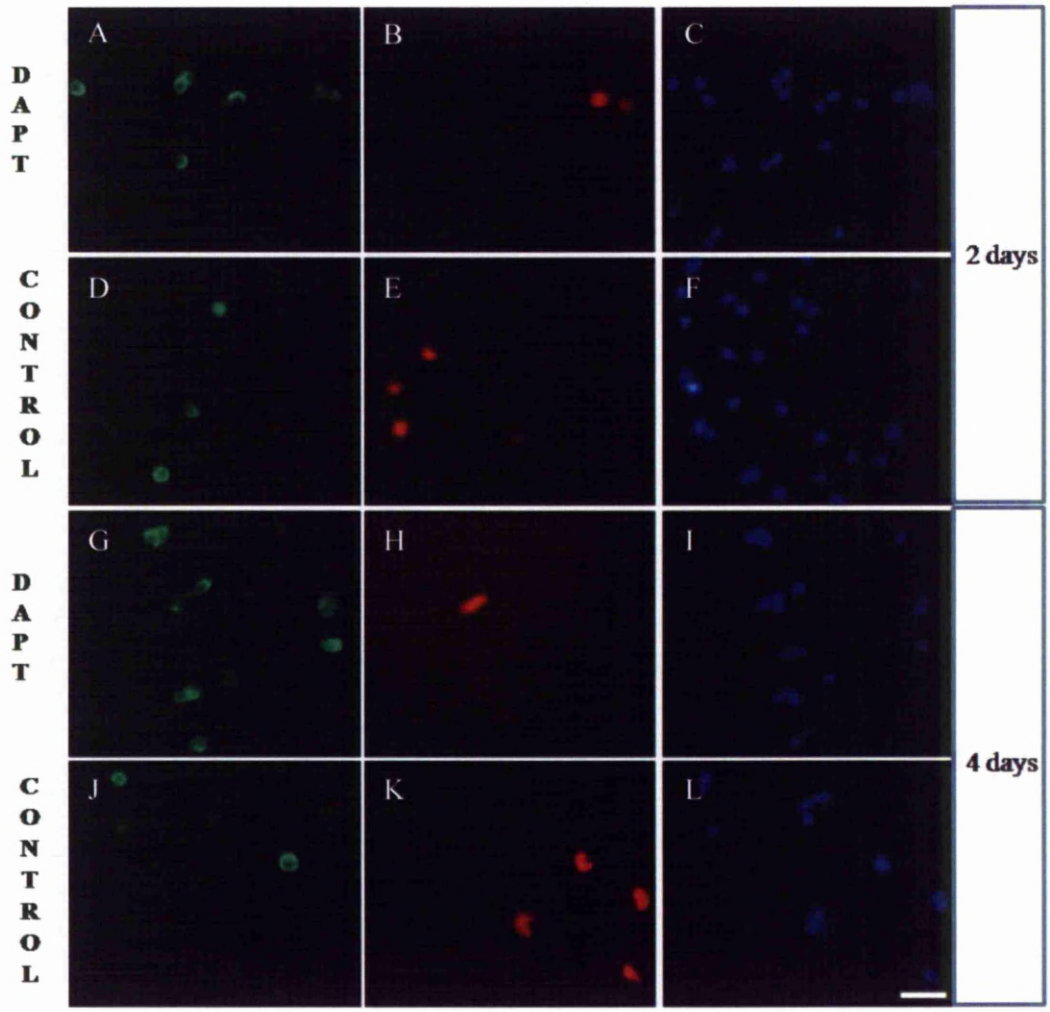

Figure 5.3. **Expression of Tuj1 and staining for EdU after 2 and 4 days DAPT treatment.**

Embryonic mouse primary neurospheres after 15 day culture in 60mm non adherent dishes were incubated for 2 (A) or 4 (B) days with medium containing 10μM DAPT. At the end of treatment neurospheres were then treated with 10μM

EdU for 1h, washed and dissociated into a single cell suspension before seeding in Permanox chamber slides. The cells were allowed to attach and spread for 3h in the presence or absence of DAPT before they were fixed and stained for Tuj1(A, D, G, J) and EdU (B, E, H, K). Nuclei were stained with DAPI (C, F, I, L). Scale bar is 25 μm.

5.2.2. Inhibition of Notch signaling promotes neuronal differentiation.

Having decided the optimum conditions to inhibit Notch signaling, neurospheres were treated for 4 days with DAPT in order to examine the effect of the Notch inhibitor on GFAP, Sox10 and S100 expression. Data (Fig. 5.4) showed an expected increase in the total number of $Tuj1^+$ cells from 23% to 48%, in addition to a reduction in the EdU^+ cells from 19% to 10%. While the number of cells expressing NOS and S100 did not change after DAPT treatment, the numbers of $Sox10^+$ and $GFAP^+$ cells decreased from 45% to 34% and from 52% to 44% respectively, but the reduction was not statistically significant (also see Fig. 5.5a, 5.5b and 5.5c). The results of the phenotypic expression of the markers examined in the sample used

as control was in agreement with what was shown in Chapter 4, Fig. 4.8 where the phenotypes of 15 days (after 1h pulse) and 19 days old (after 4 days chase) neurospheres were compared, indicating that the DMSO treatment itself didn't have any effect on expression of these markers.

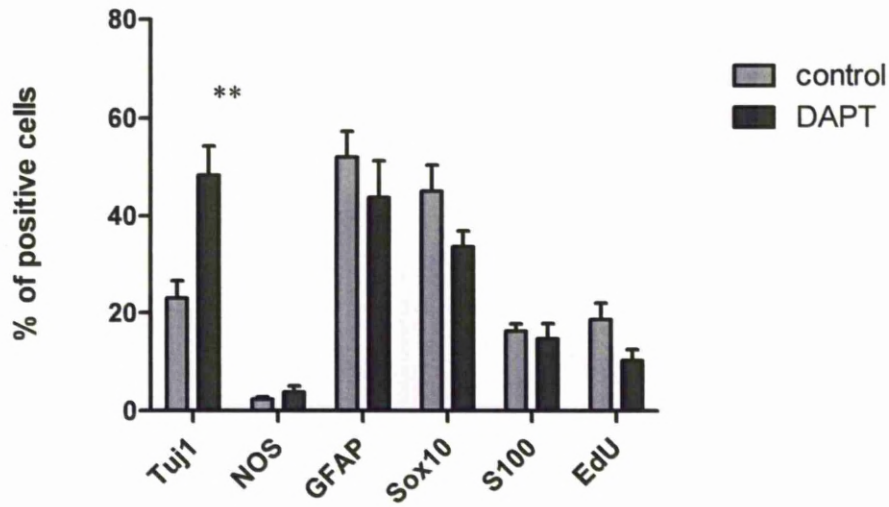

Figure 5.4. **Effect of 4 days DAPT treatment on the percentage of cells positive for each phenotype or incorporating EdU at the end of the treatment.**

Embryonic mouse primary neurospheres after 15 day culture in 60mm non adherent dishes were incubated for 4 days with medium containing 10μM DAPT. At the end of treatment neurospheres were then treated with 10μM EdU for 1h, washed and dissociated into a single cell suspension before seeding into chamber slides. The cells were allowed to attach and spread for 3h in the presence or

absence of DAPT and they were fixed and stained for the markers Tuj1, NOS, GFAP, Sox10, S100 and EdU. Immunopositive cells were counted in random optical fields (n= 5-10) of each chamber with a 40X oil objective. The total number of cells per optical field was quantified by counting the number of nuclei stained with DAPI. Error bars represent the SEM from different experiments (n= 3-5). A two tailed unpaired t-test was performed for the markers Tuj1 ($p= 0.007$), Sox10 ($p= 0.16$) and EdU ($p= 0.07$). ** = p value < 0.01.

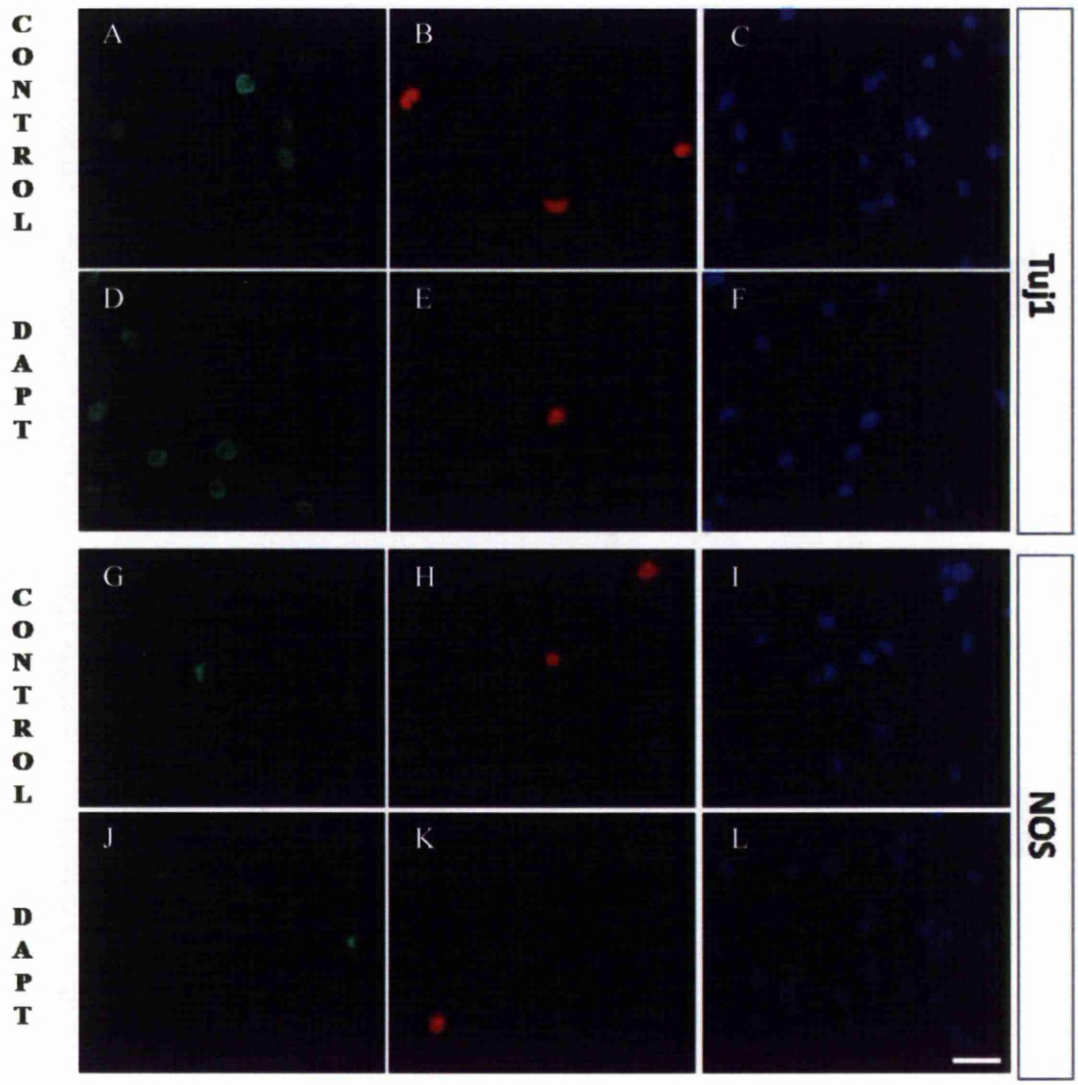

Figure 5.5a. **Phenotypic expression of neurosphere-derived cells after 4 days of treatment with DAPT.**

Neurosphere cells were treated as described in Fig. 5.4. They were stained for the markers TuJ1 (A, D), NOS (G, J), and EdU (B, E, H, K). Nuclei were stained with DAPI (blue). Scale bar is 25μm.

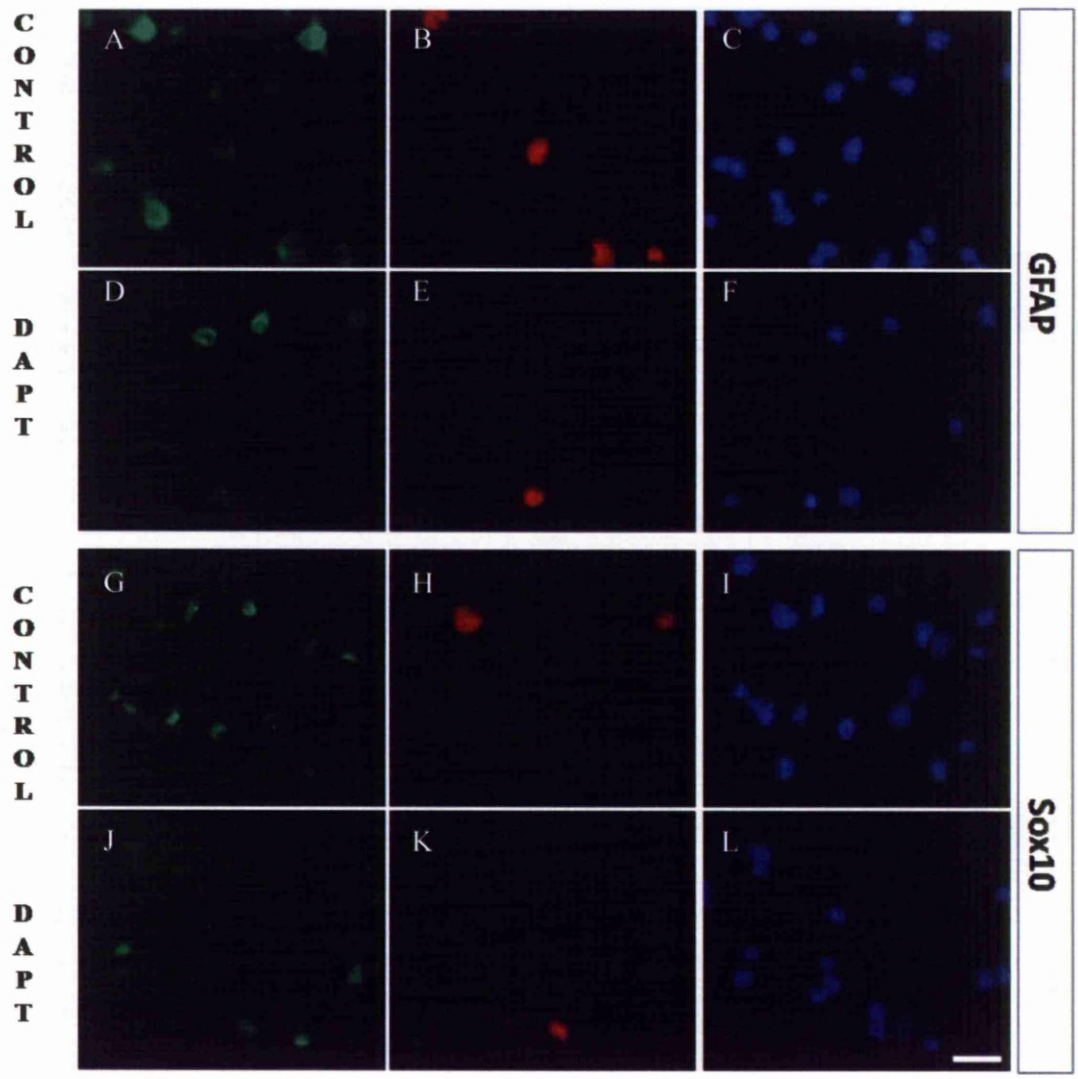

Figure 5.5b. **Phenotypic expression of neurosphere-derived cells after 4 days of treatment with DAPT.**

Neurosphere cells were treated as described in Fig. 5.4. They were stained for the markers GFAP (A, D), Sox10 (G, J) and EdU (B, E, H, K). Nuclei were stained with DAPI (blue). Scale bar is 25μm.

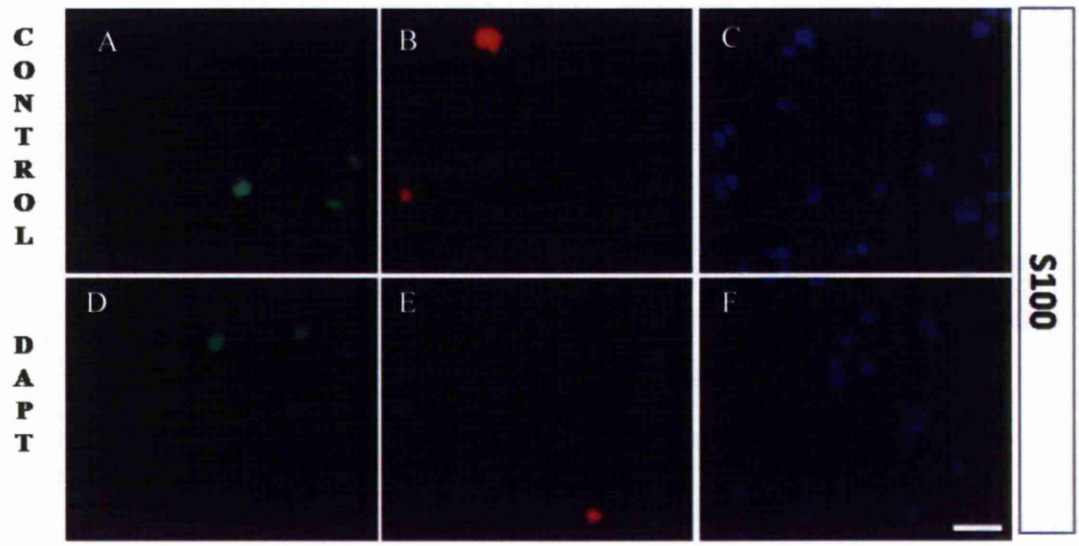

Figure 5.5c. **Phenotypic expression of neurosphere-derived cells after 4 days of treatment with DAPT.**

Neurosphere cells were treated as described in Fig. 5.4. They were stained for the markers S100 (A, D) and EdU (C, F). Nuclei were stained with DAPI (blue). Scale bar is 25μm.

5.2.3. Effect of Notch signaling inhibition in a pulse/chase experiment

The question was whether differentiation of the fast dividing cells found at the periphery of neurospheres (Chapter 4) is regulated by the Notch signaling pathway. After the pulsing with EdU for 1h followed by 4 days chase in the presence of Notch inhibitor DAPT, the percentage of total $Tuj1^+$ cells increased over 2-fold compared to that immediately after the 1h pulse or after the chase in the absence of DAPT (Fig. 5.6). The proportions of $GFAP^+$ and $Sox10^+$ cells in the DAPT treated neurospheres were also decreased but for the $GFAP^+$ population that reduction was significant when compared to the 1h values. The percentages of NOS^+ and $S100^+$ were not affected by the presence of DAPT for 4 days (See also Fig. 5.9a, 5.9b and 5.9c).

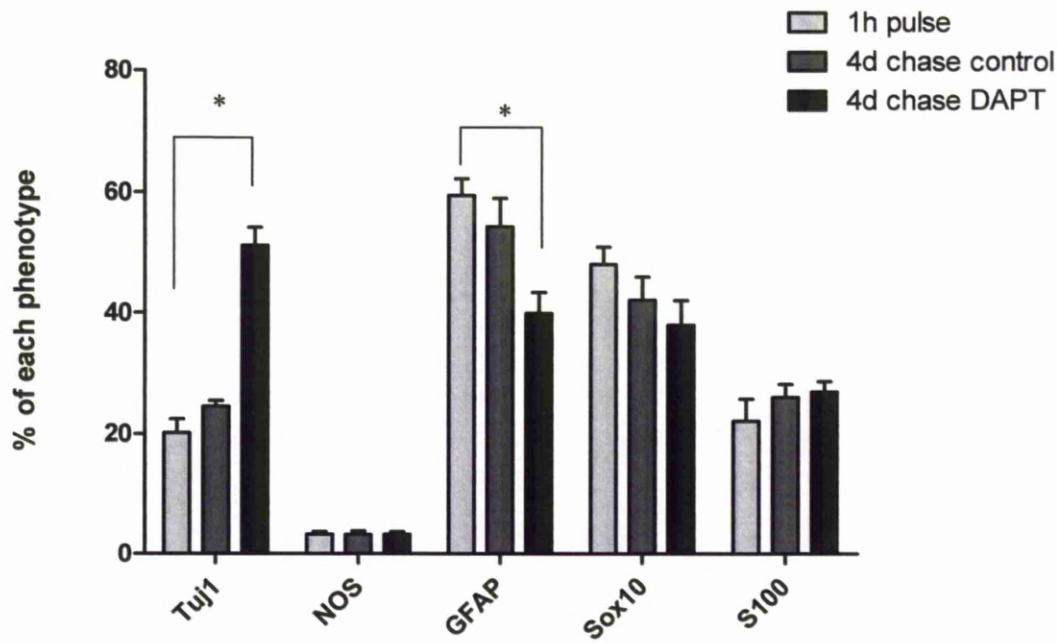

Figure 5.6. **Effect of DAPT on the percentage of neurosphere cells expressing different markers after 1h EdU pulse with and without a 4 day chase.**

Embryonic mouse primary neurospheres after 15 day culture in 60mm non adherent dishes were pulsed for 1h with 10μM EdU. Immediately after the EdU pulse and the 4 day chase with or without DAPT, neurospheres were dissociated into single cells which were allowed to attach and spread in Permanox chamber slides for 3h. Cells were then fixed and stained for different markers. Immunopositive cells were counted in random optical fields (n= 10) of each

chamber using the 40X oil objective. The total number of cells per optical field was quantified by counting the total number of nuclei stained with DAPI. Error bars represent the range from two individual experiments (n= 2). A two tailed unpaired t-test was performed for the markers Tuj1 (p= 0.02) and GFAP (p= 0.047). * = p value < 0.05.

Interestingly, with DAPT treatment, the percentage of EdU^+ cells decreased significantly when compared with both the number of EdU^+ cells straight after the pulse and in controls after the chase (Fig. 5.7 and 5.8). As shown in neurosphere sections (Fig. 5.8), levels of EdU^+ cells in DAPT treated neurospheres did not have a great variation as observed in controls. Their EdU fluorescence signal was more similar to the high level EdU^+ cells of the control.

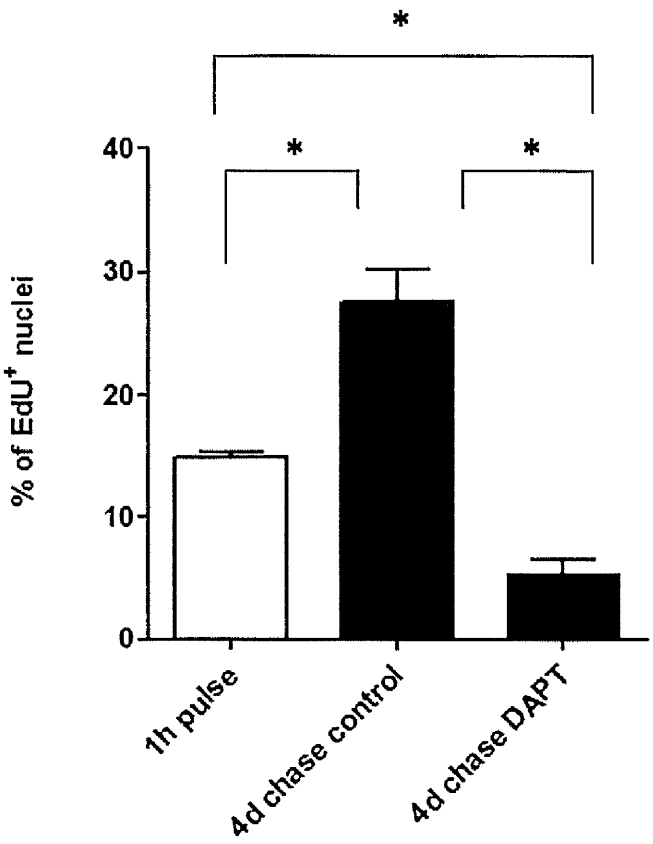

Figure 5.7. **Effect of DAPT on the percentage of EdU+ nuclei after 1h EdU pulse with and without a 4 day chase.**

Neurosphere cells were cultured and stained as described in Fig. 5.6. Error bars represent range from two experiments (n= 2). A two tailed unpaired t-test was performed. * = p value < 0.05.

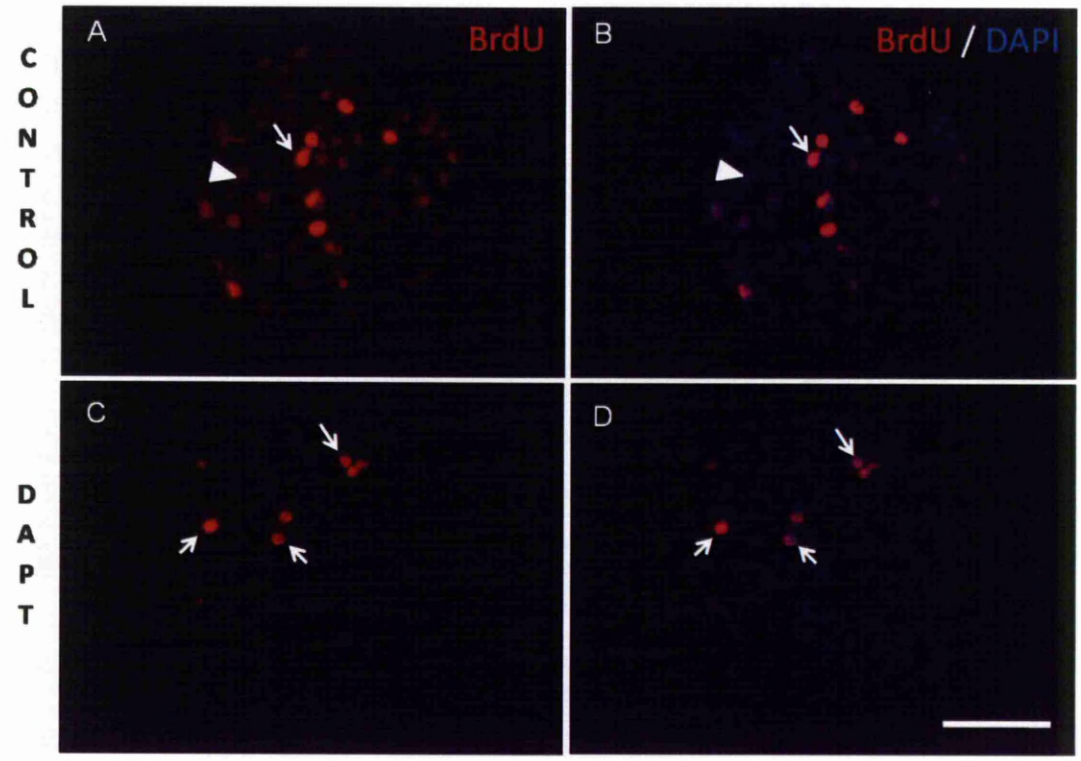

Figure 5.8. **Effect of DAPT treatment on EdU$^+$ nuclei in neurosphere sections at the end of a 4 day chase.**

Embryonic mouse primary neurospheres after 15 day culture in 60mm non adherent dishes were pulsed for 1h with 10μM EdU. At the end of the 4 day chase with (C, D) or without DAPT (A, B), neurospheres were sectioned in 8μm thick slices and stained for EdU (red). Nuclei were stained with DAPI. Arrows indicate EdU$^+$ nuclei and arrowheads nuclei with low levels of incorporated EdU. Scale bar is 50μm.

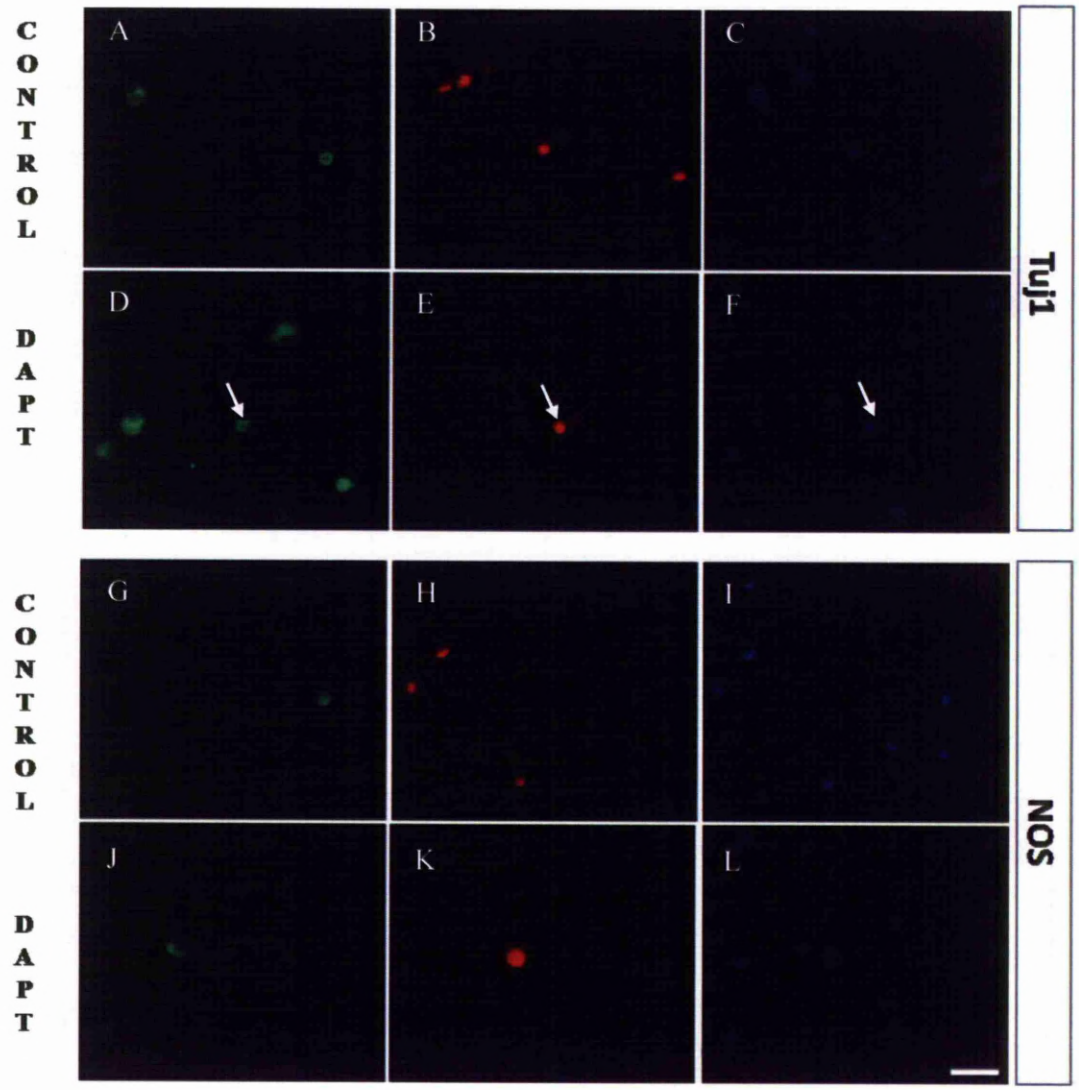

Figure 5.9a. **Co-localisation of neurosphere-derived cell markers with EdU incorporation 4 days after EdU chase in DAPT treated neurospheres.**

Embryonic mouse primary neurospheres after 15 day culture in 60mm non adherent dishes were incubated with 10μM EdU for a further 1h and then cultured

in absence of EdU for 4 days (chase). During the chase neurospheres were cultured with 10μM DAPT or without (control). At the end of the chase neurospheres were dissociated and single cells were left to attach and spread for 3h in adherent Permanox chamber slides in the presence of DAPT. They were then fixed and stained for TuJ1 (A, D), NOS (G, J) and EdU (B, E, H, K). Nuclei were stained with DAPI (blue). Arrows represent cells with dual labeling. Scale bar is 25μm.

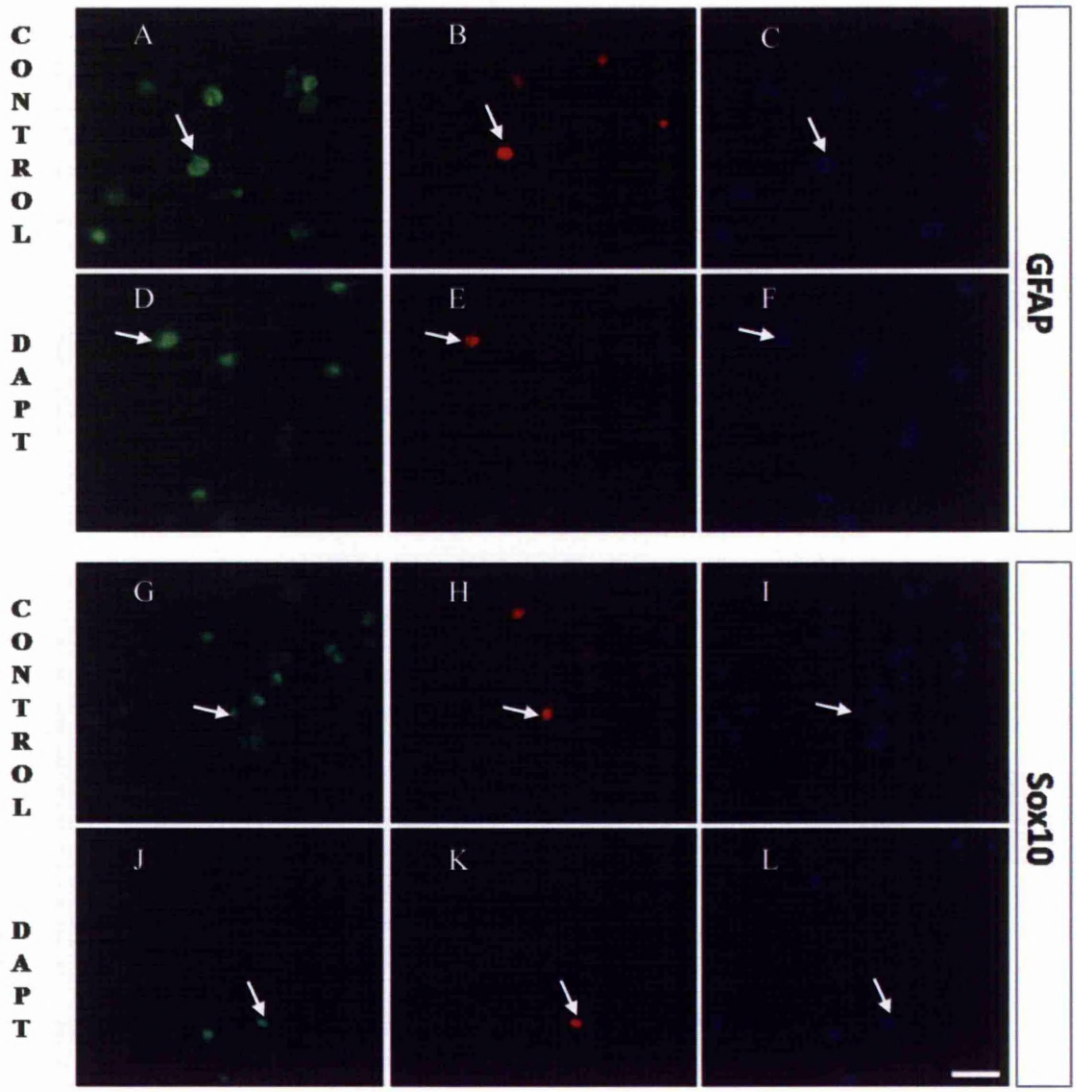

Figure 5.9b. **Co-localisation of neurosphere-derived cell markers with EdU incorporation after 4 days chase in DAPT treated neurospheres.**

Neurospheres were treated and dissociated as described in Fig. 5.9a. After fixation cells were stained for GFAP (A, D), Sox10 (G, J) and EdU (B, E, H, K). Nuclei

were stained with DAPI (blue). Arrows represent cells with dual labeling. Scale bar is 25μm.

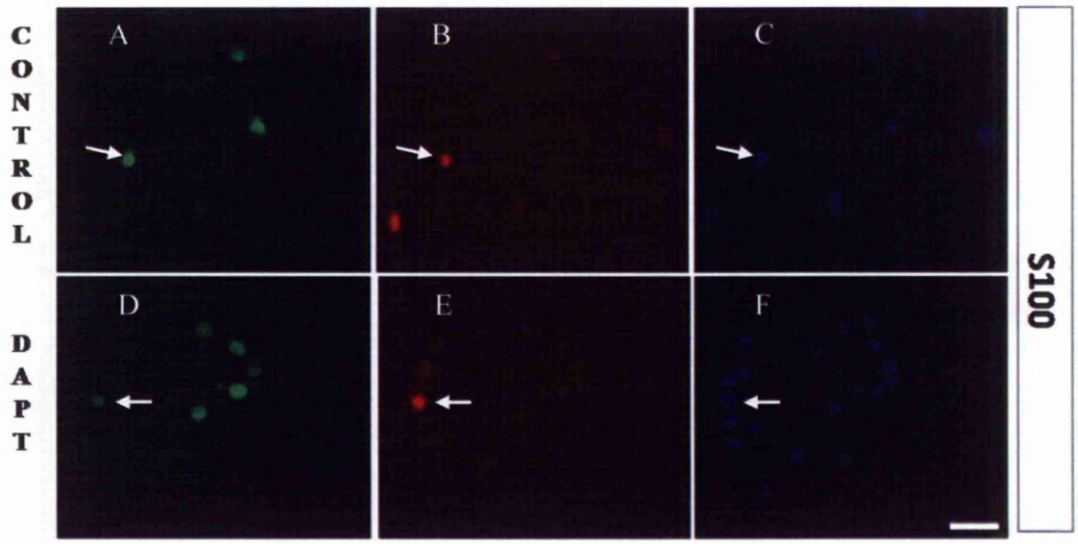

Figure 5.9c. **Co-localisation of neurosphere-derived cell markers with EdU incorporation after 4 days chase in DAPT treated neurospheres.**

Neurospheres were treated as described in Fig. 5.9a. After fixation cells were stained for S100 (A, D) and EdU (B, E). Nuclei were stained with DAPI (blue). Arrows represent cells with dual labeling. Scale bar is 25μm.

As shown in Fig. 5.10 the phenotype of EdU^+ cells changed over the 4h chase, consistent with that shown before (Chapter 4, Fig. 4.12). However, in the case of DAPT treatment the effect is greater than the control. Specifically, the number of $Tuj1^+EdU^+$ cells after the pulse was around 6% but after 4 days of chase and DAPT treatment it reached 42%. Also, the reduction of $GFAP^+EdU^+$ and $Sox10^+EdU^+$ cell populations was more pronounced when compared to the control. There was an increasing trend in the $S100^+EdU^+$ population control after 4d of chase (from 25% after pulse to 40% at the end of chase) but in the presence of DAPT during the chase, the percentage only increased to 30% which was not significant (Fig. 5.10). This result implies that the Notch inhibitor possibly blocked the differentiation of EdU^+ cells towards the $S100^+$ phenotype.

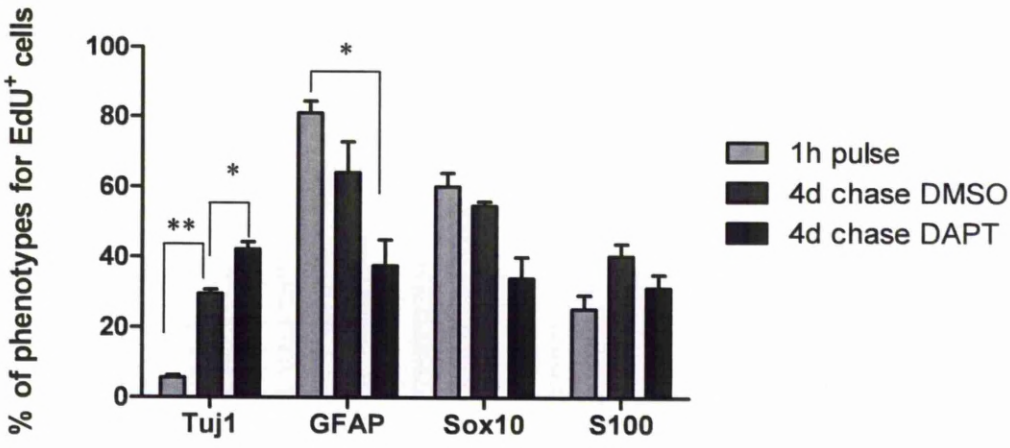

Figure 5.10. **Co-expression of phenotypic markers in EdU^+ cells after 1h EdU pulse with and without 4 day chase.**

Neurosphere cells were cultured and stained as described in Fig. 5.6. Error bars represent the range from two experiments (n= 2). A two tailed unpaired t-test was performed for all the markers. Sox10: 1h vs 4d control, p value= 0.32; 1h vs 4d DAPT, p value= 0.07; 4d control vs 4d DAPT, p value= 0.08. [S100: p value > 0.1 for all the combinations]. * = p value < 0.05, ** = p value < 0.01.

5.2.4. Downregulation of Notch targeted genes upon DAPT treatment.

In order to confirm that DAPT inhibits canonical Notch signaling pathway in neurosphere cells, mRNA was extracted and the levels of Hes1 and Hes5 were quantified using real time RT-PCR. As shown in Fig. 5.11 the levels of Hes1 with DAPT treatment were reduced by approximately 50% whereas the reduction in Hes5 was even greater. Agarose gel electrophoresis of the qRT-PCR products was also consistent with these changes in mRNA levels (Fig. 5.12). However, in the case of Hes5, 2 products can be seen, 183 and 269bp (Fig. 5.12). The cDNA and genomic sequences for Hes5 obtained from Ensembl (Fig. 5.13) and those of the sequenced PCR products (Fig. 5.14), revealed that the smaller size band (183bp) is derived from the 1^{st} and the 2^{nd} exons of the Hes5 gene, whereas the bigger band included the intron sequence (86bp) between the 1^{st} and 2^{nd} exon (unspliced product).

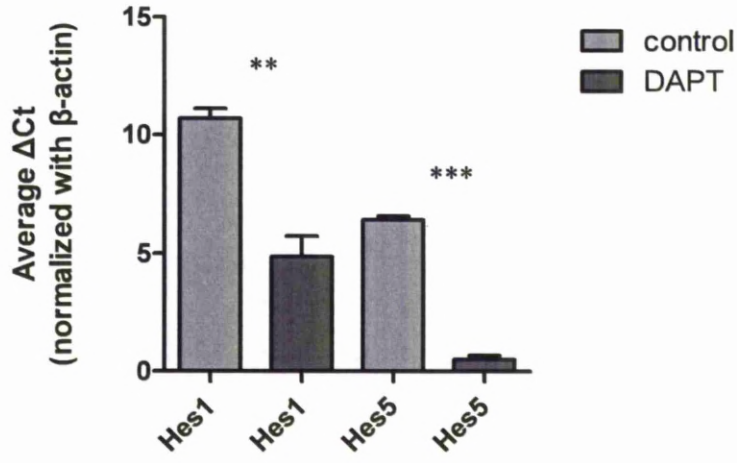

Figure 5.11. **Levels of Hes1 and Hes5 mRNA in neurospheres treated with DAPT.**

Following 4 days of treatment with DAPT as described in the previous figures, mRNA was extracted from neurospheres using Trizol. cDNA was synthetized and real-time PCR was performed to quantify the levels of Hes1 and Hes5 in control and DAPT treated neurospheres. Error bars represent SEM from 3 experiments (n=3). Levels of Hes1 and Hes5 in DAPT treated neurospheres were significantly reduced. ** = p value < 0.01, *** = p value < 0.001.

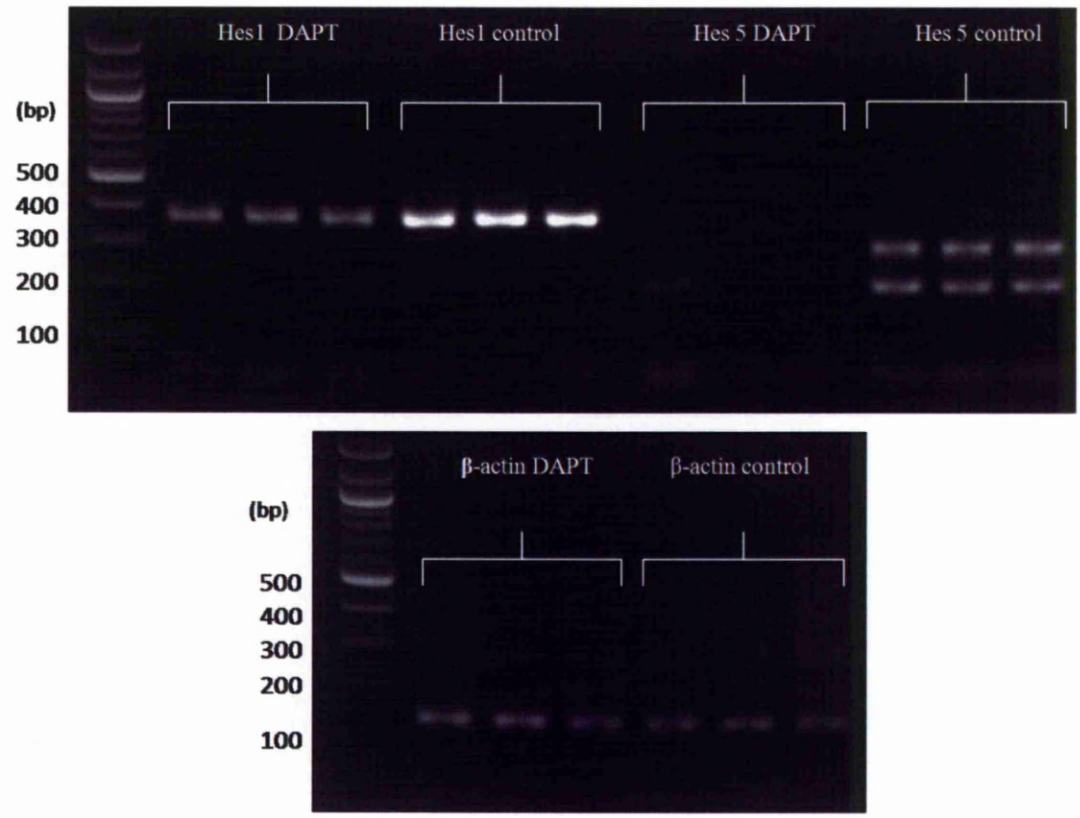

Figure 5.12. **Agarose gel electrophoresis showing the expression of Hes1, Hes5 and β-actin in DAPT treated neurospheres.**

The PCR product obtained from the experiment in Fig. 5.11 was loaded in a 2% agarose gel and an electrophoresis was performed (140V, 1000mA, 20min). Each PCR reaction was done in triplicate as shown in figure. The band sizes were: Hes 1=354bp, Hes 5= 183bp and 269bp and β-actin= 143bp.

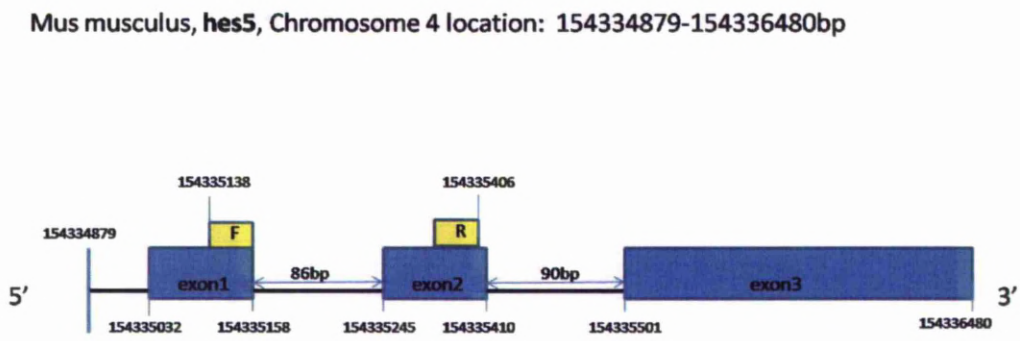

Figure 5.13. **Genomic map of Hes5. Source Ensembl.**

Figure shows that Hes 5 gene consists of 3 exons. The forward primer (F) is located at the 3' end of the first exon and the reverse primer is located to the 3' end of exon 2. If the mRNA is not spliced a band size of 269bp will be present at the end of the PCR reaction.

>Nucleotide alignment of 2 sequences: theoretical 183bp VS 183F

Identities = 146/188 (77%), Positives = 146/188 (77%), Gaps = 33/188 (17%)

```
theoretical 183bp     1 AGTCCCAAGGAGAAAAACCGACTGCGGAAGCCGGTGGTGGAGAAGATGCGTCGGGACCGC   60
                                CGA  G GG          GG GA   TGCGTCGGGA CGC
183F                  1 -----------------TCGAACGGGGG----------GGGGAGAGTGCGTCGGGA-CGC   52

theoretical 183bp    61 ATCAACAGCAGCATAGAGCAGCTGAAGCTGCTGCTGGAGCAGGAGTTCGCGCGGCACCAG  120
                        ATCAACAGCAGCATAGAGCAGCTGAAGCTGCTGCTGGAGCAGGAGTTCGCGCGGCACCAG
183F                 53 ATCAACAGCAGCATAGAGCAGCTGAAGCTGCTGCTGGAGCAGGAGTTCGCGCGGCACCAG   92

theoretical 183bp   121 CCCAACTCCAAGCTGGAGAAGGCCGACATCCTGGAGATGGCCGTCAGCTACCTGAAACAC  180
                        CCCAACTCCAAGCTGGAGAAGGCCGACATCCTGGAGATGGCCGTCAGCTACCTGAAACAC
183F                 93 CCCAACTCCAAGCTGGAGAAGGCCGACATCCTGGAGATGGCCGTCAGCTACCTGAAACAC  152

theoretical 183bp   181 AGC----- 183
                        AGC
183F                153 AGCAATCC 160
```

>Nucleotide alignment of 2 sequences: 269F VS theoretical 269bp

Identities = 236/274 (86%), Positives = 236/274 (86%), Gaps = 31/274 (11%)

```
269F                  1 --------GGGGTTATGCCG------------------GGTGGGCGCCGTCCGGTTCCCC   34
                            GG G  A  CCG                    GG G GCGCCGTCCGGTTCCCC
theoretical 269bp     1 AGTCCCAAGGAGAAAAACCGAGTAAGTGCAACTCGCCCGGCGCGCGCCGTCCGGTTCCCC   60

269F                 35 CGGGGCCTCCGGCGTCCGCCGCCCACCTGACGCCTCTCCTCCCGCAGCTGCGGAAGCCGG   94
                        CGGGGCCTCCGGCGTCCGCCGCCCACCTGACGCCTCTCCTCCCGCAGCTGCGGAAGCCGG
theoretical 269bp    61 CGGGGCCTCCGGCGTCCGCCGCCCACCTGACGCCTCTCCTCCCGCAGCTGCGGAAGCCGG  120

269F                 95 TGGTGGAGAAGATGCGTCGGGACCGCATCAACAGCAGCATAGAGCAGCTGAAGCTGCTGC  154
                        TGGTGGAGAAGATGCGTCGGGACCGCATCAACAGCAGCATAGAGCAGCTGAAGCTGCTGC
theoretical 269bp   121 TGGTGGAGAAGATGCGTCGGGACCGCATCAACAGCAGCATAGAGCAGCTGAAGCTGCTGC  180

269F                155 TGGAGCAGGAGTTCGCGCGGCACCAGCCCAACTCCAAGCTGGAGAAGGCCGACATCCTGG  214
                        TGGAGCAGGAGTTCGCGCGGCACCAGCCCAACTCCAAGCTGGAGAAGGCCGACATCCTGG
theoretical 269bp   181 TGGAGCAGGAGTTCGCGCGGCACCAGCCCAACTCCAAGCTGGAGAAGGCCGACATCCTGG  240

269F                215 AGATGGCCGTCAGCTACCTGAAACACAGCCTTGT  248
                        AGATGGCCGTCAGCTACCTGAAACACAGC
theoretical 269bp   241 AGATGGCCGTCAGCTACCTGAAACACAGC-----  269
```

Figure 5.14. **Sequencing alignment of the theoretical sequences for the Hes5 PCR products as predicted by Ensembl with the sequences of DNA from the gel-extracted bands.**

Alignments generated using the software Geneious Basic 5.4.3 (Biomatters Ltd) showed a high similarity between the theoretical sequences for 183bp (77%) and 269bp (86%) obtained from Ensembl (see also Fig. 12) and the sequences determined of the two PCR products of Hes5 cDNA.

5.2.5. Notch signaling and cell migration

As discussed previously, the notch signaling inhibitor DAPT blocked proliferation and promoted neuronal differentiation of neurosphere cells. It was therefore interesting to see whether Notch signaling inhibition had an effect on the migratory properties of neurosphere cells.

After 1 day of culture in adherent conditions (pre-coated chamber slides with poly-D-lysine and laminin), neurospheres which had been pre-treated 4 days with DAPT (Fig. 5.15B, D, and F) had much longer neurites, ~80µm (Fig. 5.15, arrows) and the number of cells that migrated away from the neurosphere was higher than in untreated controls. Not all the control neurospheres had developed neurites by day 1 and wherever these were present they were shorter in length than those in DAPT treated cultures. After 3 days in culture, there were many cells migrating away from the neurospheres in both control and DAPT-treated culture, although the DAPT treated cultures appeared to have larger outgrowths (compare Fig.

5.15E with F). Neurites were not visible on day 3, because of the large number of migratory cells moving away from the neurosphere (Fig. 5.15F).

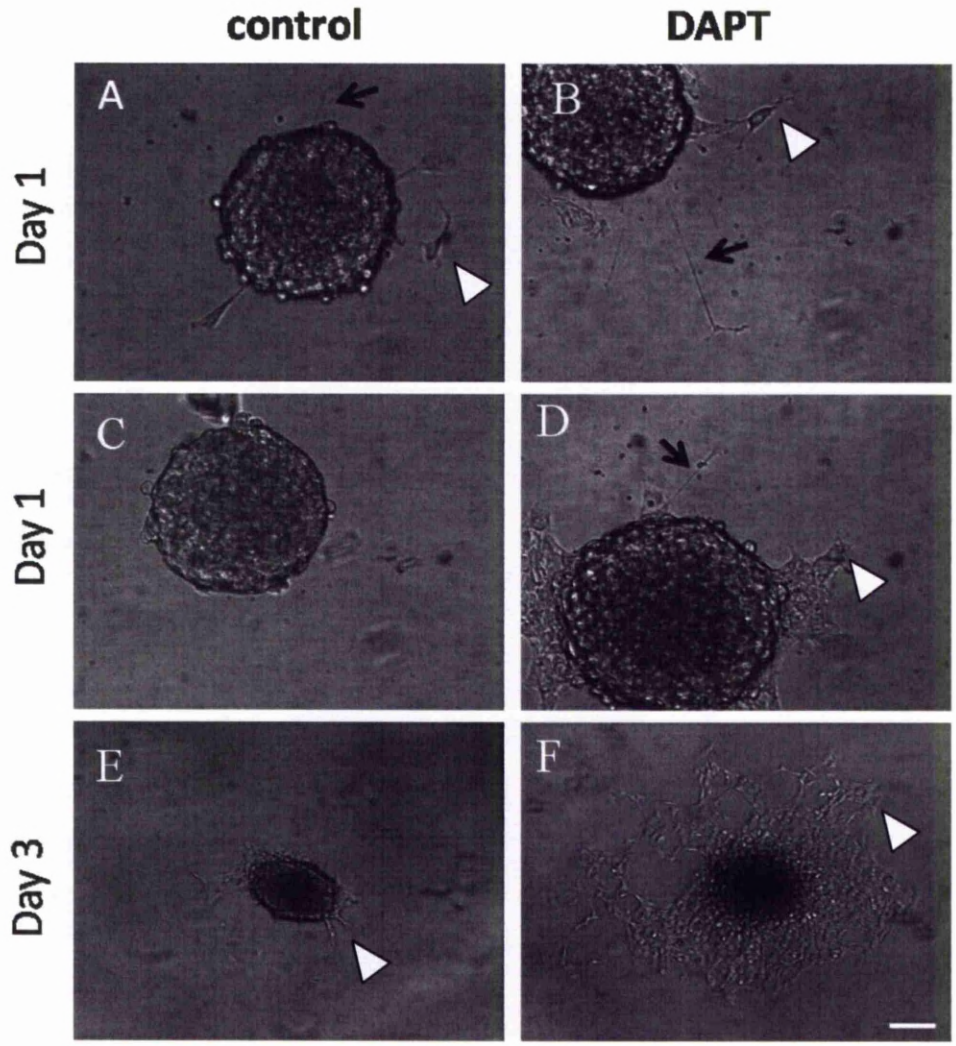

Figure 5.15. **Effect of DAPT notch signaling inhibitor on neurosphere cell migration and neurite development.**

Embryonic mouse primary neurospheres after 15 days in culture in 60mm non adherent dishes were supplemented with 10μM DAPT for 4 days. Neurospheres

were then transferred in DAPT supplemented medium to 8 well glass chamber slides (2 neurospheres per chamber) which were pre-coated with poly-D-lysine and laminin. Migratory cells (arrow heads) and neurites (arrows) were apparent after 1 day. However, in the control there were some neurospheres without any migratory cells and neurites after 1 day (C). More cells migrated out from the neurosphere by day 3 in both control (E) and DAPT treatment (F). Neurites on day 3 could not be counted due to the high number of migratory cells. Scale bar is 25μm for A-D and100μm for E and F.

Immunostaining for the markers Tuj1 and NOS (Fig. 5.16) of DAPT treated neurospheres upon adhesion onto chambers for 3 days, still in the presence of the inhibitor, revealed the presence of $Tuj1^+$ fibers among migratory cells in both control and DAPT-treated neurospheres. Also Tuj1 immunoreactivity was present in the neurospheres. High magnification pictures showed $Tuj1^+$ positive fibers adjacent to nuclei of migratory cells (Figs. 5.16C and G). In control, these fibers looked like were derived from cells in the neurosphere and not from the migratory cells (Fig. 5.16C). On the contrary, in DAPT-treated cultures, there were more $Tuj1^+$ fibers among nuclei of migratory cells and we could also observe an increase in $Tuj1^+$ signal in points where fibers were in very close proximity to some nuclei, implying that these cells could be $Tuj1^+$ (Fig. 5.16G, arrows).

In both control and DAPT-treated neurospheres most of the migratory cells were NOS^- (Fig. 5.16B, F). In the controls we observed NOS immunoreactivity at the periphery of the neurosphere but only to the part which was attached or in close proximity to the substrate (Fig. 5.16B, D). In the DAPT-treated neurospheres NOS^+ cells could be observed at the sites where cells were leaving the neurosphere and migrating on the substrate (Fig. 5.16F, H). It was difficult to observe if these NOS^+ cells were migratory or still in the neurosphere as this area of the DAPT-treated neurospheres was less clear than in the control.

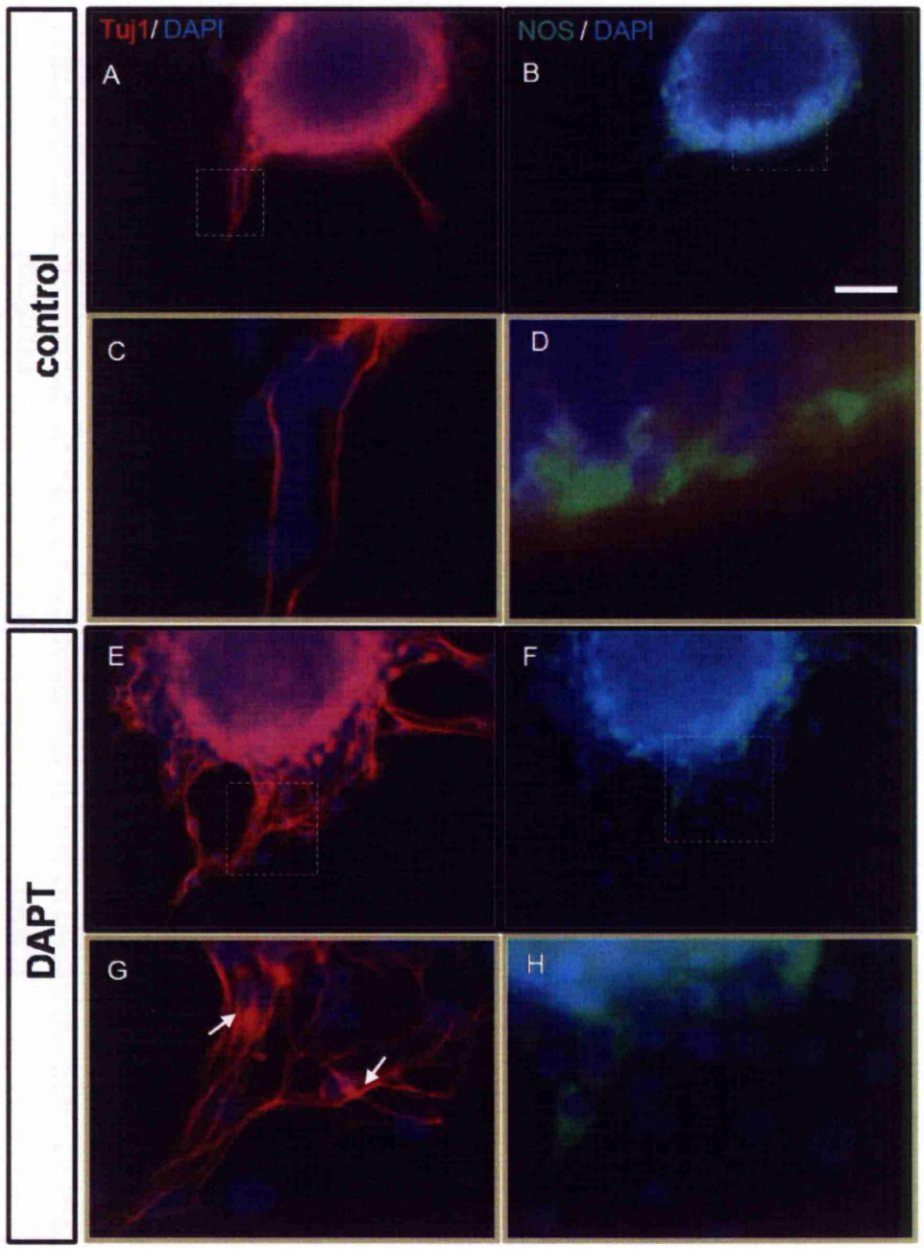

Figure 5.16. **Expression of Tuj1 and NOS in migratory neurosphere cells after DAPT treatment.**

Embryonic mouse primary neurospheres after 15 days in culture in 60mm non adherent dishes were supplemented with 10μM DAPT for 4 days or they were left untreated (control). Neurospheres were transferred to pre-coated chambers as described in Fig. 10 in the presence of DAPT . After 3 days cells were fixed and stained for the markers Tuj1 (A, C, E, G) and NOS (B, D, F, H). Pictures C, D, G and H represent higher magnification of the box inset in pictures A, B, E and F respectively. Scale bar is 50μm.

Quantification of the above observations showed that after 1 and 3 days in adherent conditions the distance covered by the most distal cell was significantly higher in the DAPT treated neurospheres compared to the control (Fig. 5.17A and B). When DAPT treated neurospheres were transferred to the chambers in the absence of DAPT, the effect of DAPT treatment was still evident at day 3 when the distance covered by the furthest migratory cell was significantly higher than the controls. In the case where untreated neurospheres were transferred to the chambers in the presence of DAPT, even after only 1 day the covered distance for the DAPT condition was significantly higher (51μm) compared to the control (8.4 μm) (Fig. 5.17E, F). These data indicate that the Notch inhibitor rapidly

stimulates the migratory behaviour of neurosphere cells and that this effect remains upon inhibitor removal.

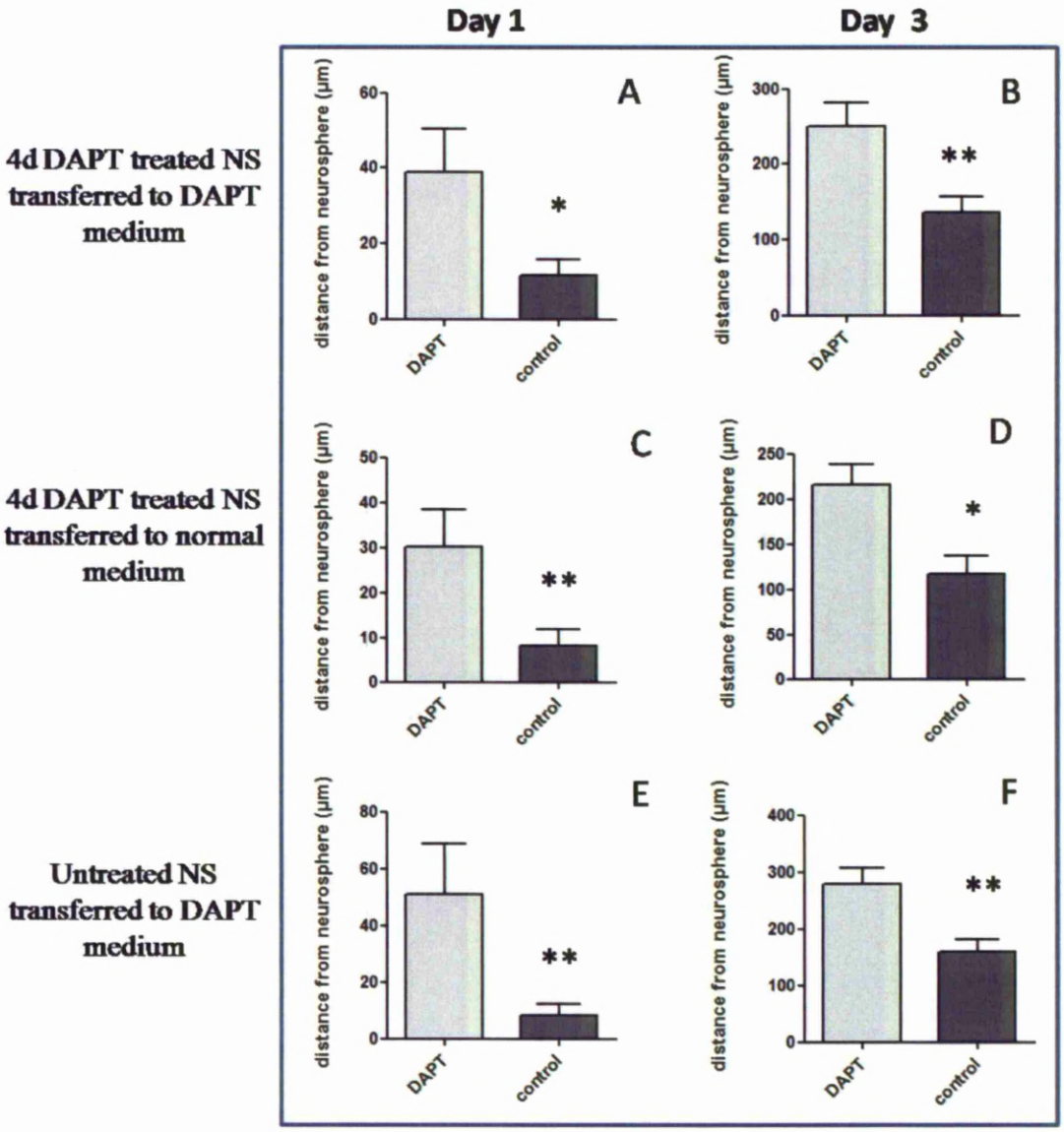

Figure 5.17. **Effect of DAPT notch signaling inhibitor on the migration of neurosphere cells.**

Embryonic mouse primary neurospheres after 15 days in culture in 60mm non adherent dishes were supplemented with 10μM DAPT for 4 days or they were left untreated. Following that, neurospheres were transferred into pre-coated 8 well glass chambers as described in Fig. 5.15. The distance covered by the furthest migratory cell was measured after 1 and 3 days using ImageJ and that was monitored in three different experimental conditions; 4 day DAPT treated neurospheres were transferred to chambers with DAPT medium (A-B), 4 day DAPT treated neurospheres were transferred to chambers with normal neurosphere medium (C-D) and untreated neurospheres were transferred to chambers with medium containing DAPT (E-F). Error bars represent SEM between different neurospheres (n= 8-10 for DAPT treated and n= 17-22 for the control). * = p value < 0.05, ** = p value < 0.01 (unpaired two tailed t-test).

In Figure 5.18 the number and the length of the longest neurite were counted after 1 day in adherent culture conditions. When DAPT treated neurospheres were transferred to the chambers in the presence of DAPT, an increase in the number of neurites per neurospheres was observed (Fig. 5.18A) but more strikingly the length of these neurites was significantly greater (89 μm) compared to the control (15 μm) (Fig. 5.18B). In the conditions where DAPT was removed from the medium upon neurosphere transfer to adherent conditions (Fig. 5.18C, D) or when it was added only in the chambers (Fig. 5.18E, F) there was no statistically significant difference with the control regarding the number of the neurites per neurosphere or their length. However, an increasing trend in the neurite length was observed in the DAPT treated neuropsheres as shown in Fig. 5.18D.

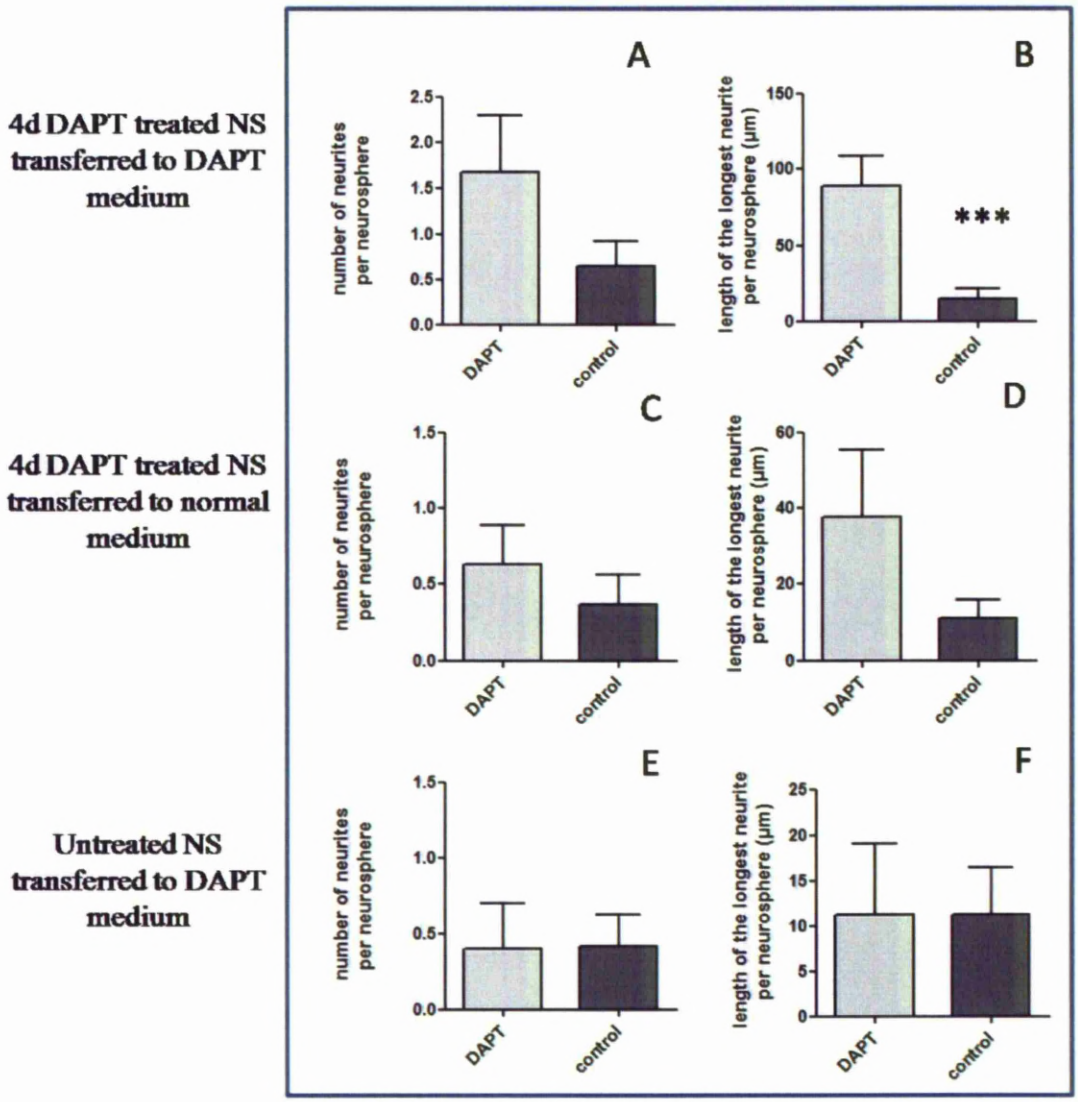

Figure 5.18. **Effect of DAPT notch signaling inhibitor on neurite number and length.**

Embryonic mouse primary neurospheres after 15 days in culture in 60mm non adherent dishes were supplemented with 10µM DAPT for 4 days or they were left untreated. Following that, neurospheres were transferred into pre- coated 8 well

glass chambers as described in Fig.5.15. After 1 day of culture in the pre-coated glass chambers the number of the neurites per neurosphere (A, C, E) as well as the length of the longest neurite per neurosphere (B, D, F) were recorded using ImageJ. Measurements were taken in three different conditions; 4 day DAPT treated neurospheres were transferred to chambers with DAPT medium (A-B), 4 day DAPT treated neurospheres were transferred to chambers with normal medium (C-D) and untreated neurospheres were transferred to chambers with medium containing DAPT (E-F). Experiment was performed once. Error bars represent SEM between different neurospheres (n= 8-10 for DAPT and n= 17-19 for the control). *** = p value < 0.001 (unpaired two tailed t-test).

5.3. Discussion

In the previous chapter, we investigated the behaviour of embryonic mouse caecum-derived neurosphere cells in terms of proliferation and differentiation. The next step was to identify mechanisms which controls this behaviour. We decided to examine the role of Notch signaling in the regulation of proliferation and differentiation of neurosphere cells, as it has been previously shown that ENS progenitors in vivo differentiate prematurely towards the neuronal lineage upon Notch signaling inhibition (Okamura et al., 2008).

5.3.1. Notch signaling inhibition decreases neurosphere cell proliferation

Treatment of neurospheres with DAPT for 4 days and a subsequent 1h pulse with EdU showed a reduction of about 50% of the EdU^+ population (Fig. 5.4). The regulation of proliferation by Notch signaling has been demonstrated before in various tissues. In neurosphere cells derived from the subventricular zone of adult rat brains, prior knock-down of Notch1 expression by siRNA, resulted in a reduction in the number of cells positive for the proliferation marker Ki-67 (Chen et al., 2008).

When the gene encoding the Notch ligand Delta1 was knocked-down by a lentivirus-mediated-RNAi in cultures of human postnatal dental pulp stem cells, their cell cycle progression was inhibited (Wang et al., 2011b). More specifically, there was a high increase of cells in G1 phase and a significant decrease of cells in S phase and also the expression of the proliferating cell nuclear antigen (PCNA), present in the S-phase, was significantly reduced (Wang et al., 2011b). Cultures of adipoce-derived stem cells (ASCs) isolated from adult mice were treated with 5 or 10μM DAPT for a period of 10 days resulting in a reduction of their proliferation in a dose-dependent manner (Jing et al., 2010). These findings together with our results indicate the role of Notch signaling in promoting the proliferation of progenitor cells from various tissues.

5.3.2. Notch signaling inhibition promotes neuronal differentiation in neurosphere cells.

A 4 day inhibition of Notch signaling using the γ-secretase inhibitor DAPT resulted in greater than 2-fold increase in the numbers of $Tuj1^+$ cells in neurospheres whereas for the untreated neurospheres the population of $Tuj1^+$ cells remained the same throughout the 4 day period. Interestingly, the numbers of cells expressing GFAP and Sox10 showed a reductin after the treatment, consistent with the differentiation of $GFAP^+/Sox10^+/Tuj1^-$ cells towards an immature neuronal phenotype $GFAP^-/Sox10^-/Tuj1^+$.

Neuronal differentiation of ENS precursors upon Notch inhibition has also been proposed by Okamura et al. (2008) where they suggested that Sox10 suppression by Mash1 and commitment towards the neuronal lineage was blocked by Notch signaling. ENS progenitors which commit to become neurons lose Sox10 expression (Young et al., 1999). Thus, the increase of the $Tuj1^+$ population after DAPT treatment in our experiments could be a result of neurogenesis from undifferentiated ENS progenitors.

The number of cells expressing S100 did not change after Notch inhibition. Maybe $S100^+$ cells do not contribute to the increase of the $Tuj1^+$ cells or if they do, that could probably happen with the increase of $S100^+$ cells which co-express Tuj1, as we already know that in normal conditions around 20% of the $S100^+$ population co-expressed Tuj1 (Chapter 4, paragraph 4.2.2., Fig. 4.6). Also, no difference was observed in the percentage of NOS^+ cells implying that although around 50% of the cells express the immature marker Tuj1 either they need more time to mature towards a nitrergic neuron or they have differentiated towards another neuronal phenotype that we did not stain for (Hao and Young, 2009).

When we investigated the phenotype of the fast dividing cells which had incorporated EdU at the end of the DAPT treatment, we also observed a significant increase of $Tuj1^+/EdU^+$ cells and a significant decrease of

$GFAP^+/EdU^+$ cells as well as a reducing trend of the $Sox10^+/EdU^+$ population; consistent with what we found by counting the phenotypic expression of all the neurosphere cells. However, in the population of the fast dividing cells at the end of the treatment there was a decreasing trend of the $S100^+/EdU^+$ cells. The marker S100 has been used to label ENS glia (Young et al., 2003) although it can be expressed by ENS neuronal progenitors in vitro (Joseph et al., 2011). Thus, the decrease of the $S100^+/EdU^+$ cells at the end of the chase could represent a decrease in the number of dividing uncommitted progenitor cells or a decrease in the number of cells which differentiate towards the glial lineage, or even both. Glial differentiation promoted by Notch signaling has been demonstrated before in cultures of embryonic rat sciatic nerve-derived neural crest cells (Morrison et al., 2000), although in that study the marker GFAP was used to identify glial cells, a marker which as we discussed before can also be expressed in non-glia neuronal progenitors making it difficult to distinguish glia from ENS progenitors.

5.3.3. Inhibition of Notch signaling could result in loss of recently dividing neurosphere cells

The percentage of EdU^+ cells at the end of the chase in the presence of DAPT shows a reduction relative both to controls at this time and is also lower than the number of cells which were labeled at the beginning of the

chase (Fig. 6). That result possibly indicates that dividing cells upon Notch inhibition not only have a reduced proliferation rate but some of them die. In fact, mutant mice lacking presenilin-1, part of the γ-secretase protein complex, showed severe loss of neural progenitors and neurons in their brains by E16.5 (Shen et al., 1997).

After administration of different concentrations of DAPT (1, 2, 5 and 10μM) in cultures of human tongue carcinoma cells (Tca8113) increased apoptosis in a dose-dependent manner was observed as revealed by caspase-3 immunostaining (Grottkau et al., 2009). In addition flow cytometry data showed a G0-G1 cell cycle arrest with DAPT treatment (Grottkau et al., 2009). Again, application of DAPT in human ovarian cancer cells in vitro provoked the arrest of their cell cycle in G1 phase which was dose-dependent. Also, by administering 50μM DAPT for 24, 48 and 72h these authors detected apoptotic cells and their increase was time-dependent. The above data indicate that the reduction of EdU^+ cells observed in our experiments could be a result of induction of apoptosis or cell cycle arrest.

However, Okamura et al. (2008) failed to detect apoptotic cells in vivo in mice with impaired Notch signaling function despite the fact that these authors observed a reduction in the number of proliferating enteric NCCs.

Sometimes though the amount of apoptotic cells can be underestimated as under in vivo conditions apoptotic cells quickly disappear by phagocytosis (Enomoto 2009), thus leaving the possibility open for induction of apoptosis in migratory enteric NCCs upon Notch inhibition.

We should bear in mind that γ-secretase activity is not Notch receptor specific similar to glycosyl-transferases (Okamura et al., 2008). The γ-secretase complex cleaves various protein intramembrane segments including those of the amyloid precursor protein and E-cadherin (De Strooper and Annaert, 2010). As a result, inhibition of γ-secretase activity in order to block Notch signaling can potentially inhibit other signaling pathways which could be involved in cell proliferation, differentiation and survival. Therefore we can conclude that the results observed from γ-secretase treatment are consistent with Notch signaling inhibition, as that was demonstrated with downregulation of Hes1 and Hes5, but we cannot exclude the involvement of other factors resulting from γ-secretase inhibition.

5.3.4. Notch signaling regulates migration of neurosphere-derived cells and neurosphere neurite formation.

Inhibition of Notch signaling in neurosphere cells resulted in the development of more and longer neurites when compared to controls (Fig. 5.18). Also, with Notch inhibition more cells migrated away and were further from the neurosphere when compared to controls (Fig. 5.15 and 5.16). Impairment of neurite outgrowth was observed in primary mouse embryonic brain-derived neurons by transient activation of Notch signaling which was promoted by transfection of plasmid encoding Notch-1 (Berezovska et al., 1999). In addition, in the same study, active Notch signaling was able to retract already formed neurites.

In the CNS, P14 mice lacking both Notch-1 and Notch-2 receptors, were shown to have morphological defects in their migratory cortical neurons, resulting in abnormal positioning of these neurons in the cortex (Hashimoto et al., 2008). Migratory defects resulting in misplacement of facial branchiomotor and cortical neurons were detected in mutant embryonic mice lacking presenilin-1 (Louvi et al., 2004), a protein critical for the intracellular cleavage of Notch receptor (Ables et al., 2011).

In comparison with our results, we did not observe any defects in the cell migration of Notch inhibited neurospheres, on the contrary we could say

that Notch inhibition promoted migration of cells away from the neurosphere. Having shown that Notch inhibition resulted in reduction of proliferating cells and the increase of cells expressing Tuj1, the number of cells coming out of the neurosphere would be unlikely to be due to increased proliferation. Therefore, it is likely to be an other mechanism which promotes the migration of cells away from the neurosphere environment in collaboration with Notch inhibition.

The transmembrane proteins N-cadherins are responsible for cell to cell adhesion and ensure that cells of a tissue are connected strongly together (Weber et al., 2011). Overexpression of N-cadherin in human arterial smooth muscle cells after transfection with a vector encoding N-cadherin, resulted in reduced migration whereas inhibition of N-cadherin with a blocking antibody provoked migration in quiescent human arterial smooth muscle cells (Blindt et al., 2004). Downregulation of Notch signaling in mouse cerebrovascular endothelial cells (ECs) using a γ-secretase inhibitor, resulted in decreased N-cadherin expression (Li et al., 2011) indicating a role for Notch signaling in the regulation of N-cadherin expression. In addition, transgenic mice lacking the Notch activated transcription factor RBP-Jk only in brain endothelial cells, demonstrated downregulation of N-cadherin expression and a perinatal intracranial hemorrhage due to the inadequate integrity of ECs (Li et al., 2011). The

above studies indicate a role for N-cadherin in cell motility and the involvement of Notch signaling in its expression, however if these mechanisms apply to neurospheres derived from enteric NCCs, further experiments will be needed to confirm it.

Another interesting observation though, is the expression of NOS and Tuj1 by migratory cells in DAPT-treated neurospheres as well as the high number of NOS^+ cells in the control in the areas where the neurosphere was attached to the substrate, which consisted of poly-D-lysine and laminin. Laminins have been shown by various groups to promote, in vitro, the migration, expansion and differentiation of neural stem cells (Barros et al., 2010). In particular, when enteric NCCs derived from embryonic chick or quail gut after immunoselection with NC-1 antibody, were cultured on different substrates including laminin, collagen and tissue culture plastic, a significant increase in the number of neurofilament-protein positive neurons in the presence of laminin resulted (Pomeranz et al., 1993). Neurospheres derived from postnatal mouse brains showed high cell outgrowth when they were cultured on laminin substrate (Kearns et al., 2003). In addition, the laminin receptor β1-integrin has been shown to be expressed at the periphery of neonatal rat brain-derived neurospheres (Campos et al., 2004). Finally, laminin acted as a permissive substrate in neurons derived from neonatal rat brains where cells survived in the

absence of glia and extended long neurites (Liesi 1992). All this evidence supports the theory that laminin promotes neuronal differentiation and migration. Therefore, the DAPT-treated neurospheres, which according to Chapter 5 had more $Tuj1^+$ neurons, migrated more extensively on the laminin substrate than the controls and hence the high number of cell outgrowth in the neurospheres. The larger number of NOS^+ cells at the periphery of control neurospheres could be due to the differentiation effect of laminin.

In summary, neurite outgrowth was promoted after Notch inhibition a result which is consistent with what has been described before (Berezovska et al., 1999). On the other hand, the migratory behaviour of neurosphere cells is in contradiction with previous literature as Notch inhibition has not before shown promotion of neurosphere cell migration. However, it is difficult to evaluate the effect of Notch inhibition on migratory cells when other factors can play important roles in cell behaviour.

5.3.5. Conclusions

In this chapter we demonstrated that by inhibiting the Notch signaling pathway we promoted induction of neuronal differentiation and reduction of neurosphere cell proliferation. In addition, Notch signaling inhibition promoted the neurite outgrowth and migration of cells away from the neurosphere on the culture substrate. Together with Chapters 2 and 3, we have analyzed in detail the behaviour of neurosphere cells in terms of proliferation, differentiation and cell migration. Next, we were interested to investigate how these cells behave in other tissues upon transplantation, properties important for any potential use of neurosphere cells for clinical applications.

CHAPTER 6

Neurosphere cell transplantation

6.1. Introduction

6.1.1. Aim

In previous chapters we investigated the proliferation, differentiation as well as the motility of cells inside the neurosphere environment. Also, it was shown that Notch signaling pathway has a regulatory role on proliferation and differentiation of neurosphere cells. The next question was to investigate how these cells behave outside the neurosphere environment once transplanted in a recipient bowel, as the overall aim of this study is to understand the behaviour of neurosphere-derived ENS progenitors so that one day they can be transplanted safely and treat ENS disorders. The following paragraphs describe briefly the migration of enteric NCCs, previous findings from transplanted gut-derived neurospheres into recipient bowel in vitro, as well as information about the cell tracking technique used in the current study and its advantages.

6.1.2. Migration of enteric NCCs

Once enteric NCCs have entered the foregut, they colonize the whole bowel in about 4 days in mice (Kapur 1999; Young et al., 2001a) and 3 weeks in humans (Wallace et al., 2005). As discussed in the introduction the colonization of the gut can be regulated by the number of enteric NCCs (Simpson et al., 2007), the increased size of the gut (Landman et al., 2007) and by various signaling pathways with the most important ones being the GDNF/Ret/GFRa1 and the EDN3/ EDNRB pathways (Burns et al., 2009).

GDNF has been shown to have a chemoattractive role in enteric NCCs in vitro whereas EDN3 inhibits that process (Young et al., 2001b; Nagy and Goldstein, 2006; Mwizerva et al., 2011). It has been suggested that EDN3 'helps' the migratory cells to overcome the chemoattraction of GDNF once they are in the caecum and thus enable the migratory cells to colonize the colon (Barlow et al., 2003; Kruger et al., 2003).

6.1.3. Transplantation of enteric NCCs in bowel explants

Many research groups in the past have tried to investigate the properties of enteric NCCs in vitro by using bowel explants, an environment where the culture conditions can be more easily modulated and the effect of drugs or inhibitory antibodies monitored (Randal et al., 2011). Over time, various approaches in ENS studies were developed to maintain the structure of gut explants in vitro for a longer period. These included transfer of embryonic mouse gut segments under the kidney capsule of adult mice (Kapur et al., 1992), transfer onto paper filter constructs (Hearn et al., 1999), floating-free in medium or in a 3D collagen matrix (Natarajan et al., 1999) or on membrane inserts (Bareiss et al., 2008).

Isolation of enteric NCCs and transplantation to embryonic mouse bowel was first demonstrated by Natarajan et al. (1999). In this study, Ret^{+} enteric NCCS were isolated from the gut of E11.0-E11.5 mice ubiquitously expressing the gene lacZ and selected by flow cytometry using anti-Ret antibodies (Lo et al., 1995). They were then injected into the stomach of E11.5 Ret-deficient and wild type mouse embryos. It was shown that these cells migrate either caudally or rostrally, proliferate and differentiate in cells expressing neuron specific-enolase or the glial marker S100 (Natarajan et al., 1999), suggesting their potential for transplantation studies and future therapeutic applications. Following this study, research groups went one

step forward and performed transplantation experiments in segments of bowel using neurospheres containing ENS progenitors as outlined below.

6.1.4. Transplantation of neurosphere cells into bowel explants

When neurospheres derived from mouse embryonic (Almond et al., 2007) or human neonatal (Almond et al., 2007; Metzger et al., 2009b) gut were transplanted into E11.0-E11.5 mouse aganglionic gut, cells migrated away from the neurosphere into the recipient tissue. In the case where immunostaining was performed subpopulations of the migratory cells were shown to express neuronal and glial markers. In the above studies, the aganglionic feature of the recipient gut, human specific antibody or staining of neurosphere cell nuclei with Hoechst 33342, were used in order to identify and stain neurosphere donor cells in the recipient gut. However, these methods have limitations in the case where migration needs to be examined in a ganglionic mouse or human recipient bowel and in the cases where the migration pattern of neurosphere cells and their progeny needs to be studied.

In another study, neurospheres were generated from E11.5 mouse whole gut digestion as well as from postnatal small intestine (Bondurand et al., 2003). Proliferating neurosphere cells were labeled with a GFP-expressing retrovirus and upon grafting into aganglionic E11.5 bowel, GFP^+ cells

migrated into the explant and gave rise to $Tuj1^+$ neurons and $GFAP^+$ glia. However this retroviral-based tracking technique was not able to permanently label all the cells of the neurosphere but only the proliferating ones, excluding the quiescent, the differentiated cells and the very slow dividing ones.

From the previous experiments it is becoming clear that the cell tracking technique is very important in transplantation experiments, as the inability to monitor live migratory cells or their selective labeling can leave many questions unanswered. Therefore, we investigated the use of another cell tracking technique based on the expression of enhanced GFP (EGFP) lentiviral vector system.

6.1.5. Lentiviral-based cell tracking

Conventional retroviruses that are being used in the labs for many years, can only transduce proliferating cells as they can access the genome and integrate on it, only when the nuclear membrane is disintegrated during cell division (Kafri et al., 2000) On the other hand, lentiviruses which are also retroviruses, can integrate to the host's DNA even when the nuclear membrane is intact, thus they are able to transduce non-dividing cells (Pfeifer et al., 2009). Therefore, lentiviruses have proven to be very effective gene-delivery vehicles for many cell types including hepatocytes,

myotubes, as well as cells of the retina (Kafri et al., 2000). In addition, CNS non dividing neurons from adult rats could be successfully labeled with a lentivirus expressing GFP (Blomer et al., 1997).

Elements of the lentiviral vector such as the central polypurine tract (cPPT) and the post-transcriptional regulatory element of Woodchuck hepatitis virus (WPRE), enhance the passage of the lentivirus through the nuclear membrane and the transgene expression respectively (Pfeifer et al., 2009). In our vector the trangene was the EGFP under the control of the spleen focus-forming virus (SFFV) promoter (Demaison, 2002; Bender et al. 2007). Using this lentiviral-approach we tried to investigate the labeling efficiency of neurosphere cells derived from E11.5 mouse caeca, study their migratory behaviour in bowel explants, and compare them with what is already known about migration of enteric NCCs. In addition we investigated the role of Notch signaling in the migratory behaviour of neurosphere cells on pre-coated substrates. These experiments would give a lot of information regarding the presence or not of mechanisms regulating the fate of neurosphere derived cells upon transplantation, important for any potential clinical applications.

6.2. Results

The production of the lentivirus and the transduction efficiency in neurosphere-derived cells is described in the sections below. In addition, transplantation experiments and the effect of Notch signaling inhibition in neurite formation and cell migration are also presented.

6.2.1. Production of the EGFP-expressing lentivirus

Triple transfection of the packaging cell line 293T (Fig. 6.1) using calcium phosphate precipitation resulted in the production of lentiviral particles in culture supernatant which was then removed and concentrated using a filter-column centrifuge tube. The number of the successfully transfected cells was around 80%.

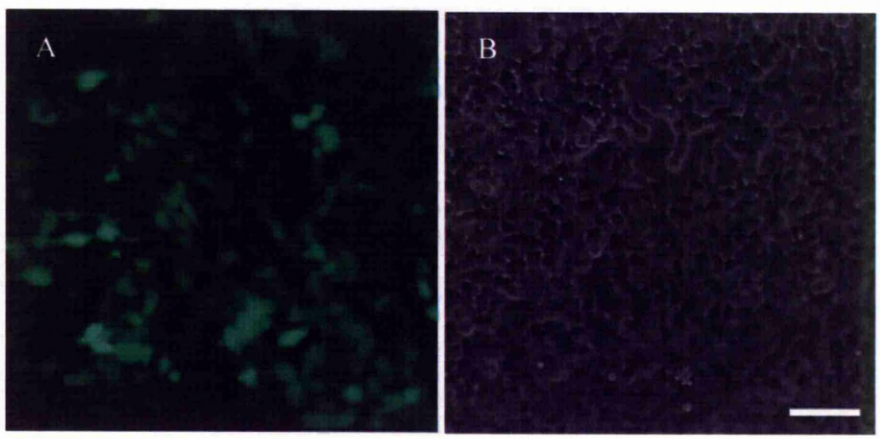

Figure 6.1. **Expression of EGFP by HEK293T cells 2 days post transfection.**

HEK293T cells were seeded ($12x10^6$) in a T175 flask ($175cm^2$). The next day cells were transiently triple transfected using calcium phosphate precipitation using the plasmids shown in Materials and Methods (2.6.1.). The following morning culture medium was replaced with fresh medium and cells remained at 37°C, 5% CO_2 overnight. Due to the fact that one of the plasmids contained the EGFP reporter gene, the transfection efficiency (~80%) could be examined under UV 2 days post transfection (A). Successful plasmid transfection indicated that all the proteins necessary for the production of the viral particles were produced. B: phase contrast; scale bar is 100μm.

The optimum concentration of the concentrated lentiviral supernatant for transduction of neurosphere derived cells was decided by transducing cells with different dilutions of the lentiviral supernatant. It was decided to use undiluted lentiviral supernatant (1:1) as we observed the highest fluorescent signal (Fig. 6.2).

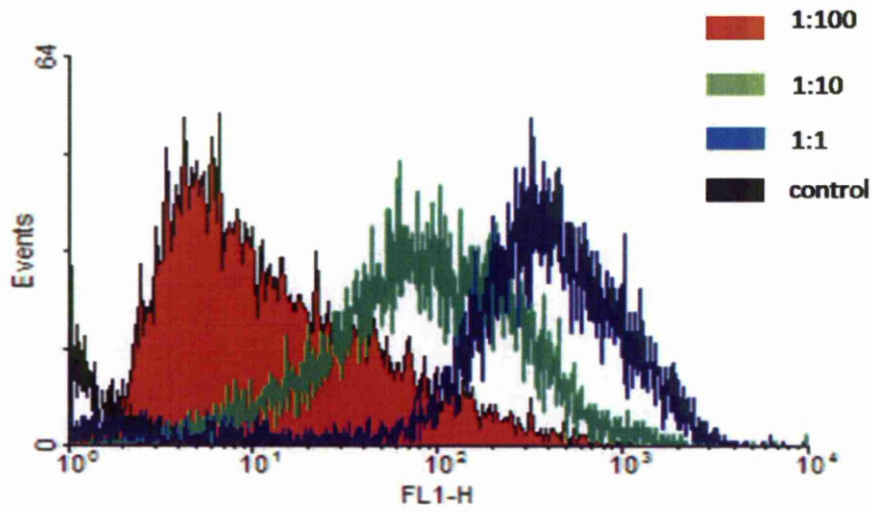

Figure 6.2. **Levels of EGFP in neurosphere-derived cells after transduction with different dilutions of lentiviral supernatant.**

Embryonic mouse primary neurospheres after 21 days in culture in 60mm non adherent dishes were dissociated using 0.05% trypsin for 10min at 37°C, followed by mechanical dissociation. The single cell population was aliquoted to 4 x 35mm adherent dishes and transduced with the lentivirus produced by the HEK293T cells. Different dilutions of the concentrated lentiviral supernatant were used in each dish; 1:100, 1:10, 1:1 and without lentiviral supernatant (control). Virus was

replaced with fresh medium after two days. Five days post transduction the levels of EGFP expression were analyzed using flow cytometry.

6.2.2. Transduction efficiency of neurosphere-derived cells

The transduction efficiency of single cells derived by dissociated neurospheres was quantified by counting $EGFP^+$ cells in 35mm adherent dishes 1, 3, 10 and 20 days post-transduction (Fig. 6.3). On day 1, cells had no expression of EGFP. The expression was apparent on day 3 and afterwards. Cells with strong expression of EGFP could be distinguished (Fig. 6.3, arrows). This variation could be a result of the number of viral particles which invaded the cell and also of how transcription-active was the sequence where the viral DNA integrated (Ahmed et al., 2004).

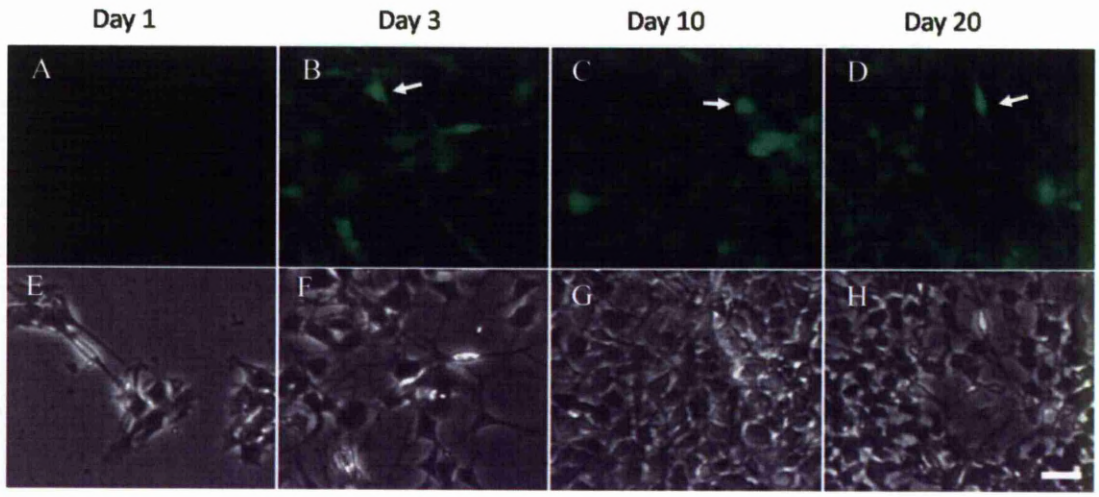

Figure 6.3. **Expression of EGFP in neurosphere-derived cells after 1, 3, 10 and 20 days post-transduction.**

Embryonic mouse primary neurospheres after 21 days in culture in 60mm non adherent dishes were dissociated using 0.05% trypsin for 10min at 37°C, followed by mechanical dissociation using a 1ml Gilson pipette. The resulted single cell population was transferred to 35mm adherent dishes and transduced with the lentivirus. Lentiviral supernatant on day 3 was replaced with fresh medium. Cells were observed under UV-microscope 1 day (A, E), 3 days (B, F), 10 days (C, G) and 20 days (D, H) post-transduction for the presence of EGFP (A, B, C, D). Arrows represent cells with strong expression of EGFP. Phase contrast pictures: E, F, G and H. Scale bar is 100μm.

Counting data showed that after 3 days post-transduction 91% of the cells were EGFP$^+$, 97% after 10 days and 98% after 20days (Fig. 6.4A). The number of strongly labeled EGFP cells was 11% after 3 days, 17% after 10 days and 11% after 20 days post-transduction (Fig. 6.4B). These data indicate that almost all the cells from day 3 until day 20 are EGFP$^+$ upon lentiviral addition to the culture medium. These data are consistent with confocal z-stack images acquired from an unfixed EGFP$^+$ neurosphere (Fig. 6.5) showing that in different planes of the neurosphere almost all the cells are labeled.

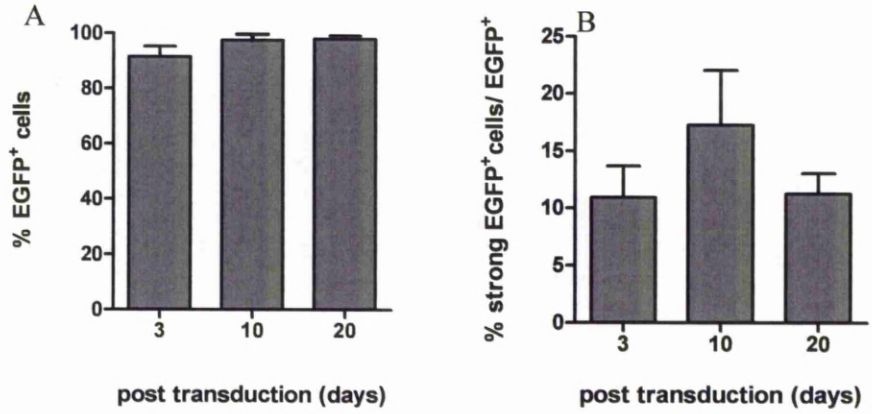

Figure 6.4. **Graph showing the percentage of cells that express EGFP over time.**

Neurosphere-derived cells which were transduced with lentivirus were used to assess the transduction efficiency of the EGFP-lentivirus. Thus EGFP$^+$ cells were counted in random optical fields (n=10) using 40X objective, 3, 10 and 20 days

post-transduction (A). Also, cells with strong expression of EGFP were counted (arrows in Fig. 6.3) and their percentage out of the total $EGFP^+$ cells was calculated (B). Scale bars represent SEM between 3 experiments (n=3). There was not a statistical difference between different days.

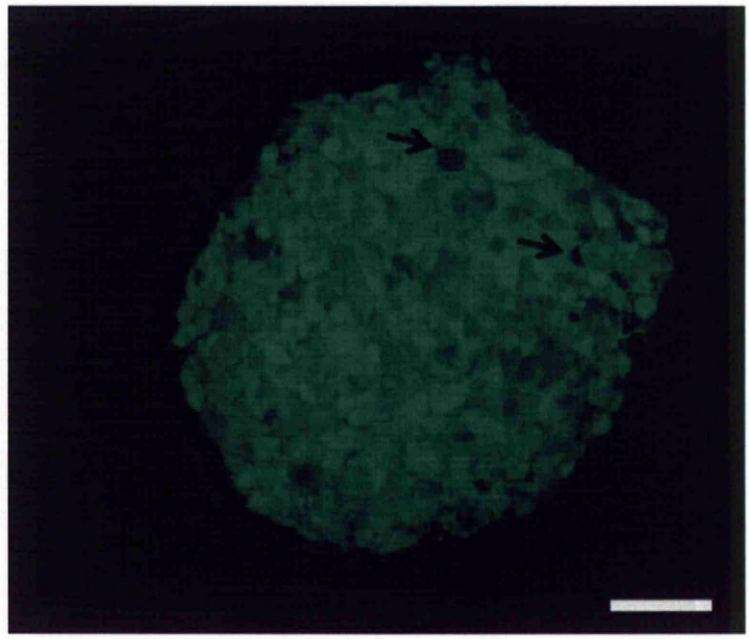

Figure 6.5. **Confocal image showing the presence of EGFP positive cells throughout a single neurosphere.**

Embryonic mouse primary neurospheres after 23 days in culture in 60mm non adherent dishes were dissociated using 0.05% trypsin for 15min at 37°C, followed by mechanical dissociation. The resulted single cell population was transferred to a 60mm non adherent dish and transduced with the lentivirus in order to form $EGFP^+$ neurospheres. After 20 days in culture the resulting $EGFP^+$ neurosphere

was transferred a 35mm adherent dish designed for confocal microscopy. After a day the neurosphere was attached on the dish and confocal z-stack pictures (2μm interval) were taken in order to identify the distribution of $EGFP^+$ cells throughout the unfixed neurosphere. Picture represents plane through the middle of the neurosphere. Arrows indicate EGFP negative cells. Scale bar is 20μm.

Flow cytometry analysis (Fig. 6.6) of dissociated labeled neurospheres of the same batch over different times post-transduction showed in more detail the fluorescence levels of $EGFP^+$ cells. In 18 day old labeled neurospheres the number of $EGFP^+$ cells was 96.4%, in 27 day old the percentage was 86.8% and in 22 day old labeled neurospheres which were dissociated 3 times before (passage after every 30 days) the percentage was 83.8%.

A closer look at the histograms in Fig. 6.6 (D, E and F) reveals the variation of the labeling in $EGFP^+$ cells. In all the graphs the vast majority of labeled cells have a Gaussian distribution but in Fig. 6.6E and 6.6F

there are more cells with lower signal and in Fig. 6.6F the number of cells that don't express detectable EGFP is higher. In Fig. 6.6F that can be explained as cells over time and multiple proliferations can find a way to minimize or even stop the expression of EGFP depending in which part of the actively-transcription area the integration of the virus took place or $EGFP^+$ cells proliferate slower than the unlabeled population.

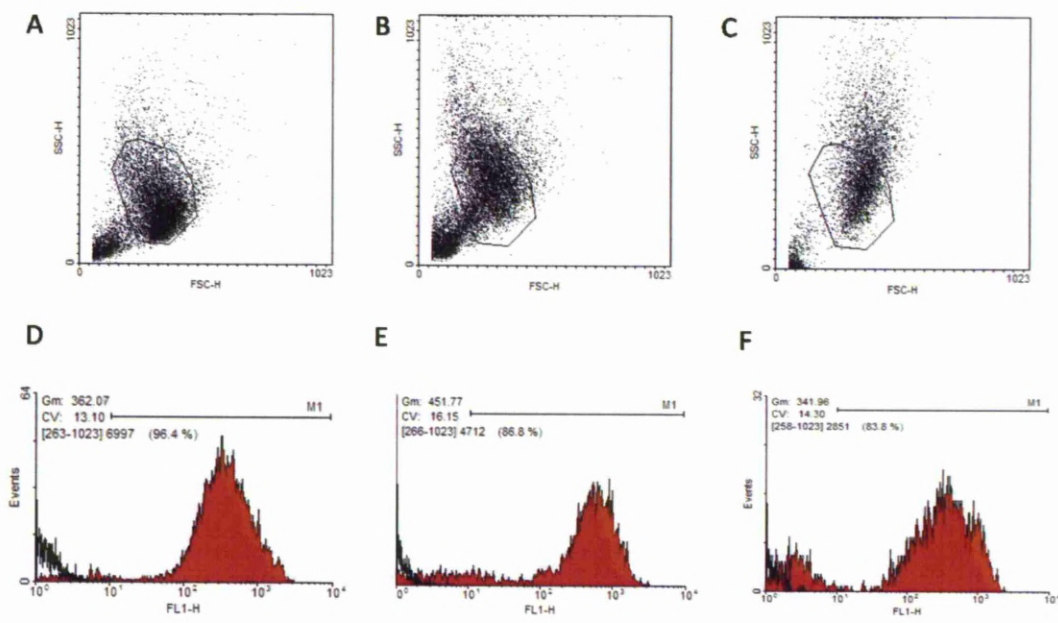

Figure 6.6. **Graph showing the levels of EGFP upon neurosphere dissociation using flow cytometry.**

Neurosphere derived cells were transduced with the EGFP-expressing lentivirus as described in figure 6.5 in order to form $EGFP^+$ neurospheres. After 18 days (A, D),

27 days (B, E) and 112 days (passaged 3 times) (C, F) labeled neurospheres were dissociated into a single cell suspension which was then analysed for the presence of $EGFP^+$ cells by FACS. Dotplots of forward and side scatter (A, B, C) represent 10000 events from which the gated ones are demonstrated in the histograms. In D, E and F the black curve represents the fluorescence levels of unlabeled gated cells (control). In each histogram the number of labeled cells as calculated by the marker line M1 is 96.4% (D), 86.8% (E) and 83.8% (F). The settings for all the runs were the same; FSC=E00, SSC=371, FL1=333.

6.2.3. Expression of PGP9.5 and GFAP in $EGFP^+$ neurospheres

Finally in order to examine if $EGFP^+$ neurospheres can express ENS markers and thus maintain their potentiality for transplantation experiments or even future clininical application, 21 day old labeled neurospheres were fixed, sectioned and stained for the ENS markers p75 (neural crest), GFAP (glia) and Protein gene product 9.5, PGP9.5 (neurons). Figure 6.7 shows abundant expression of all the above markers in $EGFP^+$ neurospheres indicating that lentiviral transduction is an efficient technique to label ENS progenitors.

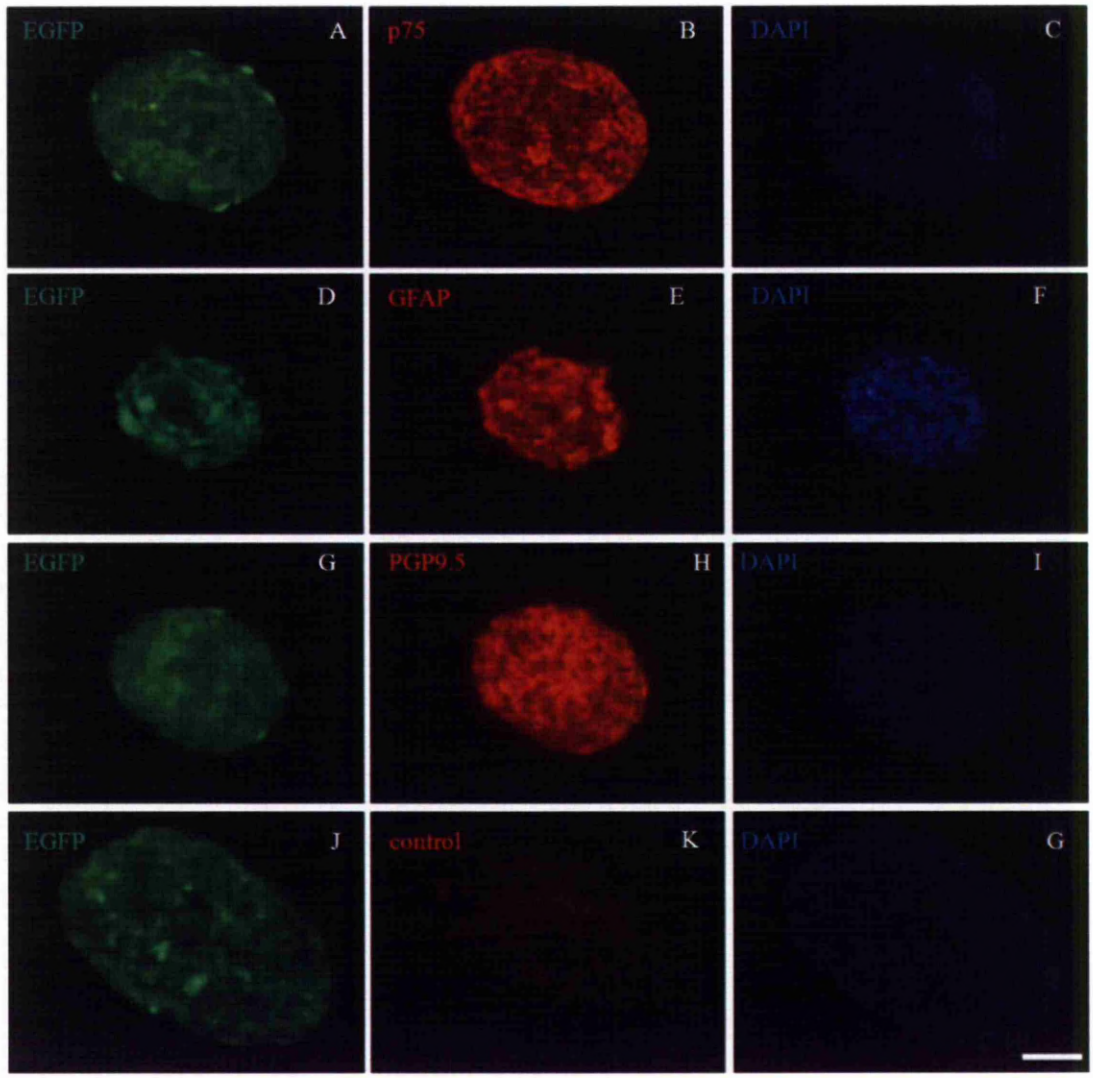

Figure 6.7. **Immunostaining of EGFP^{+} neurospheres for the presence of the markers p75, GFAP and PGP9.5.**

Embryonic mouse primary neurospheres after 21 days in culture in 60mm non adherent dishes were dissociated using 0.05% trypsin for 10min at 37°C, followed by mechanical dissociation. The single cell suspension was transferred to a 60mm non adherent dish with lentiviral supernatant. 21 days post-transduction $EGFP^+$ neurospheres were fixed, frozen and sectioned in 8μm thick slices and were immunostained for the markers p75 (B), GFAP (E), PGP9.5 (H) and control without primary antibody (K). Nuclei were stained with DAPI (C, F, I, G). EGFP: A, D, G and J. Scale bar is 25μm.

Having shown that the lentiviral labeling system efficiently labeled neuropshere cells by constitutive EGFP expression, the EGFP labeled cells were used to investigate the migration of neurosphere-derived cells into the gut and other tissue explants.

6.2.4. Transplantation of EGFP$^+$ neurospheres into embryonic and neonatal bowel

The gut explant culture technique of Hearn et al. (1999) was adapted as described in Materials and Methods (2.5). The presence of neurons in colon explants, without neurosphere transplantation, was examined in sections after 5 days (E11.5) or 4 days (P1) of culture by immunostaining with the pan-neuronal marker PGP9.5 (Fig. 6.8). Results showed that colon isolated from E11.5 mice was aganglionic as there was no immunoreactivity for the marker PGP9.5 (Fig. 6.8B). When colon was dissected out with the caecum, PGP9.5$^+$ cells were present a few layers beneath the outer surface of the gut wall (Fig. 6.8D, arrows). In the case of neonatal colon, PGP9.5$^+$ cells were distributed close to the outer surface of the bowel but also closer to the middle of the gut (Fig. 6.8F, arrows).

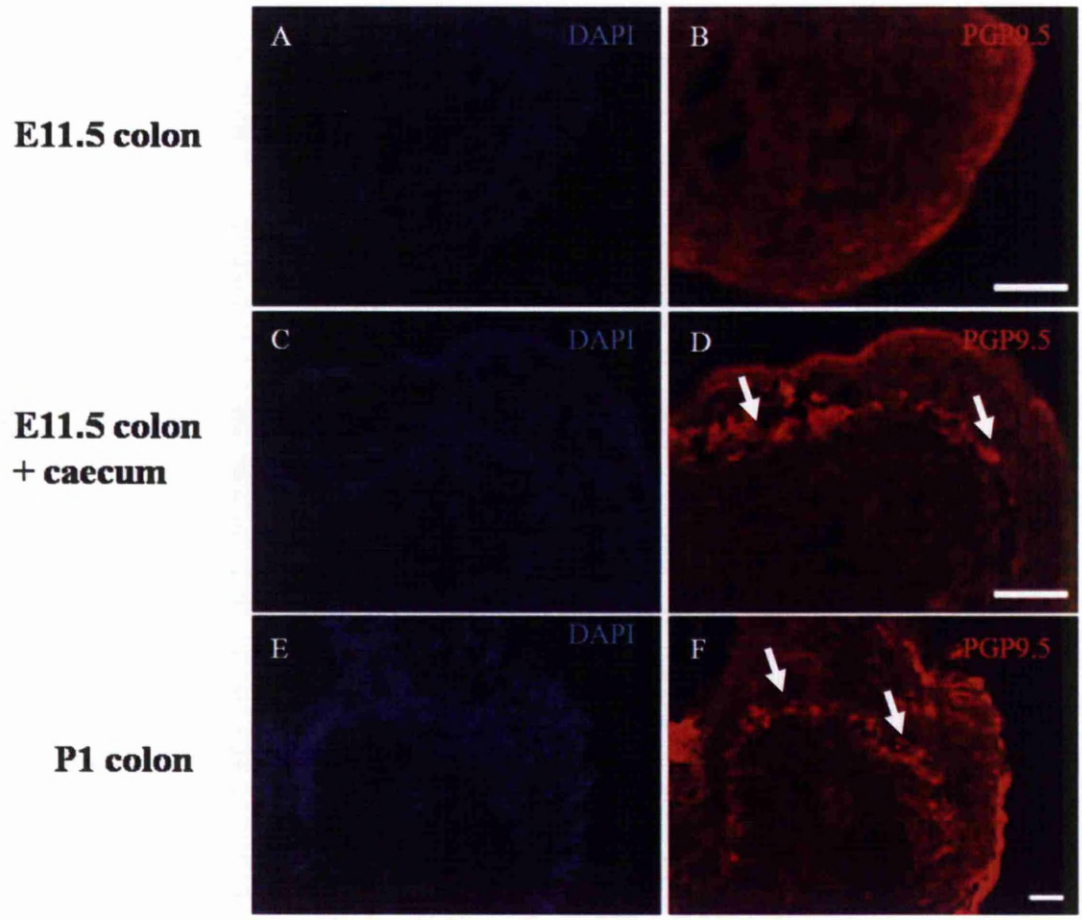

Figure 6.8. **Expression of PGP9.5 in sections of bowel explants.**

Explants of E11.5 colon (A, B), E11.5 colon with caecum (C, D) and P1 colon (E, F) were cultured for 5 days amd 4 days respectively as described in Materials and Methods (2.5). At the end of culture, explants were fixed, frozen and sectioned in 8μm at the middle of the gut and immunostained for the pan-neuronal marker PGP9.5. No immunoreactivity was found in embryonic colon (B) but there were $PGP9.5^{+}$ (arrows) cells in the case of embryonic colon with caecum (D) and in neonatal colon (F). Scale bar is 50μm.

When labeled neurospheres were transplanted at the rostral end of embryonic aganglionic colon (Fig. 6.9A), after 1 day $EGFP^+$ single cells started migrating away from the neurosphere and along the bowel in a caudal direction. However using the dissection microscope it was difficult to decide whether $EGFP^+$ cells migrate on top of the bowel or inside the gut. After 5 days (Fig. 6.9B) cells had colonized most of the gut explants visible in the V-shaped gap in the filter paper support. In order to examine whether migration is limited to the rostro-caudal direction (consistent with a possible chemoattractive gradient). labeled neurospheres were transplanted to the caudal end of the gut explants (Fig. 6.9C). As before, $EGFP^+$ cells migrated towards the opposite end from where the neurosphere was situated (Fig. 6.9D), indicating that there is no preference of neurosphere cells in migrating caudally or rostrally. At the migratory wavefront cells forming fibers (Fig. 6.9B1) and single individual cells (Fig. 6.9D1) could be observed.

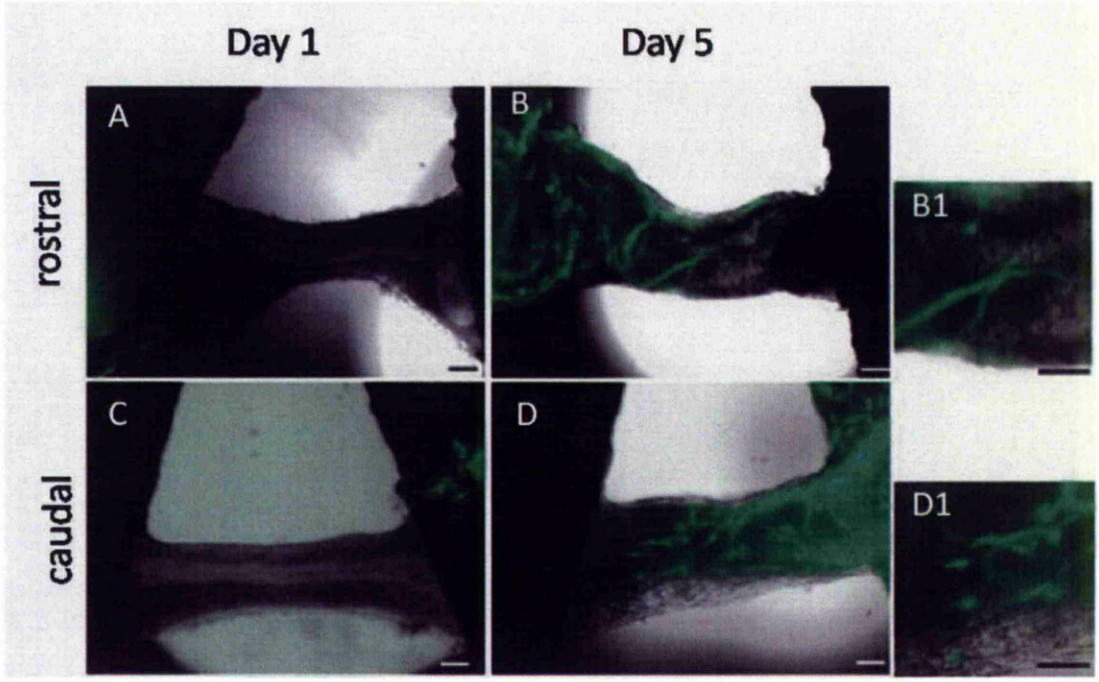

Figure 6.9. **Transplantation of EGFP-labeled mouse embryonic neurospheres onto E11.5 aganglionic mouse colon.**

Embryonic mouse $EGFP^+$ neurospheres after 2-3 weeks in culture were transplanted either onto the rostral (A) or caudal (C) end of mouse E11.5 colon. One day post transplantation $EGFP^+$ cells migrated into the gut tube from both rostral and caudal ends (A, C). Five days post transplantation $EGFP^+$ cells colonized most of the colon (B, D). Higher magnification of the migratory wavefront showed the presence of fibers (B1) and single individual cells (D1). Pictures were taken under a UV-dissection microscope. Scale bar is 100μm.

A comparison of the distance covered by the furthest migratory EGFP$^+$ cell between the rostral-caudal or caudal-rostral direction over 5 days in culture demonstrated that there are no significant differences at each time point (Fig. 6.10A). Using linear regression for each data set it was shown that the average migration rate for both directions was 181 µm/ day (Fig. 6.10B).

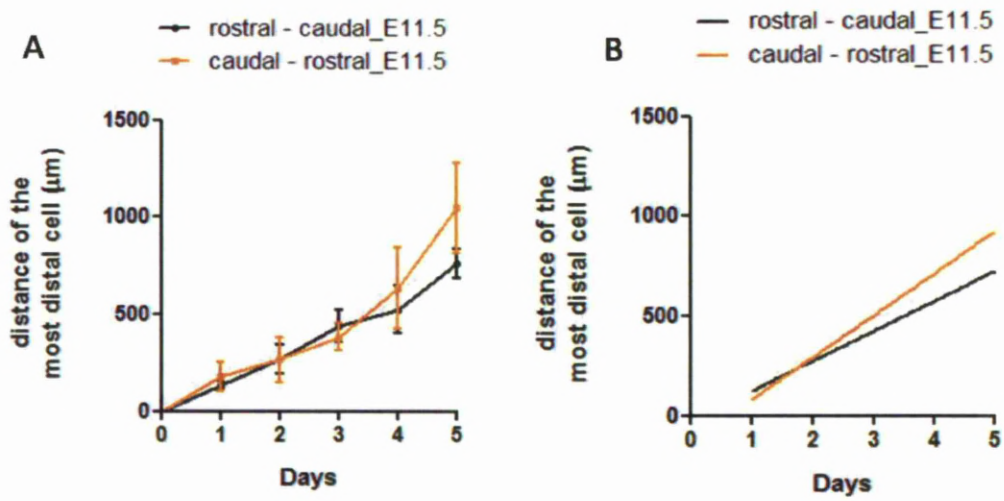

Figure 6.10. **Distance covered by the most distal migratory EGFP$^+$ cell after transplantation of embryonic mouse labeled neurosphere onto E11.5 mouse colon.**

Embryonic mouse $EGFP^+$ neurospheres were transplanted onto either the rostral or caudal ends of aganglionic E11.5 mouse colon. The distance covered by the most distal cell was measured daily and for 5 days using the software ImageJ on pictures taken under a UV-dissection microscope. Error bars represent the SEM between different experiments ($n \geq 3$). For each time point the total number of gut explants measured was 6-12. Using linear regression for each dataset (Fig. B) it was shown that there was no significant difference between the slopes in the rostral or caudal directions; slope for rostral-caudal= 151 ± 12 (R^2=0.98), slope for caudal-rostral= 211 ± 39 (R^2= 0.91); pooled slope= 181, p=0.19.

When embryonic mouse $EGFP^+$ neurospheres were transplanted into ganglionic neonatal colon (P1) migration of single labeled cells occurred (Fig 6.11). Migration was monitored up to day 4 as the explant started disintegrating at later time points. Labeled cells one day after transplantation were able to migrate away from the neurosphere (Fig. 6.11A and 6.11C) and after four days they had migrated along the bowel in both caudal (Fig. 6.11B) and rostral (Fig. 6.11D) directions. There was no significant difference in the distances covered by the most distal migratory cells in either direction at any time point (Fig. 6.12). Also, using linear regression for each data set it was shown that the average migration rate for both directions was 107 μm/ day (Fig. 6.12B), a value similar to what was calculated for embryonic colon (109 μm/ day). However in the case of neonatal recipient gut, the migration rate between day 3 and 4 seems to be reduced (Fig. 6.12A) when compared with the same time points in embryonic recipient gut (Fig. 6.10A) a possible result from the beginning of disintegration of the neonatal bowel.

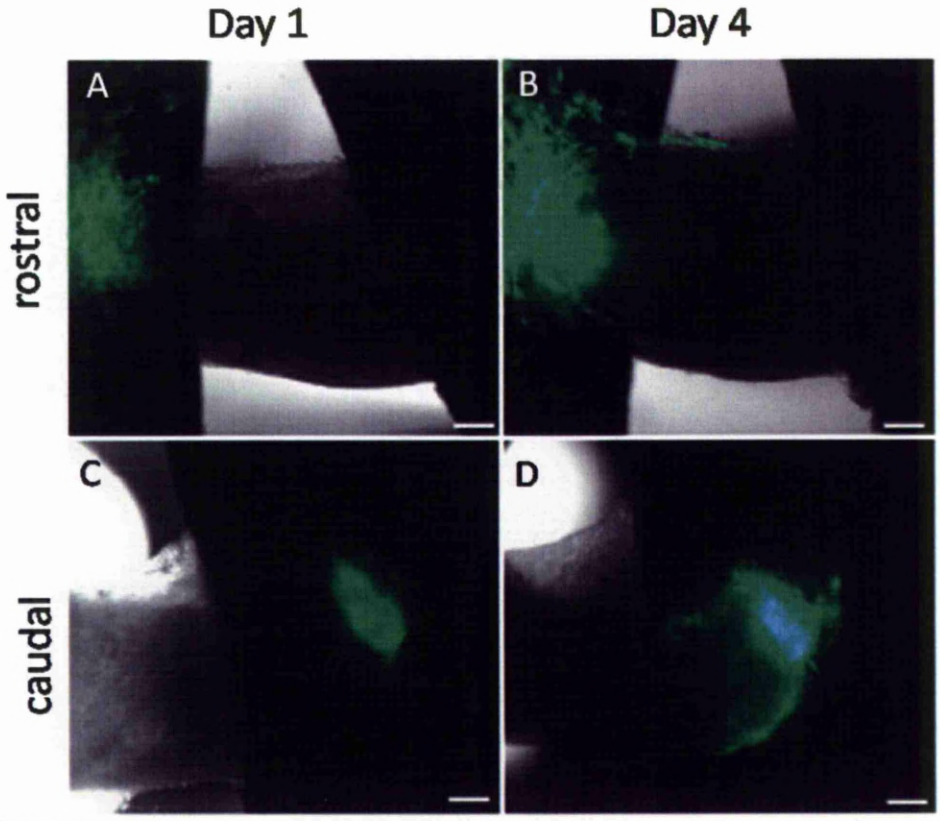

Figure 6.11. **Transplantation of labeled mouse embryonic neurospheres onto ganglionic neonatal mouse colon.**

Embryonic mouse $EGFP^+$ neurospheres after 2-3 weeks in culture were transplanted either onto rostral (A, B) or caudal (C, D) ends of P1 ganglionic mouse colon. Migration of neurosphere cells was recorded for 4 days (B, D). A day post transplantation $EGFP^+$ cells migrated into the gut tube from both rostral and caudal ends (A, C). Pictures were taken under a UV-dissection microscope. Scale bar is 200μm.

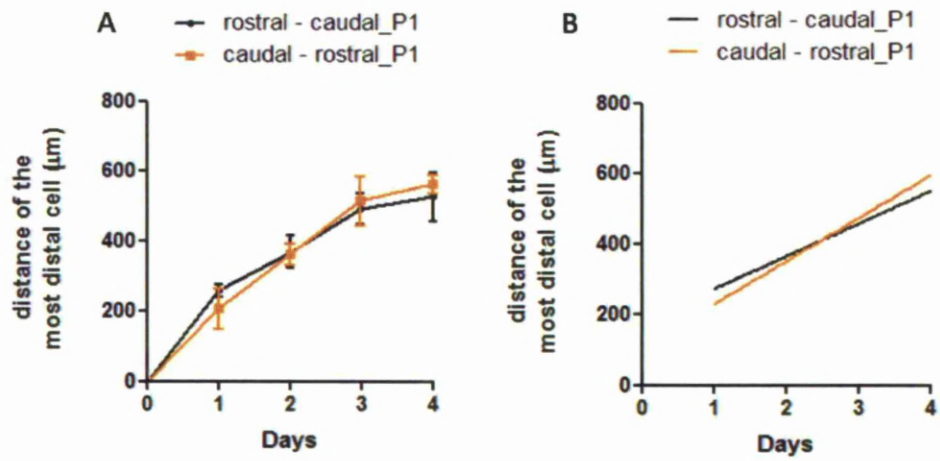

Figure 6.12. **Distance covered by transplanted labeled mouse embryonic neurosphere-derived cells into P1 mouse colon.**

Embryonic mouse EGFP$^+$ neurospheres were transplanted onto either the rostral or caudal ends of ganglionic P1 mouse colon. The distance covered by the most distal cell was measured daily and for 4 days using the software imageJ on pictures taken under a UV-dissection microscope. Error bars represent the SEM between independent experiments ($n \geq 2$). For each time point the total number of gut explants measured was 4-8. Using linear regression for each dataset (Fig. B) it was shown that there was no significant difference between the slopes in the rostral or caudal directions; slope for rostral-caudal= 93±13 (R^2=0.96), slope for caudal-rostral= 122±19 (R^2= 0.96); pooled slope= 107.16, p=0.27.

In order to assess the location and phenotype of the migratory $EGFP^+$ cells, cryostat sections of fixed frozen colon collected at the end of the explant culture were stained for the pan-neuronal marker PGP9.5 and the progenitor and glial marker GFAP (Fig. 6.13). Labeled cells were located 1-3 cell layers beneath the outer surface of the colon, a location where mouse neural crest cells migrate during early formation of the enteric nervous system (Leibl et al., 1999; Burns et al., 2005). $EGFP^+$ cells were all positive for PGP9.5 (Fig. 6.13C, arrowhead) and most of them were expressing GFAP (Fig. 6.13F, arrowhead), after 5 days in the explant culture. Cells $EGFP^+/GFAP^-$ are indicated by arrows (Fig. 6.13F, arrows).

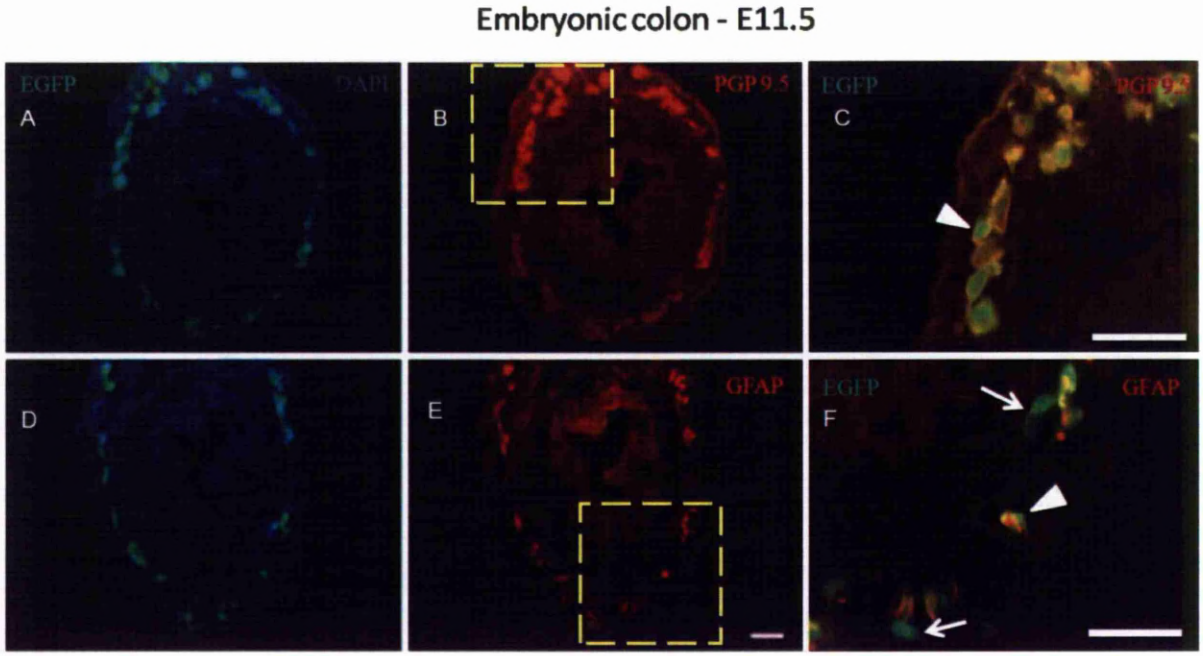

Figure 6.13. **Migratory EGFP$^+$ cells express PGP9.5 and GFAP upon transplantation into embryonic colon.**

Embryonic mouse EGFP$^+$ neurosphere after 2-3 weeks in culture was transplanted onto the rostral end of embryonic mouse E11.5 colon. After 5 days in culture explants were fixed, frozen and sectioned in 8μm slices at the middle of the bowel. Sections were immunostained for PGP9.5 (B, C) and GFAP (E, F). Nuclei were stained with DAPI. Arrowheads represent co-localization of EGFP with either PGP9.5 or GFAP. Arrows represent cells expressing only EGFP. Pictures C and F represent higher magnification of the box inset in pictures B and E respectively. Scale bar is 25μm.

The structure of neonatal gut after 4 days in culture was not as well organized as that of embryonic gut (compare Fig. 6.13 with Fig. 6.14). Cells expressing PGP9.5 and GFAP were present as expected (Figs. 6.14C and F, white arrows) and as found in the neonatal gut (for PGP9.5 see Fig. 6.8). These cells in the neonatal gut were not derived from the neurospheres as they were $EGFP^-$. Labeled cells were able to migrate inside the bowel but it was not apparent a migration pattern similar to what was observed with embryonic recipient colon, where $EGFP^+$ cells were migrating in a ring formation a few cell layers below the outer gut surface (compare Fig. 6.13 with Fig. 6.14). We could observe $EGFP^+/GFAP^+$ (Fig. 6.14F, arrowhead) and $EGFP^+/PGP9.5^+$ (Fig. 6.14C, arrowhead). Also $EGFP^+$ cells negative for both markers could be observed (Fig. 6.14, blue arrows).

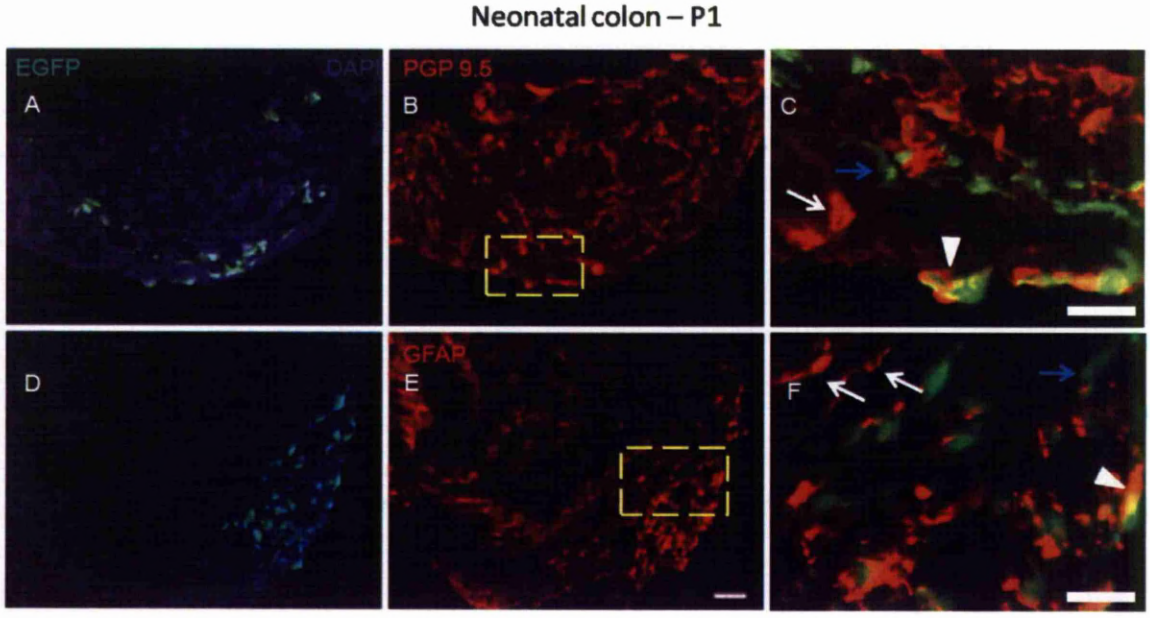

Figure 6.14. **Migratory EGFP$^+$ cells express PGP9.5 and GFAP upon transplantation into neonatal colon.**

Embryonic mouse EGFP$^+$ neurospheres after 2-3 weeks in culture were transplanted onto the rostral end of neonatal mouse P1 colon. After 4 days in culture explants were fixed, frozen and sectioned in 8μm slices at the area of the bowel where the furthest EGFP$^+$ cells had reached. Sections were immunostained for the markers PGP9.5 (B, C) and GFAP (E, F). Arrowheads represent co-localization of EGFP with either PGP9.5 or GFAP. Arrows represent PGP9.5$^+$/EGFP$^-$ or GFAP$^+$/EGFP$^-$ cells. Blue arrows indicate cells which express only EGFP. Pictures C and F represent higher magnification of the box inset in pictures B and E respectively. Scale bar is 50μm.

6.2.5. Tranplantation of embryonic EGFP$^+$ neurosphere to neonatal bladder, heart and liver.

To determine if EGFP$^+$ neurosphere cell migration into both embryonic and neonatal bowel was gut specific, embryonic mouse EGFP$^+$ neurospheres were transplanted into neonatal (P1) bladder (Fig. 6.15A-C), heart (Fig. 6.15D-F) and liver (Fig. 6.15G-I). After 4 days in culture, cells had migrated away from the neurosphere and along the recipient tissue (Fig. 6.15B, E and H). A difference in the migratory ability of labeled cells between different tissues was not observed. Frozen sections of the explants after 4 days in culture showed that EGFP$^+$ cells had migrated both at the surface of the recipient organs and in the inner cell layers (Fig. 6.15C, F, I) and not just 1-2 layers close to the outer surface as shown in the case of embryonic colon (Fig. 6.13), but similar to what was observed in the neonatal colon (Fig. 6.14). These results show that the migration of neurosphere-derived cells is not gut specific.

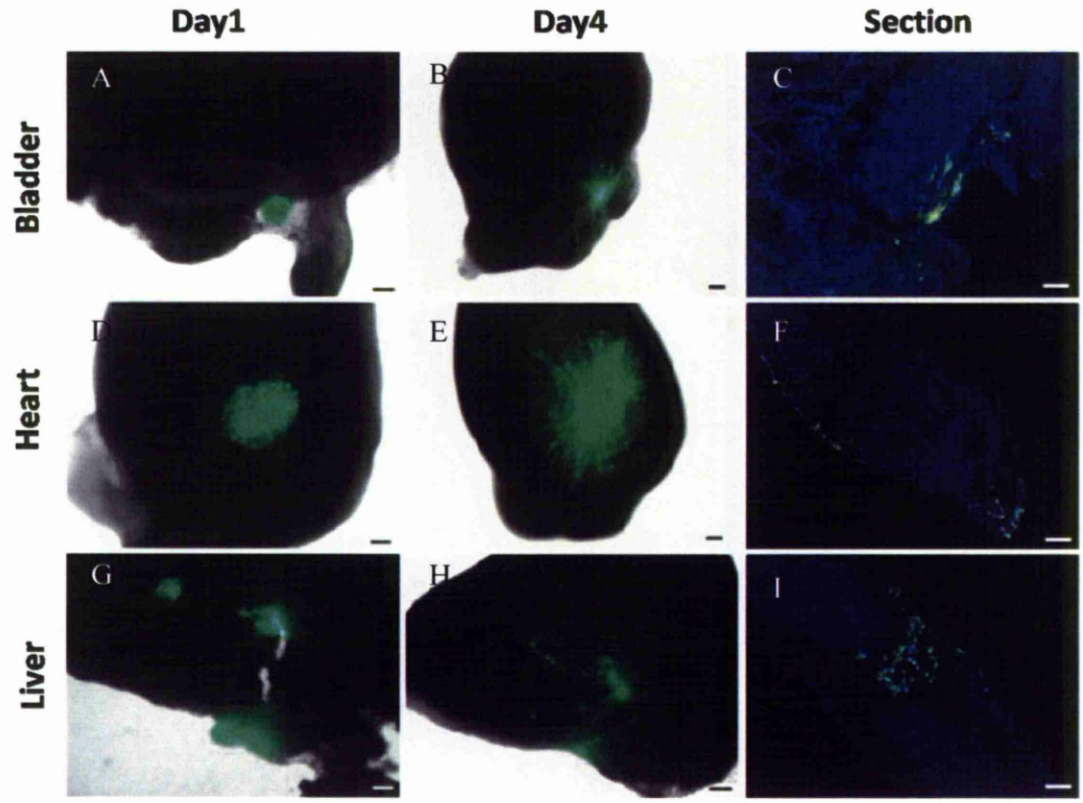

Figure 6.15. **Transplantation of EGFP^{+} neurospheres into bladder, heart and liver explants from neonatal mice P1.**

Labeled neurospheres after 2-3 weeks in culture were transplanted into neonatal P1 mouse bladder (A-C), heart (D-F) and liver (G-I). Pictures using a dissection microscope were taken on day1 and day4 of culture. After 4 days in culture explants were fixed, frozen and sectioned into 8μm thick slices. Nuclei were stained with DAPI (C, F, I). Scale bar is 100μm.

Summarizing, the above data showed that neurosphere cells can be efficiently labeled with an EGFP-expressing lentivirus and propagate in culture giving rise to $EGFP^+$ neurospheres. These labeled neurospheres when transplanted to aganglionic or ganglionic bowel, $EGFP^+$ cells could migrate equally well both caudally and rostrally, a migration which was shown to be not gut specific.

6.3. Discussion

In previous chapters we discussed the properties of cells inside the neurosphere environment, in terms of proliferation, differentiation and migration. We also demonstrated that the Notch signaling pathway regulates neurosphere cell behaviour because after Notch signaling inhibition, differentiation was promoted and proliferation was reduced. Having found a regulatory mechanism for neurosphere cell behaviour the next question was how these cells behave outside the neurosphere environment, properties important for future clinical applications of these cells. Therefore we labeled neurosphere cells with an EGFP-expressing lentivirus and studied their migration in aganglionic and ganglionic bowel as well as in explants of neonatal bladder, heart and liver.

6.3.1. EGFP-expressing lentivirus can efficiently label neurosphere-derived cells

Using the lentivirus labeling system we demonstrated that more than 95% of neurosphere-derived cells express EGFP after transduction. As a result we were able to produce neurospheres where almost all the cells were $EGFP^+$. Upon multiple passaging the fluorescence signal was reduced as shown in the data acquired by flow cytometry and the number of cells with very low signal, almost similar to the unlabeled control, was increased. However, more than 83% of the cells were expressing high levels of EGFP even after 3 passages. Stable long-term efficient transduction has also been shown when a lentivirus expressing EGFP was injected in the neocortex and hippocampus of adult mouse brains. After 4 weeks a large number of cells was expressed EGFP. However the levels of expression varied among different cells which was suggested to be due to the different number of viral particles that managed to enter the cell at the time of transduction (Ahmed et al., 2004). Similar variation of EGFP expression was observed in our transduced neurosphere-derived cells, implying that this was probably due to the different amount of lentivirus that entered the cell. In addition, in the same study they did not observe any irregularity in the morphology of $EGFP^+$ cortical neurons even 4 weeks after transduction, suggesting EGFP expression did not have any toxic effects on the labeled cells (Ahmed et al. 2004).

Also, when lentiviral particles with the encoding information for GFP were injected in the liver of nude rats, expression could be detected even after 22 weeks, indicating that lentiviral-gene delivery is an efficient process for cell labeling (Kafri et al., 1997). These findings are consistent with the expression of EGFP by most of the neurosphere cells even after multiple passaging (Fig. 6.6).

In another study, primary motor neurons, derived from the spine of 13.5 day old mice, were transduced with an EGFP-expressing lentivirus and examined 5 days later. These cells had no morphological defects in culture and their expression of the dendritic marker MAP2 and the axonal marker Tau was not different from the control as demonstrated by immunostaining (Bender et al., 2007). In our results we showed that $EGFP^{+}$ neurospheres were able to express ENS markers including the pan-neuronal marker PGP9.5 and the glial marker GFAP (Young et al., 1999; Young et al., 2003) indicating the high potential of these labeled cells in the colonization of aganglionic bowel.

6.3.2. Neurosphere-derived cells colonize aganglionic colon in both caudal and rostral directions.

We demonstrated that labeled neurosphere-derived cells were able to colonize equal distances in both caudal and rostral directions in aganglionic embryonic mouse bowel, indicating that there was not an apparent gradient of chemoattractive molecules in the colon that could alter the speed of migration (Figs. 6.9 and 6.10). Also, Anderson et al. (2007) did not observe any significant difference in the migration of enteric NCCs when they were transplanted either in the rostral or caudal end of aganglionic E11.5 small intestine from Ret deficient mice. In these experiments as donor they used segments of pre-caecal midgut from E11.5 mice where cells were expressing GFP under the control of the Ret promoter. This observation indicates that enteric NCCs that have not been exposed to the caecum can migrate in both directions when transplanted into aganglionic small intestine, resembling the behaviour of our $EGFP^+$ neurosphere-derived cells.

However, when the same group used as recipient gut an E11.5 wild type mouse colon that was not yet colonized and as donor E11.5 caecum, cells could migrate rostrocaudally but they couldn't migrate as well in the opposite direction. That impairement in migration was greater when cells were transplanted at the most distal end of the colon (Anderson et al.,

2007), implying the presence of some sort of gradient in the embryonic post-caecal gut. These results differ from our findings, where we did not observe any difference in the caudorostral migration, although the neurospheres we generated derived from E11.5 mice caeca. Thus, it seems that neurosphere-derived cells have some fundamental migratory differences from the caecal enteric NCCs in vivo or that the culture conditions make neurosphere cells resemble more pre-caecal enteric NCCs.

In terms of migratory velocity, it was found that 3 days after transplantation in aganglionic colon, the neurosphere-derived cells migrated approximately 500μm whereas in the study by Anderson et al. (2007) after 3 days in culture, cells from post-caecal midgut or from caecum covered a distance of approximately 600-700μm into E11.5 aganglionic colon, a value not that different from our results (Anderson et al., 2007). These speeds are quite slow compared to what was shown in vivo where enteric NCCs migrated caudally at an average speed of 35μm/h in both E10.5 mouse midgut and E12.5 hindgut (Young et al., 2004), indicating the effect that the experimental conditions can have on the migratory properties of enteric NCCs.

6.3.3. Presence of an already developed ENS does not inhibit the migration of neurosphere-derived cells.

We demonstrated that cells derived from $EGFP^+$ embryonic mouse gut neurospheres were able to migrate both rostrally and caudally in neonatal ganglionic gut without any apparent difference in their migration rate (Figs. 6.11 and 6.12). Also the distances covered over time by the $EGFP^+$ cells in the neonatal ganglionic bowel were similar to recipient embryonic aganglionic bowel (compare Figs. 6.10 and 6.12), indicating that migration of neurosphere cells is not affected by the age of the recipient gut and most importantly by the presence of an already formed ENS.

Contrary to our findings, in a study done by Hotta et al. (2010) aganglionic gut explants derived from Ret-/- mice of a later developmental stage than the transplanted enteric NCCs, restricted the migration of ENS precursors and the effect was stronger in ganglionic recipient gut. More specifically, E11.5 caecum consisted of enteric NCCs which expressed GFP under the control of the Ret promoter was transplanted in the rostral end of aganglionic (Ret-/-) or ganglionic (Ret+/+) explants of E11.5, E14.5 and E16.5 mouse colon. In the rare cases where enteric NCCs managed to migrate in some ganglionic explants, they were more scattered and mixed with cells of the recipient gut expressing the pan-neuronal marker Hu^+, a similar scattered distribution with what we observed in our transplantation

experiments using neonatal colon (Fig. 6.14). The migration defect observed in older aganglionic recipient guts was suggested to be the result of the maturation of the gut mesenchyme (Hotta et al., 2010) something that our neurosphere cells did not seem to be affected by.

In addition, age related defects were demonstrated with tissue grafting experiments, where ganglionic E13.5 mouse colon was grafted to aganglionic E14.5 mouse colon and enteric NCCs of the E13.5 donor showed very limited or no invasion of the E14.5 recipient gut. The inability of enteric NCCs to colonize the older colon suggested that this could be due to the higher expression of laminin at the developmental stage E14.5. In this experiment the aganglionic recipient colon was derived from Ednrb -/- mouse mutants in which enteric NCCs failed to migrate further than the proximal colon (Druckenbrod and Epstein, 2009). These findings together with our results imply that neurosphere-derived cells probably do not respond to the different concentrations of ECM proteins like laminin and thus their migratory ability is shown to be different from enteric NCCs as described in the previous ex vivo experiments.

Upon transplantation neurosphere cells were shown to express PGP9.5 and GFAP. In sections from transplants of embryonic aganglionic bowel we observed that all the neurosphere-derived cells were PGP9.5^{+} and also

almost all of them were GFAP$^+$. Regarding the marker GFAP, as it has already been discussed in 4.1.2., it can be expressed in neural progenitors in the CNS (Garcia et al., 2004) as well as in enteric neural progenitors in vitro (Joseph et al., 2011). PGP9.5 appears in the ENS as early as E12.5 and represents over 20% of the Phox2b$^+$ population (Young et al., 2003).

6.3.4. Migration of enteric neurosphere-derived cells is not tissue specific.

When EGFP$^+$ neurospheres were grafted to mouse neonatal bladder, heart and liver, we observed neurosphere cells migrating on the surface of the recipient tissue as well as in deeper cell layers. Also, the spherical formation of the neurosphere disappeared as shown after 4 days. In a previous study where E11.5 mouse gut neurospheres were placed next to E11.5 embryonic liver, it was concluded that neurosphere cells did not invade the liver (Almond et al., 2007). However, from the results demonstrated in this study, the neurosphere had lost its round boundaries and neurosphere cells mingled among liver cells. It could also be argued that some neurosphere cells migrated on the surface of the liver. The fact that E11.5 gut neurospheres behave differently in embryonic and neonatal mouse tissue could be due to different molecular mechanisms.

6.3.5. Conclusions

In this chapter we demonstrated an efficient lentiviral $EGFP^+$ labeling technique for neurosphere-derived cells. Upon transplantation in both embryonic aganglionic and neonatal ganglionic bowel $EGFP^+$ neurosphere-derived cells were able to migrate both caudally or rostrally. However, in the case of embryonic recipient gut, $EGFP^+$ cells migrated in locations inside the gut similar to vagal-derived neural crest cells in vivo, whereas in the case of neonatal bowel explants $EGFP^+$ cells migrated on the surface or in multiple cell layers below the surface. Also neurosphere cells could migrate on the surface and inside other neonatal organs upon transplantation indicating a lack of tissue specificity.

CHAPTER 7

Final Discussion

7.1. Stem cells as an alternative treatment for HSCR

The isolation of ENS progenitors and their propagation in vitro as neurospheres represented a great breakthrough as gut is an accessible tissue that allows autologous transplantations (Schafer et al., 2003). Neurospheres can be propagated over many passages in vitro, thus generating a large pool of ENS progenitors and their differentiated progeny as has been shown from in our lab and by other groups (Schafer et al., 2003; Bondurand et al., 2003; Almond et al., 2007; Metzger et al., 2009a and b). Neurospheres can also be generated from bowel tissue or gut mucosal biopsies of HSCR patients as well as from human embryonic gut (Almond et al., 2007; Metzger et al., 2009a and b).

A functional effect of human neonatal neurospheres has been shown when upon transplantation they restored a normal pattern of contractility of aganglionic embryonic mouse bowel explants in vitro (Lindley et al., 2008). In addition neurosphere cells derived from neonatal rat bowel were able to differentiate into neurons and glia and repopulate aganglionic adult colon which had been pre-treated with benzalkonium chloride, an agent that chemically ablates enteric ganglia (Pan et al., 2011). However, there is not a lot of information in the literature regarding cell behaviour in the neurosphere microenvironment and the mechanisms regulating it.

Therefore, we focused on examining properties such as neurosphere cell proliferation and differentiation in order to characterize these cells and compare these findings with the behaviour of enteric NCCs cells in vivo. The rationale was that only when we understand the behaviour of stem cells in vitro and how we can control it, will we then be able and confident to transplant them in living organisms and try to treat any disorders, as an irrational behaviour could lead to tumour formation. Proliferation and differentiation are the first things that need to be explored as they define the cell behaviour more than anything else.

7.2. Cell division in the neurospheres

Previous studies in both CNS and ENS derived neurospheres have shown that dividing cells are located at the periphery of the neurosphere (Andersen et al., 2011; Almond et al., 2007). However, the fate of these proliferating cells was not explored in these studies. Our results showed that peripheral cells can follow different fates once they have proliferated. Either they can move in the neurosphere or stay at the periphery. Cells which remain at the periphery proliferate faster than the ones nearer to the centre.

A regulatory role of the cell location in the neurosphere on the proliferation rate was demonstrated with the EGFP-chimaeric experiment, indicating that the central location of the neurosphere impairs cells proliferation.

Briefly, chimaeras were created by centrifuging together single $EGFP^+$ neurosphere cells with unlabeled neurospheres. The result was a chimaeric neurosphere where one hemisphere consisted of $EGFP^+$ cells and the other one from the unlabeled neurosphere. After a short pulse with BrdU, dividing cells were found to be located only at the periphery of the chimaera and no BrdU incorporation was observed in the interface between $EGFP^+$ cells and the unlabeled neurosphere, indicating that any dividing peripheral cells which were located in the interface either slowed down their cycle or stopped proliferation.

This model of proliferation resembles the behaviour of neuronal precursors in the subependymal zone of the lateral ventricles or the subgranular zone of the dentate gyrus. There, proliferating precursors give rise to immature neurons which migrate away from the zone following migratory pathways (Garcia et al., 2004; Kazanis et al., 2010). Also the fast dividing cells at the periphery could resemble a transit amplifying population which is generated by slow dividing cells perhaps located closer to the centre of the neurosphere because, as we have shown from the chimaera experiment, fast dividing cells were not located in the centre. Thus, the neurosphere environment could resemble the stem cell niche in the intestinal epithelium of the crypts (Shaker et al., 2010) or the epidermal niche (Jones et al., 2007), where few slow dividing stem cells give rise to transit amplifying

cells whose fate is to differentiate after multiple divisions. Therefore, the next step was to identify what is the phenotypic expression of these cells once they proliferate at the periphery of the neurosphere.

7.3. Relationship between proliferation and differentiation

Immunostaining for various markers in cells with incorporated EdU revealed that straight after the EdU pulse only a very small percentage of the fast dividing cells expressed the immature neuronal marker Tuj1 whereas the vast majority expressed the glial marker GFAP. After 4 days of chase, the proportion of cells expressing Tuj1 increased significantly and the percentage of cells expressing GFAP was significantly reduced. At the end of the 4 day chase we also observed an increased in the S100 expression and a reduction in the Sox10 expression. These data indicate that after 4 days there is an alteration in the phenotype of recently divided cells.

The correlation of cell types between in vivo and in vitro conditions according only to the phenotypic expression can be problematic, as in the case of S100 and GFAP which have been accepted as mature glia markers in the ENS (Young et al., 2003), cells in the adult gut which express S100/GFAP/nestin when transferred to *in vitro* conditions were able to differentiate into neurons (Joseph et al., 2011). In addition, GFAP

and S100 are expressed in radial glial cells in the CNS which are neural progenitors (Rakic, 2003; Namba et al., 2005). Consistent with this is our finding that there is partial overlap in the expression of S100 and GFAP with Tuj1.

However, co-expression of NOS with GFAP which was the most abundant marker of the neurosphere cells was not observed, indicating that although there might be many neural precursors or glia cells in the neurosphere expressing GFAP, mature neuronal phenotypes do not express it, a characteristic similar with what was observed in ENS in vivo where mature neurons do not express glial markers (Young et al., 2003). However, a co-expression of GFAP with another neuronal marker cannot be excluded from our experiments. Also, as discussed in Chapter 4 (4.3.1.), in an induced topical ENS injury with benzalkonium chloride, it was shown that glial cells were able to give rise to neurons *in vivo* (Laranjeira et al., 2011). Neurosphere generation could resemble an injury model *in vitro* as these aggregates are formed following gut dissociation and thus cells expressing glial markers could be potential neural progenitors.

All these data helped to assemble a picture of what is happening in the neurosphere microenvironment in terms of cell proliferation and differentiation over time. Cell behaviour which follows a specific pattern is

of great value as it can enable the application and study of different factors in order to alter and modify this behaviour, a feature important for potential clinical applications of neurosphere cells. Therefore, we investigated the role of Notch signaling, a pathway which has been shown to maintain mammalian neural stem cells in an undifferentiated state in the CNS (Hitoshi et al., 2002), and that is involved in the cell fate of many different cell types in the brain, in the heart or the kidney (Andersson et al., 2011), as well as in the fate of migratory cells of the ENS during development (Okamura et al., 2008).

7.4. Effect of Notch signaling inhibition in neurosphere cells

It has been proposed that Notch signaling maintains the proliferation of neuronal precursors and blocks their differentiation as demonstrated after retroviral activation of Notch signaling in granule neuron precursors resulting in inhibition of their differentiation towards post-mitotic granule neurons (Solecki et al., 2001). Consistent with this mechanism is our finding where upon Notch inhibition with the γ-secretase inhibitor DAPT, we observed a significant increase in the number of immature neuronal marker $Tuj1^+$ cells and a reduction in proliferation. It could be argued that the increase in the number of $Tuj1^+$ cells could be also due to de-differentiation. This process has also been suggested in a cochlear injury model in rats, where mature $NeuN^+$ neurons expressed the immature

neuronal marker doublecortin (DCX) and the neural stem cell marker nestin 48h after injury (Zheng et al., 2011). However in our case, assuming that GFAP and Sox10 are not present in mature neurons *in vitro* and considering that they are the most abundant markers in a neurosphere before the initiation of DAPT treatment, it is more likely that the high number of $Tuj1^+$ cells derives from $GFAP^+/Sox10^+$ progenitors, consistent with their observed reduction. Thus, any contribution from neuronal de-differentiation would be small.

Moreover, when we applied DAPT and examined the fate of recently divided cells after 4 days, we found that the expression of the glial marker S100 was lower than the control. As we discussed previously that cells expressing S100 in vitro could be neural progenitors or glia or both, the interpretation of S100 reduction could be that Notch signaling inhibition resulted in blockage of glial differentiation or in the increase of neuronal differentiation which resulted in fewer neural progenitors. We discussed in the previous paragraph that neuronal differentiation indeed happened after 4 day chase without though excluding the blockage of glial differentiation as Notch signaling inhibition in vivo has been shown to impair gliogenesis in both the peripheral nervous system (PNS) and CNS of mouse embryos (Taylor et al., 2007).

7.5. Migratory behaviour of neurosphere-derived cells

We showed that cells can migrate inside the neurosphere from both pulse/chase and chimaeric experiments. For the study of migratory enteric NCCs in vivo various transgenic mice have been generated expressing a fluorophore under the control of enteric NCC-specific promoters such as Ret (Young et al., 2004) and Sox10 (Corpening et al., 2011) or TH for the tracing of immature neurons (Hao and Young, 2009). Such studies have demonstrated that enteric NCCs migrate in chains in a rostro-caudal direction along the gut, forming a scaffold for the rearguard cells, whereas some leading cells can have random migratory trajectories (Young et al., 2004).

Unlike enteric NCCs in vivo, the migration of enteric-derived neurosphere cells in bowel explants is not well understood. Previous research groups have focused on the location of neurosphere-derived cells in bowel explants, after a period of time which was visualized in transplant sections (Almond et al., 2007; Metzger et al., 2009a and b). The migration rate and pattern were not examined. In this study we used a lentiviral based approach to insert the EGFP gene in the genome of neurosphere-derived cells to label them permanently. Migration experiments with embryonic $EGFP^{+}$ neurospheres showed that neurosphere cells can migrate caudally

or rostrally in both embryonic aganglionic and neonatal ganglionic bowel and this migration was not tissue specific. These results differed from what other groups have shown concerning migration of enteric NCCS where they found limitations in migration when the migratory direction was rostral and when the recipient gut was older and ganglionic (Anderson et al., 2007; Druckenbrod and Epstein, 2009; Hotta et al., 2010). These differences imply the possible regulation of migratory behaviour of neurosphere-derived cells by mechanisms different from the ones controlling enteric NCCs in vivo.

7.6. Role of Notch signaling in the migratory behaviour of neurosphere-derived cells

The role of the Notch signaling pathway in the migration of neurosphere-derived cells was also examined. Notch signaling inhibition promoted neurite formation from neurospheres and the neurite length was longer than controls. Notch signaling has been previously shown to inhibit neurite outgrowth in vitro. The induced neurite outgrowth by nerve growth factor (NGF) in the rat adrenal medulla cell line PC12 was impaired by transient overexpression of the Notch1 intracellular domain (Levy et al., 2002). Also, inhibition of Notch signaling by γ-secretase inhibitors promoted length of neurites and decreased the branching of the processes formed by human NT2N neurons which were culture on poly-D-lysine and laminin coated

coverslips, similar culture conditions to the ones used in this thesis (Figueroa et al., 2002).

Regarding migration, in neurospheres which were treated with the Notch inhibitor DAPT we observed a higher number of migrating cells away and the cells also covered longer distances compared to controls. In sections of mouse embryos lacking the Notch target gene Hes1, misplacement of hypothalamic neurons was observed, indicating the role of Notch signaling in the regulation of neuronal migratory behaviour (Aujla et al., 2011). An atypical localization pattern of CNS neurons was also observed in embryonic mice lacking presenilin1 (part of the γ-secretase protein complex) where it was suggested that Notch inhibition promoted early neuronal differentiation and thus attenuated their migratory properties (Louvi et al., 2004). We could not observe an apparent defect in migration of neurosphere-derived cells after Notch signaling inhibition but migration seemed to be promoted, implying that maybe other mechanisms are interfering with this cell behaviour.

In conclusion, we have identified a behavioural pattern in terms of proliferation, differentiation and motility in the cells of embryonic mouse-gut derived neurospheres. We demonstrated that inhibition of the Notch signaling pathway blocks proliferation and promotes differentiation of

neurosphere cells. Finally we showed that migration of neurosphere cells in gut explants is not affected by the presence of an already formed ENS. Our results contribute to a better understanding of the properties of ENS progenitor cells in vitro and advance one step closer to clinical applications for the treatment of ENS disorders such as HSCR.

7.7. Future plans

In this study we investigated the properties of neurospheres derived from embryonic mouse bowel. However, it is uncertain if the same principles apply in cells derived from postnatal tissue, as it has already been shown that in vivo postnatal enteric NCCs characterized by p75 and a4-integrin expression were not proliferating as much as E14.5 enteric NCCs. In addition, the ability of postnatal enteric NCCs to generate serotonergic neurons in vitro was lower than E14.5 enteric NCCs and impaired with increasing age (Kruger et al., 2002) indicating that there are some fundamental differences among ENS progenitors from different developmental stages. Therefore it would be interesting to investigate the differences in proliferation and phenotypic expression of neurosphere cells derived from postnatal gut and examine how their properties are regulated by Notch signaling as postnatal tissue would be a great candidate for clinical applications.

Also, we observed a really low number of recently divided cells upon Notch signaling inhibition, implying that the Notch pathway could be important for the survival of proliferating cells in the neurosphere. The role of Notch signaling in preventing apoptosis in vivo has already been shown in transgenic mouse embryos lacking normal function of the Notch-2 receptor, where embryos could not survive beyond E11.5 and increased apoptosis was observed in sections of the telencephalic region at E9.5 (Hamada et al., 1999). In addition, inhibition of Notch signaling in human and mouse pancreatic islet cultures as well as mouse insulinoma cells (MIN6) using the γ-secretase inhibitor DAPT, provoked apoptosis as shown by caspase-3 upregulation, a process which was reversible by overexpression of γ-secretase complex protein presenilin-1 (PSEN1) (Dror et al., 2007). Therefore, further investigation of apoptotic proteins like caspase-3 (Gulyaeva et al., 2004) in neurosphere cells after Notch signaling inhibition will address the question of whether the reduction in proliferating cells is due to cell death.

Finally, migration experiments with neurosphere cells showed that their behaviour is not altered whether the recipient gut is ganglionic or older and also it was not inhibited when they were transplanted in different organs. This behaviour needs to be further studied as we need to understand the mechanisms of neurosphere-derived cell migration because it is crucial for

their targeted clinical transplantation in the future. Extracellular matrix (ECM) protein receptors play an important role in cell migration. There is not much information available concerning ECM receptors expressed in neurosphere-derived cells except the fact that β1-integrin, an ECM receptor, is expressed at the periphery of neurospheres derived from rat neonatal brains (Campos et al., 2004). On the contrary in the development of the ENS a critical role has been given to ECM proteins such as fibronectin, laminin and tenascin in the regulation of migration of enteric NCCs (Newgreen et al., 1995; Breau et al., 2009). Therefore, ECM receptors can have a key role in the migration of neurosphere-derived cells, a subject which requires further investigation.

Bibliography

Ables, J. L., Breunig, J. J., Eisch, A. J. and Rakic, P. (2011). Not(ch) just development: Notch signalling in the adult brain. *Nature Reviews Neuroscience* **12**, 269-283.

Acloque, H. (2009). Epithelial-mesenchymal transitions: the importance of changing cell state in development and disease. *The Journal of Clinical Investigation* **119**, 1438-1449.

Ahmed, B., Chakravarthy, S., Eggers, R., Hermens, W., Zhang, J., Niclou, S., Levelt, C., Sablitzky, F., Anderson, P., Lieberman, A. et al. (2004). Efficient delivery of Cre-recombinase to neurons in vivo and stable transduction of neurons using adeno-associated and lentiviral vectors. *BMC Neuroscience* **5**, 4.

Airaksinen, M. S. and Saarma, M. (2002). The GDNF family: Signalling, biological functions and therapeutic value. *Nature Reviews Neuroscience* **3**, 383-394.

Allan, I. J. and Newgreen, D. F. (1980). The origin and differentiation of enteric neurons of the intestine of the fowl embryo. *American Journal of Anatomy* **157**, 137-154.

Almond, S., Lindley, R. M., Kenny, S. E., Connell, M. G. and Edgar, D. H. (2007). Characterisation and transplantation of enteric nervous system progenitor cells. *Gut* **56**, 489-496.

Alyassin, T. M. and Toner, P. G. (1977). Fine-Structure of Squamous Epithelium and Submucosal Glands of Human Esophagus. *Journal of Anatomy*, **123**, 705-721

Amiel, J. and Lyonnet, S. (2001). Hirschsprung disease, associated syndromes, and genetics: a review. *Journal of Medical Genetics* **38**, 729-739.

Amiel, J., Sproat-Emison, E., Garcia-Barcelo, M., Lantieri, F., Burzynski, G., Borrego, S., Pelet, A., Arnold, S., Miao, X., Griseri, P. et al. (2008). Hirschsprung disease, associated syndromes and genetics: a review. *Journal of Medical Genetics* **45**, 1-14.

Andersen, R. K., Johansen, M., Blaabjerg, M., Zimmer, J. and Meyer, M. (2007). Neural tissue-spheres: A microexplant culture method for propagation of precursor cells from the rat forebrain subventricular zone. *Journal of Neuroscience Methods* **165**, 55-63.

Andersen, R. K., Zimmer, J. and Meyer, M. (2011). Long-Term Propagation of Neural Stem Cells: Focus on Three-Dimensional Culture Systems and Mitogenic Factors: Humana Press Inc, 999 Riverview Dr, Ste 208, Totowa, Nj 07512-1165 USA.

Anderson, N., Young. (2006a). Neural Crest and the Development of the Enteric Nervous System. *Textbook.*

Anderson, R. B., Bergner, A. J., Taniguchi, M., Fujisawa, H., Forrai, A., Robb, L. and Young, H. M. (2007). Effects of different regions of the developing gut on the migration of enteric neural crest-derived cells: A role for Sema3A, but not Sema3F. *Developmental Biology* **305**, 287-299.

Anderson, R. B., Turner, K. N., Nikonenko, A. G., Hemperly, J., Schachner, M. and Young, H. M. (2006b). The Cell Adhesion Molecule L1 Is Required for Chain Migration of Neural Crest Cells in the Developing Mouse Gut. *Gastroenterology* **130**, 1221-1232.

Andersson, E. R., Sandberg, R. and Lendahl, U. (2011). Notch signaling: simplicity in design, versatility in function. *Development* **138**, 3593-3612.

Artavanis-Tsakonas, S., Rand, M. D. and Lake, R. J. (1999). Notch signaling: Cell fate control and signal integration in development. *Science* **284**, 770-776.

Aujla, P. K., Bora, A., Monahan, P., Sweedler, J. V. and Raetzman, L. T. (2011). The Notch effector gene Hes1 regulates migration of hypothalamic neurons, neuropeptide content and axon targeting to the pituitary. *Developmental Biology* **353**, 61-71.

Baetge, G., Pintar, J. E. and Gershon, M. D. (1990). Transiently catecholaminergic (TC) cells in the bowel of the fetal rat: Precursors of noncatecholaminergic enteric neurons. *Developmental Biology* **141**, 353-380.

Bareiss, P., Metzger, M., Sohn, K., Rupp, S., Frick, J., Autenrieth, I., Lang, F., Schwarz, H., Skutella, T. and Just, L. (2008). Organotypical tissue cultures from adult murine colon as an in vitro model of intestinal mucosa. *Histochemistry and Cell Biology* **129**, 795-804.

Barlow, A., de Graaff, E. and Pachnis, V. (2003). Enteric Nervous System Progenitors Are Coordinately Controlled by the G Protein-Coupled

Receptor EDNRB and the Receptor Tyrosine Kinase RET. *Neuron* **40**, 905-916.

Barlow, A. J., Wallace, A. S., Thapar, N. and Burns, A. J. (2008). Critical numbers of neural crest cells are required in the pathways from the neural tube to the foregut to ensure complete enteric nervous system formation. *Development* **135**, 1681-1691.

Barros, C. S., Franco, S. J., Muller, U. (2010). Extracellular Matrix: Functions in the Nervous System. Cold Spring Harbour Perspectives in Biology. Cold Spring Harbour Laboratory Press.

Baynash, A. G., Hosoda, K., Giaid, A., Richardson, J. A., Emoto, N., Hammer, R. E. and Yanagisawa, M. (1994). Interaction of endothelin-3 with endothelin-B receptor is essential for development of epidermal melanocytes and enteric neurons. *Cell* **79**, 1277-1285.

Bender, F., Fischer, M., Funk, N., Orel, N., Rethwilm, A. and Sendtner, M. (2007). High-efficiency gene transfer into cultured embryonic motoneurons using recombinant lentiviruses. *Histochemistry and Cell Biology* **127**, 439-448.

Berezovska, O., McLean, P., Knowles, R., Frosh, M., Lu, F. M., Lux, S. E. and Hyman, B. T. (1999). Notch1 inhibits neurite outgrowth in postmitotic primary neurons. *Neuroscience* **93**, 433-439.

Bixby, S., Kruger, G. M., Mosher, J. T., Joseph, N. M. and Morrison, S. J. (2002). Cell-intrinsic differences between stem cells from different regions of the peripheral nervous system regulate the generation of neural diversity. *Neuron* **35**, 643-656.

Blaugrund, E., Pham, T. D., Tennyson, V. M., Lo, L., Sommer, L., Anderson, D. J. and Gershon, M. D. (1996). Distinct subpopulations of enteric neuronal progenitors defined by time of development, sympathoadrenal lineage markers and Mash-1-dependence. *Development* **122**, 309-320.

Blindt, R., Bosserhoff, A. K., Dammers, J., Krott, N., Demircan, L., Hoffmann, R., Hanrath, P., Weber, C. and Vogt, F. (2004). Downregulation of N-cadherin in the neointima stimulates migration of smooth muscle cells by RhoA deactivation. *Cardiovascular Research* **62**, 212-222.

Blomer, U., Naldini, L., Kafri, T., Trono, D., Verma, I. M. and Gage, F. H. (1997). Highly efficient and sustained gene transfer in adult neurons with a lentivirus vector. *Journal of Virology* **71**, 6641-6649.

Bondurand, N., Natarajan, D., Barlow, A., Thapar, N. and Pachnis, V. (2006). Maintenance of mammalian enteric nervous system progenitors by SOX10 and endothelin 3 signalling. *Development* **133**, 2075-2086.

Bondurand, N., Natarajan, D., Thapar, N., Atkins, C. and Pachnis, V. (2003). Neuron and glia generating progenitors of the mammalian enteric nervous system isolated from foetal and postnatal gut cultures. *Development* **130**, 6387-6400.

Breau, M. A., Dahmani, A., Broders-Bondon, F., Thiery, J.-P. and Dufour, S. (2009). Beta-1 integrins are required for the invasion of the caecum and proximal hindgut by enteric neural crest cells. *Development* **136**, 2791-2801.

Breau, M. A., Pietri, T., Eder, O., Blanche, M., Brakebusch, C., Fassler, R., Thiery, J. P. and Dufour, S. (2006). Lack of beta 1 integrins in enteric neural crest cells leads to a Hirschsprung-like phenotype. *Development* **133**, 1725-1734.

Bronner-Fraser, M. (1986). Analysis of the early stages of trunk neural crest migration in avian embryos using monoclonal antibody HNK-1. *Developmental Biology* **115**, 44-55.

Bronner-Fraser, M. (1994). Neural crest cell formation and migration in the developing embryo. *The FASEB Journal* **8**, 699-706.

Brookes, S. J. H. (1993). Neuronal nitric-oxide in the gut. *Journal of Gastroenterology and Hepatology* **8**, 590-603.

Brou, C. (2009). Intracellular trafficking of Notch receptors and ligands. *Experimental Cell Research* **315**, 1549-1555.

Buck, S. B., Bradford, J., Gee, K. R., Agnew, B. J., Clarke, S. T. and Salic, A. (2008). Detection of S-phase cell cycle progression using 5-ethynyl-2 '-deoxyuridine incorporation with click chemistry an alternative to using 5-bromo-2 '-deoxyuridine antibodies. *Biotechniques* **44**, 927-929.

Burns, A. J. (2005). Migration of neural crest-derived enteric nervous system precursor cells to and within the gastrointestinal tract. *Int. J. Dev. Biol* **49**, 143-150.

Burns, A. J., Champeval, D. and Le Douarin, N. M. (2000). Sacral Neural Crest Cells Colonise Aganglionic Hindgut in Vivo but Fail to Compensate for Lack of Enteric Ganglia. *Developmental Biology* **219**, 30-43.

Burns, A. J. and Le Douarin, N. M. (1998). The sacral neural crest contributes neurons and glia to the post-umbilical gut: spatiotemporal analysis of the development of the enteric nervous system. *Development* **125**, 4335-4347.

Burns, A. J., Roberts, R. R., Bornstein, J. C. and Young H.M. (2009). Development of the enteric nervous system and its role in intestinal motility during fetal and early postnatal stages. *Seminars in pediatric surgery* **18**, 196-205.

Burzynski, G., Shepherd, I. T. and Enomoto, H. (2009). Genetic model system studies of the development of the enteric nervous system, gut motility and Hirschsprung's disease. *Neurogastroenterology and Motility* **21**, 113-127.

Cacalano, G., Farinas, I., Wang, L. C., Hagler, K., Forgie, A., Moore, M., Armanini, M., Phillips, H., Ryan, A. M., Reichardt, L. F. et al. (1998). GFR alpha 1 is an essential receptor component for GDNF in the developing nervous system and kidney. *Neuron* **21**, 53-62.

Campos, L. S., Decker, L., Taylor, V. and Skarnes, W. (2006). Notch, epidermal growth factor receptor, and β1-integrin pathways are coordinated in neural stem cells. *Journal of Biological Chemistry* **281**, 5300-5309.

Campos, L. S., Leone, D. P., Relvas, J. B., Brakebusch, C., Fassler, R., Suter, U. and ffrench-Constant, C. (2004). B-1 integrins activate a MAPK signalling pathway in neural stem cells that contributes to their maintenance. *Development* **131**, 3433-3444.

Cantrell, V. A., Owens, S. E., Bradley, K. M., Smith, J. R. and Southard-Smith, E. M. (2004). Interactions between Sox10 and EdnrB modulate penetrance and severity of aganglionosis in the Sox10(Dom) mouse model of Hirschsprung disease. *Human Molecular Genetics* **13**, 2289-2301.

Chalazonitis, A., D'Autreaux, F., Guha, U., Pham, T. D., Faure, C., Chen, J. J., Roman, D., Kan, L. X., Rothman, T. P., Kessler, J. A. et al. (2004). Bone morphogenetic protein-2 and-4 limit the number of enteric neurons but promote development of a TrkC-expressing neurotrophin-3-dependent subset. *Journal of Neuroscience* **24**, 4266-4282.

Chalazonitis, A., Pham, T. D., Li, Z. S., Roman, D., Guha, U., Gomes, W., Kan, L. X., Kessler, J. A. and Gershon, M. D. (2008). Bone morphogenetic protein regulation of enteric neuronal phenotypic diversity: Relationship to timing of cell cycle exit. *Journal of Comparative Neurology* **509**, 474-492.

Chalazonitis, A., Rothman, T. P., Chen, J. and Gershon, M. D. (1998). Age-Dependent Differences in the Effects of GDNF and NT-3 on the Development of Neurons and Glia from Neural Crest-Derived Precursors Immunoselected from the Fetal Rat Gut: Expression of GFR[alpha]-1in Vitroandin Vivo. *Developmental Biology* **204**, 385-406.

Chalazonitis, A.,Tennyson, V. M.,Kibbey, M. C.,Rothman, T. P. and Gershon, M. D. (1997). The A1 Subunit of Laminin-1 Promotes the Development of Neurons by Interacting with Lbp110 Expressed by Neural

Crest-Derived Cells Immunoselected from the Fetal Mouse Gut. *Journal of Neurobiology*, **33**(2), 118-138.

Chan, K. K., Chen, Y. S., Yau, T. O., Fu, M., Lui, V. C. H., Tam, P. K. H. and Sham, M. H. (2005). Hoxb3 vagal neural crest-specific enhancer element for controlling enteric nervous system development. *Developmental Dynamics* **233**, 473-483.

Chen, J., Zacharek, A., Li, A., Cui, X., Roberts, C., Lu, M. and Chopp, M. (2008). Atorvastatin Promotes Presenilin-1 Expression and Notch1 Activity and Increases Neural Progenitor Cell Proliferation After Stroke. *Stroke* **39**, 220-226.

Chumpitazi, B. P. and Nurko, S. (2011). Defecation Disorders in Children after Surgery for Hirschsprung Disease. *Journal of Pediatric Gastroenterology and Nutrition*, **53**(1), 75-79.

Conner, P. J., Focke, P. J., Noden, D. M. and Epstein, M. L. (2003). Appearance of neurons and glia with respect to the wavefront during colonization of the avian gut by neural crest cells. *Developmental Dynamics* **226**, 91-98.

Cooper-Kuhn, C. M. and Georg Kuhn, H. (2002). Is it all DNA repair?: Methodological considerations for detecting neurogenesis in the adult brain. *Developmental Brain Research* **134**, 13-21.

Cornell, R. A. and Eisen, J. S. (2005). Notch in the pathway: The roles of Notch signaling in neural crest development. *Seminars in Cell & Developmental Biology* **16**, 663-672.

Corpening, J. C., Deal, K. K., Cantrell, V. A., Skelton, S. B., Buehler, D. P. and Southard-Smith, E. M. (2011). Isolation and Live Imaging of Enteric Progenitors Based on Sox10-Histone2BVenus Transgene Expression. *genesis* **49**, 599-618.

Crawford, T. Q. and Roelink, H. (2007). The Notch response inhibitor DAPT enhances neuronal differentiation in embryonic stem cell-derived embryoid bodies independently of sonic hedgehog signaling. *Developmental Dynamics* **236**, 886-892.

de Graaff, E., Srinivas, S., Kilkenny, C., D'Agati, V., Mankoo, B. S., Costantini, F. and Pachnis, V. (2001). Differential activities of the RET tyrosine kinase receptor isoforms during mammalian embryogenesis. *Genes & Development* **15**, 2433-2444.

De Strooper, B. and Annaert, W. (2010). Novel Research Horizons for Presenilins and gamma-Secretases in Cell Biology and Disease. In *Annual Review of Cell and Developmental Biology, Vol 26*, vol. 26 (ed. R. Schekman L. Goldstein and R. Lehmann), pp. 235-260. Palo Alto: Annual Reviews.

Del Bene, F. (2011). Interkinetic nuclear migration: cell cycle on the move. *Embo Journal* **30**, 1676-1677.

Delalande, J.-M., Barlow, A. J., Thomas, A. J., Wallace, A. S., Thapar, N., Erickson, C. A. and Burns, A. J. (2008). The receptor tyrosine kinase RET regulates hindgut colonization by sacral neural crest cells. *Developmental Biology* **313**, 279-292.

Deloulme, J. C., Raponi, E., Gentil, B. J., Bertacchi, N., Marks, A., Labourdette, G. and Baudier, J. (2004). Nuclear expression of S10013 in oligodendrocyte progenitor cells correlates with differentiation toward the oligodendroglial lineage and modulates oligodendrocytes maturation. *Molecular and Cellular Neuroscience* **27**, 453-465.

Demaison, C. (2002). High-Level Transduction and Gene Expression in Hematopoietic Repopulating Cells Using a Human Imunodeficiency Virus

Type 1-Based Lentiviral Vector Containing an Internal Spleen Focus Forming Virus Promoter.

Dennis, K., Uittenbogaard, M., Chiaramello, A. and Moody, S. A. (2002). Cloning and characterization of the 5 '-flanking region of the rat neuron-specific Class III beta-tubulin gene. *Gene* **294**, 269-277.

Doetsch, F. (2003). The glial identity of neural stem cells. *Nature Neuroscience* **6**, 1127-1134.

Dong, Y. F., Jesse, A. M., Kohn, A., Gunnell, L. M., Honjo, T., Zuscik, M. J., O'Keefe, R. J. and Hilton, M. J. (2010). RBPj kappa-dependent Notch signaling regulates mesenchymal progenitor cell proliferation and differentiation during skeletal development. *Development* **137**, 1461-1471.

Dong, Y. L., Liu, W., Gao, Y. M., Wu, R. D., Zhang, Y. H., Wang, H. F. and Wei, B. (2008). Neural Stem Cell Transplantation Rescues Rectum Function in the Aganglionic Rat. *Transplantation Proceedings* **40**, 3646-3652.

Dormann, D. and Weijer, C. J. (2003). Chemotactic cell movement during development. *Current Opinion in Genetics & Development* **13**, 358-364.

Dovey, H. F., John, V., Anderson, J. P., Chen, L. Z., Andrieu, P. D., Fang, L. Y., Freedman, S. B., Folmer, B., Goldbach, E., Holsztynska, E. J. et al. (2001). Functional gamma-secretase inhibitors reduce beta-amyloid peptide levels in brain. *Journal of Neurochemistry* **76**, 173-181.

Draberova, E., Del Valle, L., Gordon, J., Markova, V., Smejkalova, B., Bertrand, L., de Chadarevian, J. P., Agamanolis, D. P., Legido, A., Khalili, K. et al. (2008). Class III beta-tubulin is constitutively coexpressed with glial fibrillary acidic protein and nestin in midgestational human fetal astrocytes: Implications for phenotypic identity. *Journal of Neuropathology and Experimental Neurology* **67**, 341-354.

Dror, V., Nguyen, V., Walia, P., Kalynyak, T., Hill, J. and Johnson, J. (2007). Notch signalling suppresses apoptosis in adult human and mouse pancreatic islet cells. *Diabetologia* **50**, 2504-2515.

Druckenbrod, N. R. and Epstein, M. L. (2005). The pattern of neural crest advance in the cecum and colon. *Developmental Biology* **287**, 125-133.

Druckenbrod, N. R. and Epstein, M. L. (2007). Behavior of enteric neural crest-derived cells varies with respect to the migratory wavefront. *Developmental Dynamics* **236**, 84-92.

Druckenbrod, N. R. and Epstein, M. L. (2009). Age-dependent changes in the gut environment restrict the invasion of the hindgut by enteric neural progenitors. *Development* **136**, 3195-3203.

Druckenbrod, N. R., Powers, P. A., Bartley, C. R., Walker, J. W. and Epstein, M. L. (2008). Targeting of endothelin receptor-B to the neural crest. *genesis* **46**, 396-400.

Durbec, P. L., Larsson-Blomberg, L. B., Schuchardt, A., Costantini, F. and Pachnis, V. (1996). Common origin and developmental dependence on c-ret of subsets of enteric and sympathetic neuroblasts. *Development* **122**, 349-358.

Eggers, R., Hendriks, W. T. J., Tannemaat, M. R., van Heerikhuize, J. J., Pool, C. W., Carlstedt, T. P., Zaldumbide, A., Hoeben, R. C., Boer, G. J. and Verhaagen, J. (2008). Neuroregenerative effects of lentiviral vector-mediated GDNF expression in reimplanted ventral roots. *Molecular and Cellular Neuroscience* **39**, 105-117.

Ehninger, D. and Kempermann, G. (2008). Neurogenesis in the adult hippocampus. *Cell and Tissue Research* **331**, 243-250.

Eisch, A. J. and Mandyam, C. D. (2007). Adult neurogenesis: Can analysis of cell cycle proteins move us "Beyond BrdU"? *Current Pharmaceutical Biotechnology* **8**, 147-165.

Elworthy, S., Pinto, J. P., Pettifer, A., Cancela, M. L. and Kelsh, R. N. (2005). Phox2b function in the enteric nervous system is conserved in zebrafish and is Sox10-dependent. *Mechanisms of Development* **122**, 659-669.

Enomoto. (2009). Death comes early: apoptosis observed in ENS precursors. *Neurogastroenterology & Motility* **21**, 684-687.

Enomoto, H., Araki, T., Jackman, A., Heuckeroth, R. O., Snider, W. D., Johnson, E. M. and Milbrandt, J. (1998). GFR alpha 1-deficient mice have deficits in the enteric nervous system and kidneys. *Neuron* **21**, 317-324.

Enomoto, H., Hughes, I., Golden, J., Baloh, R. H., Yonemura, S., Heuckeroth, R. O., Johnson, E. M. and Milbrandt, J. (2004). GFR alpha

1 expression in cells lacking RET is dispensable for organogenesis and nerve regeneration. *Neuron* **44**, 623-636.

Epstein, M. L., Mikawa, T., Brown, A. M. C. and McFarlin, D. R. (1994). Mapping the origin of the avian enteric nervous system with a retroviral marker. *Developmental Dynamics.* **201**, 236-244.

Epstein, M. L., Poulsen, K. T. and Thiboldeaux, R. (1991). Formation of ganglia in the gut of the chick embryo. *The Journal of comparative neurology.* **307**, 189-199.

Estrada-Mondaca, S., Carreon-Rodriguez, A. and Belkind-Gerson, J. (2007). Biology of the adult enteric neural stem cell. *Developmental Dynamics* **236**, 20-32.

Fan, X., Khaki, L., Zhu, T. S., Soules, M. E., Talsma, C. E., Gul, N., Koh, C., Zhang, J., Li, Y.-M., Maciaczyk, J. et al. (2010). NOTCH Pathway Blockade Depletes CD133-Positive Glioblastoma Cells and Inhibits Growth of Tumor Neurospheres and Xenografts. *Stem Cells* **28**, 5-16.

Faure, C., Chalazonitis, A., Rheaume, C., Bouchard, G., Sampathkumar, S. G., Yarema, K. J. and Gershon, M. D. (2007).

Gangliogenesis in the enteric nervous system: Roles of the polysialylation of the neural cell adhesion molecule and its regulation by bone morphogenetic protein-4. *Developmental Dynamics* **236**, 44-59.

Fekete, E., Timmermans, J. P., Resch, B. A. and Scheuermann, D. W. (1999). Different distribution of S-100 protein and glial fibrillary acidic protein (GFAP) immunoreactive cells and their relations with nitrergic neurons in the human fetal small intestine. *Histology and Histopathology* **14**, 785-790.

Figueroa, D. J., Morris, J. A., Ma, L., Kandpal, G., Chen, E., Li, Y.-M. and Austin, C. P. (2002). Presenilin-Dependent Gamma-Secretase Activity Modulates Neurite Outgrowth. *Neurobiology of Disease* **9**, 49-60.

Fre, S., Huyghe, M., Mourikis, P., Robine, S., Louvard, D. and Artavanis-Tsakonas, S. (2005). Notch signals control the fate of immature progenitor cells in the intestine. *Nature* **435**, 964-968.

Fu, M., Lui, V. C. H., Sham, M. H., Cheung, A. N. Y. and Tam, P. K. H. (2003). HOXB5 expression is spatially and temporarily regulated in human embryonic gut during neural crest cell colonization and differentiation of enteric neuroblasts. *Developmental Dynamics* **228**, 1-10.

Fu, M., Lui, V. C. H., Sham, M. H., Pachnis, V. and Tam, P. K. H. (2004). Sonic hedgehog regulates the proliferation, differentiation, and migration of enteric neural crest cells in gut. *Journal of Cell Biology* **166**, 673-684.

Fu, M., Sato, Y., Lyons-Warren, A., Zhang, B., Kane, M. A., Napoli, J. L. and Heuckeroth, R. O. (2010). Vitamin A facilitates enteric nervous system precursor migration by reducing Pten accumulation. *Development* **137**, 631-640.

Furness, J. B. (2006). The Enteric Nervous System. Malden (MA): Blackwell Publishing.

Furness, J. B. (2008). The enteric nervous system: normal functions and enteric neuropathies. *Neurogastroenterology & Motility* **20**, 32-38.

Fusaoka-Nishioka, E., Shimono, C., Taniguchi, Y., Togawa, A., Yamada, A., Inoue, E., Onodera, H., Sekiguchi, K. and Imai, T. (2011). Differential effects of laminin isoforms on axon and dendrite development in hippocampal neurons. *Neuroscience Research*.

Gamm, Lynda, S. W., Elizabeth, E. C., Rebecca, L. S., Jason, S. M., Hyun-Jung, K., Bernard, L. S., John Nicholas, M. and Clive, N. S.

(2008). Regulation of Prenatal Human Retinal Neurosphere Growth and Cell Fate Potential by Retinal Pigment Epithelium and Mash1. *Stem Cells* **26**, 3182-3193.

Gammill, L. S. and Bronner-Fraser, M. (2003). Neural crest specification: migrating into genomics. *Nat Rev Neurosci* **4**, 795-805.

Garcia, A. D. R.,Doan, N. B.,Imura, T.,Bush, T. G. and Sofroniew, M. V. (2004). Gfap-Expressing Progenitors Are the Principal Source of Constitutive Neurogenesis in Adult Mouse Forebrain. *Nature Neuroscience*, **7**(11), 1233-1241.

Gariepy, C. E., Williams, S. C., Richardson, J. A., Hammer, R. E. and Yanagisawa, M. (1998). Transgenic expression of the endothelin-B receptor prevents congenital intestinal aganglionosis in a rat model of Hirschsprung disease. *Journal of Clinical Investigation* **102**, 1092-1101.

Gerdes, J., Schwab, U., Lemke, H. and Stein, H. (1983). Production of a mouse monoclonal antibody reactive with a human nuclera antigen associated with cell proliferation. *International Journal of Cancer* **31**, 13-20.

Gershon, M. D. (1997). Genes and lineages in the formation of the enteric nervous system. *Current Opinion in Neurobiology* **7**, 101-109.

Gershon, M. D. (1999). Endothelin and the development of the enteric nervous system. *Clinical and Experimental Pharmacology and Physiology* **26**, 985-988.

Gershon, M. D. (2007). Transplanting the enteric nervous system: a step closer to treatment for aganglionosis. *Gut* **56**, 459-461.

Gershon, M. D. (2010). Developmental determinants of the independence and complexity of the enteric nervous system. *Trends in Neurosciences* **33**, 446-456.

Gershon, M. D. (2011). Behind an enteric neuron there may lie a glial cell. *Journal of Clinical Investigation* **121**, 3386-3389.

Gershon, M. D., Rothman, T. P., John, T. H. and Teitelman, G. N. (1984). Transient and differential expression of aspects of the catecholaminergic phenotype during development of the fetal bowel of rats and mice. *Journal of Neuroscience* **4**, 2269-2280.

Gianino, S., Grider, J. R., Cresswell, J., Enomoto, H. and Heuckeroth, R. O. (2003). GDNF availability determines enteric neuron number by controlling precursor proliferation. *Development* **130**, 2187-2198.

Gilbert, S. (2000). Developmental Biology, 6th edition. *Sunderland (MA)* Sinauer Associates.

Goldstein, A. M., Brewer, K. C., Doyle, A. M., Nagy, N. and Roberts, D. J. (2005). BMP signaling is necessary for neural crest cell migration and ganglion formation in the enteric nervous system. *Mechanisms of Development* **122**, 821-833.

Goldstein, A. M. and Nagy, N. (2008). A bird's eye view of enteric nervous system development: Lessons from the avian embryo. *Pediatric Research* **64**, 326-333.

Grottkau, B. E., Chen, X.-R., Friedrich, C. C., Yang, X.-m., Jing, W., Wu, Y., Cai, X.-x., Liu, Y.-r., Huang, Y.-d. and Lin, Y.-f. (2009). DAPT Enhances the Apoptosis of Human Tongue Carcinoma Cells. *International Journal of Oral Science* **1**, 81-89.

Guillemot, F., Lo, L. C., Johnson, J. E., Auerbach, A., Anderson, D. J. and Joyner, A. L. (1993). Mammalian achaete-scute homolog-1 is required for the early development of olfactory and autonomic neurons. *Cell* **75**, 463-476.

Gulyaeva, N. V. (2004). "Apoptotic" mechanisms in normal brain plasticity: Caspase-3 and long-term potentiation. *Zhurnal Vysshei Nervnoi Deyatelnosti Imeni I P Pavlova* **54**, 437-447.

Hall K. B. (2008). The neural crest and neural crest cells: discovery and signifi cance for theories of embryonic organization. *J. Biosci.* **33**(5), 781–793.

Hamada, Y.,Kadokawa, Y.,Okabe, M.,Ikawa, M.,Coleman, J. R. and Tsujimoto, Y. (1999). Mutation in Ankyrin Repeats of the Mouse Notch2 Gene Induces Early Embryonic Lethality. *Development*, **126**(15), 3415-3424.

Hansen, D. V.,Lui, J. H.,Parker, P. R. L. and Kriegstein, A. R. (2010). Neurogenic Radial Glia in the Outer Subventricular Zone of Human Neocortex. *Nature*, **464**(7288), 554-561.

Hao, M. M., Anderson, R. B., Kobayashi, K., Wittington, P. M., Young, H. M. (2008). The migratory behavior of immature enteric neurons. *Developmental Neurobiology* **69, 22-35**

Hao, M. M. and Young, H. M. (2009). Development of enteric neuron diversity. *Journal of Cellular and Molecular Medicine* **13**, 1193-1210.

Hashimoto-Torii, K.,Torii, M.,Sarkisian, M. R.,Bartley, C. M.,Shen, J.,Radtke, F.,Gridley, T.,Sestan, N. and Rakic, P. (2008). Interaction between Reelin and Notch Signaling Regulates Neuronal Migration in the Cerebral Cortex. *Neuron*, **60**(2), 273-284.

Hearn, C. J., Murphy, M. and Newgreen, D. (1998). GDNF and ET-3 differentially modulate the numbers of avian enteric neural crest cells and enteric neurons in vitro. *Developmental Biology* **197**, 93-105.

Hearn C.J., Y. H. M., Ciampoli D., Lomax Don Newgreen A. E. G. (1999). Catenary cultures of embryonic gastrointestinal tract support organ morphogenesis, motility, neural crest cell migration, and cell differentiation. *Developmental Dynamics* **214**, 239-247.

Heuckeroth, R. O., Lampe, P. A., Johnson, E. M. and Milbrandt, J. (1998). Neurturin and GDNF promote proliferation and survival of enteric neuron and glial progenitors in vitro. *Developmental Biology* **200**, 116-129.

Hitoshi, S.,Alexson, T.,Tropepe, V.,Donoviel, D.,Elia, A. J.,Nye, J. S.,Conlon, R. A.,Mak, T. W.,Bernstein, A. and van der Kooy, D. (2002). Notch Pathway Molecules Are Essential for the Maintenance, but Not the Generation, of Mammalian Neural Stem Cells. *Genes & Development*, **16**(7), 846-858.

Hofstra, R. M. W., Wu, Y., Stulp, R. P., Elfferich, P., Osinga, J., Maas, S. M., Siderius, L., Brooks, A. S., Von der Ende, J. J., Heydendael, V. M., Hosoda, K., Hammer, R. E., Richardson, J. A., Baynash, A. G., Cheung, J. C., Giaid, A. and Yanagisawa, M. (1994). Targeted and natural (piebald-lethal) mutations of endothelin-B gene produce megacolon associated with spotted coat color in mice. *Cell* **79**, 1267-1276.

Hosoda, K.,Hammer, R. E.,Richardson, J. A.,Baynash, A. G.,Cheung, J. C.,Giaid, A. and Yanagisawa, M. (1994). Targeted and Natural (Piebald-Lethal) Mutations of Endothelin-B Receptor Gene Produce Megacolon Associated with Spotted Coat Color in Mice. *Cell*, **79**(7), 1267-1276.

Hotta, R., Anderson, R. B., Kobayashi, K., Newgreen, D. F. and Young, H. M. (2010). Effects of tissue age, presence of neurones and endothelin-3 on the ability of enteric neurone precursors to colonize recipient gut: implications for cell-based therapies. *Neurogastroenterology & Motility* **22**, 331-341.

Ieiri, S., Nakatsuji, T., Akiyoshi, J., Higashi, M., Hashizume, M., Suita, S. and Taguchi, T. (2010). Long-term outcomes and the quality of life of Hirschsprung disease in adolescents who have reached 18 years or older—a 47-year single-institute experience. *Journal of Pediatric Surgery* **45**, 2398-2402.

Ishizaki, Y. (2006). Control of Proliferation and Differentiation of Neural Precursor Cells: Focusing on the Developing Cerebellum. *Journal of Pharmacological Sciences*, **101**(3), 183-188.

Iso, T.,Kedes, L. and Hamamori, Y. (2003). Hes and Herp Families: Multiple Effectors of the Notch Signaling Pathway. *Journal of Cellular Physiology*, **194**(3), 237-255.

Iwashita, T., Kruger, G. M., Pardal, R., Kiel, M. J. and Morrison, S. J. (2003). Hirschsprung disease is linked to defects in neural crest stem cell function. *Science* **301**, 972-976.

Iwasaki, Y.,Shiojima, T. and Kinoshita, M. (1997). S100β Prevents the Death of Motor Neurons in Newborn Rats after Sciatic Nerve Section. *Journal of the Neurological Sciences*, **151**(1), 7-12.

Jarvi, K.,Laitakari, E. M.,Koivusalo, A.,Rintala, R. J. and Pakarinen, M. P. (2010). Bowel Function and Gastrointestinal Quality of Life among Adults Operated for Hirschsprung Disease During Childhood: A Population-Based Study. *Annals of Surgery*, **252**(6), 977-981 910.1097/SLA.1090b1013e3182018542.

Jia, H.,Zhang, K.,Chen, Q.,Gao, H. and Wang, W. (2011). Downregulation of Notch-1/Jagged-2 in Human Colon Tissues from Hirschsprung Disease Patients. *International Journal of Colorectal Disease*, 1-5.

Jing, W.,Xiong, Z.,Cai, X.,Huang, Y.,Li, X.,Yang, X.,Liu, L.,Tang, W.,Lin, Y. and Tian, W. (2010). Effects of Γ-Secretase Inhibition on the Proliferation and Vitamin D3 Induced Osteogenesis in Adipose Derived

Stem Cells. *Biochemical and Biophysical Research Communications*, **392**(3), 442-447.

Jones, P. H.,Simons, B. D. and Watt, F. M. (2007). Sic Transit Gloria: Farewell to the Epidermal Transit Amplifying Cell? *Cell Stem Cell*, **1**(4), 371-381.

Joseph, N. M.,He, S. H.,Quintana, E.,Kim, Y. G.,Nunez, G. and Morrison, S. J. (2011). Enteric Glia Are Multipotent in Culture but Primarily Form Glia in the Adult Rodent Gut. *Journal of Clinical Investigation*, **121**(9), 3398-3411.

Kafri, T.,Blomer, U.,Peterson, D. A.,Gage, F. H. and Verma, I. M. (1997). Sustained Expression of Genes Delivered Directly into Liver and Muscle by Lentiviral Vectors. *Nat Genet*, **17**(3), 314-317.

Kafri, T.,van Praag, H.,Gage, F. H. and Verma, I. M. (2000). Lentiviral Vectors: Regulated Gene Expression. *Mol Ther*, **1**(6), 516-521.

Kapur, R. P. (1999). Early Death of Neural Crest Cells Is Responsible for Total Enteric Aganglionosis in Sox10(Dom)/Sox10(Dom) Mouse Embryos. *Pediatric and Developmental Pathology*, **2**(6), 559-569.

Kapur, R. P. (2000). Colonization of the Murine Hindgut by Sacral Crest-Derived Neural Precursors: Experimental Support for an Evolutionarily Conserved Model. *Developmental Biology* **227**, 146-155.

Kapur, R. P.,Yost, C. and Palmiter, R. D. (1992). A Transgenic Model for Studying Development of the Enteric Nervous-System in Normal and Aganglionic Mice. *Development*, **116**(1), 167-&.

Katsetos, C. D.,Herman, M. M. and Mork, S. J. (2003). Class Iii Beta-Tubulin in Human Development and Cancer. *Cell Motility and the Cytoskeleton*, **55**(2), 77-96.

Kazanis, I.,Lathia, J. D.,Vadakkan, T. J.,Raborn, E.,Wan, R. Q.,Mughal, M. R.,Eckley, D. M.,Sasaki, T.,Patton, B.,Mattson, M. P., et al. (2010). Quiescence and Activation of Stem and Precursor Cell Populations in the Subependymal Zone of the Mammalian Brain Are Associated with Distinct Cellular and Extracellular Matrix Signals. *Journal of Neuroscience*, **30**(29), 9771-9781.

Kearns, S. M.,Laywell, E. D.,Kukekov, V. K. and Steindler, D. A. (2003). Extracellular Matrix Effects on Neurosphere Cell Motility. *Experimental Neurology*, **182**(1), 240-244.

Kee, N.,Sivalingam, S.,Boonstra, R. and Wojtowicz, J. M. (2002). The Utility of Ki-67 and Brdu as Proliferative Markers of Adult Neurogenesis. *Journal of Neuroscience Methods*, **115**(1), 97-105.

Kenny, S. E.,Tam, P. K. H. and Garcia-Barcelo, M. (2010). Hirschsprung's Disease. *Seminars in pediatric surgery*, **19**(3), 194-200.

Kim, J., Lo, L., Dormand, E. and Anderson, D. J. (2003). SOX10 maintains multipotency and inhibits neuronal differentiation of neural crest stem cells. *Neuron* **38**, 17-31.

Kligman, D. and Hilt, D. C. (1988). The S100 Protein Family. *Trends in Biochemical Sciences*, **13**(11), 437-443.

Kirby, ML and KL Waldo. 1990. Role of Neural Crest in Congenital Heart Disease. *Circulation*, **82**(2), 332-340.

Kruger, G. M.,Mosher, J. T.,Bixby, S.,Joseph, N.,Iwashita, T. and Morrison, S. J. (2002). Neural Crest Stem Cells Persist in the Adult Gut but Undergo Changes in Self-Renewal, Neuronal Subtype Potential, and Factor Responsiveness. *Neuron*, **35**(4), 657-669.

Kruger, G. M., Mosher, J. T., Tsai, Y.-H., Yeager, K. J., Iwashita, T., Gariepy, C. E. and Morrison, S. J. (2003). Temporally Distinct Requirements for Endothelin Receptor B in the Generation and Migration of Gut Neural Crest Stem Cells. *Neuron* **40**, 917-929.

LaBonne, C. and Bronner-Fraser, M. (1998). Induction and patterning of the neural crest, a stem cell-like precursor population. *Journal of Neurobiology* **36**, 175-189.

LaBonne, C. and Bronner-Fraser, M. (1999). Molecular mechanisms of neural mechanisms of neural crest formation. *Annual Review of Cell and Developmental Biology* **15**, 81-112.

Landman, K. A.,Simpson, M. J. and Newgreen, D. F. (2007). Mathematical and Experimental Insights into the Development of the Enteric Nervous System and Hirschsprung's Disease. *Development, Growth & Differentiation*, **49**(4), 277-286.

Lane, P. W. and Liu, H. M. (1984). Association of Megacolon with a New Dominant Spotting Gene (Dom) in the Mouse. *Journal of Heredity*, **75**(6), 435-439.

Lang, D., Chen, F., Milewski, R., Li, J., Lu, M. M. and Epstein, J. A. (2000). Pax3 is required for enteric ganglia formation and functions with Sox10 to modulate expression of c-ret. *The Journal of Clinical Investigation* **106**, 963-971.

Lang, D. and Epstein, J. A. (2003). Sox10 and Pax3 Physically Interact to Mediate Activation of a Conserved C-Ret Enhancer. *Human Molecular Genetics*, **12**(8), 937-945.

Laranjeira, C. and Pachnis, V. (2009). Enteric nervous system development: Recent progress and future challenges. *Autonomic Neuroscience-Basic & Clinical* **151**, 61-69.

Laranjeira, C.,Sandgren, K.,Kessaris, N.,Richardson, W.,Potocnik, A.,Berghe, P. V. and Pachnis, V. (2011). Glial Cells in the Mouse Enteric Nervous System Can Undergo Neurogenesis in Response to Injury. *Journal of Clinical Investigation*, **121**(9), 3412-3424.

Le Douarin, N. M. and Teillet, M.-A. (1973). The migration of neural crest cells to the wall of the digestive tract in avian embryo. *Journal of Embryology and Experimental Morphology* **30**, 31-48.

Lee, H. O., Levorse, J. M. and Shin, M. K. (2003). The endothelin receptor-B is required for the migration of neural crest-derived melanocyte and enteric neuron precursors. *Developmental Biology* **259**, 162-175.

Leibl, M. A., Ota, T., Woodward, M. N., Kenny, S. E., Lloyd, D. A., Vaillant, C. R. and Edgar, D. H. (1999). Expression of endothelin 3 by mesenchymal cells of embryonic mouse caecum. *Gut* **44**, 246-252.

Lemke, G. (2009). Developmental Neurobiology. London; Burlington MA, Elsevier, Academic Press.

Leon, T. Y. Y.,Ngan, E. S. W.,Poon, H.-C.,So, M.-T.,Lui, V. C. H.,Tam, P. K. H. and Garcia-Barcelo, M. M. (2009). Transcriptional Regulation of Ret by Nkx2-1, Phox2b, Sox10, and Pax3. *Journal of Pediatric Surgery*, **44**(10), 1904-1912.

Levy, O. A.,Lah, J. J. and Levey, A. I. (2002). Notch Signaling Inhibits Pc12 Cell Neurite Outgrowth Via Rbp-J-Dependent and -Independent Mechanisms. *Developmental Neuroscience*, **24**(1), 79-88.

Li, F.,Lan, Y.,Wang, Y.,Wang, J.,Yang, G.,Meng, F.,Han, H.,Meng, A.,Wang, Y. and Yang, X. (2011). Endothelial Smad4 Maintains

Cerebrovascular Integrity by Activating N-Cadherin through Cooperation with Notch. *Developmental Cell*, **20**(3), 291-302.

Lin, L. F. H.,Doherty, D. H.,Lile, J. D.,Bektesh, S. and Collins, F. (1993). Gdnf - a Glial-Cell Line Derived Neurotrophic Factor for Midbrain Dopaminergic-Neurons. *Science*, **260**(5111), 1130-1132.

Lindley, R. M., Hawcutt, D. B., Connell, M. G., Almond, S. N., Vannucchi, M.-G., Faussone-Pellegrini, M. S., Edgar, D. H. and Kenny, S. E. (2008). Human and Mouse Enteric Nervous System Neurosphere Transplants Regulate the Function of Aganglionic Embryonic Distal Colon. *Gastroenterology* **135**, 205-216.

Lo, L. C. and Anderson, D. J. (1995). Postmigratory Neural Crest Cells Expressing C-Ret Display Restricted Developmental and Proliferative Capacities. *Neuron*, **15**(3), 527-539.

Lo, L. C., Tiveron, M. C. and Anderson, D. J. (1998). MASH1 activates expression of the paired homeodomain transcription factor Phox2a, and couples pan-neuronal and subtype-specific components of autonomic neuronal identity. *Development* **125**, 609-620.

Louvi, A.,Sisodia, S. S. and Grove, E. A. (2004). Presenilin 1 in Migration and Morphogenesis in the Central Nervous System. *Development*, **131**(13), 3093-3105.

McKeown, S. J., Chow, C. W. and Young, H. M. (2001). Development of the submucous plexus in the large intestine of the mouse. *Cell and Tissue Research* **303**, 301-305.

Metzger, M., Bareiss, P. M., Danker, T., Wagner, S., Hennenlotter, J., Guenther, E., Obermayr, F., Stenzl, A., Koenigsrainer, A., Skutella, T. et al. (2009b). Expansion and Differentiation of Neural Progenitors Derived From the Human Adult Enteric Nervous System. *Gastroenterology* **137**, 2063-2073.e4.

Metzger, M., Caldwell, C., Barlow, A. J., Burns, A. J. and Thapar, N. (2009a). Enteric Nervous System Stem Cells Derived From Human Gut Mucosa for the Treatment of Aganglionic Gut Disorders. *Gastroenterology* **136**, 2214-2225

Micci, M. A.,Kahrig, K. M.,Simmons, R. S.,Sarna, S. K.,Espejo-Navarro, M. R. and Pasricha, P. J. (2005). Neural Stem Cell Transplantation in the

Stomach Rescues Gastric Function in Neuronal Nitric Oxide Synthase-Deficient Mice. *Gastroenterology*, **129**(6), 1817-1824.

Moore, M. W., Klein, R. D., Farinas, I., Sauer, H., Armanini, M., Phillips, H., Reichardt, L. F., Ryan, A. M., CarverMoore, K. and Rosenthal, A. (1996). Renal and neuronal abnormalities in mice lacking GDNF. *Nature* **382**, 76-79.

Mori, H.,Ninomiya, K.,Kino-oka, M.,Shofuda, T.,Islam, M. O.,Yamasaki, M.,Okano, H.,Taya, M. and Kanemura, Y. (2006). Effect of Neurosphere Size on the Growth Rate of Human Neural Stem/Progenitor Cells. *Journal of Neuroscience Research*, **84**(8), 1682-1691.

Morrison, S. J., Perez, S. E., Qiao, Z., Verdi, J. M., Hicks, C., Weinmaster, G. and Anderson, D. J. (2000). Transient notch activation initiates an irreversible switch from neurogenesis to gliogenesis by neural crest stem cells. *Cell* **101**, 499-510.

Mwizerwa, O., Das, P., Nagy, N., Akbareian, S. E., Mably, J. D. and Goldstein, A. M. (2011). Gdnf Is Mitogenic, Neurotrophic, and Chemoattractive to Enteric Neural Crest Cells in the Embryonic Colon. *Developmental Dynamics* **240**, 1402-1411.

Nagy, N. and Goldstein, A. M. (2006). Endothelin-3 regulates neural crest cell proliferation and differentiation in the hindgut enteric nervous system. *Developmental Biology* **293**, 203-217.

Namba, T.,Mochizuki, H.,Onodera, M.,Mizuno, Y.,Namiki, H. and Seki, T. (2005). The Fate of Neural Progenitor Cells Expressing Astrocytic and Radial Glial Markers in the Postnatal Rat Dentate Gyrus. *European Journal of Neuroscience*, **22**(8), 1928-1941.

Natarajan, D., G., M., Marcos-Gutierrez, C. V., Atkins, C. and Pachnis, V. (1999). Multipotential progenitors of the mammalian enteric nervous system capable of colonising aganglionic bowel in organ culture. *Development* **126**, 157-168.

Natarajan, D., Marcos-Gutierrez, C., Pachnis, V. and de Graaff, E. (2002). Requirement of signalling by receptor tyrosine kinase RET for the directed migration of enteric nervous system progenitor cells during mammalian embryogenesis. *Development* **129**, 5151-5160.

Newgreen, D. F. and Hartley, L. (1995). Extracellular matrix and adhesive molecules in the early development of the gut and its innervation in normal and spotting lethal rat embryos. *Acta Anatomica* **154**, 243-260.

Ngan, E. S.-W., Garcia-Barcelo, M.-M., Yip, B. H.-K., Poon, H.-C., Lau, S.-T., Kwok, C. K.-M., Sat, E., Sham, M.-H., Wong, K. K.-Y., Wainwright, B. J. et al. (2011). Hedgehog/Notch-induced premature gliogenesis represents a new disease mechanism for Hirschsprung disease in mice and humans. *The Journal of Clinical Investigation* **121**, 3467-78.

Niederreither, K.,Vermot, J.,Messaddeq, N.,Schuhbaur, B.,Chambon, P. and Dolle, P. (2001). Embryonic Retinoic Acid Synthesis Is Essential for Heart Morphogenesis in the Mouse. *Development*, **128**(7), 1019-1031.

Okamura, Y. and Saga, Y. (2008). Notch Signaling Is Required for the Maintenance of Enteric Neural Crest Progenitors. *Development*, **135**(21), 3555-3565.

Ott, D. and Lachance, P. (1979). Retinoic Acid--a Review. *The American Journal of Clinical Nutrition*, **32**(12), 2522-2531.

Pachnis, V., Mankoo, B. and Costantini, F. (1993). Expression of the c-ret proto-oncogene during mouse embryogenesis. *Development* **119**, 1005-1017.

Pan, W. K.,Zheng, B. J.,Gao, Y.,Qin, H. and Liu, Y. (2011). Transplantation of Neonatal Gut Neural Crest Progenitors Reconstructs Ganglionic Function in Benzalkonium Chloride-Treated Homogenic Rat Colon. *Journal of Surgical Research*, **In Press, Corrected Proof**.

Pattyn, A.,Morin, X.,Cremer, H.,Goridis, C. and Brunet, J. F. (1999). The Homeobox Gene Phox2b Is Essential for the Development of Autonomic Neural Crest Derivatives. *Nature*, **399**(6734), 366-370.

Peters-Van Der Sanden, M. J. H.,Kirby, M. L.,Gittenberger-De Groot, A.,Tibboel, D.,Mulder, M. P. and Meijers, C. (1993). Ablation of Various Regions within the Avian Vagal Neural Crest Has Differential Effects on Ganglion Formation in the Fore-, Mid- and Hindgut. *Developmental Dynamics*, **196**(3), 183-194.

Pfeifer, A. and Hofmann, A. (2009). Lentiviral Transgenesis Gene Knockout Protocols. **530**, 391-405

Pichel, J. G., Shen, L. Y., Sheng, H. Z., Granholm, A. C., Drago, J., Grinberg, A., Lee, E. J., Huang, S. P., Saarma, M., Hoffer, B. J., Sariola H. and Westphal H. (1996). Defects in enteric innervation and kidney development in mice lacking GDNF. *Nature* **382**, 73-76.

Pierfelice, T.,Alberi, L. and Gaiano, N. (2011). Notch in the Vertebrate Nervous System: An Old Dog with New Tricks. *Neuron*, **69**(5), 840-855.

Pingault, V.,Bondurand, N.,Kuhlbrodt, K.,Goerich, D. E.,Prehu, M. O.,Puliti, A.,Herbarth, B.,Hermans-Borgmeyer, I.,Legius, E.,Matthijs, G., et al. (1998). Sox10 Mutations in Patients with Waardenburg-Hirschsprung Disease. *Nature Genetics*, **18**(2), 171-173.

Pitera, J. E.,Smith, V. V.,Woolf, A. S. and Milla, P. J. (2001). Embryonic Gut Anomalies in a Mouse Model of Retinoic Acid-Induced Caudal Regression Syndrome - Delayed Gut Looping, Rudimentary Cecum, and Anorectal Anomalies. *American Journal of Pathology*, **159**(6), 2321-2329.

Platel, J. C.,Gordon, V.,Heintz, T. and Bordey, A. (2009). Gfap-Gfp Neural Progenitors Are Antigenically Homogeneous and Anchored in Their Enclosed Mosaic Niche. *Glia*, **57**(1), 66-78.

Poelmann, R. E.,Mikawa, T. and Gittenberger-De Groot, A. C. (1998). Neural Crest Cells in Outflow Tract Septation of the Embryonic Chicken Heart: Differentiation and Apoptosis. *Developmental Dynamics*, **212**(3), 373-384.

Pomeranz, H. D.,Rothman, T. P.,Chalazonitis, A.,Tennyson, V. M. and Gershon, M. D. (1993). Neural Crest-Derived Cells Isolated from the Gut by Immunoselection Develop Neuronal and Glial Phenotypes When Cultured on Laminin. *Developmental Biology*, **156**(2), 341-361.

Pomeranz, H. D., Rothman, T. P. and Gershon, M. D. (1991). Colonization of the post-umbilical bowel by cells derived from the sacral neural crest: direct tracing of cell migration using an intercalating probe and a replication-deficient retrovirus. *Development* **111**, 647-655.

Prajerova, I.,Honsa, P.,Chvatal, A. and Anderova, M. (2010). Neural Stem/Progenitor Cells Derived from the Embryonic Dorsal Telencephalon of D6/Gfp Mice Differentiate Primarily into Neurons after Transplantation into a Cortical Lesion. *Cellular and Molecular Neurobiology*, **30**(2), 199-218.

Radtke, F. and Clevers, H. (2005). Self-Renewal and Cancer of the Gut: Two Sides of a Coin. *Science*, **307**(5717), 1904-1909.

Rakic, P. (2002). Adult Neurogenesis in Mammals: An Identity Crisis. *Journal of Neuroscience*, **22**(3), 614-618.

Rakic, P. (2003). Developmental and Evolutionary Adaptations of Cortical Radial Glia. *Cerebral Cortex*, **13**(6), 541-549.

Ramalho-Santos, M.,Melton, D. A. and McMahon, A. P. (2000). Hedgehog Signals Regulate Multiple Aspects of Gastrointestinal Development. *Development*, **127**(12), 2763-2772.

Randall, K. J.,Turton, J. and Foster, J. R. (2011). Explant Culture of Gastrointestinal Tissue: A Review of Methods and Applications. *Cell Biology and Toxicology*, **27**(4), 267-284.

Redmond, L.,Oh, S. R.,Hicks, C.,Weinmaster, G. and Ghosh, A. (2000). Nuclear Notch1 Signaling and the Regulation of Dendritic Development. *Nature Neuroscience*, **3**(1), 30-40.

Reichenbach, B.,Delalande, J. M.,Kolmogorova, E.,Prier, A.,Nguyen, T.,Smith, C. M.,Holzschuh, J. and Shepherd, I. T. (2008). Endoderm-Derived Sonic Hedgehog and Mesoderm Hand2 Expression Are Required for Enteric Nervous System Development in Zebrafish. *Developmental Biology*, **318**(1), 52-64.

Reynolds, W. (1992). Generation of Neurons and Astrocytes from Isolated Cells of the Adult Mammalian Central Nervous System. *Science*, **255**(5052), 1707-1710.

Rickmann, M. and Wolff, J. R. (1995). S100 Protein Expression in Subpopulations of Neurons of Rat-Brain. *Neuroscience*, **67**(4), 977-991.

Rosario, D. (1999). Functional roles of S100 proteins, calcium-binding proteins of the EF-hand type. *Biochimica et Biophysica Acta (BBA) - Molecular Cell Research* **1450**, 191-231.

Rothman, T. P. and Gershon, M. D. (1982). Phenotypic-Expression in the Developing Murine Enteric Nervous-System. *Journal of Neuroscience*, **2**(3), 381-393.

Rothman, T. P.,Tennyson, V. M. and Gershon, M. D. (1986). Colonization of the Bowel by the Precursors of Enteric Glia - Studies of Normal and Congenitally Aganglionic Mutant Mice. *Journal of Comparative Neurology*, **252**(4), 493-506.

Ruhrberg, C. and Schwarz, Q. (2010). In the Beginning: Generating Neural Crest Cell Diversity. *Cell Adhesion & Migration*, **4**(4), 622-630.

Sanalkumar, R.,Dhanesh, S. and James, J. (2010). Non-Canonical Activation of Notch Signaling/Target Genes in Vertebrates. *Cellular and Molecular Life Sciences*, **67**(17), 2957-2968.

Sanchez, M. P., SilosSantiago, I., Frisen, J., He, B., Lira, S. A. and Barbacid, M. (1996). Renal agenesis and the absence of enteric neurons in mice lacking GDNF. *Nature* **382**, 70-73.

Sander, G. R.,Brookes, S. J. H. and Powell, B. C. (2003). Expression of Notch1 and Jagged2 in the Enteric Nervous System. *Journal of Histochemistry & Cytochemistry*, **51**(7), 969-972.

Santos, T. G.,Silva, I. R.,Costa-Silva, B.,Lepique, A. P.,Martins, V. R. and Lopes, M. H. (2011). Enhanced Neural Progenitor/Stem Cells Self-Renewal Via the Interaction of Stress-Inducible Protein 1 with the Prion Protein. *Stem Cells*, **29**(7), 1126-1136.

Sariola, H. and Saarma, M. (2003). Novel Functions and Signalling Pathways for Gdnf. *Journal of Cell Science*, **116**(19), 3855-3862.

Sato, Y. and Heuckeroth, R. O. (2008). Retinoic Acid Regulates Murine Enteric Nervous System Precursor Proliferation, Enhances Neuronal Precursor Differentiation, and Reduces Neurite Growth in Vitro. *Developmental Biology*, **320**(1), 185-198.

Schäfer, K.-H., Hagl, C. I. and Rauch, U. (2003). Differentiation of neurospheres from the enteric nervous system. *Pediatric Surgery International* **19**, 340-344.

Shaker, A. and Rubin, D. C. (2010). Intestinal Stem Cells and Epithelial–Mesenchymal Interactions in the Crypt and Stem Cell Niche. *Translational Research*, **156**(3), 180-187.

Shen, J., Bronson, R. T., Chen, D. F., Xia, W., Selkoe, D. J. and Tonegawa, S. (1997). Skeletal and CNS Defects in Presenilin-1-Deficient Mice. *Cell* **89**, 629-639.

Shen, L., Pichel, J. G., Mayeli, T., Sariola, H., Lu, B. and Westphal, H. (2002). Gdnf haploinsufficiency causes Hirschsprung-like intestinal obstruction and early-onset lethality in mice. *American Journal of Human Genetics* **70**, 435-447.

Schuchardt, A., Dagati, V., Larssonblomberg, L., Costantini, F. and Pachnis, V. (1994). Defects in the kidney and enteric nervous system of mice lacking the tyrosine kinase receptor Ret. *Nature* **367**, 380-383.

Sidebotham, E. L., Woodward, M. N., Kenny, S. E., Lloyd, D. A., Vaillant, C. R. and Edgar, D. H. (2002). Localization and endothelin-3 dependence of stem cells of the enteric nervous system in the embryonic colon. *Journal of Pediatric Surgery* **37**, 145-150.

Sieber-Blum, M. (2000). Factors Controlling Lineage Specification in the Neural Crest. *International Review of Cytology*, **197**, 1-33.

Simpson, M. J., Zhang, D. C., Mariani, M., Landman, K. A. and Newgreen, D. F. (2007). Cell proliferation drives neural crest cell invasion of the intestine. *Developmental Biology* **302**, 553-568.

Solecki, D. J.,Liu, X.,Tomoda, T.,Fang, Y. and Hatten, M. E. (2001). Activated Notch2 Signaling Inhibits Differentiation of Cerebellar Granule Neuron Precursors by Maintaining Proliferation. *Neuron*, **31**(4), 557-568.

Southard-Smith, E. M.,Angrist, M.,Ellison, J. S.,Agarwala, R.,Baxevanis, A. D.,Chakravarti, A. and Pavan, W. J. (1999). The

Sox10(Dom) Mouse: Modeling the Genetic Variation of Waardenburg-Shah (Ws4) Syndrome. *Genome Research*, **9**(3), 215-225.

Southard-Smith, E. M.,Kos, L. and Pavan, W. J. (1998). Sox10 Mutation Disrupts Neural Crest Development in Dom Hirschsprung Mouse Model. *Nature Genetics*, **18**(1), 60-64.

Stanchina, L.,Baral, V.,Robert, F.,Pingault, V.,Lemort, N.,Pachnis, V.,Goossens, M. and Bondurand, N. (2006). Interactions between Sox10, Edn3 and Ednrb During Enteric Nervous System and Melanocyte Development. *Developmental Biology*, **295**(1), 232-249.

Swenson, O. (1996). Early history of the therapy of Hirschsprung's disease: Facts and personal observations over 50 years. *Journal of Pediatric Surgery* **31**, 1003-1008.

Taraviras, S., Marcos-Gutierrez, C. V., Durbec, P., Jani, H., Grigoriou, M., Sukumaran, M., Wang, L. C., Hynes, M., Raisman, G. and Pachnis, V. (1999). Signalling by the RET receptor tyrosine kinase and its role in the development of the mammalian enteric nervous system. *Development* **126**, 2785-2797.

Taylor, M. K.,Yeager, K. and Morrison, S. J. (2007). Physiological Notch Signaling Promotes Gliogenesis in the Developing Peripheral and Central Nervous Systems. *Development*, **134**(13), 2435-2447.

Teitelman, G.,Gershon, M. D.,Rothman, T. P.,Joh, T. H. and Reis, D. J. (1981). Proliferation and Distribution of Cells That Transiently Express a Catecholaminergic Phenotype During Development in Mice and Rats. *Developmental Biology*, **86**(2), 348-355.

Theocharatos, S. and Kenny, S. E. (2008). Hirschsprung's disease: Current management and prospects for transplantation of enteric nervous system progenitor cells. *Early Human Development* **84**, 801-804.

Toshihide Iwashita, G. M. K., Ricardo Pardal, Mark J. Kiel, and Sean J. and Morrison†. (2003). Hirschsprung Disease Is Linked to Defects in Neural Crest Stem Cell Function. *Science* **301**, 5.

Turker Yardan, A. K. E., Ahmet Baydin, Keramettin Aydin, Cengiz Cokluk. (2011). Usefulness of S100b Protein in Neurological Disorders. *Journal of Pakistan Medical Association*, **61**(3), 6.

Uesaka, T. and Enomoto, H. (2010). Neural Precursor Death Is Central to the Pathogenesis of Intestinal Aganglionosis in Ret Hypomorphic Mice. *Journal of Neuroscience* **30**, 5211-5218.

Uesaka, T., Jain, S., Yonemura, S., Uchiyama, Y., Milbrandt, J. and Enomoto, H. (2007). Conditional ablation of GFR alpha 1 in postmigratory enteric neurons triggers unconventional neuronal death in the colon and causes a Hirschsprung's disease phenotype. *Development* **134**, 2171-2181.

Uesaka, T., Nagashimada, M., Yonemura, S. and Enomoto, H. (2008). Diminished Ret expression compromises neuronal survival in the colon and causes intestinal aganglionosis in mice. *Journal of Clinical Investigation* **118**, 1890-1898.

van Es, J. H.,van Gijn, M. E.,Riccio, O.,van den Born, M.,Vooijs, M.,Begthel, H.,Cozijnsen, M.,Robine, S.,Winton, D. J.,Radtke, F., et al. (2005). Notch/[Gamma]-Secretase Inhibition Turns Proliferative Cells in Intestinal Crypts and Adenomas into Goblet Cells. *Nature*, **435**(7044), 959-963.

Wallace, A. S. and Burns, A. J. (2005). Development of the Enteric Nervous System, Smooth Muscle and Interstitial Cells of Cajal in the Human Gastrointestinal Tract. *Cell and Tissue Research*, **319**(3), 367-382.

Walters, L. C.,Cantrell, V. A.,Weller, K. P.,Mosher, J. T. and Southard-Smith, E. M. (2010). Genetic Background Impacts Developmental Potential of Enteric Neural Crest-Derived Progenitors in the Sox10(Dom) Model of Hirschsprung Disease. *Human Molecular Genetics*, **19**(22), 4353-4372.

Wang, H. T., Hughes, I., Planer, W., Parsadanian, A., Grider, J. R., Vohra, B. P. S., Keller-Peck, C. and Heuckeroth, R. O. (2010). The Timing and Location of Glial Cell Line-Derived Neurotrophic Factor Expression Determine Enteric Nervous System Structure and Function. *Journal of Neuroscience* **30**, 1523-1538.

Wang, J.,Fu, L.,Gu, F. and Ma, Y. (2011). Notch1 Is Involved in Migration and Invasion of Human Breast Cancer Cells. *Oncology reports*, **26**(5), 1295-1303.

Wang, X.,Chan, A. K. K.,Sham, M. H.,Burns, A. J. and Chan, W. Y. (2011). Analysis of the Sacral Neural Crest Cell Contribution to the Hindgut

Enteric Nervous System in the Mouse Embryo. *Gastroenterology*, **141**(3), 992-1002.e1006.

Wang, Z. X.,Dolle, P.,Cardoso, W. V. and Niederreither, K. (2006). Retinoic Acid Regulates Morphogenesis and Patterning of Posterior Foregut Derivatives. *Developmental Biology*, **297**(2), 433-445.

Weber, G. F.,Bjerke, M. A. and DeSimone, D. W. (2011). Integrins and Cadherins Join Forces to Form Adhesive Networks. *Journal of Cell Science*, **124**(8), 1183-1193.

Wegner, M. (1999). From Head to Toes: The Multiple Facets of Sox Proteins. *Nucleic Acids Research*, **27**(6), 1409-1420.

Wegner, M. and Stolt, C. C. (2005). From Stem Cells to Neurons and Glia: A Soxist's View of Neural Development. *Trends in Neurosciences*, **28**(11), 583-588.

Woodward, M. N., Sidebotham, E. L., Connell, M. G., Kenny, S. E., Vaillant, C. R., Lloyd, D. A. and Edgar, D. H. (2003). Analysis of the effects of endothelin-3 on the development of neural crest cells in the embryonic mouse gut. *Journal of Pediatric Surgery* **38**, 1322-1328.

Worley, D. S., Pisano, J. M., Choi, E. D., Walus, L., Hession, C. A., Cate, R. L., Sanicola, M. and Birren, S. J. (2000). Developmental regulation of GDNF response and receptor expression in the enteric nervous system. *Development* **127**, 4383-4393.

Wu, J. J., Chen, J. X., Rothman, T. P. and Gershon, M. D. (1999). Inhibition of in vitro enteric neuronal development by endothelin-3: mediation by endothelin B receptors. *Development* **126**, 1161-1173.

Xu, X., Francis, R., Wei, C. J., Linask, K. L. and Lo, C. W. (2006). Connexin 43-mediated modulation of polarized cell movement and the directional migration of cardiac neural crest cells. *Development* **133**, 3629-3639.

Xu, X., Li, W. E. I., Huang, G. Y., Meyer, R., Chen, T., Luo, Y., Thomas, M. P., Radice, G. L. and Lo, C. W. (2001). Modulation of mouse neural crest cell motility by N-cadherin and connexin 43 gap junctions. *The Journal of Cell Biology* **154**, 217-230.

Yang, Q. E.,Hamberger, A.,Khatibi, N.,Stigbrand, T. and Haglid, K. G. (1996). Presence of S-100 Beta in Cholinergic Neurones of the Rat Hindbrain. *Neuroreport*, **7**(18), 3093-3099.

Yntema, C. L. and Hammond, W. S. (1954). The origin of intrinsic ganglia of trunk viscera from vagal neural crest in the chick embryo. *The Journal of Comparative Neurobiology* **101**, 515-541.

Young, H. M., Bergner, A. J. and Muller T. (2003). Acquisition of neuronal and glial markers by neural crest-derived cells in the mouse intestine. *The journal of Comparative Neurology* **456**, 1-11.

Young, H. M., Bergner, A. J., Anderson, R. B., Enomoto, H., Milbrandt, J., Newgreen, D. F. and Whitington, P. M. (2004). Dynamics of neural crest-derived cell migration in the embryonic mouse gut. *Developmental Biology* **270**, 455-473.

Young, H. M., Ciampoli, D., Hsuan, J. and Canty, A. J. (1999). Expression of Ret-, p75NTR-, Phox2a-, Phox2b-, and tyrosine hydroxylase-immunoreactivity by undifferentiated neural crest-derived cells and different classes of enteric neurons in the embryonic mouse gut. *Developmental Dynamics* **216**, 137-152.

Young, H. M., Hearn, C. J., Ciampoli, D., Southwell, B. R., Brunet, J. F. and Newgreen, D. F. (1998). A Single Rostrocaudal Colonization of the Rodent Intestine by Enteric Neuron Precursors Is Revealed by the

Expression of Phox2b, Ret, and p75 and by Explants Grown under the Kidney Capsule or in Organ Culture. *Developmental Biology* **202**, 67-84.

Young, H. M., Hearn, C. J., Farlie, P. G., Canty, A. J., Thomas, P. Q. and Newgreen, D. F. (2001b). GDNF Is a Chemoattractant for Enteric Neural Cells. *Developmental Biology* **229**, 503-516.

Young, H. M.,Hearn, C. J. and Newgreen, D. F. (2000). Embryology and Development of the Enteric Nervous System. *Gut*, **47**(90004), iv12-14.

Young, H.M., Newgreen. D. (2001a). Enteric neural crest-derived cells: Origin, identification, migration, and differentiation. *The Anatomical Record* **262**, 1-15.

Young, H. M., Turner, K. N. and Bergner, A. J. (2005). The location and phenotype of proliferating neural-crest-derived cells in the developing mouse gut. *Cell and Tissue Research* **320**, 1-9.

Zheng, Y., Begum, S., Zhang, C., Fleming, K., Masumura, C., Zhang, M., Smith, P. and Darlington, C. (2011). Increased BrdU incorporation reflecting DNA repair, neuronal de-differentiation or possible neurogenesis

in the adult cochlear nucleus following bilateral cochlear lesions in the rat. *Experimental Brain Research* **210**, 477-487.

Zhu, L.,Lee, H. O.,Jordan, C. R. S.,Cantrell, V. A.,Southard-Smith, E. M. and Shin, M. K. (2004). Spatiotemporal Regulation of Endothelin Receptor-B by Sox10 in Neural Crest-Derived Enteric Neuron Precursors. *Nature Genetics*, **36**(7), 732-737.

Zwijsen, A., Verschueren, K. and Huylebroeck, D. (2003). New intracellular components of bone morphogenetic protein/Smad signaling cascades. *Febs Letters* **546**, 133-139.